A Linear Algebra Approach to Graph Melting

Najlaa Alalwan

Department of Mathematics and Statistics

University of Strathclyde, Glasgow, UK

March 11, 2022

This thesis is the result of the author's original research. It has been composed by the author and has not been previously submitted for examination which has led to the award of a degree.

Signed:

Date:

Acknowledgements

Many thanks and appreciation to my dear mother **Ameena Khalaf** and father **Sadeq Abdullah** who encouraged and supported me to study a PhD in the UK. Special thanks to my dear sister **Ghadaa**, who has had a huge impact by supporting me psychologically. Thanks for all the advice you gave me, and for being the best listener.

Many thanks to my country **Iraq** and ministry of higher education - **Basra university** for supporting me financially to study a PhD in the UK.

Thanks, appreciation and respect to Prof. **John Mackenzie** for everything.

Thanks, appreciation and respect to Dr. **Francesca Arrigo**, Dr. **Michael Grinfeld**, Dr. **Sergey Kitaev** and Dr. **Matthias Langer** for reading this work and the excellent comments on the work and its presentation.

Many thanks to my friends **Michael Doherty**, **Jamie**, **Andrew**, **James**, **Alistair**, **Ewan**, **Irene** and **Mary**.

Abstract

Robustness is often regarded as the ability of a given system to maintain its functionality when faced with some external perturbation or when some of its parts fail to operate. The ability of the system to cope with disturbances vary from system to system, and there are many examples in daily life which illustrate this concept. Communication networks, for example, transportation and telephone networks, or the internet, often manage to cope with errors or damage within some of their components without leading to the system failing entirely. As an example, within a social network of employees within a company, the absence of some employees within some given threshold will not lead to failure of the company. However, in a financial network, economic failure in some parts of the system could lead to the complete failure of the entire system.

In order to understand how external perturbations or failures within particular parts of the system affect a network we can study the robustness of the network. The robustness of a complex system in graph theory, is the ability of the network to maintain its connectivity after the removal of some nodes or edges. The process of changing of a graph from being connected to being disconnected, via deletion of nodes or edges, is called graph melting. We introduce a melting phase transition for simple connected graphs and networks faced with external perturbations with positive second largest eigenvalue $\lambda_2 > 0$.

In order to calibrate our method of studying network robustness, we consider the network-theoretic representation of some materials which, in the real-world, are affected by melting. In particular, we will consider granular materials. A granular material is a material which is composed of discrete macroscopic solid particles, for example, sand, rice, and coffee. Granular materials are commonly used in a wide range of real world

applications. There are already various models of granular materials within network theory, which has allowed us to study the structure and physical behaviour of such systems when they have an external perturbations applied to them.

In this thesis, we represent granular solids by simple graphs capturing their topological structure and ordering, in order to study their robustness and the melting process. The melting process is related to the algebraic structure of the adjacency matrix of the graph and the concept of network communicability. At the melting phase transition, a graph in question transfers from being connected to being disconnected. We study melting in graphs with the second largest eigenvalue being positive, namely, in windmill graphs, dumbbell graphs and cycle graphs. Also, we investigate melting in complete multipartite graphs where the second largest eigenvalue is non-positive. We found a melting phase transition in simple connected graphs with $\lambda_2 > 0$ and $\lambda_2 \gg \lambda_3$, which resembles the melting process of a given system. We found that there is no melting phase transition in complete multipartite graphs. Also, we found the spectral decomposition for dumbbell graphs and complete multipartite graphs, which until now have not been done.

Moreover, in this thesis, we show that crystalline-like granular materials melt at lower temperatures and display a sharper transition between solid to liquid phases than amorphous granular materials. In addition, we show the evolution mechanism of melting in these granular materials with tools from network theory. In the particular case of crystalline materials, the process starts by melting the central core of the crystal network, then melting spreads out from the central core until the whole network (material) transfers into a liquid. We also investigate computationally the melting process in some real-world networks. We found that the melting process of a network correlates well with the topological structure of the network.

Contents

List of Figures

List of Figures

List of Tables

List of Tables

List of Symbols

Γ	simple connected graph
V	set of vertices
E	set of edges
n	size of V
m	size of E
A	adjacency matrix
A_{ij}	(i, j) entry of A
λ_i	ith eigenvalue of A
$\boldsymbol{\psi}_i$	ith eigenvector of A that corresponds λ_i
$\psi_i(p)$	pth entry of the eigenvector ψ_i
$\boldsymbol{\psi}_1$	Perron-Frobenius eigenvector of A
β	external stress
β_c	critical external stress
$G_{pq}(\Gamma, \beta)$	communicability function of Γ between nodes p and q at β
$\Delta G_{pq}(\Gamma, \beta)$	communicability graph funtion of Γ between nodes p and q at β
$\Delta \tilde{G}_{pq}(\beta)$	modified communicability graph function between p and q at β
$M(\Gamma, \beta)$	maximum vibration of any pair of distinct nodes at β
$\tilde{H}(\Gamma, \beta)$	modified communicability graph of $\Gamma = (V, E)$
$K_{\eta_1, \eta_2, \ldots, \eta_k}$	complete multipartite graph with $n = \sum_{i=1}^{k} \eta_i$
$K_{\eta, \eta, \ldots, \eta}$	complete k–partitie graph with $n = \eta k$
$K_{\eta, \eta, l}$	complete 3–partitie graph with $n = 2\eta + l$

List of Symbols

RGG	random geometric graphs
RNG	relative neighbourhood graphs
$P_n \times P_n$	square grid (lattice) graph
CC	closeness centrality
BC	betweenness centrality
EC	eigenvector centrality
SC	subgraph centrality
r	Pearson correlation coefficient
CV	coefficient of variation
$\bar{k}$	average degree
K_{max}	maximum degree
$\bar{C}$	average Watts-Strogatz clustering coefficient
$\bar{l}$	average path length
Ef	shortest path efficiency
λ_1	spectral radius of the adjacency matrix
λ_2	second largest eigenvalue of the adjacency matrix
$\bar{\xi}$	average communicability distance
$\bar{\Omega}$	average resistance distance
$\bar{\theta}$	average communicability angle
$\varrho(G)$	scaled isotropy
S_η	Star graph with η nodes
C_n	cycle graph with n nodes
K_η	complete graph with η nodes
N_n	null graph with n nodes
K_η-K_η	Dumbbell graph with 2η nodes
$\Theta(c, s, \eta)$	core-satellite graph of η copies of K_s (the satellites) with core K_c
$W(\eta, s)$	Windmill graph of s copies of K_η

Chapter 1

Introduction

A complex system is a system comprised of many interconnected components that interact with each other, where the behaviour of one component might be affected by the behaviour of the other components [20]. In everyday life, we deal with such complex systems. For example, granular materials, the human brain, power grids, communication and transportation systems, ecosystems, and social organizations fall into the category of complex systems. These systems are difficult to model due to the behaviour of their components. With this mind, it can be useful to study the relationships between such components and consider how they interact with each other in such a system. For this reason, these complex systems are represented using *network theory*, which is regarded as a powerful framework for modelling such systems.

Network theory, using graphs (or networks) consisting of vertices and edges, has been used to model many real world systems in science and technology [16, 45, 107]. The vertices are used to represent the components of the system, and an edge between two given vertices represents the relationship between the two corresponding components. Network theory has attracted a great deal of attention as a result of its applicability to many real world systems. It is an active area throughout various disciplines of research such as statistical and particle physics, computer science, electrical engineering, biology, economics, finance, operational research, climatology and sociology [28, 86]. For instance, a particle of a granular material can be represented in graph theory by a node, and two particles in contact can be represented by two nodes being connected by an edge. However, in reality it is not always possible to determine exactly if two

particles have been in contact; therefore we need to use approximations to model this phenomenon. There are many different approaches and experimental techniques in two dimensions that have been developed for approximating the contact between particles of granular materials [4]. In this thesis, using network theory, we model granular material systems as simple graphs. We use regular and irregular graph structures such as square lattices and Gabriel graphs, respectively, to approximate the contact between the particles of granular solids, using the assumption that all of the particles are identical.

Physically, melting of a solid begins when the internal energy of the solid increases due to being subject to heat or pressure [3, 57]. We recall that the properties of a solid depend on its chemical characterization, as well as the structure of its atoms and molecules [98, 45]. There are many theoretical models explaining the mechanisms of melting solids. The most successful models are based on the Lindemann and Born criteria. Lindemann [66] found that when the temperature of the solid increases, the amplitudes of the vibrations of the atoms become large. Once a critical temperature is reached, the atoms break down and disturb their neighbouring atoms. This is how the melting process starts in reality. In 1937, Born suggested a new criterion for melting solids [11]. He found that the spaces between the atoms increase as a result of the increase in temperature of the solids. At a critical temperature, a solid suffers mechanical instability within its structure which initiates the melting process. Since the work of Lindemann, many studies have been published based on these two criteria [53].

The vibrations of the atoms or molecules of solids can be interpreted using graph theory in order to study the melting process. The first successful approach for interpreting this phenomenon was done in 2012 by Estrada and Hatano. They defined a measure to capture the vibrations between the nodes by using graph theory. Estrada and Hatano [36, 33] proved that the vibrations between the nodes can be determined using the communicability function. They found that a network of a solid substance melts (that is to say it becomes fully disconnected) when the communicability between their nodes disappears. On the other hand, when the communicability between the nodes is very high, the network is solidified.

1. Introduction

In this work we propose a melting phase transition for some simple connected graphs and networks when faced with external perturbations. We consider a vibrational model of the communicability function based on the Lindemann criterion to study melting of certain simple connected graphs. Namely, we investigate melting in certain graph families where the second largest eigenvalue λ_2 of the graph is positive and other families where it is non-positive. In particular, for graphs with positive second largest eigenvalue, we study the melting in windmill graphs, dumbbell graphs and cycle graphs. Also, we investigated melting in complete multipartite graphs where the second largest eigenvalue is non-positive. We found the melting phase transition in the communicability graph structures of simple connected graphs with $\lambda_2 > 0$ and $\lambda_2 \gg \lambda_3$, which resembles the melting process of a given system. We found that there is no melting phase transition in complete multipartite graphs.

Moreover, we model amorphous and crystal solids in graph theory as regular and irregular graphs respectively, in order to investigate the differences in their melting processes. We compare the melting percentage and melting temperature of amorphous and crystal solids like regular and irregular graphs by applying a wide range of temperatures to them. Our results satisfy the two main physical attributes for melting these two kinds of solids, namely, the melting point and the melting percentage with increased temperature.

We investigate computationally the melting phase transition in several real-world networks. We find that the melting process in these networks correlates with their topological structure. In addition, we discover and prove that melting of nodes (a node is melted when it is disconnected from the rest of the graph) correlates well with its corresponding eigenvector centrality. That is, melting of a network starts with the nodes having the highest values of the Perron–Frobenius eigenvector, because these nodes require a lower temperature to melt (to be disconnected) than the nodes with the smaller values of the Perron–Frobenius eigenvector.

The thesis is organised as follows. In Chapter 2, we present general concepts in graph theory including definitions of various types of graphs to be considered in the thesis. Moreover, we find the spectrum of some of these graph types which we will

deal with in depth in Chapter 4. For windmill graphs, we find the exact values of the entries of the associated eigenvectors corresponding to the largest and smallest eigenvalues. Also, we find the spectrum (eigenvalues and eigenvectors) of dumbbell graphs. Moreover, we find the eigenvectors corresponding to $\lambda = 0$ and $\lambda = -\eta_i$, $i \in \{1, 2, \ldots, k\}$ for complete multipartite graph $K_{\eta_1,\eta_2,\cdots,\eta_k}$, $\eta_1 \leq \eta_2 \leq \cdots \leq \eta_k$, and the exact entries of the normalized eigenvectors corresponding to the negative eigenvalues $\lambda \neq -\eta_i$ and the largest eigenvalue. Then, we discuss several topological network properties for investigating network robustness.

In Chapter 3, we define a melting phase transition in graphs. First, we include some fundamentals about melting solids physically. Then we include a discussion about melting of graphs; vibrations (communicability) and pure vibrations (communicability graphs) of nodes in graph theory.

In Chapter 4, we investigate melting in certain graph families that covers the cases when the second eigenvalue is positive or nonpositive. We study melting in windmill, dumbbell and complete multipartite graphs. For these graphs, we find the communicability graph functions in terms of the inverse temperature β. We can determine explicitly the possible melting patterns for windmill and dumbbell graphs. Moreover, we show that the communicability graph functions for complete multipartite graphs are not connected regardless of the value of β.

In Chapter 5, we study computationally melting in cycle graphs. Again, we can determine explicitly the possible melting patterns for these graphs. Then, we present our result about the existence of the melting phase transition in simple connected graphs with $\lambda_2 > 0$ and $\lambda_2 \gg \lambda_3$. Also, we model granular material solids using graph theory in order to study the melting process in such materials.

In Chapter 6, we analyse the melting process of a series of real-world networks as a means of investigating the global and local structural characteristics of networks which drive their melting processes.

Finally, Chapter 7 presents the conclusion for the entire thesis, as well as some remarks on possible directions of future work based on our thesis. We also included, in the appendix, details of the real world data that was employed in this work, tables of

simulation results, and scripts used for our calculations.

Part I

Background and Preliminary Results

Chapter 2

Graph and Network Theory

In this chapter, we highlight some fundamental properties of networks. Moreover, we find the spectrum of certain graph types, which we will deal with in depth in Chapter 4. Throughout this chapter, we let I_n denote an $n \times n$ identity matrix, $\mathbf{1}_n$ a vector of n ones, and $\mathbf{0}_n$ a vector of n zeros.

2.1 Networks and Graphs

The study of graphs is a branch of mathematics known as graph theory. Graph theory is relevant to the structure of many systems [28, 47], and can, for example, be used to represent the relationships between various components within such a given system. In order to study complex systems in terms of graphs, we first need to review some essential concepts that we will deal with frequently throughout this work. The main concept we would like to establish here is that of a graph (or network). We use the term graph or network to refer to the skeleton of the system that is considered. A graph (or network) is comprised of nodes and links. The nodes represent the entities of the system and the links represent the relationships between those entities. The term network is used to refer to real world systems while the concept of a graph is usually used as a mathematical representation of such systems. Due to strong links between the two concepts, we will use them interchangeably.

2.1.1 Definition of Graph

A graph $\Gamma = (V, E)$ is an ordered pair of a set of vertices V and a set of edges $E \subseteq V \times V$, where $v_i, v_j \in V$ are connected in Γ if there exists an edge $e = (v_i, v_j) \in E$ connecting v_i to v_j [28]. The sizes of V and E are denoted by $|V| = n$ and $|E| = m$, respectively. Another way to represent the graph $\Gamma = (V, E)$ is via its *adjacency matrix* A, which is an $n \times n$ matrix defined by

$$A_{ij} = \begin{cases} 1 & \text{if } (v_i, v_j) \in E, \\ 0 & \text{otherwise.} \end{cases} \tag{2.1}$$

If the graph is *weighted* then each edge $(v_i, v_j) \in E$ has an associated real positive number, weight, and the A_{ij} entry denotes that weight. An edge of the form $(v_i, v_i) \in E$ for some $v_i \in V$ is called a *loop*. If there is more than one edge connecting two given vertices, then we say that those vertices are connected through multiple edges. *A directed* graph is a graph whose edges are associated with a direction such that if $(v_i, v_j) \in E$ then (v_j, v_i) is not necessarily in E. However, in undirected graphs if $(v_i, v_j) \in E$ then necessarily $(v_j, v_i) \in E$, which means that both entries (v_i, v_j) and (v_j, v_i) equal 1 in the corresponding adjacency matrix. An undirected graph is *simple* if there are no multiple edges and loops in it. In the rest of this work, we will deal with simple graphs.

2.1.2 Structural Concepts of Graphs

In this subsection, we introduce some basic notions in graph theory. There is much literature explaining various concepts and structural properties related to graphs; e.g. see [28, 47].

Definition 2.1.1. Adjacent and Incident Nodes
In a graph $\Gamma = (V, E)$, two nodes v_i and v_j in V are *adjacent* if they are connected by an edge $e = (v_i, v_j) \in E$. In this case, we say that v_i and v_j are *incident* to the edge e and e is incident to v_i and v_j. Similarly, two edges $e_{ij} = (v_i, v_j)$ and $e_{jk} = (v_j, v_k)$ are adjacent if they are both incident to the same node.

Definition 2.1.2. Neighbourhood of a Node

The *neighbourhood* of a node v_i, denoted by $N(v_i)$, in a graph $\Gamma = (V, E)$ is the set of nodes which are adjacent to v_i. That is, $N(v_i) = \{v_j \in V \mid (v_i, v_j) \in E\}$.

Definition 2.1.3. Degree of a Node

The *degree* of a node $v_i \in V$, denoted by k_i, in a graph $\Gamma = (V, E)$ is the number of edges incident to v_i, and this is equivalent to the sum of the entries of the ith row, or the ith column, in the adjacency matrix of Γ.

Definition 2.1.4. Regular Graph

A simple graph is *regular* if all its nodes have the same degree.

Definition 2.1.5. Walk and Path in a Graph

A *walk* of length k in a graph $\Gamma = (V, E)$ is an ordered set of vertices (not necessarily distinct) $v_1, v_2, ..., v_{k+1} \in V$ such that for all $1 \leq i \leq k$, there exists an edge in E that connects v_i and v_{i+1}. A walk is *closed* if $v_1 = v_{k+1}$. Additionally, if a walk contains no repeated vertices then it is called a *path*.

Definition 2.1.6. Connected Graph

A graph is *connected* if for every pair of vertices there exists a path connecting them. A graph that is not connected is called a *disconnected graph*.

Definition 2.1.7. Subgraph

A graph $\grave{\Gamma} = (\grave{V}, \grave{E})$ is a *subgraph* of $\Gamma = (V, E)$, denoted by $\grave{\Gamma} \subseteq \Gamma$, if $\grave{V} \subseteq V$ and $\grave{E} \subseteq E$.

Definition 2.1.8. Clique

A *clique* in a simple graph is a subgraph such that every two distinct nodes are adjacent.

Definition 2.1.9. Connected Component

A disconnected graph can be regarded as a collection of a number of connected subgraphs known as *components*, or *connected components*. A connected graph has one connected component.

Definition 2.1.10. Community Structure

A network has a community structure if its nodes can be clustered into groups, where

the nodes in each group are more connected with each other (internally) than with other nodes of the network (externally), and each group is called a *community*.

2.2 Spectral Graph Properties

To study the structural properties of graphs, we shall use *spectral graph theory*. We start by defining *eigenvalues* and *eigenvectors* [28]. Let $\Gamma = (V, E)$ be a simple connected graph (in the rest of this thesis, we deal with simple connected graphs only), where $|V| = n$ and $|E| = m$, with the adjacency matrix A. A non-zero vector x is an eigenvector if $Ax = \lambda x$. In this case, λ is an eigenvalue. The eigenvalues and eigenvectors contain important information about the structure of the graph Γ.

If the graph Γ is simple then its adjacency matrix is symmetric, hence its eigenvalues are real. The eigenvalues of A can be ordered as $\lambda_1 \geq \lambda_2 \geq \cdots \geq \lambda_n$ with corresponding eigenvectors $\boldsymbol{\psi}_1, \boldsymbol{\psi}_2, ..., \boldsymbol{\psi}_n$. A can be decomposed into the form $A = S\Lambda S^T$, where Λ is the diagonal matrix of the eigenvalues and $S = [\boldsymbol{\psi}_1, \boldsymbol{\psi}_2, ..., \boldsymbol{\psi}_n]$ is the orthonormal matrix of the corresponding eigenvectors of A. A matrix is orthonormal if $SS^T = S^T S = I_n$, where S^T is the transpose of S. That is, each row is of length 1, and the rows are mutually perpendicular. Similarly, each column is of length 1, and the columns are mutually perpendicular.

The graphs considered in this work are connected, so A is irreducible and from the *Perron-Frobenius Theorem*, the largest eigenvalue λ_1 of A is positive and unique. Thus, the eigenvalues of A can be written in the form $\lambda_1 > \lambda_2 \geq \cdots \geq \lambda_n$. In addition, all entries of the corresponding to λ_1 eigenvector $\boldsymbol{\psi}_1$ can be chosen to be positive.

Another important concept in graph theory is the *Laplacian matrix* L that can be defined by

$$L_{ij} = \begin{cases} -1 & \text{if } (v_i, v_j) \in E, \\ k_i & \text{if } i = j, \\ 0 & \text{otherwise,} \end{cases} \tag{2.2}$$

where k_i is the degree of vertex v_i. The adjacency and Laplacian matrices of a graph are regarded as key tools in the study of complex networks. The Laplacian matrix is

important for studying networks as its spectral properties can be used to investigate many different aspects such as clustering and pattern recognition. The Laplacian matrix can also be represented in terms of the adjacency matrix A of the graph by

$$L = K - A, \tag{2.3}$$

where K is the diagonal matrix of the degrees of the nodes in the graph. The Laplacian matrix is symmetric and positive semidefinite. Thus, the eigenvalues of L can be ordered as $0 = \mu_1 \leq \mu_2 \leq \cdots \leq \mu_n$ with the corresponding eigenvectors $\boldsymbol{\phi}_1, \boldsymbol{\phi}_2, ..., \boldsymbol{\phi}_n$. If the graph is connected then eigenvector $\boldsymbol{\phi}_2$ that corresponds to the second smallest eigenvalue μ_2 is known as the Fiedler vector. The spectral decomposition of the Laplacian matrix is $L = \Psi M \Psi^T$, where M is the diagonal matrix of the eigenvalues, and $\Psi = [\boldsymbol{\phi}_1, \boldsymbol{\phi}_2, ..., \boldsymbol{\phi}_n]$ is the orthogonal matrix of the eigenvectors of L [22, 40]. For simple connected graphs, the spectral decomposition can be more important than the matrix itself in studying graph properties. It can help to understand the effects of a function on the adjacency matrix of a graph.

In this thesis, we investigate the spectra of the Laplacian matrix in order to study the robustness of graphs. The multiplicity of 0 as an eigenvalue in the Laplacian matrix of the graph represents the number of connected components in that graph. In addition, we consider the spectra of the adjacency matrix of the graph. We explore the relationship between the robustness of graphs and the second largest eigenvalue λ_2.

2.3 Matrix Function

There are many ways to define a function of a matrix. In this thesis, we will often consider the following power series, which we apply to an $n \times n$ adjacency matrix A. The power series function for $x \in \mathbb{R}$ can be expressed as [63],

$$f(x) = \sum_{k=0}^{\infty} c_k x^k,$$

where $c_k \in \mathbb{R}$. Then, the power series function for an adjacency matrix A is

$$f(A) = \sum_{k=0}^{\infty} c_k A^k.$$

The power series function of $f(A)$ converges if and only if $\rho(A) < R$, where R is the radius of convergency of the power series, $\rho(A) = \max\{|\lambda_1|, |\lambda_2|, \ldots, |\lambda_n|\}$ and λ_i are the eigenvalues of A [63].

The adjacency matrix to the power of k can be shown to coincide with

$$A^k = S\Lambda^k S^T.$$

Then, the sum of the main diagonal elements of A^k is given by

$$\mathrm{tr}(A^k) = \mathrm{tr}(\Lambda^k), \tag{2.4}$$

and

$$\mathrm{tr}(A^k) = \sum_{i=1}^{n} \lambda_i^k, \tag{2.5}$$

such that for any matrix function, we have

$$\mathrm{tr}\big(f(A)\big) = \sum_{i=1}^{n} f(\lambda_i). \tag{2.6}$$

The matrix exponential can be defined in terms of a series, which always converges

$$e^A = \sum_{k=0}^{\infty} \frac{A^k}{k!},$$

then

$$\mathrm{tr}\big(e^A\big) = \sum_{i=1}^{n} e^{\lambda_i}. \tag{2.7}$$

If the spectral gap $\lambda_1 - \lambda_2$ is large then $\mathrm{tr}(e^A)$ is dominated by the term with the largest eigenvalue λ_1 such that $\mathrm{tr}(e^A) \simeq e^{\lambda_1}$.

A function f is *monotonic increasing*, if for all x and y such that $x \leq y$, we have

$f(x) \leq f(y)$, and if $f(x) < f(y)$ for all $x < y$, then f is *strictly increasing*. Likewise, a function f is *monotonic decreasing*, if for all $x \leq y$, we have $f(x) \geq f(y)$, and if $f(x) > f(y)$ for all $x < y$, then f is *strictly decreasing*. A real-valued function f is *concave* if the line segment between any two points on the graph of the function lies below the graph between the two points.

2.4 Counting Zeros of Dirichlet Polynomials

A function of the form $f(x) = \sum_{j=1}^{n} a_j e^{p_j x}$, $x \in \mathbb{R}$, with a_j, $p_j \in \mathbb{R}$ is called (*generalized*) *Dirichlet polynomial*. In what follows, we always assume that the coefficients in the exponents are ordered: $p_1 > p_2 > \cdots > p_n$. Further, we introduce the partial sums $A_k = a_1 + a_2 + \cdots + a_k$ for $k = 1, 2, \ldots, n$. We denote by $S[(a_j)]$ and $S[(A_j)]$ the number of sign changes in the sequences (a_j) and (A_j), respectively. In other words, the number of terms that have the opposite sign to the previous term (leaving out any zero terms). For example, $(a_j) = (2, -1, 1, -2, 0, -2, 1, 0, -1, 2)$ has six sign changes, hence $S[(a_j)] = 6$. Note that, by [55, Lemma 4.1], $S[(A_j)] \leq S[(a_j)]$. The following result, which is a generalization of Descartes' Rule of Signs and basically goes back to Laguerre, will be used in later chapters of the thesis.

Lemma 2.4.1. ([55, Theorem 4.7]) *Let $f(x) = \sum_{j=1}^{n} a_j e^{p_j x}$ with $p_1 > \cdots > p_n$ and $a_j \in \mathbb{R}$, and let A_j be as above. Then, the number of zeros of f in the interval $(0, \infty)$ is not greater than $S[(A_j)]$.*

If $A_1, \ldots, A_n$ all have the same sign, then $f(x) \neq 0$ for all $x \in (0, \infty)$.

2.5 Some Types of Graphs

In this section, we consider special types of graphs. One can find many more types in [28]. In Figures 2.1–2.3, we present some such types.

2.5.1 Null Graph

A graph $\Gamma = (V, E)$ with n nodes is called the *null graph* N_n if it does not have any edges (E is the empty set).

2.5.2 Path Graph

A *path graph* P_n is a simple connected graph with all vertices having degree 2, except for two vertices that have degree 1. The adjacency matrix of P_n is an $n \times n$ matrix that can be presented in the form

$$A = \begin{pmatrix} 0 & 1 & 0 & \cdots & 0 & 0 \\ 1 & 0 & 1 & \cdots & 0 & 0 \\ 0 & 1 & 0 & \cdots & 0 & 0 \\ 0 & 0 & 1 & \cdots & 0 & 0 \\ \vdots & \vdots & \vdots & \ddots & \vdots & \vdots \\ 0 & 0 & 0 & \cdots & 0 & 1 \\ 0 & 0 & 0 & \cdots & 1 & 0 \end{pmatrix}.$$

2.5.3 Cycle Graph

A *cycle graph* with n nodes, denoted by C_n, is a simple connected regular graph where each of the vertices has degree 2. The adjacency matrix of C_n is an $n \times n$ matrix that can be presented in the form

$$A = \begin{pmatrix} 0 & 1 & 0 & 0 & \cdots & 0 & 1 \\ 1 & 0 & 1 & 0 & \cdots & 0 & 0 \\ 0 & 1 & 0 & 1 & \cdots & 0 & 0 \\ 0 & 0 & 1 & 0 & \cdots & 0 & 0 \\ \vdots & \vdots & \vdots & \vdots & \ddots & \vdots & \vdots \\ 0 & 0 & 0 & 0 & \cdots & 0 & 1 \\ 1 & 0 & 0 & 0 & \cdots & 1 & 0 \end{pmatrix}.$$

The eigenvalues of A are

$$\lambda = 2\cos\left(\frac{2\pi j}{n}\right), \qquad j = 0, 1, \ldots, n-1, \tag{2.8}$$

with eigenvectors

$$\boldsymbol{x} = \frac{1}{\sqrt{n}} \begin{bmatrix} 1 \\ \omega_n^j \\ \omega_n^{2j} \\ \vdots \\ \omega_n^{(n-1)j} \end{bmatrix}, \qquad j = 0, 1, \ldots, n-1, \qquad \text{with} \quad \omega_n = e^{\frac{2\pi i}{n}}.$$

The eigenvalues in (2.8) coincide for j and $n-j$. Hence the distinct eigenvalues are obtained for $j = 0, 1, \ldots, \frac{n}{2}$ when n is even, and for $j = 0, 1, \ldots, \frac{n-1}{2}$ when n is odd.

2.5.4 Tree

A *tree* is a simple connected graph that contains no cycle graphs as subgraphs.

2.5.5 Spanning Tree

A *spanning tree* for a connected graph $\Gamma = (V, E)$ is a subgraph of Γ that is a tree and includes all the nodes of Γ.

2.5.6 Triangle

A *triangle* is a cycle graph of three nodes.

2.5.7 Square Grid Graph (Lattice)

A *square grid graph* $P_n \times P_n$ is the Cartesian product of two path graphs P_n. Its vertices can be labelled by $\{v_1, v_2, ..., v_{n^2}\}$ and its adjacency matrix is an $n^2 \times n^2$ matrix, that

can be defined by

$$A(P_n \times P_n) = \begin{pmatrix} A(P_n) & I_n & O_n & \cdots & O_n & O_n \\ I_n & A(P_n) & I_n & \cdots & O_n & O_n \\ O_n & I_n & A(P_n) & \cdots & O_n & O_n \\ \vdots & \vdots & \vdots & \ddots & \vdots & \vdots \\ O_n & O_n & O_n & \cdots & A(P_n) & I_n \\ O_n & O_n & O_n & \cdots & I_n & A(P_n) \end{pmatrix},$$

where $A(P_n)$ is the adjacency matrix of the path graph P_n, I_n is an $n \times n$ identity matrix with all entries equal to 0 except for the entries in the main diagonal which are all 1, and O_n is an $n \times n$ zero matrix.

2.5.8 Complete Graph

A *complete graph* with η nodes, K_η, is a simple graph with $\eta(\eta-1)/2$ edges. The adjacency matrix $A(K_\eta)$ of K_η is an $\eta \times \eta$ matrix with all entries equal to 1 except for the entries in the main diagonal which are all 0. That is, $A(K_\eta) = \mathbf{1}_\eta \mathbf{1}_\eta^T - I$, where $\mathbf{1}_\eta$ is the column vector of all 1s of size η and I is the $\eta \times \eta$ identity matrix.

Lemma 2.5.1. *The spectrum of the adjacency matrix A of the complete graph $A(K_\eta)$ with η nodes consists of*

1. *the largest eigenvalue $\lambda_1 = \eta - 1$ with the corresponding eigenvector*

$$\boldsymbol{y}_1 = \frac{1}{\sqrt{\eta}} \mathbf{1}_\eta.$$

2. *the eigenvalue $\lambda = -1$ with multiplicity $\eta - 1$ and the corresponding eigenvectors*

$$\boldsymbol{y}_h = \left[y_1^{(h)}, y_2^{(h)}, \ldots, y_\eta^{(h)} \right]^T,$$

where $h = \{2, \ldots, \eta\}$, $y_i^{(h)} \in \mathbb{R}$, $h = 2, \ldots, \eta$ and $\boldsymbol{y}_h \neq \boldsymbol{y}_\eta$.

2.5.9 Core-satellite Graph

Let $c \geq 1$, $s \geq 1$ and $\eta \geq 2$. The core-satellite graph $\Theta(c, s, \eta)$ is the graph consisting of η copies of K_s (the satellites) meeting in a common clique K_c (the core). So that every vertex in K_c is connected to every vertex in each copy of K_s; see Figure 2.3 for an example.

2.5.10 Windmill Graph

A windmill graph $W(\eta, s) := \Theta(1, \eta, s)$ is a simple graph consisting of s copies of the complete graph K_η with every node being connected to a common one, see Figure 2.3 for an example. The adjacency matrix of $W(\eta, s)$ is an $n \times n$ matrix, where $n = s\eta + 1$ and has the form

$$A = \begin{pmatrix} 0 & \mathbf{1}_\eta^T & \mathbf{1}_\eta^T & \cdots & \mathbf{1}_\eta^T \\ \mathbf{1}_\eta & A(K_\eta) & O_\eta & \cdots & O_\eta \\ \mathbf{1}_\eta & O_\eta & A(K_\eta) & \vdots & O_\eta \\ \vdots & \vdots & \vdots & \ddots & \vdots \\ \mathbf{1}_\eta & O_\eta & O_\eta & \cdots & A(K_\eta) \end{pmatrix}, \tag{2.9}$$

where $A(K_\eta) = \mathbf{1}_\eta \mathbf{1}_\eta^T - I$ is the adjacency matrix of K_η, $\mathbf{1}_\eta$ is a column vector of all 1s of length η and O_η is an $\eta \times \eta$ zero matrix. The adjacency matrix A in (2.9) induces a labelling of the nodes in $W(\eta, s)$ which we will assume throughout this work; in particular, node 1 will be the node of largest degree. By specializing a result from [30, 31] about the spectrum of $\Theta(c, s, \eta)$ to the case of $W(\eta, s)$, we obtain the following lemma.

Lemma 2.5.2. ([31], Theorem 8) *The spectrum of the adjacency matrix A of a windmill graph $W(\eta, s)$ with $n = s\eta + 1$ nodes consists of*

1. *the eigenvalue $\lambda = -1$ with multiplicity $s(\eta - 1)$;*
2. *the eigenvalue $\lambda = \eta - 1$ with multiplicity $s - 1$;*
3. *the largest and smallest eigenvalues, λ_1 and λ_n, given by the roots of the quadratic*

equation

$$\lambda^2 - \lambda(\eta - 1) - s\eta = 0, \tag{2.10}$$

i.e.,

$$\lambda_1 = \frac{\eta - 1}{2} + \sqrt{\left(\frac{\eta - 1}{2}\right)^2 + s\eta}, \tag{2.11}$$

and

$$\lambda_n = \frac{\eta - 1}{2} - \sqrt{\left(\frac{\eta - 1}{2}\right)^2 + s\eta}. \tag{2.12}$$

Remark 2.5.3. *The fact that* λ_1 *and* λ_n *satisfy the quadratic equation* (2.10) *implies that* $\lambda_1 + \lambda_n = \eta - 1$ *and* $\lambda_1\lambda_n = -s\eta$.

Structure of the Eigenvectors

In [30, 31], the authors also describe the structure of the eigenvectors associated with the eigenvalues considered in Lemma 2.5.2. We need to refine their results; in particular, we derive orthonormality conditions for the eigenvectors described in [30, 31]. Throughout this work, the eigenvectors are partitioned according to the partition of A in (2.9).

I. It is easy to verify from (2.13) and the eigenvalue equation $A\boldsymbol{x}_k = \lambda\boldsymbol{x}_k$ that the $s-1$ eigenvectors corresponding to the eigenvalue $\lambda = \eta - 1$ are

$$\boldsymbol{x}_k = \begin{bmatrix} 0 \\ \alpha_1^{(k)}\mathbf{1}_\eta \\ \vdots \\ \alpha_s^{(k)}\mathbf{1}_\eta \end{bmatrix} \quad \text{for } k = 2, 3, \ldots, s, \tag{2.13}$$

where $[\alpha_1^{(k)}, \ldots, \alpha_s^{(k)}]^T$ are linearly independent vectors satisfying $\sum_{h=1}^{s} \alpha_h^{(k)} = 0$. By requiring these eigenvectors to be normalized in the 2-norm, we also get that the coefficients must satisfy

$$\sum_{h=1}^{s} \left(\alpha_h^{(k)}\right)^2 = \frac{1}{\eta}.$$

II. The $s(\eta - 1)$ eigenvectors $\boldsymbol{x}_k$, $k = s+1, \ldots, n-1$, corresponding to the eigenvalue

$\lambda = -1$ can be written in the form

$$\boldsymbol{x}_k = \begin{bmatrix} 0 \\ \mathbf{0}_\eta \\ \vdots \\ \mathbf{0}_\eta \\ \boldsymbol{y}_h \\ \mathbf{0}_\eta \\ \vdots \\ \mathbf{0}_\eta \end{bmatrix}, \qquad \begin{aligned} &k = s + (l-1)(\eta - 1) + h, \\ &h = 1, \dots, \eta - 1, \\ &\boldsymbol{y}_h \text{ in the } l^{\text{th}} \text{ block, } l = 1, \dots, s, \end{aligned} \tag{2.14}$$

where $\boldsymbol{y}_1, \dots, \boldsymbol{y}_{\eta-1}$ builds an orthonormal system of eigenvectors of $A(K_\eta)$ corresponding to the eigenvalue -1.

III. Finally, the eigenvectors that correspond to the eigenvalues λ_1 in (2.11) and λ_n in (2.12) can be written in the form

$$\boldsymbol{x}_1 = \begin{bmatrix} z_1 \\ z_2 \mathbf{1}_{s\eta} \end{bmatrix} \tag{2.15}$$

and

$$\boldsymbol{x}_n = \begin{bmatrix} z_3 \\ z_4 \mathbf{1}_{s\eta} \end{bmatrix} \tag{2.16}$$

respectively, where $z_1, z_2, z_3, z_4 \in \mathbb{R}$ are not all zeros.

In the next lemma, we find the explicit value of the coefficients appearing above in order for $\boldsymbol{x}_1$ and $\boldsymbol{x}_n$ to be normalized in the 2-norm.

Lemma 2.5.4. *The normalized eigenvectors corresponding to the largest and smallest eigenvalues λ_1 and λ_n for windmill graphs $W(\eta, s)$ are*

$$\boldsymbol{x}_1 = \frac{1}{\sqrt{\lambda_n^2 + s\eta}} \begin{bmatrix} -\lambda_n \\ \mathbf{1}_{s\eta} \end{bmatrix} \tag{2.17}$$

and

$$\boldsymbol{x}_n = \frac{1}{\sqrt{\lambda_1^2 + s\eta}} \begin{bmatrix} -\lambda_1 \\ \mathbf{1}_{s\eta} \end{bmatrix}. \tag{2.18}$$

Proof. To find the entries of the normalized eigenvector corresponding to λ_1 we consider the associated eigenvalue problem:

$$A \begin{bmatrix} z_1 \\ z_2 \mathbf{1}_{s\eta} \end{bmatrix} = \begin{bmatrix} s\eta z_2 \\ z_1 + (\eta - 1) z_2 \mathbf{1}_{s\eta} \end{bmatrix} = \lambda_1 \begin{bmatrix} z_1 \\ z_2 \mathbf{1}_{s\eta} \end{bmatrix}$$

which yields

$$\begin{cases} z_1 + (\eta - 1) z_2 = \lambda_1 z_2 \\ s\eta z_2 = \lambda_1 z_1 \end{cases} \qquad \Rightarrow \quad z_1 = -\lambda_n z_2$$

where we have used the expression for $\boldsymbol{x}_1$ described in (2.15) and Remark 2.5.3. By imposing normalization of the eigenvector in the 2-norm, we get:

$$z_1^2 + s\eta z_2^2 = 1$$

which, together with the fact that $z_1 = -\lambda_n z_2$, yields $z_2 = \left(\sqrt{s\eta + \lambda_n^2}\right)^{-1}$, and hence the desired expression (2.17). The same argument yields the expression for $\boldsymbol{x}_n$ in (2.18). □

2.5.11 Complete Multipartite Graphs

Let $1 \leq \eta_1 \leq \eta_2 \leq \cdots \leq \eta_k$ with $k \geq 2$. A *complete multipartite graph* $K_{\eta_1, \eta_2, \ldots, \eta_k}$ with $n = \sum_{i=1}^{k} \eta_i$ vertices is a graph that consists of k pairwise disjoint sets $V_1, V_2, \ldots, V_k$ of nodes where each set V_i has η_i nodes ($i \in \{1, 2, \ldots, k\}$), there is no edge between nodes in the same set and there is an edge between any two nodes in distinct subsets, i.e. if $v \in V_i$ and $w \in V_j$, then there is an edge between v and w if and only if $i \neq j$; see Figure 2.3 for an example. The adjacency matrix A of $K_{\eta_1, \eta_2, \ldots, \eta_k}$ is an $n \times n$ matrix

of the form

$$A = \begin{pmatrix} O_{\eta_1\times\eta_1} & 1_{\eta_1\times\eta_2} & 1_{\eta_1\times\eta_3} & \dots & 1_{\eta_1\times\eta_k} \\ 1_{\eta_2\times\eta_1} & O_{\eta_2\times\eta_2} & 1_{\eta_2\times\eta_3} & \dots & 1_{\eta_2\times\eta_k} \\ 1_{\eta_3\times\eta_1} & 1_{\eta_3\times\eta_2} & O_{\eta_3\times\eta_3} & \dots & 1_{\eta_3\times\eta_k} \\ \vdots & \vdots & \vdots & \ddots & \vdots \\ 1_{\eta_k\times\eta_1} & 1_{\eta_k\times\eta_2} & 1_{\eta_k\times\eta_3} & \dots & O_{\eta_k\times\eta_k} \end{pmatrix}, \tag{2.19}$$

where $O_{\eta_i\times\eta_j}$ is the $\eta_i \times \eta_j$ zero matrix and $1_{\eta_i\times\eta_j}$ is the $\eta_i \times \eta_j$ matrix with all entries equal 1.

Spectrum of $K_{\eta_1,\eta_2,\dots,\eta_k}$

We start our considerations about the spectrum of the adjacency matrix for a complete multipartite graph with two lemmas from the literature.

Lemma 2.5.5 ([101])**.** *A graph has exactly one positive eigenvalue if and only if the non-isolated points form a complete multipartite graph.*

The following lemma is Lemma 1 and Theorem 1 in [23].

Lemma 2.5.6 ([23])**.** *For an eigenvalue λ of the adjacency matrix of a complete multipartite graph $K_{\eta_1,\eta_2,\dots,\eta_k}$ with $n = \sum_{i=1}^{k} \eta_i$ vertices and k disjoint sets $V_1, V_2, \dots V_k$ of nodes, where set V_i has η_i nodes, $i \in \{1, 2, \dots, k\}$, and $\eta_1 \leq \eta_2 \leq \dots \leq \eta_k$, the following statements hold.*

1. *If $\eta_k > 1$, then $\lambda = 0$ is an eigenvalue of multiplicity $n - k$; the corresponding eigenvectors are of the form*

$$\boldsymbol{x} = \begin{bmatrix} \boldsymbol{y}_1 \\ \boldsymbol{y}_2 \\ \vdots \\ \boldsymbol{y}_k \end{bmatrix}$$

   where $\boldsymbol{y}_i = \left[y_1^{(i)}, y_2^{(i)}, \dots, y_{\eta_i}^{(i)}\right]^T$ with $\sum_{j=1}^{\eta_i} y_j^{(i)} = 0$, $i \in \{1, 2, \dots, k\}$.

2. *There is exactly one positive eigenvalue, λ_1, and $k - 1$ negative eigenvalues; the*

latter satisfy

$$-\eta_k \leq \lambda_n \leq -\eta_{k-1} \leq \lambda_{n-1} \leq -\eta_{k-2} \leq \cdots \leq -\eta_2 \leq \lambda_{n-k+2} \leq -\eta_1, \tag{2.20}$$

i.e. $-\eta_{j-n+k} \leq \lambda_j \leq -\eta_{j-n+k-1}$, $j \in \{n-k+2, \ldots, n\}$. *If* $-\eta_{j-n+k} < -\eta_{j-n+k-1}$, *then* $-\eta_{j-n+k} < \lambda_j < -\eta_{j-n+k-1}$. *The eigenvalue* λ_1 *and those negative eigenvalues that are not in* $\{-\eta_1, \ldots, -\eta_k\}$ *satisfy the equation*

$$\sum_{i=1}^{k} \frac{\eta_i}{\lambda + \eta_i} = 1. \tag{2.21}$$

3. *If* $\lambda \neq 0$, *then the eigenvectors corresponding to non-zero eigenvalues* λ *can be written in the form*

$$\boldsymbol{x} = \begin{bmatrix} x_1 \mathbf{1}_{\eta_1} \\ x_2 \mathbf{1}_{\eta_2} \\ \vdots \\ x_k \mathbf{1}_{\eta_k} \end{bmatrix}, \tag{2.22}$$

where $x_i \in \mathbb{R}$, $i \in \{1, 2, \ldots, k\}$ *and they satisfy*

$$\lambda (x_i - x_j) = \eta_j x_j - \eta_i x_i, \tag{2.23}$$

for all $i, j \in \{1, 2, \ldots, k\}$.

Throughout this work, the eigenvectors will be partitioned according to the partition of A in (2.19). We need to refine the results about the eigenvectors and find the exact entries of these. Let us first consider an eigenvalue $\lambda \notin \{0, -\eta_1, \ldots, -\eta_k\}$.

Lemma 2.5.7. *Let* $K_{\eta_1, \eta_2, \ldots, \eta_k}$ *be the complete multipartite graph with* $n = \sum_{i=1}^{k} \eta_i$ *nodes and* $\eta_1 \leq \eta_2 \leq \cdots \leq \eta_k$ *with adjacency matrix* A *defined in* (2.19). *Every eigenvalue* $\lambda \notin \{0, -\eta_1, -\eta_2, \ldots, -\eta_k\}$ *is simple. The corresponding normalized eigenvector is given by* (2.22) *with*

$$x_i = \frac{\alpha}{\lambda + \eta_i}, \qquad i \in \{1, \ldots, k\} \tag{2.24}$$

and

$$\alpha = \left(\sum_{i=1}^{k} \frac{\eta_i}{(\lambda + \eta_i)^2} \right)^{-\frac{1}{2}}. \tag{2.25}$$

Proof. That λ is a simple eigenvalue follows from the inequalities (2.20). Since $\lambda \neq 0$, we obtain from Lemma 2.5.6 that an eigenvector $\boldsymbol{x}$ must be of the form (2.22) where the coefficients x_i satisfy (2.23). The latter relation implies

$$(\lambda + \eta_i)x_i = (\lambda + \eta_j)x_j \tag{2.26}$$

for all $i, j \in \{1, \ldots, k\}$. The expression in (2.26) is independent of i and j, and therefore must be equal to some constant α. We choose α such that the eigenvector is normalized. From the normalization condition $\sum_{i=1}^{k} \eta_k x_i^2 = 1$ we can easily derive (2.25). □

In the next lemma we consider the situation when some of the η_i coincide.

Lemma 2.5.8. *Let $K_{\eta_1,\eta_2,\ldots,\eta_k}$ be the complete multipartite graph with $n = \sum_{i=1}^{k} \eta_i$ nodes and $\eta_1 \leq \eta_2 \leq \cdots \leq \eta_k$ with adjacency matrix A defined in (2.19). If $\eta_i = \eta_{i+1} = \cdots = \eta_{i+r-1}$ for some $i \in \{1, 2, \ldots, k\}$ and $r \geq 2$ such that $i + r - 1 \leq k$, then $\lambda = -\eta_i$ is an eigenvalue of A with multiplicity $r - 1$. The corresponding complete set of orthonormal eigenvectors is given by*

$$\boldsymbol{x}_h = \begin{bmatrix} \mathbf{0}_{\eta_1} \\ \vdots \\ \mathbf{0}_{\eta_{i-1}} \\ y_1^{(h)} \mathbf{1}_{\eta_i} \\ \vdots \\ y_r^{(h)} \mathbf{1}_{\eta_i} \\ \mathbf{0}_{\eta_{i+r}} \\ \vdots \\ \mathbf{0}_{\eta_k} \end{bmatrix}, \qquad h = 1, 2, \ldots, r-1, \tag{2.27}$$

where $\left[y_1^{(h)}, \ldots, y_r^{(h)}\right]^T$, $h = 1, 2, \ldots, r-1$, *are orthogonal vectors satisfying*

$$\sum_{j=1}^{r} y_j^{(h)} = 0, \qquad \sum_{j=1}^{r} \left(y_j^{(h)}\right)^2 = \frac{1}{\eta_i}, \qquad h = 1, 2, \ldots, r-1. \tag{2.28}$$

Proof. It follows from (2.20) that $-\eta_i$ is an eigenvalue with multiplicity at least $r-1$. Further, Lemma 2.5.6 implies that a corresponding eigenvector $\boldsymbol{x}$ must be of the form (2.22) where the coefficients x_i satisfy (2.23). For $j \notin \{i, i+1, \ldots, i+r-1\}$ we obtain from (2.23) that $-\eta_i(x_i - x_j) = \eta_j x_j - \eta_i x_i$, which implies $x_j = 0$ since $\eta_j \neq \eta_i$. Hence the eigenvector $\boldsymbol{x}$ has the form

$$\boldsymbol{x} = \begin{bmatrix} \mathbf{0}_{\eta_1} \\ \vdots \\ \mathbf{0}_{\eta_{i-1}} \\ y_1 \mathbf{1}_{\eta_i} \\ \vdots \\ y_r \mathbf{1}_{\eta_i} \\ \mathbf{0}_{\eta_{i+r}} \\ \vdots \\ \mathbf{0}_{\eta_k} \end{bmatrix}.$$

If we plug this vector into the eigenvalue equation $A\boldsymbol{x} = -\eta_i \boldsymbol{x}$, we obtain, for the components in the jth block ($j \in \{i, i+1, \ldots, i+r\}$),

$$\sum_{\substack{s=1 \\ s \neq j}}^{r} \eta_s y_s = -\eta_j y_j,$$

which yields $\sum_{s=1}^{r} y_s = 0$. There are $r-1$ linearly independent vectors satisfying this constraint, which shows that the multiplicity of the eigenvalue is $r-1$. The normalization of the eigenvectors yields the second condition in (2.28). □

In the next lemma, we find the eigenvectors that correspond to the eigenvalue $\lambda = 0$ of A for $K_{\eta_1, \eta_2, \ldots, \eta_k}$ when $\eta_1 \leq \eta_2 \leq \cdots \leq \eta_k$.

Lemma 2.5.9. *Let* $K_{\eta_1, \eta_2, \ldots, \eta_k}$ *be the complete multipartite graph with* $n = \sum_{i=1}^{k} \eta_i$

nodes and $\eta_1 \leq \eta_2 \leq \cdots \leq \eta_k$ *with adjacency matrix* A *defined in* (2.19)*. Then, a complete orthonormal set of* $n-k$ *eigenvectors corresponding to the eigenvalue* $\lambda = 0$ *is given by*

$$\boldsymbol{x}_h = \begin{bmatrix} \mathbf{0}_{\eta_1} \\ \vdots \\ \mathbf{0}_{\eta_{i-1}} \\ \boldsymbol{y}_{i,j} \\ \mathbf{0}_{\eta_{i+1}} \\ \vdots \\ \mathbf{0}_{\eta_k} \end{bmatrix}, \qquad \begin{aligned} &h = 1 + \textstyle\sum_{s=1}^{i-1}(\eta_s - 1) + j, \\ &i = 1, \ldots, k, \\ &j = 1, \ldots, \eta_i - 1, \end{aligned} \tag{2.29}$$

where, for each $i \in \{1, \ldots, k\}$*, the vectors* $\boldsymbol{y}_{i,1}, \ldots, \boldsymbol{y}_{i,\eta_i - 1}$ *form an orthonormal system such that* $\mathbf{1}_{\eta_i}^T \boldsymbol{y}_{i,j} = 0$*,* $j = 1, \ldots, \eta_i - 1$*, i.e. if* $\boldsymbol{y}_{i,j} = \left[y_1^{(i,j)}, \ldots, y_{\eta_i}^{(i,j)}\right]^T$*, then* $\sum_{s=1}^{\eta_i} y_s^{(i,j)} = 0$*.*

Proof. The vectors in (2.29) are eigenvectors corresponding to the eigenvalue 0 according to Lemma 2.5.6; they are orthonormal and span a space of dimension $\sum_{i=1}^{k}(\eta_i - 1) = n - k$, which is the multiplicity of the eigenvalue 0 by Lemma 2.5.6. Hence we have found a complete orthonormal set of eigenvectors. □

Spectrum of a Complete k-partite Graph with equal-sized Parts

Let us consider the case of a multipartite graph $K_{\eta_1,\eta_2,\ldots,\eta_k}$ where $\eta_1 = \eta_2 = \cdots = \eta_k = \eta$, i.e. all subgroups V_i are of equal size. (Note that, for $\eta = 1$, we obtain the complete graph K_k.) In the next lemma, we describe the spectrum of such a multipartite graph $K_{\eta,\eta,\ldots,\eta}$.

Lemma 2.5.10. *The spectrum of the adjacency matrix* A *of the complete* k*-partite graph* $K_{\eta,\eta,\ldots,\eta}$ *with* $n = k\eta$ *nodes consists of the following eigenvalues:*

1. *the largest eigenvalue* $\lambda_1 = \eta(k-1)$*, which is simple, with corresponding normalized eigenvector*

$$\boldsymbol{x}_1 = \frac{1}{\sqrt{n}} \mathbf{1}_n; \tag{2.30}$$

2. the smallest eigenvalue $\lambda_{n-k+2} = \cdots = \lambda_n = -\eta$ *with multiplicity* $k-1$ *and corresponding orthonormal eigenvectors*

$$\boldsymbol{x}_h = \begin{bmatrix} x_1^{(h)}\mathbf{1}_\eta \\ x_2^{(h)}\mathbf{1}_\eta \\ \vdots \\ x_k^{(h)}\mathbf{1}_\eta \end{bmatrix}, \qquad h = n-k+2, \dots, n, \tag{2.31}$$

where $\left[x_1^{(h)}, \dots, x_k^{(h)}\right]^T$, $h = n-k+2, \dots, n$, *are orthogonal vectors satisfying*

$$\sum_{j=1}^{k} x_j^{(h)} = 0, \qquad \sum_{j=1}^{k} \left(x_j^{(h)}\right)^2 = \frac{1}{\eta}, \qquad h = n-k+2, \dots, n;$$

3. the eigenvalue $\lambda_2 = \cdots = \lambda_{n-k+1} = 0$ *with multiplicity* $k(\eta-1)$ *and corresponding orthonormal eigenvectors*

$$\boldsymbol{x}_h = \begin{bmatrix} \mathbf{0}_\eta \\ \vdots \\ \mathbf{0}_\eta \\ \boldsymbol{y}_j \\ \mathbf{0}_\eta \\ \vdots \\ \mathbf{0}_\eta \end{bmatrix}, \qquad \begin{aligned} &h = (i-1)(\eta-1) + j + 1, \\ &i = 1, \dots, k; \;\; j = 1, \dots, \eta-1, \end{aligned} \tag{2.32}$$

where the vector in (2.32) *has a non-zero entry in the* i^{th} *block and where the vectors* $\boldsymbol{y}_1, \dots, \boldsymbol{y}_{\eta-1}$ *form an orthonormal system such that, with* $\boldsymbol{y}_j = \left[y_1^{(j)}, \dots, y_\eta^{(j)}\right]^T$, *one has* $\sum_{s=1}^{\eta} y_s^{(j)} = 0$.

Proof.

1. The eigenvalue λ_1 satisfies equation (2.21), which is

$$\frac{k\eta}{\lambda_1 + \eta} = 1,$$

and hence $\lambda_1 = (k-1)\eta$. The corresponding eigenvector must be of the form (2.22) where the coefficients x_i satisfy (2.23), which in our case is $\lambda_1(x_i - x_j) = \eta(x_j - x_i)$. This implies that $x_i = x_j$ for all $i, j \in \{1, \ldots, k\}$. A normalized eigenvector is therefore given by (2.30).

2. The statement follows directly from Lemma 2.5.8.

3. The assertion is a direct consequence of Lemma 2.5.9 with $\eta_1 = \cdots = \eta_k$. The enumeration of the eigenvectors can be easily checked.

□

Spectrum of Certain Complete 3-partite Graphs

In this subsection, and in particular, in the next lemma we consider complete 3-partite graphs where $\eta_1 = \eta_2 = \eta < \eta_3 = l$.

Lemma 2.5.11. *Let $l > \eta > 0$. The spectrum of the adjacency matrix A of $K_{\eta,\eta,l}$ consists of*

1. *the largest and smallest eigenvalues given by the roots of the quadratic equation $\lambda^2 - \eta\lambda - 2\eta l = 0$, i.e.,*

$$\lambda_1 = \frac{\eta + \sqrt{\eta^2 + 8\eta l}}{2}, \tag{2.33}$$

$$\lambda_n = \frac{\eta - \sqrt{\eta^2 + 8\eta l}}{2}, \tag{2.34}$$

and their corresponding eigenvectors given by

$$\boldsymbol{x}_h = \begin{bmatrix} x_h \mathbf{1}_{2\eta} \\ y_h \mathbf{1}_l \end{bmatrix}, \tag{2.35}$$

where $x_h = \left(2\eta + l\left(\frac{2\eta}{\lambda_h}\right)^2\right)^{-\frac{1}{2}}$, $y_h = \frac{2\eta}{\lambda_h} x_h$ and $h \in \{1, n\}$;

2. the eigenvalue $\lambda = 0$ with multiplicity $n-3$ with the corresponding eigenvectors

$$\boldsymbol{x}_{1+i} = \begin{bmatrix} \boldsymbol{y}_i \\ \mathbf{0}_\eta \\ \mathbf{0}_l \end{bmatrix}, \qquad \boldsymbol{x}_{\eta+i} = \begin{bmatrix} \mathbf{0}_\eta \\ \boldsymbol{y}_i \\ \mathbf{0}_l \end{bmatrix}, \qquad i = 1, 2, \ldots, \eta - 1,$$

and

$$\boldsymbol{x}_{2\eta-1+i} = \begin{bmatrix} \mathbf{0}_\eta \\ \mathbf{0}_\eta \\ \boldsymbol{z}_j \end{bmatrix}, \qquad j = 1, 2, \ldots, l - 1,$$

where $\boldsymbol{y}_i = \left[y_1^{(i)}, \ldots, y_\eta^{(i)}\right]^T$, $i = 1, \ldots, \eta - 1$, and $\boldsymbol{z}_j = \left[z_1^{(j)}, \ldots, z_l^{(j)}\right]^T$, $j = 1, \ldots, l-1$, are orthonormal systems such that $\sum_{s=1}^{\eta} y_s^{(i)} = 0$ for $i = 1, \ldots, \eta - 1$, and $\sum_{s=1}^{l} z_s^{(j)} = 0$ for $j = 1, \ldots, l - 1$;

3. the simple eigenvalue $\lambda = -\eta$ with the corresponding eigenvector

$$\boldsymbol{x}_{n-1} = \frac{1}{\sqrt{2\eta}} \begin{bmatrix} x\mathbf{1}_\eta \\ -x\mathbf{1}_\eta \\ \mathbf{0}_l \end{bmatrix}. \tag{2.36}$$

Proof. It follows from Lemma 2.5.6 (see, in particular, (2.20)) that the non-zero eigenvalues satisfy

$$-l < \lambda_n < -\eta = \lambda_{n-1} < 0 < \lambda_1.$$

Now let us consider the eigenvalues and the corresponding eigenvectors separately.

1. The eigenvalues λ_1 and λ_n satisfy (2.21), i.e.,

$$\frac{2\eta}{\lambda + \eta} + \frac{l}{\lambda + l} = 1,$$

which is equivalent to the quadratic equation $\lambda^2 - \eta\lambda - 2\eta l = 0$. The solutions of the latter equation are given by (2.33) and (2.34). The corresponding eigenvectors

must be of the form (2.22), i.e.,

$$\boldsymbol{x} = \begin{bmatrix} x_1\mathbf{1}_\eta \\ x_2\mathbf{1}_\eta \\ x_3\mathbf{1}_l \end{bmatrix},$$

where x_1, x_2, x_3 satisfy (2.23). For $i = 1$, $j = 2$ we obtain $\lambda(x_1 - x_2) = \eta(x_2 - x_1)$, which implies that $x_1 = x_2$. Hence, we can write $\boldsymbol{x} = \begin{bmatrix} x\mathbf{1}_{2\eta} \\ y\mathbf{1}_l \end{bmatrix}$. Substituting $\boldsymbol{x}$ into the eigenvalue equation we obtain

$$\eta x + ly = \lambda x, \tag{2.37}$$

$$2\eta x = \lambda y. \tag{2.38}$$

The second equation yields $y = \frac{2\eta}{\lambda}x$. The normalization condition is $2\eta x^2 + ly^2 = 1$, which then leads to $x = \left(2\eta + l\left(\frac{2\eta}{\lambda}\right)^2\right)^{-\frac{1}{2}}$.

2. The form of the eigenvectors follows directly from Lemma 2.5.9.

3. We can apply Lemma 2.5.8 with $r = 2$, which yields that $-\eta$ is a simple eigenvalue. The form of the eigenvector also follows from that lemma.

□

2.5.12 Star Graphs

A star graph S_η is a complete bipartite graph with $\eta_1 = 1$ and $\eta_2 = \eta - 1$ (i.e. $S_\eta = S_{1,\eta-1}$). The adjacency matrix of S_η is an $\eta \times \eta$ matrix that can be expressed by

$$A(S_\eta) = \begin{pmatrix} 0 & \mathbf{1}_{\eta-1}^T \\ \mathbf{1}_{\eta-1} & O_{\eta-1} \end{pmatrix}, \tag{2.39}$$

where $\mathbf{1}_{\eta-1}$ is the vector of all 1s size $\eta - 1$ and $O_{\eta-1}$ is an $(\eta-1)\times(\eta-1)$ zero matrix.

Lemma 2.5.12 ([51])**.** *The spectrum of the adjacency matrix $A(S_\eta)$ of the star graph with η nodes consists of*

1. the largest eigenvalue is $\lambda_1 = \sqrt{\eta - 1}$ *with the corresponding eigenvector*

$$\boldsymbol{x}_1 = \frac{1}{\sqrt{2}} \begin{bmatrix} 1 \\ \frac{1}{\sqrt{\eta-1}} \mathbf{1}_{\eta-1} \end{bmatrix};$$

2. the smallest eigenvalue is $\lambda_\eta = -\sqrt{\eta - 1}$ *with the corresponding eigenvector*

$$\boldsymbol{x}_\eta = \frac{1}{\sqrt{2}} \begin{bmatrix} -1 \\ \frac{1}{\sqrt{\eta-1}} \mathbf{1}_{\eta-1} \end{bmatrix};$$

3. the eigenvalue $\lambda_h = 0$, $2 \leq h \leq \eta - 1$ *with corresponding eigenvectors*

$$\boldsymbol{x}_h = \begin{bmatrix} 0, x_1^{(h)}, x_2^{(h)}, \cdots, x_{\eta-1}^{(h)} \end{bmatrix}^T,$$

$x_i^{(h)} \in \mathbb{R}$, $i = \{1, \ldots, \eta - 1\}$ *and* $\boldsymbol{x}_h \neq \mathbf{0}_\eta$.

2.5.13 Dumbbell Graphs

A dumbbell graph K_η–K_η, where $\eta \geq 2$, is a simple graph consisting of two copies of the complete graph K_η with a single edge connecting these two copies. The adjacency matrix of K_η–K_η is an $n \times n$ matrix where $n = 2\eta$, $\eta \geq 2$, and has the form

$$A = \left(\begin{array}{cccc|cccc} & & & & 0 & 0 & \cdots & 0 \\ & A(K_\eta) & & & \vdots & \vdots & & \vdots \\ & & & & 0 & 0 & \cdots & 0 \\ & & & & 1 & 0 & \cdots & 0 \\ \hline 0 & \cdots & 0 & 1 & & & & \\ 0 & \cdots & 0 & 0 & & & & \\ \vdots & & \vdots & \vdots & & A(K_\eta) & & \\ 0 & \cdots & 0 & 0 & & & & \end{array}\right). \tag{2.40}$$

where the adjacency matrix A in (2.40) induces a labelling of the nodes in K_η–K_η, which we will assume throughout this work; in particular, we partitioned the set of

nodes V into subsets $V_1 = \{1, 2, \ldots, \eta - 1\}$ and $V_2 = \{\eta + 2, \eta + 3, \ldots, 2\eta\}$ and two single nodes η and $\eta + 1$ (i.e $V = V_1 \cup \{\eta\} \cup \{\eta + 1\} \cup V_2$). In other words, the two cliques of a dumbbell graph are connected via the nodes η and $\eta + 1$.

In the next theorem we find the spectrum of dumbbell graphs.

Theorem 2.5.13. *The spectrum of the adjacency matrix A of the dumbbell graph K_η–K_η with $\eta \geq 2$ and $n = 2\eta$ nodes consists of:*

1. *the eigenvalues given by the roots of the quadratic equation $\lambda^2 - (\eta - 1)\lambda - 1 = 0$,*

$$\lambda_\pm = \frac{\eta - 1}{2} \pm \frac{\sqrt{(\eta - 1)^2 + 4}}{2}, \tag{2.41}$$

with corresponding eigenvectors given by

$$\boldsymbol{x}_\pm = \alpha_\pm \begin{bmatrix} \mathbf{1}_{\eta-1} \\ \lambda_\pm - \eta + 2 \\ \lambda_\pm - \eta + 2 \\ \mathbf{1}_{\eta-1} \end{bmatrix}, \tag{2.42}$$

where

$$\alpha_\pm = \left[2(\lambda_\pm - \eta + 2)^2 + 2(\eta - 1)\right]^{-\frac{1}{2}}; \tag{2.43}$$

2. *the eigenvalues given by the roots of the quadratic equation $\lambda^2 - (\eta - 3)\lambda - (2\eta - 3) = 0$,*

$$\lambda_\pm = \frac{\eta - 3}{2} \pm \frac{\sqrt{(\eta + 1)^2 - 4}}{2}, \tag{2.44}$$

with corresponding eigenvectors given by

$$\boldsymbol{x}_\pm = \alpha_\pm \begin{bmatrix} -\mathbf{1}_{\eta-1} \\ -(\lambda_\pm - \eta + 2) \\ \lambda_\pm - \eta + 2 \\ \mathbf{1}_{\eta-1} \end{bmatrix}, \tag{2.45}$$

where

$$\alpha_\pm = \left[2(\lambda_\pm - \eta + 2)^2 + 2(\eta - 1)\right]^{-\frac{1}{2}}; \tag{2.46}$$

3. the eigenvalue $\lambda = -1$ with the multiplicity $2\eta - 4$ and with the corresponding eigenvectors given by

$$\boldsymbol{x}_k = \begin{bmatrix} \boldsymbol{y}_k \\ 0 \\ 0 \\ \mathbf{0}_{\eta-1} \end{bmatrix}, \quad \boldsymbol{x}'_k = \begin{bmatrix} \mathbf{0}_{\eta-1} \\ 0 \\ 0 \\ \boldsymbol{y}_k \end{bmatrix}, \quad k = 1, \ldots, \eta - 2, \tag{2.47}$$

where the vectors $\boldsymbol{y}_1, \ldots \boldsymbol{y}_{\eta-2}$ (of size $\eta-1$) are an orthonormal set of eigenvectors of the complete graph $K_{\eta-1}$ corresponding to the eigenvalue $\lambda = -1$.

Proof. Let us consider the following vectors, $\boldsymbol{x}_1$, $\boldsymbol{x}_2$, $\boldsymbol{x}_3$ and $\boldsymbol{x}_4$, which are partitioned according to the partition of A in (2.40).

$$\boldsymbol{x}_1 = \begin{bmatrix} z_1\mathbf{1}_{\eta-1} \\ z_2 \\ z_2 \\ z_1\mathbf{1}_{\eta-1} \end{bmatrix},$$

where $z_1, z_2 \neq 0$,

$$\boldsymbol{x}_2 = \begin{bmatrix} -z_3\mathbf{1}_{\eta-1} \\ -z_4 \\ z_4 \\ z_3\mathbf{1}_{\eta-1} \end{bmatrix},$$

where $z_3, z_4 \neq 0$, and

$$\boldsymbol{x}_3 = \begin{bmatrix} \boldsymbol{y} \\ 0 \\ 0 \\ \mathbf{0}_{\eta-1} \end{bmatrix}, \quad \boldsymbol{x}_4 = \begin{bmatrix} \mathbf{0}_{\eta-1} \\ 0 \\ 0 \\ \boldsymbol{y} \end{bmatrix},$$

where, $\boldsymbol{y} = \begin{bmatrix} y_1, y_2, \cdots, y_{\eta-1} \end{bmatrix}^T \neq \mathbf{0}_{\eta-1}$.

Now, by substituting the vector $\boldsymbol{x}_1$ into the eigenvalue problem $A\boldsymbol{x}_1 = \lambda\boldsymbol{x}_1$, we obtain

$$(\eta - 2)z_1 + z_2 = \lambda z_1, \tag{2.48}$$

$$(\eta - 1)z_1 + z_2 = \lambda z_2. \tag{2.49}$$

Then we have

$$z_2 = (\lambda - \eta + 2)z_1, \tag{2.50}$$

$$\lambda^2 - (\eta - 1)\,\lambda - 1 = 0, \tag{2.51}$$

from which we immediately obtain the two eigenvalues,

$$\lambda_\pm = \frac{\eta - 1}{2} \pm \frac{\sqrt{(\eta - 1)^2 + 4}}{2}. \tag{2.52}$$

The eigenvectors are normalized if and only if

$$2(\eta - 1)z_1^2 + 2z_2^2 = 1;$$

by (2.50), this implies

$$z_1 = \left[2\big((\lambda_\pm - \eta + 2)^2 + (\eta - 1)\big)\right]^{-\frac{1}{2}}, \quad z_2 = (\lambda_\pm - \eta + 2)z_1,$$

which yields (2.70) and (2.71).

Similarly, let us consider the vector $\boldsymbol{x}_2$, substituted into the eigenvalue problem $A\boldsymbol{x}_2 = \lambda\boldsymbol{x}_2$. We obtain that

$$-(\eta - 2)z_3 - z_4 = -\lambda z_3, \tag{2.53}$$

$$-(\eta - 1)z_3 + z_4 = -\lambda z_4 \tag{2.54}$$

and hence

$$z_4 = (\lambda - \eta + 2)z_3, \tag{2.55}$$

$$\lambda^2 - (\eta - 3)\,\lambda - (2\eta - 3) = 0, \tag{2.56}$$

from which we obtain the two eigenvalues,

$$\lambda_\pm = \frac{\eta - 3}{2} \pm \frac{\sqrt{(\eta+1)^2 - 4}}{2}. \tag{2.57}$$

The normalization condition for the eigenvector is

$$2(\eta - 1)z_3^2 + 2z_4^2 = 1,$$

which, by (2.55), implies

$$\begin{aligned} z_3 &= \left[2\big((\lambda_\pm - \eta + 2)^2 + (\eta - 1)\big)\right]^{-\frac{1}{2}}, \\ z_4 &= (\lambda_\pm - \eta + 2)z_3, \end{aligned}$$

and therefore (2.72).

Finally, with the same ordering of the nodes, the adjacency matrix of K_η–K_η can be written as the block matrix

$$A = \left(\begin{array}{ccccc|cccc} & & & & & 0 & 0 & \cdots & 0 \\ & A(K_{\eta-1}) & & & \mathbf{1}_{\eta-1} & \vdots & \vdots & & \vdots \\ & & & & & 0 & 0 & \cdots & 0 \\ & \mathbf{1}_{\eta-1}^T & & & 0 & 1 & 0 & \cdots & 0 \\ \hline 0 & \cdots & 0 & 1 & & 0 & & \mathbf{1}_{\eta-1}^T & \\ 0 & \cdots & 0 & 0 & & & & & \\ \vdots & & \vdots & \vdots & & \mathbf{1}_{\eta-1} & & A(K_{\eta-1}) & \\ 0 & \cdots & 0 & 0 & & & & & \end{array}\right). \tag{2.58}$$

Substitution of the vector $\boldsymbol{x}_3$ into the eigenvalue problem $A\boldsymbol{x}_3 = \lambda\boldsymbol{x}_3$, or $\boldsymbol{x}_4$ into the eigenvalue problem $A\boldsymbol{x}_4 = \lambda\boldsymbol{x}_4$, yields

$$A(K_{\eta-1})\boldsymbol{y} = \lambda\boldsymbol{y}, \tag{2.59}$$

$$\sum_{i=1}^{\eta-1} y_i = 0. \tag{2.60}$$

Explicitly, relation (2.59) can be written as

$$y_2 + \sum_{i=3}^{\eta-1} y_i = \lambda y_1, \tag{2.61}$$

$$y_1 + \sum_{i=3}^{\eta-1} y_i = \lambda y_2, \tag{2.62}$$

$$y_1 + y_2 + \sum_{i=4}^{\eta-1} y_i = \lambda y_3, \tag{2.63}$$

$$\vdots$$

$$\sum_{i=1}^{\eta-2} y_i = \lambda y_{\eta-1}. \tag{2.64}$$

Taking differences of two such equations we obtain

$$y_i - y_j = \lambda \left(y_j - y_i \right),$$

for all $i, j \in \{1, 2, \ldots, \eta - 1\}$ with $i \neq j$. At least one of the terms $y_i - y_j$ must be non-zero by (2.60), which implies $\lambda = -1$. Hence, $\boldsymbol{y}$ is an eigenvector of $A(K_{\eta-1})$ corresponding to the eigenvalue -1, which has multiplicity $\eta - 2$. This shows that we have $\eta-2$ linearly independent vectors of the form $\boldsymbol{x}_3$ and also $\eta-2$ linearly independent vectors of the form $\boldsymbol{x}_4$, which gives a total multiplicity of $2\eta - 4$ of the eigenvalue -1 of the matrix A. Since the total multiplicity of the eigenvectors of the forms $\boldsymbol{x}_1, \ldots, \boldsymbol{x}_4$ is $2 + 2 + (2\eta - 4) = 2\eta = n$, we have found all eigenvalues of A. □

In the next lemma, we find an ordering and bounds for the eigenvalues of a dumbbell graph.

Lemma 2.5.14. *The eigenvalues of the dumbbell graph K_η–K_η, $\eta \geq 2$, can be ordered*

and bounded as follows

$$\lambda_1 > \lambda_2 > 0 > \lambda_3 > \lambda_4 = \cdots = \lambda_{n-1} = -1 > \lambda_n, \tag{2.65}$$

$$\eta - 1 < \lambda_1 = \frac{\eta - 1}{2} + \frac{\sqrt{(\eta-1)^2 + 4}}{2} < \eta, \tag{2.66}$$

$$\eta - 2 < \lambda_2 = \frac{\eta - 3}{2} + \frac{\sqrt{(\eta+1)^2 - 4}}{2} < \eta - 1, \tag{2.67}$$

$$-\frac{1}{\eta - 1} < \lambda_3 = \frac{\eta - 1}{2} - \frac{\sqrt{(\eta-1)^2 + 4}}{2} < -\frac{1}{\eta}, \tag{2.68}$$

$$-2 < \lambda_n = \frac{\eta - 3}{2} - \frac{\sqrt{(\eta+1)^2 - 4}}{2} < -1. \tag{2.69}$$

Proof. Let us first consider the eigenvalues $\lambda_\pm = \frac{\eta-1}{2} \pm \frac{\sqrt{(\eta-1)^2+4}}{2}$. Since $\eta > 1$, we have

$$\eta - 1 = \sqrt{(\eta-1)^2} < \sqrt{(\eta-1)^2 + 4} < \sqrt{(\eta-1)^2 + 4\eta} = \sqrt{(\eta+1)^2} = \eta + 1,$$

which implies (2.66). By Theorem 2.5.13, the eigenvalues λ_+ and λ_- satisfy the quadratic equation $\lambda^2 - (\eta - 1)\lambda - 1 = 0$, and therefore $\lambda_+\lambda_- = -1$, or $\lambda_- = -\frac{1}{\lambda_+}$. Together with (2.66), this implies (2.68). For $\lambda_\pm = \frac{\eta-3}{2} \pm \frac{\sqrt{(\eta+1)^2-4}}{2}$ we use again the fact that $\eta > 1$, which yields

$$\eta - 1 = \sqrt{(\eta-1)^2} = \sqrt{(\eta+1)^2 - 4\eta} < \sqrt{(\eta+1)^2 - 4} < \sqrt{(\eta+1)^2} = \eta + 1,$$

and we obtain (2.67) and (2.69). Now, the inequalities in (2.65) follow easily. □

Remark 2.5.15. *The fact that the eigenvalues satisfy the quadratic equations in Theorem 2.5.13 implies the following relations:*

1. $\lambda_1 + \lambda_3 = \eta - 1$ *and* $\lambda_1\lambda_3 = -1$*;*

2. $\lambda_2 + \lambda_n = \eta - 3$ *and* $\lambda_2\lambda_n = -(2\eta - 3)$*.*

Remark 2.5.16. *The orthonormal eigenvectors corresponding to the eigenvalues* λ_k*,*

$k \in \{1, 3\}$, can be written in the form

$$\boldsymbol{x}_k = \alpha_k \begin{bmatrix} \mathbf{1}_{\eta-1} \\ (\lambda_k - \eta + 2) \\ (\lambda_k - \eta + 2) \\ \mathbf{1}_{\eta-1} \end{bmatrix}, \tag{2.70}$$

where

$$\alpha_k = \left[2(\lambda_k - \eta + 2)^2 + 2(\eta - 1)\right]^{-\frac{1}{2}}. \tag{2.71}$$

The orthonormal eigenvectors corresponding to the eigenvalues λ_k, $k \in \{2, n\}$, can be written in the form

$$\boldsymbol{x}_k = \alpha_k \begin{bmatrix} -\mathbf{1}_{\eta-1} \\ -(\lambda_k - \eta + 2) \\ (\lambda_k - \eta + 2) \\ \mathbf{1}_{\eta-1} \end{bmatrix}, \tag{2.72}$$

where

$$\alpha_k = \left[2(\lambda_k - \eta + 2)^2 + 2(\eta - 1)\right]^{-\frac{1}{2}}. \tag{2.73}$$

2.5.14 Random Geometric Graph

A *random geometric graph* is an undirected graph defined by placing n nodes randomly and independently in $\mathbb{R}^N$. The nodes in a random geometric graph are connected as follows. A disk of radius $r > 0$ centered at each node v_i is placed, then v_i is connected to every other node found in the disk. In other words, v_i is connected to a node v_j if the Euclidean distance between these nodes is at most r [43].

2.5.15 β-Skeleton Graph

A *β-skeleton graph* [56, 104] is a simple graph defined by forming a set V with random points in $\mathbb{R}^N$. Two points $p = (p_1, p_2, \ldots, p_N)$ and $q = (q_1, q_2, \ldots, q_N)$ in a β-skeleton graph are connected as follows. Let $B(x, r)$ be the circle centered at x with radius r. If the intersection of the two circles $B((1 - \frac{\beta}{2})p + \frac{\beta}{2}q, \frac{\beta}{2}L)$ and $B((1 - \frac{\beta}{2})q + \frac{\beta}{2}p, \frac{\beta}{2}L)$

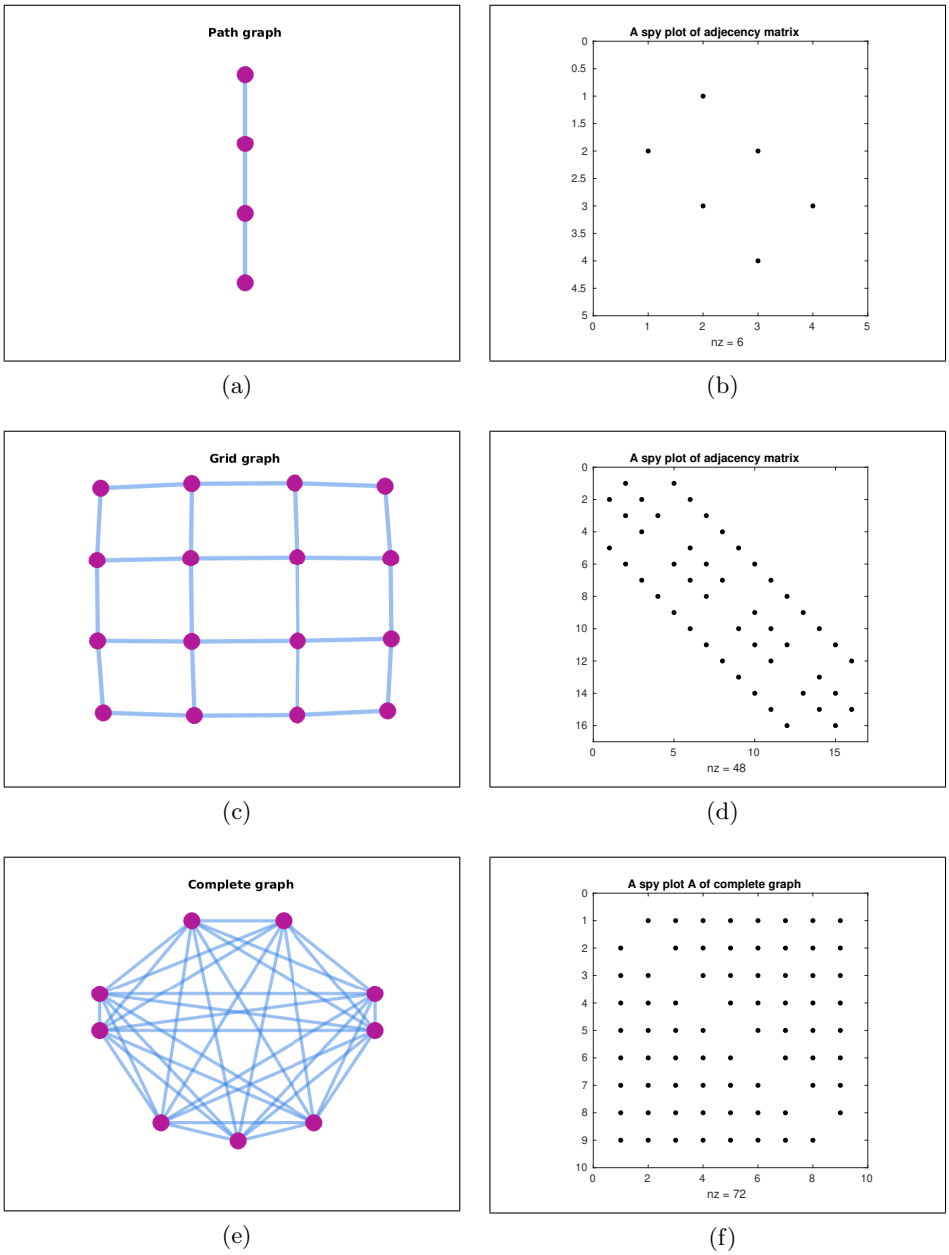

Figure 2.1: Examples of graphs: (a) path graph, (c) grid graph and (e) complete graph, and the Spy plots of their adjacency matrices in (b), (d) and (f), respectively. The Spy(A) plots the sparsity pattern of the matrix A: the non-zero values are colored black while zero values are white.

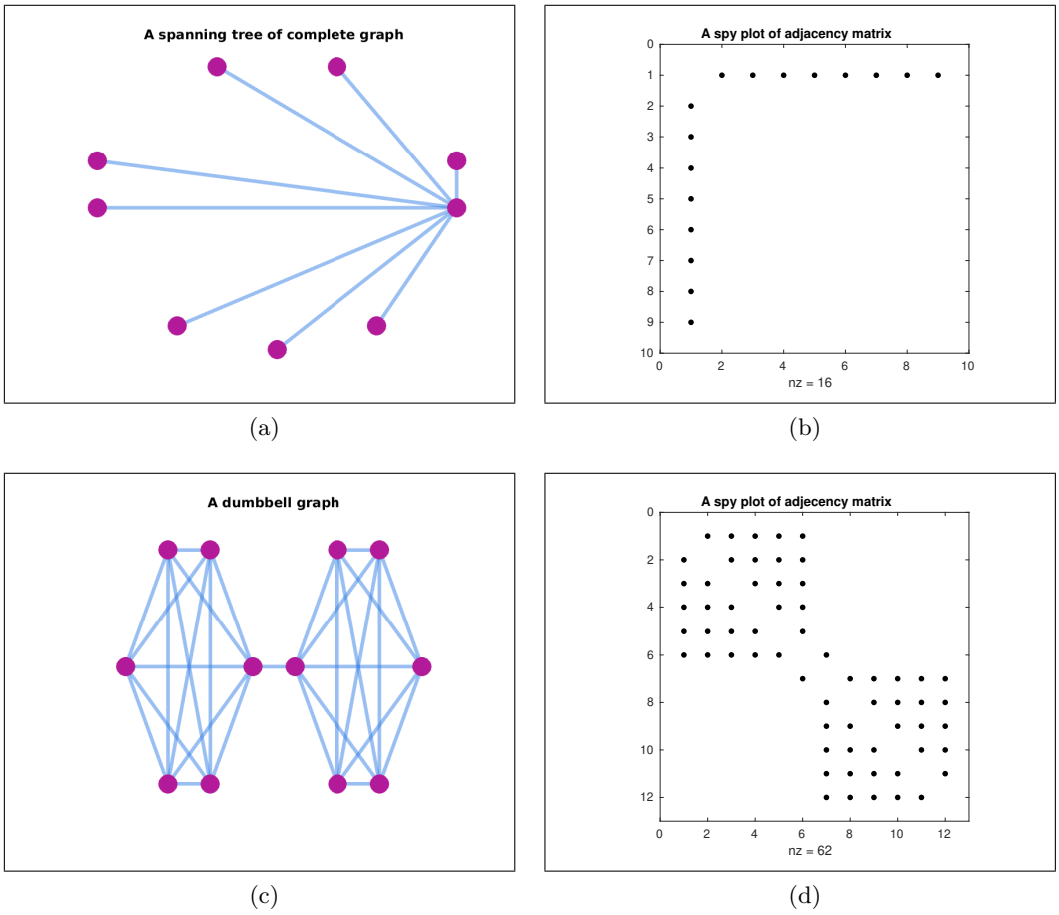

Figure 2.2: Examples of graphs: (a) a spanning tree of the complete graph K_9, (c) a dumbbell graph, and the Spy plots of their adjacency matrices in (b) and (d), respectively.

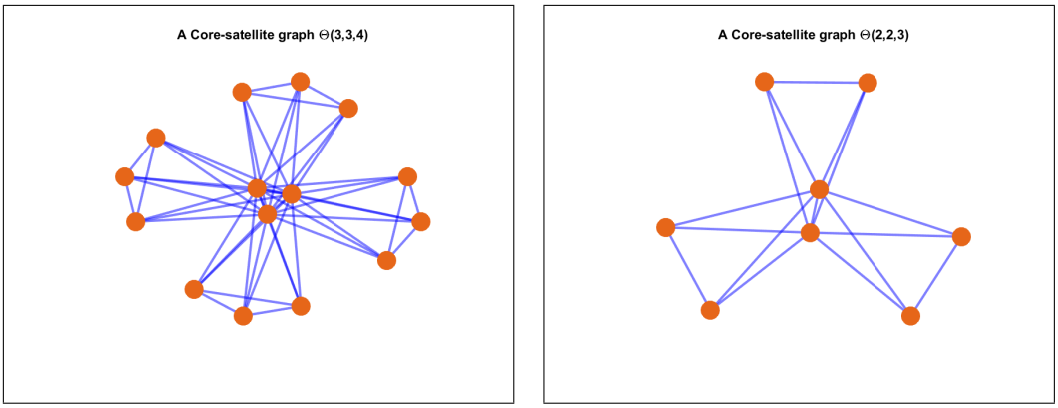

(a)

(b)

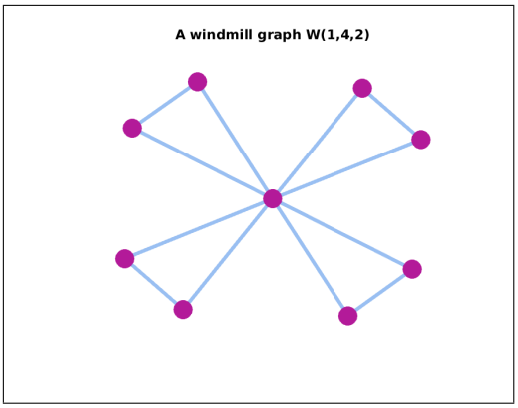

(c)

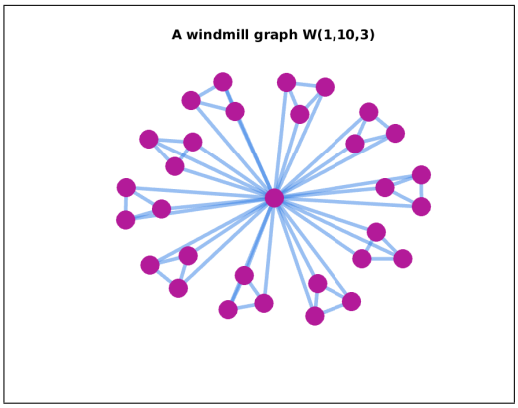

(d)

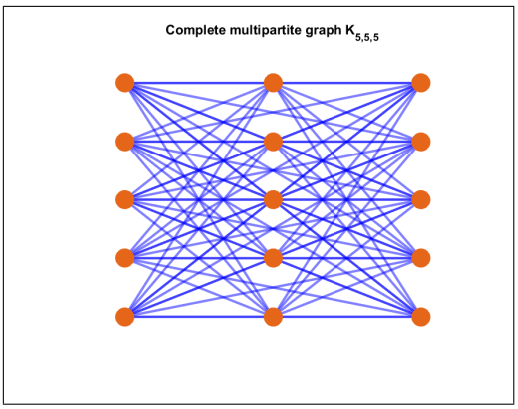

(e)

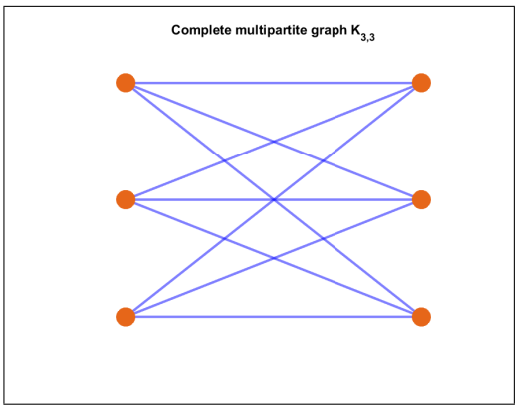

(f)

Figure 2.3: Examples of core-satellite graphs in (a) and (b), windmill graphs in (c) and (d), and complete multipartite graphs in (e) and (f).

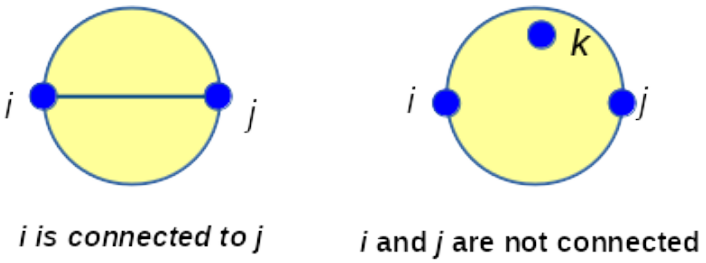

Figure 2.4: Illustration of connection between nodes in a Gabriel graph, where nodes i and j are connected in the left picture because there is no node in the constructed disk between i and j. In the right picture, i and j are disconnected because of the existence of the node k inside the disk between i and j.

contains no other points from V, where $\beta \geq 0$ and $L = \sqrt{\sum_{i=1}^{N}(p_i - q_i)^2} = \|p - q\|$ is the Euclidean distance between p and q, then p and q are connected by an edge in β-Skeleton graph.

2.5.16 Gabriel Graph and Relative Neighbourhood Graph

If $\beta = 1$ in a β-skeleton graph then the resulting graph is called a Gabriel graph, and if $\beta = 2$ then the resulting graph is called a relative neighbourhood graph. Figure 2.4 illustrates connection between nodes in this graph. In Figures 2.5 and 2.6, we give two examples of β-skeleton graphs with $n = 500$ nodes for $\beta = 1$ (Gabriel graph) and $\beta = 2$ (relative neighbourhood graph) in 2 and 3 dimensions, respectively.

2.6 Network Measures

In order to investigate the robustness of a network, we examine some network structural measures which depend on the network topology, and its global and local properties. These measures will allow us, in this thesis, to investigate the structural properties that affect the robustness of the studied networks.

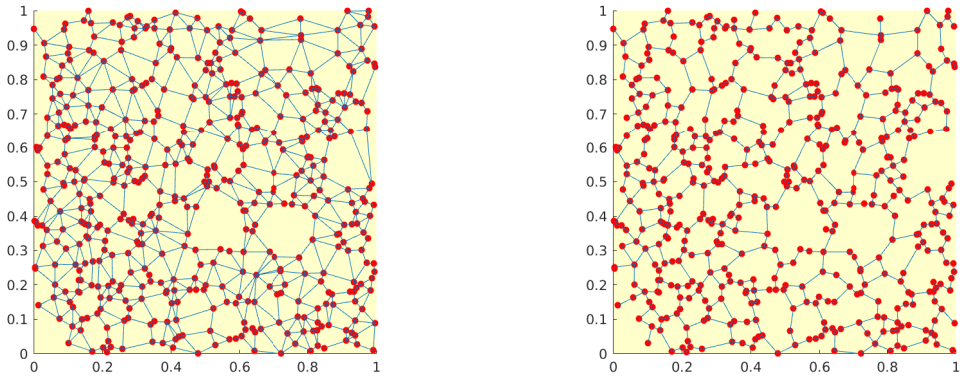

(a) Gabriel graph

(b) Relative neighbourhood graph

Figure 2.5: Examples of two β-skeleton graphs with $n = 500$ nodes each in 2 dimensions for $\beta = 1$ (Gabriel graph) and $\beta = 2$ (relative neighbourhood graph).

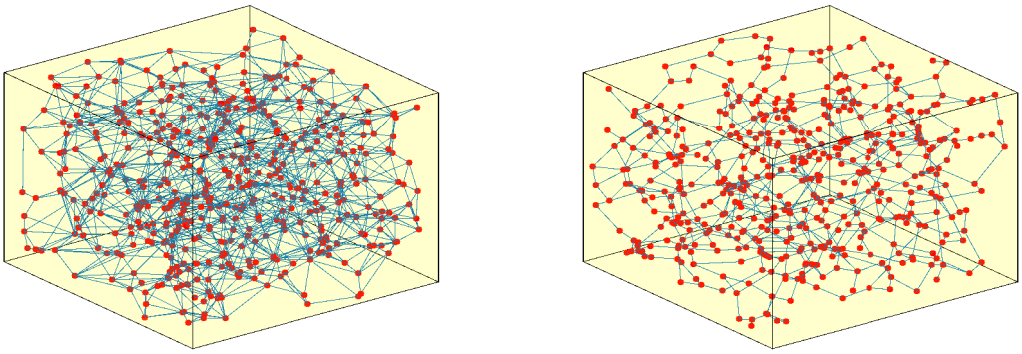

(a) Gabriel graph

(b) Relative neighbourhood graph

Figure 2.6: Examples of two β-skeleton graphs with $n = 500$ nodes each in 3 dimensions for $\beta = 1$ (Gabriel graph) and $\beta = 2$ (relative neighbourhood graph).

2.6.1 Network Connectivity

Let $\Gamma = (V, E)$ be a simple connected graph with $|V| = n$ and $|E| = m$. The maximum node degree is $k_{max} = \max_i k_i$, where k_i is the degree of the node v_i, $i = \{1, \ldots, n\}$. The average node degree $\bar{k}$ is given by

$$\bar{k} = \frac{1}{n} \sum_{i=1}^{n} k_i = \frac{2m}{n}. \tag{2.74}$$

In addition, we will consider another aspect of node degrees called the *Collatz-Sinogowitz Index* [109] given by

$$CS(\Gamma) = \lambda_1 - \bar{k}. \tag{2.75}$$

The $CS(\Gamma)$ is widely used to capture the regularity of the graph [109], where, in general, the largest eigenvalue λ_1 of the adjacency matrix A of Γ satisfies

$$k_{max} \geq \lambda_1 \geq \bar{k}. \tag{2.76}$$

For regular graphs $\lambda_1 = \bar{k}$. According to edge connectivity, we investigate the *edge density* δ given in [28]:

$$\delta = \frac{2m}{n(n-1)} = \frac{\bar{k}}{n-1}. \tag{2.77}$$

The edge density is bounded between 0 and 1.

2.6.2 Average Distance

The *distance* d_{ij} is the shortest path length from node v_i to node v_j. The distance between each pair of nodes in the graph can be displayed in a matrix form called the distance matrix D. For simple graphs, D is a symmetric matrix. The distance d_{ij} between v_i and v_j is given at the ith row (or column) and jth column (or row) of the matrix D. Then the average distance (path length) $\bar{l}$ over all pairs of nodes in a graph can be defined as in [28]:

$$\bar{l} = \frac{2}{n(n-1)} \sum_{i=1}^{n-1} \sum_{j=i+1}^{n} d_{ij}. \tag{2.78}$$

2.6.3 Efficiency

The *efficiency* of a graph measure Ef is the averaged sum of the multiplicative inverses of the distance over all pairs of nodes in a graph, and it is defined in [91, 62] as

$$Ef = \frac{2}{n(n-1)} \sum_{i=1}^{n-1} \sum_{j=i+1}^{n} \frac{1}{d_{ij}}. \tag{2.79}$$

We have $Ef \in (0, 1]$, where the upper bound is defined by the complete graph [28].

2.6.4 Closeness Centrality

The *closeness centrality* CC_i of a node v_i is the reciprocal of the sum of the shortest path lengths from v_i to every other node v_j in the graph [42]:

$$CC_i = \frac{1}{\sum_{j \neq i} d_{ij}}. \tag{2.80}$$

2.6.5 Eigenvector Centrality

The eigenvector centrality EC_i is the ith entry of the eigenvector $\boldsymbol{\psi}_1$ which corresponds to the largest eigenvalue λ_1 of the adjacency matrix A of the graph.

2.6.6 Betweenness Centrality

The *betweenness centrality* BC_x is defined as the fraction of the shortest paths between pairs of nodes passing through a node or an edge x, and can be defined by

$$BC_x = \sum_{i=1}^{n-1} \sum_{j=i+1}^{n} \frac{p_{ij}(x)}{p_{ij}}, \tag{2.81}$$

where $p_{ij}(x)$ represents the number of shortest paths between i and j passing through x, and p_{ij} represents the total number of the shortest paths between nodes i and j [42, 41].

2.6.7 Subgraph Centrality

The *subgraph centrality* of a node accounts for the number of closed walks in a graph. There are many ways for characterizing this centrality measure. One approach considers the weighted sum of the powers of the the adjacency matrix A,

$$f(A) = \sum_{k=0}^{\infty} c_k A^k. \tag{2.82}$$

In order to give more weights to smaller subgraphs, we will consider in this work $c_k = \frac{1}{k!}$ [24, 38], hence

$$f(A) = \sum_{k=0}^{\infty} \frac{A^k}{k!} = e^A. \tag{2.83}$$

The main diagonal of A^k counts the number of closed walks of length k from each node to itself. Each entry of the main diagonal of e^A represents the weighted sum of the numbers of closed walks of length $k = 1, 2, \ldots$, from each node v_i to itself, where $i \in \{1, \ldots, n\}$. Then, the subgraph centrality of node v_i can be defined by

$$SC(i) = \left(e^A\right)_{ii}. \tag{2.84}$$

The sum of all subgraph centralities $SC = \sum_{i=1}^{n} SC(i)$, known as the Estrada index, considers all possible closed walks in a graph [24]. It can be related to the sum of the eigenvalues of the adjacency matrix of the graph. By using the spectral decomposition of the adjacency matrix A of the graph, we have that $e^A = Se^{\Lambda}S^T$and then the average subgraph centrality of all the nodes in the graph can be written as

$$\overline{SC} = \frac{\sum_{i=1}^{n} e^{\lambda_i}}{n}. \tag{2.85}$$

2.6.8 Clustering Coefficient

The *clustering coefficient* captures the presence of triangles in a graph. This concept was proposed by Watts and Strogatz in 1998 [112]. The clustering coefficient compares the number of triangles to the number of connected triples. The number of triangles

incident to the node v_i of a graph can be expressed by the main diagonal of A^3 and can be evaluated as

$$t_i = \frac{1}{2}\left(A^3\right)_{ii}. \tag{2.86}$$

In general, A^3 captures all paths of length 3 and the diagonal of A^3 captures the number of closed walks of length 3. However, the triangles may be counted in each direction of v_i, therefore we multiply by a half to avoid double counting. The number of all paths of length 2 centred on a node v_i is the number of all possible ways to pick two edges from the k_i edges incident to v_i, and can be expressed as

$$P_2(i) = \binom{k_i}{2} = \frac{k_i(k_i-1)}{2}. \tag{2.87}$$

Hence, the clustering coefficient C_i of a node v_i of degree k_i and related number of triangles, is calculated by

$$C_i = \frac{\left(A^3\right)_{ii}}{k_i(k_i-1)}. \tag{2.88}$$

The average clustering coefficient $\bar{C}$ can hence be calculated by

$$\bar{C} = \frac{1}{n}\sum_{i=1}^{n}\frac{\left(A^3\right)_{ii}}{k_i(k_i-1)}. \tag{2.89}$$

The average clustering coefficient is also known as the *Watts-Strogatz* clustering coefficient. It ranges between zero and one [112]. If, for any given graph, one has that $\bar{C} = 1$, then this indicates that all possible triangles exist in the graph.

2.6.9 Average Resistance Distance

The resistance distance was introduced by Kirchhoff [59]. The resistance distance is induced in graph theory by placing fixed electrical resistors on the edges of a graph and connecting a battery across the nodes. Then the resistance distance between the nodes can be found by using Kirchhoff's and Ohm's laws. The effective graph resistance is defined based on the set of spanning trees in the graph [28]. The average effective graph resistance (or Kirchhoff index) is the sum of effective resistances of all pairs of nodes in the graph. It has been proven [59] that the Kirchhoff index can be written as a function

of the non-zero eigenvalues of the Laplacian graph as

$$\Omega_{ij} = \sum_{k=2}^{n} \frac{1}{\mu_k} (\phi_k(i) - \phi_k(j))^2. \tag{2.90}$$

Then, the average resistance distance is

$$\bar{\Omega} = \sum_{i<j} \Omega_{ij}, \tag{2.91}$$

where μ_k is the kth eigenvalue of the Laplacian matrix L of A and $\phi_k(i)$ is the ith entry of the eigenvector $\boldsymbol{\phi}_k$ that corresponds to μ_k. The values of $\bar{\Omega}$ can be diverse and grow incredibly large.

2.7 Network Communicability

A measure named communicability was proposed by Estrada [25]. This measure quantify how well information flows between nodes in a network. Communicability is computed as the number of walks in a graph, where larger weights are given to shorter walks. The communicability between any two vertices $p, q \in V$ in a graph $\Gamma = (V, E)$ is defined mathematically as the weighted sum of the number of all possible walks between p and q. Then, the communicability can be defined as

$$G_{pq}(\Gamma) = \sum_{k=0}^{\infty} \frac{\left(A^k\right)_{pq}}{k!} = \left(\exp(A)\right)_{pq} = \sum_{j=1}^{n} \psi_j(p)\psi_j(q)e^{\lambda_j}, \tag{2.92}$$

where $\psi_j(p)$ is the pth component of the jth orthogonal eigenvector associated with the eigenvalue λ_j of the adjacency matrix A [33, 37]. The weight $\frac{1}{k!}$ makes the communicability function focus more on the shortest walks, where recall that shorter walks receive more weights than longer walks. In the next two sections we present communicability in more detail and in general depth. Other two measures for investigating robustness considered in this work (and based on communicability) are the *communicability distance* and *communicability angle*. Estrada defines these measures by considering the distance between nodes as the Euclidean distance [26, 27].

The meaning of communicability distance and communicability angle can be induced by embedding the graph into a hypersphere, which allows us to define the Euclidean distance between nodes [26, 27]. To define the Euclidean distance between nodes p and q, let the vectors $\boldsymbol{x}_p = e^{\frac{\Lambda}{2}}\boldsymbol{\psi}_p$ and $\boldsymbol{x}_q = e^{\frac{\Lambda}{2}}\boldsymbol{\psi}_q$ be located on the surface of a hypersphere. The matrix Λ is the diagonal matrix of eigenvalues of the adjacency matrix A and $\boldsymbol{\psi}_p = [\psi_1(p), \psi_2(p), ..., \psi_n(p)]^T$, where $\psi_i(p)$ is the pth entry of eigenvector $\boldsymbol{\psi}_i$ of A. Then the distance ξ_{pq} between nodes p and q can be considered as an Euclidean distance, and the communicability angle is represented by the angle between the two vectors $\boldsymbol{x}_p$ and $\boldsymbol{x}_q$ such that [26, 27]

$$\begin{aligned}
\xi^2 =& \parallel \boldsymbol{x}_p - \boldsymbol{x}_q \parallel^2, \\
&= (\boldsymbol{x}_p - \boldsymbol{x}_q)^T (\boldsymbol{x}_p - \boldsymbol{x}_q), \\
&= \left(\boldsymbol{x}_p^T - \boldsymbol{x}_q^T\right)(\boldsymbol{x}_p - \boldsymbol{x}_q), \\
&= \boldsymbol{x}_p^T\boldsymbol{x}_p - \boldsymbol{x}_p^T\boldsymbol{x}_q - \boldsymbol{x}_q^T\boldsymbol{x}_p + \boldsymbol{x}_q^T\boldsymbol{x}_q, \\
&= \boldsymbol{x}_p^T\boldsymbol{x}_p - 2\boldsymbol{x}_p^T\boldsymbol{x}_q + \boldsymbol{x}_q^T\boldsymbol{x}_q.
\end{aligned}$$

Then

$$\xi_{pq}^2 = G_{pp} + G_{qq} - 2\sqrt{G_{pp}G_{qq}}\cos\theta_{pq},$$

and

$$\begin{aligned}
\boldsymbol{x}_p \cdot \boldsymbol{x}_q =& \parallel \boldsymbol{x}_p \parallel \cdot \parallel \boldsymbol{x}_q \parallel \cos\theta_{pq}, \\
\cos\theta_{pq} =& \frac{G_{pq}}{\sqrt{G_{pp}G_{qq}}},
\end{aligned}$$

where $p \neq q$, ξ_{pq} is the communicability distance and θ_{pq} is the communicability angle between the nodes p and q. The average communicability distance $\bar{\xi}$ and the average communicability angle $\bar{\theta}$ [35] are defined, respectively, by

$$\bar{\xi} = \frac{\sum_{p\neq q}\left(G_{pp} + G_{qq} - 2\sqrt{G_{pp}G_{qq}}\right)^{\frac{1}{2}}}{n(n-1)}, \tag{2.93}$$

$$\bar{\theta} = \frac{\sum_{p \neq q} \arccos\left(\frac{G_{pq}}{\sqrt{G_{pp}G_{qq}}}\right)}{n(n-1)}. \tag{2.94}$$

The average communicability angle $\bar{\theta}$ is a measure for the spatial efficiency of a network, and it holds $0 \leq \bar{\theta} \leq 90$ where a value close to the lower bound indicates high spatial efficiency and a value close to the upper bound indicates poor spatial efficiency. The average communicability angle and distance depend on two factors: the amount of information which departs from p (resp., q) and then goes back to p (resp., q) as is represented by G_{pp} (resp., G_{qq}), and the amount of information which departs from p (resp., q) then arrives to q (resp., p) as is represented by G_{pq} (resp., G_{qp}). Therefore, the quality of communication depends on the amount of information which arrives at its goal G_{pq} while the amount of information that arrives to G_{pp} and G_{qq} represents the information that returns to its origin and decreases the quality of communication. Both a low value of the average communicability angle and a high value of the average communicability distance indicate a more robust graph.

2.8 Summary

In this chapter, we reviewed the necessary background in graph theory. We provided an overview of network theory including, in particular, definitions, structural graph concepts, as well as relevant to us graph types.

Additionally, we found the exact values of the entries of the associated eigenvectors corresponding to the largest and smallest eigenvalues of windmill graphs. Also, we found the spectrum of dumbbell graphs. Moreover, we found the eigenvectors corresponding to $\lambda = 0$ and $\lambda = -\eta_i$, $i \in \{1, 2, \ldots, k\}$, for complete multipartite graph $K_{\eta_1,\eta_2,\cdots,\eta_k}$, $\eta_1 \leq \eta_2 \leq \cdots \leq \eta_k$, and the exact entries of the normalized eigenvectors corresponding to the negative eigenvalues $\lambda \neq -\eta_i$ and the largest eigenvalue. Moreover, we found the spectrum of complete k-partite graphs $K_{\eta,\eta,\ldots,\eta}$ and complete 3-partite graphs $K_{\eta,\eta,l}$. Finally, we discussed several topological network properties for investigating network robustness.

Chapter 3

Topological Melting in Networks

3.1 Melting in Solids

In presenting the melting theory in this chapter, we follow closely [1]. Physically, the melting or transforming from a solid to a liquid at a microscopic scale occurs as a result of an increase in the internal energy of the solid by applying heat or pressure [3, 13]. One of the most successful criteria for explaining the melting of solids at the microscopic level was developed by Lindemann in 1910 [67]. The Lindemann criterion states that melting in solids occurs when the square root of the mean range of the vibrations VI of a solid reaches a critical fraction of distance d to the nearest neighbour [67]. It can be defined as

$$\sqrt{VI} = L_p d,$$

where the critical fraction L_p is called *Lindemann parameter*.

According to the Lindemann criterion [57, 67], melting occurs due to vibrational instability in the crystal lattice as a result of an increase in the temperature. In fact, every substance is characterized by a melting point, i.e. the temperature at which the melting process starts. We study the vibrations between nodes in graphs in order to study the change of state resulting from raising the temperature, as described by the Lindemann criterion.

The successful use of networks to represent several granular materials has bolstered their ubiquity as an object of study in this area of research [89]. We understand "gran-

ular materials" as a far ranging concept which includes, for instance, granular crystals [93, 97], microsphere monolayers [50], soft glassy materials [6], and colloidal crystals [100] among others [82]. An important aspect of this area of research is related to the robustness of such networks against any external stress they may be subjected to [89]. For instance, Walker and Tordesillas [110] have studied the evolution of deformations in granular material networks under axial strain. In their work, they have found that measures related to the network communicability function [33, 36] perform very well in describing such deformations. If we bear in mind the network representation as a system of balls and springs submerged in a thermal bath at a given inverse temperature $\beta = (k_B T)^{-1}$, where k_B is the Boltzmann constant, the communicability function acquires the interpretation of being the thermal Green's function of the network [36]. This represents the capacity of a node to transmit a perturbation to another node in the network at a given β.

3.2 Vibrations on Graphs

In 2012 Estrada, Hatano and Benzi [36] defined a measure for the *vibrations* between the nodes in graphs. They defined a communicability function which measures the perturbations or vibrations between any two nodes in a network due to the thermal external stress $\beta = (k_B T)^{-1}$, where k_B is Boltzmann constant and T is the temperature. The generalized communicability function $G_{pq}(\Gamma, \beta)$ is a communicability function defined using the weights $\frac{\beta^k}{k!}$. It takes into account longer walks as well as shorter walks depending on the value of β [32, 36]. For a graph $\Gamma = (V, E)$ with n nodes and adjacency matrix A, they define

$$G_{pq}(\Gamma, \beta) = \sum_{k=0}^{\infty} \frac{\beta^k \left(A^k\right)_{pq}}{k!} = \left(\exp(\beta A)\right)_{pq} = \sum_{j=1}^{n} \psi_j(p)\, \psi_j(q)\, e^{\beta \lambda_j} \tag{3.1}$$

where $p, q \in V$, $\beta > 0$ and $\psi_j(p)$ is the pth entry of the eigenvector $\boldsymbol{\psi}_j$ that corresponds to the eigenvalue λ_j of A. In what follows, we assume that $\lambda_1 > \lambda_2 \geq \cdots \geq \lambda_n$. The inverse temperature β might have different meanings depending on the network that is being considered [32]. In general, using the generalized communicability function

allows us to regard β as the strength of the links in the network. Thus, the generalized communicability function accounts for the strength of the interactions among the nodes with different temperatures T. When $\beta \to 0$, the temperature goes to infinity, and there is no communicability (that is, the vibrations are very high) between any two vertices in the network. All the edges in the network vanish since all the edges are weighted by β, and the graph will be fully disconnected, which could correspond to a gas. However, if the temperature goes to zero, then $\beta \to \infty$, which corresponds to high communicability between the nodes in the network. In this case, there are many routes through which information can be transferred from one node to another, where the graph is fully connected similarly to a rigid solid. Mathematically, when β is large and the spectral gap is significantly large then the communicability function $G_{pq}(\Gamma, \beta)$ is dominated by the term of the largest eigenvalue λ_1, which is positive according to the Perron-Frobenius Theorem for matrices.

Communicability in graph theory has many uses in a wide range of real world applications. For instance, in detecting changes in the contralesional hemisphere following strokes in humans [19], in the detection of symptoms of multiple sclerosis [64], in the study of variants of epilepsy [15], in the prediction of abnormal brain states [54], in the early detection of Alzheimer's disease [73], in the prediction of functional protein complexes [70], in the analysis of genetic diseases [14], in the optimization of wireless networks [17], in the evolution of granular materials [110], in the classification of grass pollen [75] and vegetation patterns [74], and in the identification of the transcription factor critically involved with self-renewal of undifferentiated embryonic stem cells [71].

3.3 The Communicability Graph

To study pure vibrations of nodes, or the community structure of networks, Estrada and Hatano [25, 34] defined the communicability graph function $\Delta G(\Gamma, \beta)$ of a graph $\Gamma = (V, E)$. They decomposed the generalized communicability function into terms depending on the sign of the components of the eigenvectors of the adjacency matrix. The signs can be interpreted as the direction of the vibrations of the nodes. In Figure 3.1, we display a schematic representation for the eigenvectors of the adjacency

matrix of a small graph with $n = 8$ nodes. The positive (resp., negative) entries of each eigenvector $\boldsymbol{\psi}_j$, where $1 \leq j \leq n$, are illustrated as vibrations in the positive (resp., negative) directions of the y-axis. However, the magnitude of the entries of the eigenvectors is not represented for the sake of simplicity. The first eigenvector $\boldsymbol{\psi}_1$ that corresponds to the largest eigenvalue λ_1 shows coordinated vibrations of all the nodes in the graph.

The term $\psi_1(p)\psi_1(q)e^{\beta\lambda_1}$ represents the coordinated vibrations of all the nodes at the given value β. Consequently, to obtain the pure vibrations between the nodes, they subtracted the first term $\psi_1(p)\psi_1(q)e^{\beta\lambda_1}$ to define the communicability graph function $\Delta G_{pq}(\Gamma, \beta)$ by

$$\begin{aligned}
\Delta G_{pq}(\beta) &= G_{pq}(\Gamma, \beta) - \psi_1(p)\psi_1(q)e^{\beta\lambda_1} \\
&= \sum_{j=2}^{n} \psi_j(p)\psi_j(q)e^{\beta\lambda_j} \\
&= \sum_{\substack{j\geq 2: \\ \operatorname{sgn}\psi_j(p)=\operatorname{sgn}\psi_j(q)}} \psi_j(p)\psi_j(q)e^{\beta\lambda_j} - \sum_{\substack{j\geq 2: \\ \operatorname{sgn}\psi_j(p)\neq\operatorname{sgn}\psi_j(q)}} \left|\psi_j(p)\psi_j(q)\right|e^{\beta\lambda_j}.
\end{aligned}$$

The first term on the right-hand side represents the positive components, since both nodes have the same sign of the jth eigenvector component. The first term is known as the *in-phase*, and the second term is known as the *out-of-phase*, which represents the negative components, since the two nodes in it have different signs of the jth eigenvector component. The function $\Delta G_{pq}(\beta)$ accounts for the difference between the in-phase and out-of-phase vibrations of the corresponding pair of nodes. This allows to define a new graph, called the *communicability graph*, that represents the pure vibrations between the nodes.

Definition 3.3.1. Communicability Graph

The *communicability graph* $H(V, E', \beta)$ of a graph Γ is a simple graph, which has the same nodes as $\Gamma = (V, E)$ and the edges are determined according to the values of $\Delta G(\Gamma, \beta)$. Two distinct nodes p and q are connected in $H(V, E', \beta)$ if and only if $\Delta G_{pq}(\Gamma, \beta) \geq 0$.

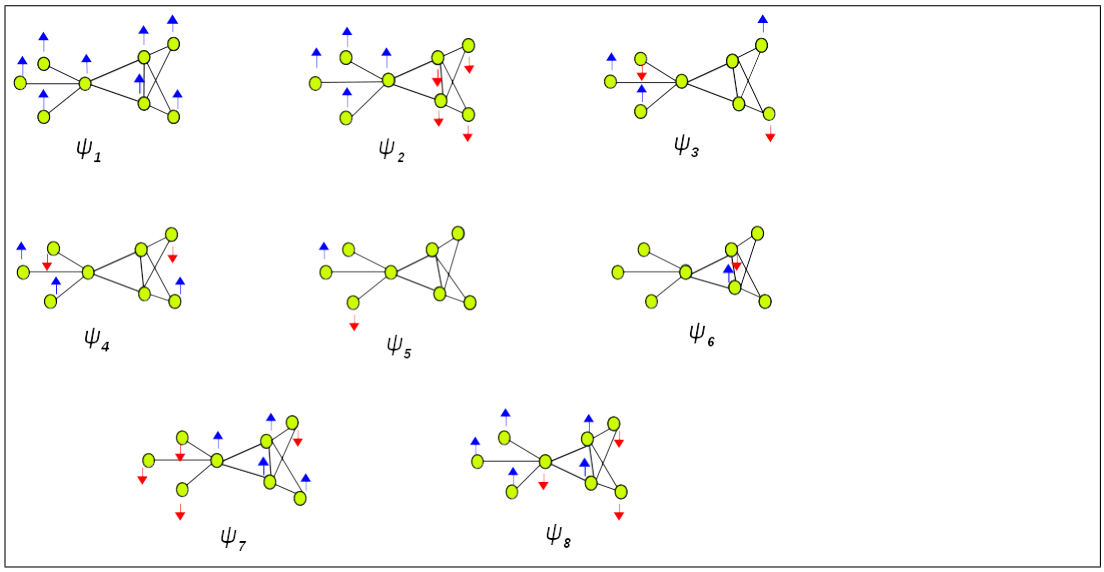

Figure 3.1: Illustration of the sign pattern of the eigenvectors in a simple graph. The signs of the positive components of the eigenvectors are represented by blue arrows and the negative entries by red arrows. The magnitude of the eigenvector components are not represented. Also, the absence of an arrow implies the corresponding eigenvector entry is zero.

3.4 Melting of Graphs

In this section, we propose a new melting phase transition for networks based on the communicability function between nodes. We define a communicability graph function that accounts for the vibrations between any given pair of nodes based on the Lindemann criterion for melting solids. We then define the melting phase transition of networks.

Let us now reconnect with the Lindemann melting criterion: this asserts that melting should be expected when the root mean-square amplitude of vibrations exceeds a certain threshold value [67]. We will assume that in a graph Γ such a threshold is given by

$$M(\Gamma,\beta) = \max_{s\neq t\in V} \sum_{j=2}^{n} \psi_j(s)\,\psi_j(t)\,e^{\beta\lambda_j}.$$

Therefore, we assume that an edge between the nodes p and q melts (i.e. disappears) in the graph when the vibration between p and q at a given temperature measured by $\Delta G_{pq}(\beta)$, exceeds the value of the maximum vibration of any pair of distinct nodes in

that graph at the same temperature, $M(\Gamma, \beta)$. In order to implement the Lindemann criterion on graphs we define a new communicability graph function, the *modified communicability graph function* $\Delta\tilde{G}_{pq}(\beta)$ for networks, as

$$\Delta\tilde{G}_{pq}(\beta) = M(\Gamma, \beta) + \Delta G_{pq}(\beta). \tag{3.2}$$

To illustrate the melting process of edges, we discuss the following cases.

If $M(\Gamma, \beta) > 0$ then we have the following scenarios. When $\Delta G_{pq}(\beta) \geq 0$ then $\Delta\tilde{G}_{pq}(\beta) > 0$, indicating a *reinforcement* of the in-phase vibrations from the two nodes. That means that p and q are strictly connected to each other. When $\Delta G_{pq}(\beta) < 0$ then we have the following two cases. If $\Delta\tilde{G}_{pq}(\beta) \geq 0$ then the difference between in-phase and out-of-phase vibration of the nodes p and q (i.e. $\Delta G_{pq}(\beta)$) does not exceed the maximum in-phase vibrations of any pair of nodes in the graph; then there is an edge between p and q. Otherwise, $\Delta\tilde{G}_{pq}(\beta) < 0$ indicating that the out-of-phase vibrations of these two nodes have overtaken not only their in-phase vibrations but also the maximum in-phase vibrations of any pair of nodes in the graph. In this case, the edge between p and q is melted.

On the other hand, if $M(\Gamma, \beta) < 0$ then it is necessary that $\Delta G_{pq}(\beta) < 0$, for all $p, q \in V$, which means that $\Delta\tilde{G}_{pq}(\beta) < 0$, and the edge necessarily melts. In this case, there are no edges between the nodes. Let us define the following representation of $\Delta\tilde{G}_{pq}(\beta)$ in the form of a new graph.

Definition 3.4.1. Let $\Gamma = (V, E)$ be a simple graph. The *modified communicability graph* $\tilde{H}(V, E', \beta)$ of Γ is a simple graph with the same set of nodes as Γ. Two distinct nodes $p, q \in V$ are connected in $\tilde{H}$ if and only if $\Delta\tilde{G}_{pq}(\beta) \geq 0$.

Remark 3.4.1. *In the modified communicability graph there could be edges connecting pairs of nodes which are not connected in the original graph Γ. In a similar way, for some β, there could be pairs of nodes not connected in $\tilde{H}(V, E', \beta)$ which correspond to edges in Γ. In other words, Γ is not necessarily a subgraph of $\tilde{H}(V, E', \beta)$.*

In the graph presented in Figure 3.2, at $\beta = 0.25$ the pairs of nodes (5,6), (5,8) and (6,8) are not connected in the modified communicability graph whereas they are

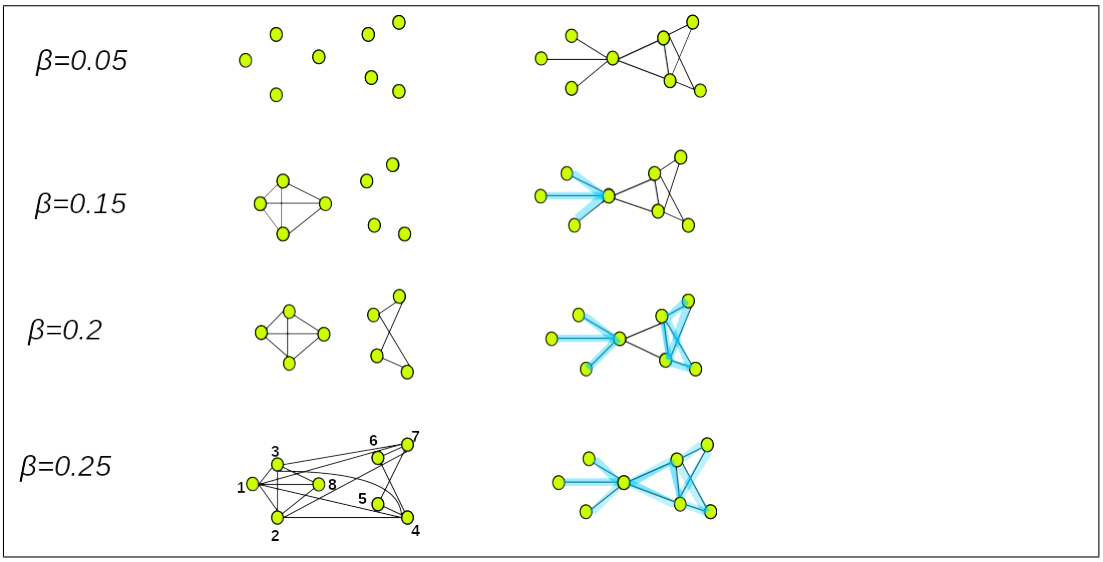

Figure 3.2: Modified communicability graphs in the middle column at different values of β for the small graph Γ with degree sequence 1, 1, 1, 2, 2, 4, 4, 5, presented in the last column with black thin lines. In the right column the edges of the Lindemann graph are represented as thick blue lines over the edges of the original graph Γ.

connected in the original graph. These nodes can be seen to be the out-of-phase. However, there are paths connecting those nodes such as 5-4-6, 8-3-7-5 and 8-3-7-6. These nodes could vibrate in phase at temporal stages of the process, so then the modified communicability graph could be connected in this case. For this reason we introduce the following definitions.

Definition 3.4.2. Let $\Gamma = (V, E)$ be a simple graph and let $\tilde{H}(V, E', \beta)$ be its modified communicability graph. For $p, q \in V$ we say that there exists a *Lindemann path* $L_{p,q}$ between the nodes p and q in Γ at a given value of β if there is a path connecting these nodes in $\tilde{H}(V, E', \beta)$.

Now we define a graph that contains all the information about the in- and out-of-phase nature of the vibrations in Γ.

Definition 3.4.3. Let $\Gamma = (V, E)$ be a simple graph and let $\tilde{H}(V, E', \beta)$ be its modified communicability graph. The *Lindemann graph* $F(V, E'', \beta)$ of Γ is a subgraph of Γ with the same set of vertices as Γ. The two distinct nodes $p, q \in V$ are connected in F if and only if $(p, q) \in E$ and there exists a Lindemann path $L_{p,q}$.

Next, we state the definition of the modified communicability graph melting.

Definition 3.4.4. A modified communicability graph of a graph Γ starts melting when deleting one or more edges makes it transfer from being a connected graph to a disconnected graph. The modified communicability graph is fully connected when the communicability between the nodes is very high (i.e. $\Delta\tilde{G}_{pq}(\beta) \geq 0$, for all $p, q \in V$). However, the communicability between the nodes decreases as β decreases, where the modified communicability graph is disconnected when $\Delta\tilde{G}_{pq}(\beta) < 0$, for some $p, q \in V$.

To illustrate the previously defined concepts we return to the small graph with 8 nodes and degree sequence 1, 1, 1, 2, 2, 4, 4, 5 at different values of β as illustrated in Figure 3.2. For $\beta = 0.25$ the modified communicability graph has many more edges than the original graph Γ, but there are missing edges which connect the pairs of nodes (5,6), (5,8) and (6,8) in the original graph. However, the Lindemann graph at this value of β is connected with the same edges as in the original graph Γ, since there is a path between every pair of nodes in the corresponding modified communicability graph. The modified communicability graphs are in the middle column and the Lindemann graphs are in the right column represented as thick blue lines over the edges of the original graph Γ in Figure 3.2. When $\beta = 0.2$ the modified communicability graph is disconnected with two components of four nodes each. Then, the Lindemann graph consists of all the edges of Γ, except the edges that connect the pairs of nodes (6,8) and (5,8), because there is no path connecting these pairs of nodes in the corresponding modified communicability graph. At this value of β, we can say that the melting process of the modified communicability graph has already started.

If we decrease β to 0.15, then more edges vanish, where the modified communicability graph at this point consists of four isolated nodes and one clique of four nodes. Although, there are paths connecting the nodes in the clique, there are no paths connecting the isolated nodes in the modified communicability graph. In this case, the Lindemann graph is disconnected. Finally, when β is dropped to 0.05 then all edges in the modified communicability graph vanish, where now the modified communicability graph consists of eight isolated nodes as does the Lindemann graph. At this point there is no connections between any pair of nodes and the Lindemann graph is the null

graph. Physically, the modified communicability graph is completely melted.

In Figure 3.3, we plot the number of connected components of the Lindemann graphs versus the values of β. At the point $\beta \approx 0.2$, there is a transition between connected and disconnected Lindemann graphs. Let us call this critical value of β which we identified previously β_c; this is the melting temperature of the graph.

Remark 3.4.2. *The modified communicability graph is null graph when the communicability between the nodes is very low (i.e. $\Delta\tilde{G}_{pq}(\beta) < 0$, for all $p, q \in V$). However, the communicability between the nodes increases as β increases. The nodes p and q are connected (freeze) by an edge in the modified communicability graph if $\Delta\tilde{G}_{pq}(\beta) \geq 0$. We will call this process* freezing.

Definition 3.4.5. The critical value β_c (melting temperature or the melting phase transition) of a graph Γ is the value of β by which $\Delta\tilde{G}_{pq}(\beta)$ makes the modified communicability graph and Lindemann graph of Γ transfer from being connected to disconnected graphs. The lower the value of β_c the more robust is the graph.

Definition 3.4.6. Let $\Gamma = (V, E)$ be a simple connected graph. The *melting signature* of Γ is the sequence of inverse temperatures β, starting with the lowest, at which the structure of the associated modified communicability graph changes.

Remark 3.4.3. *We compute β_c for a simple connected graph by finding the number of connected components of its modified communicability graph as the value of β changes. The number of connected components of a graph is equal to the multiplicity of the zero eigenvalue of its Laplacian matrix. Then β_c is the value of β by which the modified communicability graph transfers from one connected component to more than one component.*

In the next chapter, we will study and investigate melting of graphs in some graph families, before that we need to include the following results.

Lemma 3.4.4. *The existence of the transition in Lindemann graphs from connected to disconnected, is sufficient for the existence of the transition in the modified communicability graphs of a simple connected graph.*

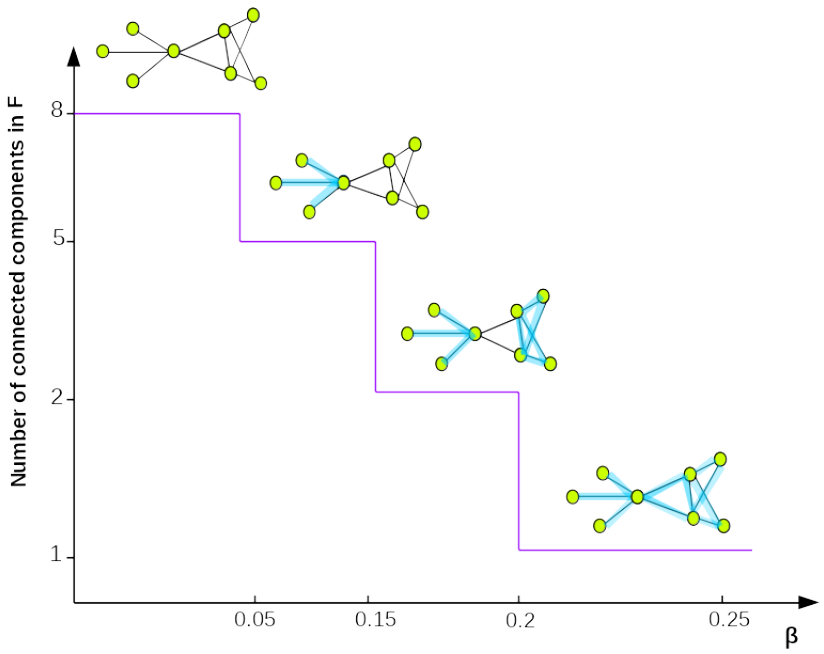

Figure 3.3: Illustration of the transition between connected (for all $\beta \geq 0.2$) and disconnected (for all $\beta < 0.2$) Lindemann graphs as a function of β for the simple graph illustrated in Figure 3.2

Proof. When the modified communicability graph is connected, so is the Lindemann graph, due to the fact that there is a path between every pair of nodes in the connected graph. In the same way, if the modified communicability graph is disconnected, so is the Lindemann graph because there will be pairs of adjacent nodes of the original graph for which there are no paths connecting them in the modified communicability graph. □

Lemma 3.4.5. *Let $\Gamma = (V, E)$ be a simple connected graph with adjacency matrix A, and $\lambda_1 > \lambda_2 \geq \cdots \geq \lambda_n$ be the eigenvalues of A, with the corresponding eigenvectors $\psi_1, \psi_2, \ldots, \psi_n$. Then the modified communicability graph function*

$$\Delta\tilde{G}_{pq}(\beta) = M(\Gamma, \beta) + \sum_{j=2}^{n} \psi_j(p)\,\psi_j(q)\,e^{\beta\lambda_j},$$

where $M(\Gamma, \beta) = \max_{s \neq t \in V} \sum_{j=2}^{n} \psi_j(s)\,\psi_j(t)\,e^{\beta\lambda_j}$, is a continuous function of β.

Proof. It is clear that $\Delta\tilde{G}_{pq}(\beta)$ is a finite sum of exponential functions and the maxi-

mum of exponential functions. Thus, $\Delta\tilde{G}_{pq}(\beta)$ is a continuous function. □

3.5 Summary

In this chapter, we defined a melting phase transition in graphs. This transition takes place when we consider a Lindemann-like model on graphs, which is based on the vibrational approach to the problem. First, we discussed some basics about melting solids physically. Then we discussed melting of graphs including vibrations (communicability) and pure vibrations (communicability graphs).

Part II

Results and Discussion

Chapter 4

Melting in some Graph Families

In this chapter, we study and investigate melting in some graph families which could allow us to cover the cases when the second eigenvalue is positive or nonpositive. Hence, we can find a generalization about the melting phase transition in graphs.

In the next two sections, we study melting in two families of graphs, windmill and dumbbell graphs introduced in Chapter 2. The reason for this choice is that in these families of graphs, on the one hand, the second eigenvalue λ_2 is positive and, on the other hand, the number of different types of edges in the associated modified communicability graph is very low: it is at most 3 in the case of windmill graphs and at most 5 in the case of dumbbell graphs. Even in these relatively simple cases the analysis of monotonicity and ordering of the elements of $\Delta G(\beta)$ and $\Delta\tilde{G}(\beta)$ as β changes is non-trivial. In the case of windmill graphs it is made easier by the fact that the smallest and the largest eigenvalues are solutions to a quadratic equation. Also, in the case of dumbbell graphs the eigenvalues are related algebraically. However, in both cases of windmill graphs and dumbbell graphs not everything can be done analytically. Though we can determine explicitly possible patterns of melting. Somewhat surprisingly we will show that the case when $s = 2$ is different from the case when $s > 2$ in windmill graphs. Also, in dumbbell graphs there are two possible patterns of melting, when $\eta > 2$ and $\eta = 2$.

4.1 Windmill Graphs

Windmill graphs are core-satellite graphs with $c = 1$; see Section 2.5.10. Therefore, in windmill graphs $W(\eta, s)$ there are s cliques of size η which share a common node. Hence, there are at most three different types of edges in the modified communicability graph of $W(\eta, s)$: edges between vertices in a clique, edges connecting vertices in a clique to the common node, and edges connecting vertices in different cliques.

To discuss melting, we use the explicit formulae for eigenvalues and normalized eigenvectors of the adjacency matrix of a windmill graph in Section 2.5.10 to construct the communicability function and hence the functions $\Delta G(\beta)$ and $\Delta\tilde{G}(\beta)$.

4.1.1 Communicability Function

To understand melting in windmill graphs, we need to compute the off-diagonal entries of $\Delta\tilde{G}(\beta)$. The diagonal elements of this matrix are uninteresting for the purposes of this work, since we are concerned with communicability measures between different nodes, and are therefore ignored. Moreover, since the case of $W(1, s)$ is that of a star graph, from now on we assume $\eta \geq 2$, in which case the second eigenvalue $\lambda_2 = \eta - 1$ is strictly positive.

We begin by finding an explicit expression for the off-diagonal entries of the matrix function $G(\beta) = e^{\beta A}$. The result is summarized in the following lemma.

Lemma 4.1.1. *Let $W(\eta, s) = (V, E)$ be a windmill graph and assume the nodes to be labelled as in the definition of A in (2.9). Moreover, suppose that the set $V \setminus \{1\}$ is partitioned into s subsets $V_1, V_2, \ldots, V_s$, each corresponding to a clique of η nodes in the graph. The communicability function $G(\beta)$ for all $p, q \in V$, $p \neq q$, is given by*

$$G_{pq}(\beta) = \begin{cases} -\lambda_n \alpha_1^2 e^{\beta\lambda_1} - \lambda_1 \alpha_2^2 e^{\beta\lambda_n} & \text{if } p = 1, q \neq 1 \text{ or } p \neq 1, q = 1, \\ \alpha_1^2 e^{\beta\lambda_1} - \frac{1}{s\eta} e^{\beta(\eta-1)} + \alpha_2^2 e^{\beta\lambda_n} & \text{if } p \in V_i, q \in V_j,\ 1 \leq i \neq j \leq s, \\ \alpha_1^2 e^{\beta\lambda_1} + \frac{s-1}{s\eta} e^{\beta(\eta-1)} - \frac{1}{\eta} e^{-\beta} + \alpha_2^2 e^{\beta\lambda_n} & \text{if } p, q \in V_j,\ 1 \leq j \leq s, \end{cases}$$

where

$$\alpha_1 = \frac{1}{\sqrt{\lambda_n^2 + s\eta}} \quad \textit{and} \quad \alpha_2 = \frac{1}{\sqrt{\lambda_1^2 + s\eta}},$$

and λ_1 *and* λ_n *are as in* (2.11) *and* (2.12)*, respectively.*

Proof. Throughout the proof, we make use of the results presented in Lemma 2.5.2 on the eigenvalues of A in (2.9), as well as the explicit expressions for the associated orthonormal eigenvectors described in (2.13)–(2.18). We also recall that the eigenvectors are partitioned according to the partition of A. First, we consider the case $p = 1, q \neq 1$; by symmetry of A, the result holds also for $p \neq 1, q = 1$. It is straightforward to see that

$$G_{1q}(\beta) = \sum_{k=1}^{n} x_k(1)x_k(q)e^{\beta\lambda_k} = -\lambda_n\alpha_1^2 e^{\beta\lambda_1} - \lambda_1\alpha_2^2 e^{\beta\lambda_n}.$$

Suppose now that $p \in V_i$ and $q \in V_j$, $i \neq j \in \{1, 2, \ldots, s\}$; we want to evaluate the expression

$$\begin{aligned} G_{pq}(\beta) = x_1(p)x_1(q)e^{\beta\lambda_1} + e^{\beta(\eta-1)} \sum_{k=2}^{s} x_k(p)x_k(q) \\ + e^{-\beta} \sum_{k=s+1}^{n-1} x_k(p)x_k(q) + x_n(p)x_n(q)e^{\beta\lambda_n}. \end{aligned}$$

We first note that $x_k(p)x_k(q) = 0$ for all $k = s+1, \ldots, n-1$, since the two nodes under consideration belong to distinct cliques, namely $p \in V_i$ and $q \in V_j$, and that $x_k(p)x_k(q) = \alpha_i^{(k)}\alpha_j^{(k)}$ for all $k = 2, \ldots, s$. Let $X = [\boldsymbol{x}_1, \boldsymbol{x}_2, \ldots, \boldsymbol{x}_n]$ be the orthonormal matrix of eigenvectors of A. Then, it is easy to verify that

$$0 = (XX^T)_{pq} = \alpha_1^2 + \sum_{k=2}^{s} \alpha_i^{(k)}\alpha_j^{(k)} + \alpha_2^2 \iff \sum_{k=2}^{s} \alpha_i^{(k)}\alpha_j^{(k)} = -(\alpha_1^2 + \alpha_2^2).$$

We therefore have

$$G_{pq}(\beta) = \alpha_1^2 e^{\beta\lambda_1} - (\alpha_1^2 + \alpha_2^2)e^{\beta(\eta-1)} + \alpha_2^2 e^{\beta\lambda_n},$$

from which the desired expression follows by noticing that

$$\alpha_1^2 + \alpha_2^2 = \frac{1}{s\eta}. \tag{4.1}$$

We now consider the final case, where the two nodes belong to the same clique $p, q \in V_j$, $j \in \{1, 2, \ldots, s\}$. Again, we want to evaluate

$$\begin{aligned} G_{pq}(\beta) = x_1(p)x_1(q)e^{\beta\lambda_1} + e^{\beta(\eta-1)} \sum_{k=2}^{s} x_k(p)x_k(q) \\ + e^{-\beta} \sum_{k=s+1}^{n-1} x_k(p)x_k(q) + x_n(p)x_n(q)e^{\beta\lambda_n}. \end{aligned}$$

The eigenvectors $\boldsymbol{y}_h$ of $A(K_\eta)$ that appear in (2.14) are orthogonal to the eigenvector $\mathbf{1}_\eta$ corresponding to the eigenvalue $\eta - 1$. Let $Y = \left[\frac{1}{\sqrt{\eta}}\mathbf{1}, \boldsymbol{y}_1, \ldots, \boldsymbol{y}_{\eta-1}\right]$ be the orthogonal matrix of eigenvectors of $A(K_\eta)$. Then,

$$0 = (YY^T)_{pq} = \frac{1}{\eta} + \sum_{h=1}^{\eta-1} y_h(p)y_h(q)$$

and hence

$$\sum_{k=s+1}^{n-1} x_k(p)x_k(q) = \sum_{h=1}^{\eta-1} y_h(p)y_h(q) = -\frac{1}{\eta}.$$

Moreover, from the orthonormality of the eigenvectors of A and (4.1) we can also deduce that

$$0 = (XX^T)_{pq} = \alpha_1^2 - \frac{1}{\eta} + \sum_{k=2}^{s} \left(\alpha_j^{(k)}\right)^2 + \alpha_2^2 \iff \sum_{k=2}^{s} \left(\alpha_j^{(k)}\right)^2 = \frac{s-1}{s\eta},$$

and hence

$$\sum_{k=2}^{s} x_k(p)x_k(q) = \sum_{k=2}^{s} \left(\alpha_j^{(k)}\right)^2 = \frac{s-1}{s\eta}.$$

Overall, we thus have

$$G_{pq}(\beta) = \alpha_1^2 e^{\beta\lambda_1} + \frac{s-1}{s\eta} e^{\beta(\eta-1)} - \frac{1}{\eta} e^{-\beta} + \alpha_2^2 e^{\beta\lambda_n}.$$

This concludes the proof. □

Now that the communicability function $G(\beta)$ between any two distinct nodes has been computed, we immediately obtain $\Delta G(\beta)$ by removing the $e^{\beta\lambda_1}$ terms from $G(\beta)$. As a result, we have:

$$\Delta G_{pq}(\beta) = \begin{cases} -\lambda_1\alpha_2^2 e^{\beta\lambda_n} & \text{if } p=1, q\neq 1 \text{ or } p\neq 1, q=1, \\ -\frac{1}{s\eta}e^{\beta(\eta-1)} + \alpha_2^2 e^{\beta\lambda_n} & \text{if } p\in V_i, q\in V_j,\ 1\leq i\neq j\leq s, \\ \frac{s-1}{s\eta}e^{\beta(\eta-1)} - \frac{1}{\eta}e^{-\beta} + \alpha_2^2 e^{\beta\lambda_n} & \text{if } p,q\in V_j,\ 1\leq j\leq s, \end{cases}$$

Next we need to understand the order relations among the different entries in $\Delta G(\beta)$. This will allow us to describe $\max_{p\neq q}\Delta G_{pq}(\beta)$ for $\beta > 0$ and, hence, define $\Delta\tilde{G}(\beta)$. We set

$$\begin{aligned} f_1(\beta) &= -\lambda_1\alpha_2^2 e^{\beta\lambda_n}, \\ f_2(\beta) &= -\frac{1}{s\eta}e^{\beta(\eta-1)} + \alpha_2^2 e^{\beta\lambda_n}, \\ f_3(\beta) &= \frac{s-1}{s\eta}e^{\beta(\eta-1)} - \frac{1}{\eta}e^{-\beta} + \alpha_2^2 e^{\beta\lambda_n}. \end{aligned}$$

Claim 4.1.2. *The function $f_3(\beta)$ is strictly increasing in β.*

Proof. Consider the derivative of $f_3(\beta)$,

$$f_3'(\beta) = \frac{(s-1)(\eta-1)}{s\eta}e^{\beta(\eta-1)} + \frac{1}{\eta}e^{-\beta} + \alpha_2^2\lambda_n e^{\beta\lambda_n}.$$

We will show, using Lemma 2.4.1, that this function has no zeros for $\beta\in[0,\infty)$. We have $\frac{(s-1)(\eta-1)}{s\eta} > 0$, and $\frac{(s-1)(\eta-1)}{s\eta} + \frac{1}{\eta} > 0$, since $s,\eta\geq 2$. Hence to use the above theorem, we need to show that $\frac{(s-1)(\eta-1)}{s\eta} + \frac{1}{\eta} + \alpha_2^2\lambda_n > 0$. Using the relations in

Remark 2.5.3 we get:

$$\begin{aligned}\frac{(s-1)(\eta-1)}{s\eta}+\frac{s}{s\eta}+\frac{\lambda_n}{s\eta+\lambda_1^2} &= \frac{\lambda_1\lambda_n+\lambda_1+\lambda_n}{\lambda_1\lambda_n}+\frac{\lambda_n}{\lambda_1(\lambda_1-\lambda_n)}\\ &= \frac{(\lambda_1-\lambda_n)(\lambda_1\lambda_n+\lambda_1+\lambda_n)+\lambda_n^2}{\lambda_1\lambda_n(\lambda_1-\lambda_n)}\\ &= \frac{\lambda_1^2\lambda_n+\lambda_1^2-\lambda_1\lambda_n^2}{\lambda_1\lambda_n(\lambda_1-\lambda_n)}=\frac{\lambda_1(1+\lambda_n)-\lambda_n^2}{\lambda_n(\lambda_1-\lambda_n)}>0,\end{aligned}$$

since $\lambda_n<-1$. Therefore $f_3'(\beta)$ has constant sign. Since for large β, $f_3'(\beta)$ is dominated by the positive $e^{\beta(\eta-1)}$ term, this means that $f_3(\beta)$ is strictly increasing. □

Claim 4.1.3. *$f_3(\beta)>f_2(\beta)$ for all $\beta\in(0,\infty)$.*

Proof. Since the derivative of $f_2(\beta)$ is always negative and, by Claim 4.1.2, $f_3(\beta)$ is strictly increasing, $f_3(\beta)-f_2(\beta)$ is a strictly increasing function. Furthermore,

$$f_3(0)-f_2(0)=\frac{s}{s\eta}-\frac{1}{\eta}=0,$$

so that $f_3(\beta)>f_2(\beta)$ for all $\beta>0$. □

Claim 4.1.4. *$f_3(\beta)>f_1(\beta)$ for all $\beta\in[0,\infty)$.*

Proof. Here, again, we use Lemma 2.4.1 and the equations described in Remark 2.5.3. The derivative of $f_3(\beta)-f_1(\beta)$ is

$$\big(f_3(\beta)-f_1(\beta)\big)'=\frac{(s-1)(\eta-1)}{s\eta}e^{\beta(\eta-1)}+\frac{1}{\eta}e^{-\beta}+\alpha_2^2(1+\lambda_1)\lambda_n e^{\beta\lambda_n},$$

$\frac{(s-1)(\eta-1)}{s\eta}>0$ and $\frac{(s-1)(\eta-1)}{s\eta}+\frac{1}{\eta}>0$ since $s,\eta\geq 2$. To show that the derivative is of one sign, we need to prove that $\frac{(s-1)(\eta-1)}{s\eta}+\frac{1}{\eta}+\alpha_2^2(1+\lambda_1)\lambda_n>0$. We have

$$\begin{aligned}\frac{(s-1)(\eta-1)}{s\eta}+\frac{s}{s\eta}+\frac{\lambda_n(1+\lambda_1)}{-\lambda_1\lambda_n+\lambda_1^2} &= \frac{\lambda_1\lambda_n+\lambda_1+\lambda_n}{\lambda_1\lambda_n}+\frac{\lambda_n(1+\lambda_1)}{\lambda_1(\lambda_1-\lambda_n)}\\ &= \frac{\lambda_1^2\lambda_n+\lambda_1^2}{\lambda_1\lambda_n(\lambda_1-\lambda_n)}=\frac{\lambda_1^2(1+\lambda_n)}{\lambda_1\lambda_n(\lambda_1-\lambda_n)}>0,\end{aligned}$$

since $\lambda_n<-1$. So the derivative of $f_3(\beta)-f_1(\beta)$ has constant sign; hence this function must be monotonic increasing as for large β the positive $e^{\beta(\eta-1)}$ term dominates. Now,

since

$$f_3(0) - f_1(0) = \frac{(s-1)}{s\eta} - \frac{1}{\eta} + \alpha_2^2 (1 + \lambda_1) = \frac{\lambda_1 (1 + \lambda_n)}{\lambda_1 \lambda_n (\lambda_1 - \lambda_n)} > 0$$

as $\lambda_n < -1$, we can conclude that $f_3(\beta) > f_1(\beta)$ for all $\beta \geq 0$. □

The take-home message from the previous three claims is that, for all $\beta \in [0, \infty)$, the maximum value of $\Delta G_{pq}(\beta)$ is attained by $f_3(\beta)$, i.e., at entries of $\Delta G(\beta)$ corresponding to two nodes that belong to the same clique. Hence, we have proved the following result.

Theorem 4.1.5. *Let $W(\eta, s) = (V, E)$ be a windmill graph and suppose that $s, \eta \geq 2$. Moreover, assume that the nodes are labelled as in the definition of A in (2.9) and that the set $V \setminus \{1\}$ is partitioned into s subsets $V_1, V_2, \ldots, V_s$, each corresponding to a clique of η nodes in the graph. Then, for all $p \neq q \in V$,*

$$\Delta \tilde{G}_{pq}(\beta) = \begin{cases} \frac{s-1}{s\eta} e^{\beta(\eta-1)} - \frac{1}{\eta} e^{-\beta} + (1 - \lambda_1)\alpha_2^2 e^{\beta\lambda_n} & \text{if } p = 1, q \neq 1 \text{ or } p \neq 1, q = 1 \\ \frac{s-2}{s\eta} e^{\beta(\eta-1)} - \frac{1}{\eta} e^{-\beta} + 2\alpha_2^2 e^{\beta\lambda_n} & \text{if } p \in V_i, q \in V_j,\ 1 \leq i \neq j \leq s \\ 2\left(\frac{s-1}{s\eta} e^{\beta(\eta-1)} - \frac{1}{\eta} e^{-\beta} + \alpha_2^2 e^{\beta\lambda_n}\right) & \text{if } p, q \in V_j,\ 1 \leq j \leq s. \end{cases}$$

4.1.2 Melting in Windmill Graphs

To characterize melting in windmill graphs, we need to understand in what order the functions $f_1(\beta) + f_3(\beta)$, $f_2(\beta) + f_3(\beta)$ and $2f_3(\beta)$, corresponding to the three different values appearing in the off-diagonal entries of $\Delta \tilde{G}(\beta)$, cross the β-axis and to ensure that such crossing point is unique for each function. We will show that these conditions are satisfied for $2f_3(\beta)$ and $f_1(\beta) + f_3(\beta)$, while they are satisfied for $f_2(\beta) + f_3(\beta)$ only when $s > 2$.

First of all, we have the following result.

Claim 4.1.6. *The function $2f_3(\beta)$ crosses the β-axis first and once.*

Proof. Note that

$$f_3(0) = -\frac{1}{s\eta} + \frac{1}{s\eta + \lambda_1^2} < 0.$$

The result follows from Claim 4.1.2 and the fact that for large β the function is dominated by the positive $e^{\beta(\eta-1)}$ term. The fact that this function crosses the β-axis first

follows immediately from Claims 4.1.3 and 4.1.4 □

We have already proved that

$$f_1(0) < f_3(0) = f_2(0) < 0; \tag{4.2}$$

see Claims 4.1.3 and 4.1.4. We also have the following result.

Claim 4.1.7. *The function $f_1(\beta) + f_3(\beta)$ is strictly increasing and crosses the β-axis once.*

Proof. Monotonicity is obvious as both $f_3(\beta)$ and $f_1(\beta)$ are strictly increasing; the first by Claim 4.1.2 and the second by inspection. The fact that $f_1(\beta) + f_3(\beta)$ crosses the β-axis once follows immediately as well, using (4.2) and the presence of the positive term $e^{\beta(\eta-1)}$ which dominates the function for large values of β. □

It remains to deal with $f_2(\beta) + f_3(\beta)$.

Claim 4.1.8. *The function $f_2(\beta) + f_3(\beta)$ is monotonic increasing.*

Proof. Consider the derivative

$$\big(f_2(\beta) + f_3(\beta)\big)' = \frac{(s-2)\,(\eta-1)}{s\eta} e^{\beta(\eta-1)} + \frac{1}{\eta} e^{-\beta} + 2\alpha_2^2 \lambda_n e^{\beta\lambda_n}.$$

Again, we apply Lemma 2.4.1. We will need to consider two separate cases: $s = 2$ and $s > 2$.

Suppose $s > 2$; the proof for $s = 2$ follows the same lines. We have $\frac{(s-2)(\eta-1)}{s\eta} > 0$ and $\frac{(s-2)(\eta-1)}{s\eta} + \frac{1}{\eta} > 0$. Now, we need to show that

$$\frac{(s-2)\,(\eta-1)}{s\eta} + \frac{1}{\eta} + 2\alpha_2^2\lambda_n = \frac{(s-2)\,(\eta-1)}{s\eta} + \frac{1}{\eta} + \frac{2\lambda_n}{s\eta + \lambda_1^2} > 0.$$

Note that

$$\frac{2\lambda_n}{s\eta + \lambda_1^2} = \frac{2\lambda_n}{\lambda_1(\lambda_1 - \lambda_n)} = \frac{2\lambda_n}{(\eta - 1 - \lambda_n)(\eta - 1 - 2\lambda_n)}.$$

Now, consider the function

$$g(x) = \frac{2x}{(\eta - 1 - x)(\eta - 1 - 2x)}$$

for $x < 0$. This function has a global minimum at some point $x_{\min} < 0$ and hence for all x we have that $g(x) \geq g(x_{\min})$. Differentiating, we have $x_{\min} = -\frac{\sqrt{2}}{2}(\eta - 1)$ and $g(x_{\min}) = -\frac{b}{\eta - 1}$, where

$$b = \frac{2\sqrt{2}}{(1 + \sqrt{2})(2 + \sqrt{2})}.$$

Clearly,

$$\frac{(s-2)(\eta - 1)}{s\eta} + \frac{1}{\eta} + 2\alpha_2^2\lambda_n \geq \frac{(s-2)(\eta - 1)}{s\eta} + \frac{1}{\eta} - \frac{b}{\eta - 1} > 0,$$

as $\eta \geq 2$. □

The proof just presented shows that there are two separate cases to consider when studying the zeros of $f_2(\beta) + f_3(\beta)$, namely, $s = 2$ and $s > 2$. The following result shows that, depending on the value of s, the function $f_2(\beta) + f_3(\beta)$ may or may not cross the β-axis.

Claim 4.1.9. *The function $f_2(\beta) + f_3(\beta)$*

- *crosses the β-axis once when $s > 2$; and*
- *never crosses the β-axis when $s = 2$.*

Proof. Suppose that $s > 2$. The result follows from (4.2) and from the fact that the function is dominated by the positive term $e^{\beta(\eta-1)}$ for large values of β. The result for the case $s = 2$ follows from (4.2), Claim 4.1.8, and the fact that

$$\lim_{\beta \to \infty} f_2(\beta) + f_3(\beta) = 0.$$

□

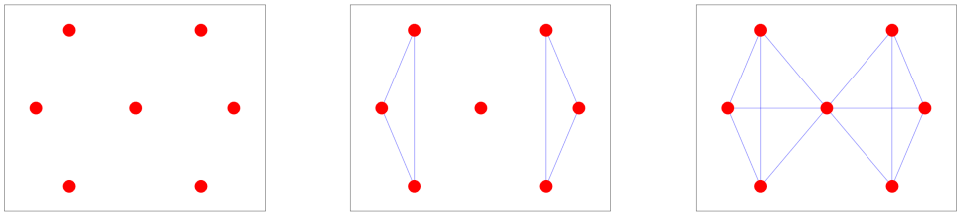

(a) $0 \leq \beta < \beta_3$ (b) $\beta_3 \leq \beta < \beta_1$ (c) $\beta \geq \beta_1$

Figure 4.1: Illustration of the structure of the modified communicability graph of $W(3,2)$ for different values of β.

4.1.3 Melting Signatures of Windmill Graphs

We want to discuss here how the structure of the modified communicability graph associated to a given $W(\eta, s)$ changes with $\beta \in [0, \infty)$. Throughout this section, we denote by $\beta_i = \beta_i(\eta, s)$ the unique point, if it exists, where the function $f_i(\beta) + f_3(\beta)$ crosses the β-axis, for $i = 1, 2, 3$. The simplest case to treat is when $s = 2$. In this case, Claims 4.1.4 and 4.1.9 allow us to conclude that the melting signature of $W(\eta, 2)$ is (β_3, β_1) for all $\eta \geq 2$. The melting of the associated modified communicability graph goes as follows. At $\beta = \beta_3$ the modified communicability graph of $W(\eta, 2)$ changes from being the null graph N_n to a collection of s complete graphs K_η, and at $\beta = \beta_1$ the modified communicability graph becomes just the graph $W(\eta, 2)$ itself. This means that there is no temperature at which the modified communicability graph of $W(\eta, 2)$ is the complete graph $K_{s\eta+1}$. As an example of this behaviour, in Figure 4.1 we show the evolution of the modified communicability graphs of $W(3, 2)$ as β varies.

Suppose now that $s > 2$. The graphs $W(\eta, s)$ have two possible melting signatures: $(\beta_3, \beta_2, \beta_1)$ and $(\beta_3, \beta_1, \beta_2)$. Below, we show that both are possible, and that most windmill graphs have $(\beta_3, \beta_2, \beta_1)$ as signature; however all $W(\eta, 3)$ graphs have $(\beta_3, \beta_1, \beta_2)$ as signature.

We start with yet another claim:

Claim 4.1.10. *The graphs of $f_1(\beta) + f_3(\beta)$ and $f_2(\beta) + f_3(\beta)$ always cross.*

This is obvious because $f_1(0) < f_2(0)$ by (4.2), and for large enough β, $f_1(\beta) + f_3(\beta)$ grows faster as $s - 1 > s - 2$.

The point of intersection β^* is unique, and in fact has a very neat expression:

$$\beta^*(\eta, s) = \frac{1}{\lambda_1} \ln \left[\frac{s\eta(1+\lambda_1)}{s\eta + \lambda_1^2} \right]. \tag{4.3}$$

Hence, the locus of points separating the values of (η, s) of graphs $W(\eta, s)$ with the $(\beta_3, \beta_2, \beta_1)$ signature from the ones with the $(\beta_3, \beta_1, \beta_2)$ signature, is given by $F(\eta, s) = 0$, where

$$F(\eta, s) := f_1\big(\beta^*(\eta, s)\big) + f_3\big(\beta^*(\eta, s)\big).$$

Indeed, when $F(\eta, s) < 0$ this means that the functions $f_1(\beta) + f_3(\beta)$ and $f_2(\beta) + f_3(\beta)$ intersect *before* crossing the β-axis, and hence the melting signature of the associated graph will be $(\beta_3, \beta_1, \beta_2)$. On the other hand, when $F(\eta, s) > 0$, the two functions will intersect *after* having crossed the β-axis, and thus the melting signature of the associated windmill graph will be $(\beta_3, \beta_2, \beta_1)$.

The zero set $F(\eta, s) = 0$ defines s as a function of η, $s = E(\eta)$, which can be plotted in the (η, s) plane. The graphs with (η, s) below the curve exhibit the $(\beta_3, \beta_1, \beta_2)$ signature. On the other hand, all graphs with (η, s) above the curve exhibit the $(\beta_3, \beta_2, \beta_1)$ signature.

In windmill graphs with the $(\beta_3, \beta_1, \beta_2)$ melting signature the transitions of the modified communicability graph are, as we increase β from 0, as follows: at β_3 there is a transition from the null graph to s separate K_η graphs, at β_1 the graph changes to a connected graph identical to $W(\eta, s)$ itself, and finally, at β_2 to the $K_{s\eta+1}$ graph. In windmill graphs with melting signature $(\beta_3, \beta_1, \beta_2)$, as we increase β from 0, the sequence is different: at β_3 there is a transition from the null graph to s separate K_η graphs, at β_2 the graph changes to a disconnected graph with two connected components, namely $K_{s\eta}$ and an isolated node, and finally at β_2, the modified communicability graph coincides with $K_{s\eta+1}$. In Figure 4.2, we show the evolution of the structure of the modified communicability graph of $W(3, 3)$, which exhibits the $(\beta_3, \beta_2, \beta_1)$ melting signature, while in Figure 4.3, we show the changes in the structure of the modified communicability graph of $W(4, 5)$, which has melting signature $(\beta_3, \beta_1, \beta_2)$.

The zero set $F(\eta, s) = 0$ is easily found numerically: it is found that $E(\eta)$ behaves

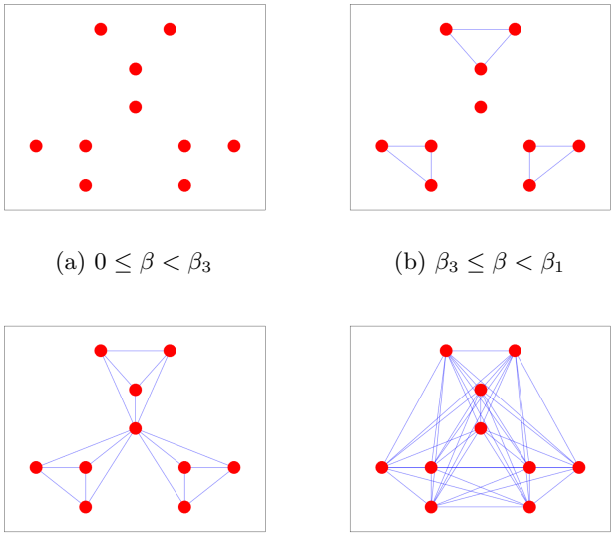

(a) $0 \leq \beta < \beta_3$ (b) $\beta_3 \leq \beta < \beta_1$

(c) $\beta_1 \leq \beta < \beta_2$ (d) $\beta \geq \beta_2$

Figure 4.2: Illustration of the structure of the modified communicability graph of $W(3,3)$ for different values of β.

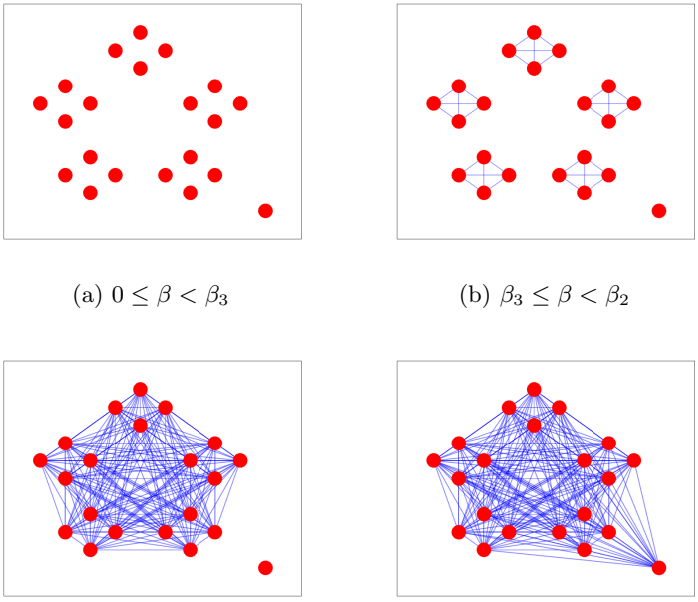

(a) $0 \leq \beta < \beta_3$ (b) $\beta_3 \leq \beta < \beta_2$

(c) $\beta_2 \leq \beta < \beta_1$ (d) $\beta \geq \beta_1$

Figure 4.3: Illustration of the structure of the modified communicability graph of $W(4,5)$ for different values of β.

as

$$E(\eta) \approx 3 + \frac{4.2}{\eta} + O\left(\frac{1}{\eta^2}\right),$$

and moreover the following statement has been verified numerically.

Conjecture 4.1.11. *$E(\eta)$ is a monotonically decreasing function of η, $E(2) \approx 5.06$ and*

$$\lim_{\eta\to\infty} E(\eta) = 3.$$

As we noted above, the graph of the function $E(\eta)$, plotted in magenta in Figure 4.4, separates, for $s > 2$, windmill graphs into two classes with different melting signatures. Let us call $\mathcal{S}_1$ the smaller class that has the $(\beta_3, \beta_1, \beta_2)$ signature and $\mathcal{S}_2$ the bigger one.

Now, the locus of points in the (η, s) plane, such that $\lambda_n = -3$ is given by

$$s = 3 + \frac{6}{\eta}.$$

We plot this function in blue in Figure 4.4. It is striking to see that, with the one exception of $W(4,5)$, the set of windmill graphs having $\lambda_n \leq -3$ coincides with the set $\mathcal{S}_2$. In this section, we have thus proved the following result which fully characterizes the melting signature of windmill graphs assuming Conjecture 4.1.11 is true.

Theorem 4.1.12. *Assuming Conjecture 4.1.11 is true, all graphs $W(\eta, 2)$ with $\eta \geq 2$ have the (β_3, β_1) melting signature; only the graphs $W(\eta, 3)$ for all $\eta \geq 2$, $W(2,4)$, $W(2,5)$, $W(3,4)$, and $W(4,4)$ have the $(\beta_3, \beta_1, \beta_2)$ signature; all other windmill graphs exhibit the $(\beta_3, \beta_2, \beta_1)$ signature.*

Conjecture 4.1.13. *The values of β_i for $i = 1, 2, 3$ in the melting signatures $(\beta_3, \beta_1, \beta_2)$, $(\beta_3, \beta_2, \beta_1)$ and (β_3, β_1) go to zero as η goes to infinity.*

4.1.4 Conclusions

We have been able to give a complete picture of the melting process in windmill graphs basically for two reasons: there are very few (just three) different types of edges, only

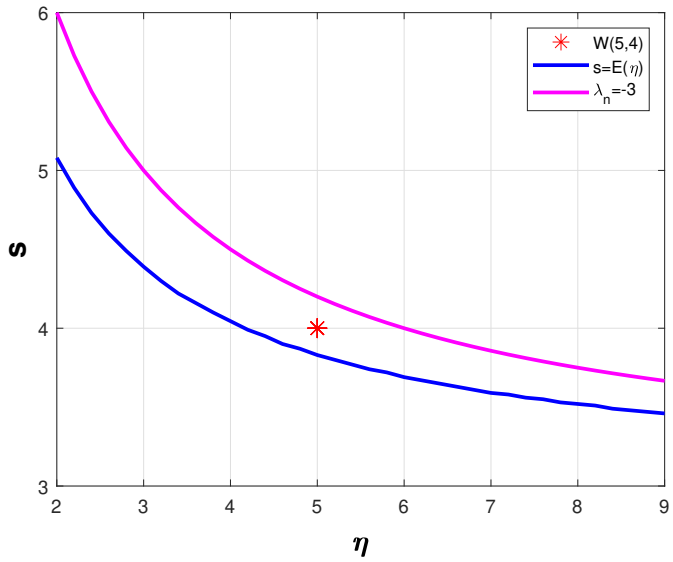

Figure 4.4: Graphs of the functions $s = E(\eta)$ (blue curve) and $s = 3 + \frac{6}{\eta}$ or $\lambda_n = -3$ (magenta curve).

four eigenvalues to deal with, so only three terms remain in $\Delta G(\beta)$ so that the Theorem of Jameson in Lemma 2.4.1 is relatively easy to apply, and finally the smallest eigenvalue λ_n and the largest one λ_1 are related by a quadratic equation.

We have proved analytically, and using numerical investigations, that for the whole class of windmill graphs $W(\eta, s)$ there are three types of melting signatures: (β_3, β_1) in the case of $s = 2$ and $(\beta_3, \beta_2, \beta_1)$ or $(\beta_3, \beta_1, \beta_2)$ in the case of $s > 2$. The evolution of the modified communicability graph of a graph with $s > 2$, as temperature is decreased to a sufficiently low value, gives us a modified communicability graph that is a complete graph, while for $s = 2$, we can only recover the graph $W(\eta, 2)$ itself and not $K_{2\eta+1}$. Also, the evolution of the modified communicability graph $(\beta_3, \beta_1, \beta_2)$ will include the graph $W(\eta, s)$, while that of $(\beta_3, \beta_2, \beta_1)$ will not include it.

4.2 Dumbbell graphs

Recall that in dumbbell graphs K_η–K_η there are two cliques of size η connected by an edge. Hence, there are at most five different types of edges in the modified communicability graph of K_η–K_η: edges between vertices in a clique, edges connecting the

two cliques, edges connecting vertices in a clique to the vertices in the other clique that connects the two cliques in the graph, and edges connecting vertices in different cliques. To discuss melting, we use the explicit formulae for eigenvalues and normalised eigenvectors of the adjacency matrix of a dumbbell graph in Section 2.5.13 to construct the communicability function of the graph and hence the functions $\Delta G(\beta)$ and $\Delta\tilde{G}(\beta)$. As the case of K_2–K_2 is that of a path graph which has four different types of edges in the modified communicability graph, and the case of $\eta \geq 3$ is that of a dumbbell graph which has five different types of edges in the modified communicability graph, we will consider the two cases separately, where in both cases the second eigenvalue λ_2 is positive.

4.2.1 Communicability Function

To understand melting in dumbbell graphs with $\eta \geq 3$, we need to compute the matrix function $\Delta\tilde{G}(\beta)$. First, we need the matrix function $\Delta G(\beta)$. We begin by finding an explicit expression for the off-diagonal entries of the matrix function $G(\beta) = e^{\beta A}$ by using the explicit formulae for eigenvalues and normalised eigenvectors of the adjacency matrix of a dumbbell graph in Section 2.5.13. The result is summarized in the following lemma.

Lemma 4.2.1. *Let K_η–$K_\eta = (V, E)$ be a dumbbell graph, and assume that the labelling of nodes is given by the matrix of A in (2.40). Moreover, suppose that the set V is partitioned into $V = V_1 \cup \{\eta\} \cup \{\eta + 1\} \cup V_2$, where $V_1 = \{1, 2, \ldots, \eta - 1\}$, and $V_2 = \{\eta + 2, \eta + 3, \ldots, 2\eta\}$. The communicability function $G_{pq}(\beta)$, for all $p \neq q \in V$,*

of K_η–K_η is given by

$$G_{pq}(\beta) = \begin{cases} \sum_{k\in\{1,2,3,n\}} \alpha_k^2 e^{\beta\lambda_j} - \frac{e^{-\beta}}{\eta-1} & \text{if } p,q \in V_1 \text{ or } p,q \in V_2 \\ \sum_{k\in\{1,2,3,n\}} (-1)^{k+1}\alpha_k^2 e^{\beta\lambda_k} & \text{if } p \in V_1, q \in V_2 \\ \sum_{k\in\{1,2,3,n\}} (\lambda_k - \eta + 2)\alpha_k^2 e^{\beta\lambda_k} & \text{if } p \in V_1, q = \eta \text{ or } p \in V_2, q = (\eta+1) \\ \sum_{k\in\{1,2,3,n\}} (-1)^{k+1}(\lambda_k - \eta + 2)\alpha_k^2 e^{\beta\lambda_k} & \text{if } p \in V_1, q = \eta+1 \text{ or } p \in V_2, q = \eta \\ \sum_{k\in\{1,2,3,n\}} (-1)^{k+1}(\lambda_k - \eta + 2)^2\alpha_k^2 e^{\beta\lambda_k} & \text{if } p = \eta, q = \eta+1 \end{cases} \tag{4.4}$$

where λ_1, λ_2, λ_3, and λ_n are defined in (2.66), (2.67), (2.68), *and* (2.69), *respectively, and α_k for all $k \in \{1,2,3,n\}$ are defined in* (2.71) *and* (2.73).

Proof. Throughout the proof, we will make use of the results presented in Theorem 2.5.13 and Lemma 2.5.14 on the eigenvalues in (2.66)–(2.69) and their associated orthonormal eigenvectors in (2.70), (2.72) and (2.47) of A in (2.40). We also recall that the eigenvectors are partitioned according to A. First, we consider the case when $p,q \in V_1$ or $p,q \in V_2$. We want to evaluate the expression

$$G_{pq}(\beta) = \sum_{k\in\{1,2,3,n\}} x_k(p)x_k(q)e^{\beta\lambda_k} + \sum_{k=4}^{n-1} x_k(p)x_k(q)e^{-\beta}. \tag{4.5}$$

The non-zero entries of the eigenvectors of A corresponding to $\lambda = -1$, the vectors $\mathbf{y}_{\eta-1}$ are the orthonormal eigenvectors of $A(K_{\eta-1})$ of the complete graph $K_{\eta-1}$ associated to the eigenvalue -1. Thus, if we let $Y = \left[\frac{1}{\sqrt{\eta-1}}\mathbf{1}, \mathbf{y}_1, \ldots, \mathbf{y}_{\eta-2}\right]$ be the orthonormal matrix of eigenvectors of $A(K_{\eta-1})$, it follows that

$$(YY^T)_{pq} = \frac{1}{\eta-1} + \sum_{h=1}^{\eta-2} y_h(p)y_h(q) = 0, \tag{4.6}$$

and hence,

$$\sum_{k=4}^{n-1} x_k(p)x_k(q) = \sum_{h=1}^{\eta-2} y_h(p)y_h(q) = -\frac{1}{\eta-1}. \tag{4.7}$$

Thus, by substituting (4.7), the eigenvalues λ_k, for $k = \{1, 2, 3, n\}$, and the entries $x_k(p)$, $x_k(q)$ of their corresponding orthonormal eigenvectors into (4.5), the desired expression follows immediately

$$G_{pq}(\beta) = \sum_{k\in\{1,2,3,n\}} \alpha_k^2 e^{\beta\lambda_k} - \frac{e^{-\beta}}{\eta-1}, \tag{4.8}$$

where α_k for $k \in \{1, 2, 3, n\}$ are defined in (2.71) and (2.73).

Consider now the case when $p \in V_1$, $q \in V_2$ or $q \in V_1$, $p \in V_2$. Again, we want to evaluate the expression

$$G_{pq}(\beta) = \sum_{k\in\{1,2,3,n\}} x_k(p)x_k(q)e^{\beta\lambda_k} + \sum_{k=4}^{n-1} x_k(p)x_k(q)e^{-\beta}. \tag{4.9}$$

The entry $x_k(p)x_k(q) = 0$, for all $k \in \{4, \ldots, n-1\}$, of all the eigenvectors that correspond to $\lambda = -1$. We have that

$$\sum_{k=4}^{n-1} x_k(p)x_k(q) = 0. \tag{4.10}$$

Thus, by substituting the eigenvalues λ_k , for $k = \{1, 2, 3, n\}$, and the entries $x_k(p)$, $x_k(q)$ of their corresponding orthonormal eigenvectors into (4.9), the desired expression follows immediately

$$G_{pq}(\beta) = \sum_{k\in\{1,2,3,n\}} (-1)^{k+1}\alpha_k^2 e^{\beta\lambda_k}, \tag{4.11}$$

where α_k for $k \in \{1, 2, 3, n\}$ are defined in (2.71) and (2.73).

In the last three cases where at least one of p and q is in $\{\eta, \eta+1\}$, we substitute the eigenvalues and eigenvectors of A into $G_{pq}(\beta) = \sum_{k=1}^{n} x_k(p)x_k(q)e^{\beta\lambda_k}$, to obtain

$$G_{pq}(\beta) = \sum_{k\in\{1,2,3,n\}} x_k(p)x_k(q)e^{\beta\lambda_k}, \tag{4.12}$$

since the entries η and $\eta+1$ of all the eigenvectors that correspond the eigenvalue $\lambda=-1$, are zeros and so $x_k(\eta)=x_k(\eta+1)=0$ for all $k\in\{4,5,\ldots,n-1\}$. Thus, by substituting the eigenvalues λ_k, $k=\{1,2,3,n\}$, and their corresponding orthonormal eigenvectors into (4.12), the desired expressions follow immediately. In particular,

- when $p\in V_1, q=\eta$ or $p\in V_2, q=(\eta+1)$, we have

$$G_{pq}(\beta)=\sum_{k\in\{1,2,3,n\}}(\lambda_k-\eta+2)\alpha_k^2 e^{\beta\lambda_k};$$

- when $p\in V_1, q=\eta+1$ or $p\in V_2, q=\eta$, we have

$$G_{pq}(\beta)=\sum_{k\in\{1,2,3,n\}}(-1)^{k+1}(\lambda_k-\eta+2)\alpha_k^2 e^{\beta\lambda_k};$$

- when $p=\eta$, $q=\eta+1$, we have

$$G_{pq}(\beta)=\sum_{k\in\{1,2,3,n\}}(-1)^{k+1}(\lambda_k-\eta+2)^2\alpha_k^2 e^{\beta\lambda_k},$$

where α_k, for $k\in\{1,2,3,n\}$, are defined in (2.71) and (2.73) and λ_1, λ_2, λ_3, and λ_n are defined in (2.66), (2.67), (2.68), and (2.69), respectively. So, we obtain the desired result.

□

Once the communicability function $G(\beta)$ has been computed, we immediately obtain $\Delta G(\beta)$ by removing the $e^{\beta\lambda_1}$ terms from $G(\beta)$. As a result, we have:

$$\Delta G_{pq}(\beta) = \begin{cases} \sum_{k=\{2,3,n\}} \alpha_k^2 e^{\beta\lambda_k} - \frac{e^{-\beta}}{\eta-1} & \text{if } p,q \in V_1 \text{ or } p,q \in V_2 \\ \sum_{k=\{2,3,n\}} (-1)^{k+1} \alpha_k^2 e^{\beta\lambda_k} & \text{if } p \in V_1, q \in V_2 \\ \sum_{k=\{2,3,n\}} (\lambda_k - \eta + 2)\alpha_k^2 e^{\beta\lambda_k} & \text{if } p \in V_1, q = \eta \text{ or } p \in V_2, q = (\eta+1) \\ \sum_{k=\{2,3,n\}} (-1)^{k+1} (\lambda_k - \eta + 2)\alpha_k^2 e^{\beta\lambda_k} & \text{if } p \in V_1, q = \eta+1 \text{ or } p \in V_2, q = \eta \\ \sum_{k=\{2,3,n\}} (-1)^{k+1} (\lambda_k - \eta + 2)^2 \alpha_k^2 e^{\beta\lambda_k} & \text{if } p = \eta, q = \eta+1. \end{cases} \tag{4.13}$$

Next, we need to understand the order relations among the different entries in $\Delta G_{pq}(\beta)$. This will allow us to describe $\max_{p\neq q} \Delta G_{pq}(\beta)$ for $\beta > 0$ and, hence, define $\Delta \tilde{G}_{pq}(\beta)$. We introduce the following functions, which are equal to the entries in $\Delta \tilde{G}_{pq}(\beta)$:

$$f_1(\beta) = \sum_{k\in\{2,3,n\}} \alpha_k^2 e^{\beta\lambda_k} - \frac{e^{-\beta}}{\eta-1}, \tag{4.14}$$

$$f_2(\beta) = \sum_{k\in\{2,3,n\}} (-1)^{k+1} \alpha_k^2 e^{\beta\lambda_k}, \tag{4.15}$$

$$f_3(\beta) = \sum_{k\in\{2,3,n\}} (\lambda_k - \eta + 2)\alpha_k^2 e^{\beta\lambda_k}, \tag{4.16}$$

$$f_4(\beta) = \sum_{k\in\{2,3,n\}} (-1)^{k+1} (\lambda_k - \eta + 2)\alpha_k^2 e^{\beta\lambda_k}, \tag{4.17}$$

$$f_5(\beta) = \sum_{k\in\{2,3,n\}} (-1)^{k+1} (\lambda_k - \eta + 2)^2 \alpha_k^2 e^{\beta\lambda_k}. \tag{4.18}$$

Claim 4.2.2. *For all $\eta \geq 2$, we have that*

$$\sum_{k\in\{1,2,3,n\}} \alpha_k^2 = \frac{1}{\eta-1} \qquad \text{and} \qquad \sum_{k\in\{1,2,3,n\}} (-1)^{k+1} \alpha_k^2 = 0, \tag{4.19}$$

where α_k, for $k \in \{1,2,3,n\}$, are defined in (2.71) *and* (2.73).

Note that n is an even number.

Proof. Let $p, q \in V_1$ or $p, q \in V_2$. From the orthonormality of the eigenvectors of A of a dumbbell graph, we can deduce that

$$\begin{aligned} & \sum_{k\in\{1,2,3,n\}} x_k(p)x_k(q) + \sum_{k=4}^{n-1} x_k(p)x_k(q) = 0 \\ \Rightarrow \quad & \sum_{k\in\{1,2,3,n\}} \alpha_k^2 + \sum_{k=4}^{n-1} x_k(p)x_k(q) = 0 \\ \Rightarrow \quad & \sum_{k=4}^{n-1} x_k(p)x_k(q) = -\sum_{k\in\{1,2,3,n\}} \alpha_k^2, \end{aligned}$$

and from (4.7) we obtain the first relation in (4.19).

Now, let $p \in V_1$, $q \in V_2$ or $q \in V_1$, $p \in V_2$. From the orthonormality of the eigenvectors of A of a dumbbell graph, we can also deduce that

$$\begin{aligned} & \sum_{k\in\{1,2,3,n\}} x_k(p)x_k(q) + \sum_{k=4}^{n-1} x_k(p)x_k(q) = 0 \\ \Rightarrow & \sum_{k\in\{1,2,3,n\}} (-1)^{k+1}\alpha_k^2 + \sum_{k=4}^{n-1} x_k(p)x_k(q) = 0 \\ \Rightarrow \quad & \sum_{k=4}^{n-1} x_k(p)x_k(q) = -\sum_{k\in\{1,2,3,n\}} (-1)^{k+1}\alpha_k^2. \end{aligned}$$

We now obtain the second relation in (4.19) from (4.10). □

Claim 4.2.3. *For $\eta \geq 2$ and $B = \{1, 2, 3, n\}$, we have*

$$\sum_{k\in B} \lambda_k^m \alpha_k^2 = \frac{P_m(\eta)}{\eta - 1}, \qquad \sum_{k\in B} (-1)^{k+1} \lambda_k^m \alpha_k^2 = Q_m(\eta), \qquad m = 0, 1, 2, 3, 4, \tag{4.20}$$

where

$$\begin{aligned} P_0(\eta) &= 1, \\ P_1(\eta) &= \eta - 2, \\ P_2(\eta) &= \eta^2 - 3\eta + 3, \\ P_3(\eta) &= \eta^3 - 4\eta^2 + 6\eta - 4, \\ P_4(\eta) &= \eta^4 - 5\eta^3 + 10\eta^2 - 9\eta + 4, \end{aligned}$$

and

$$Q_0(\eta) = 0, \qquad Q_1(\eta) = 0, \qquad Q_2(\eta) = 0, \qquad Q_3(\eta) = 1, \qquad Q_4(\eta) = 2(\eta - 2).$$

Proof. Set

$$a_m(\eta) = \lambda_1^m \alpha_1^2 + \lambda_3^m \alpha_3^2, \qquad b_m(\eta) = \lambda_2^m \alpha_2^2 + \lambda_n^m \alpha_n^2, \qquad m = 0, 1, 2, \ldots.$$

From Claim 4.2.2 we obtain

$$\begin{aligned} a_0(\eta) &= \frac{1}{2}\left[\sum_{k\in\{1,2,3,n\}} \alpha_k^2 + \sum_{k\in\{1,2,3,n\}} (-1)^{k+1} \alpha_k^2 \right] = \frac{1}{2(\eta - 1)}, \\ b_0(\eta) &= \frac{1}{2}\left[\sum_{k\in\{1,2,3,n\}} \alpha_k^2 - \sum_{k\in\{1,2,3,n\}} (-1)^{k+1} \alpha_k^2 \right] = \frac{1}{2(\eta - 1)}. \end{aligned}$$

A lengthy but elementary calculation yields

$$a_1(\eta) = b_1(\eta) = \frac{\eta - 2}{2(\eta - 1)}.$$

Since λ_1, λ_3 satisfy the quadratic equation (2.51), we obtain the recurrence relation (for

$m \geq 2$):

$$\begin{aligned} a_m(\eta) &= \lambda_1^2 \lambda_1^{m-2} \alpha_1^2 + \lambda_3^2 \lambda_3^{m-2} \alpha_3^2 \\ &= \big[(\eta-1)\lambda_1 + 1\big] \lambda_1^{m-2} \alpha_1^2 + \big[(\eta-1)\lambda_3 + 1\big] \lambda_3^{m-2} \alpha_3^2 \\ &= (\eta-1) a_{m-1}(\eta) + a_{m-2}(\eta). \end{aligned}$$

In a similar way, we can use (2.56) to deduce the recurrence relation

$$b_m(\eta) = (\eta-3) b_{m-1}(\eta) + (2\eta-3) b_{m-2}(\eta)$$

for $m \geq 2$. With these recurrence relations we obtain

$$\begin{aligned} a_2(\eta) &= \frac{\eta^2 - 3\eta + 3}{2(\eta-1)}, & b_2(\eta) &= \frac{\eta^2 - 3\eta + 3}{2(\eta-1)}, \\ a_3(\eta) &= \frac{\eta^3 - 4\eta^2 + 7\eta - 5}{2(\eta-1)}, & b_3(\eta) &= \frac{\eta^3 - 4\eta^2 + 5\eta - 3}{2(\eta-1)}, \\ a_4(\eta) &= \frac{\eta^4 - 5\eta^3 + 12\eta^2 - 15\eta + 8}{2(\eta-1)}, & b_4(\eta) &= \frac{\eta^4 - 5\eta^3 + 8\eta^2 - 3\eta}{2(\eta-1)}. \end{aligned}$$

Now, with

$$\sum_{k \in B} \lambda_k^m \alpha_k^2 = a_m(\eta) + b_m(\eta) \qquad \text{and} \qquad \sum_{k \in B} (-1)^{k+1} \lambda_k^m \alpha_k^2 = a_m(\eta) - b_m(\eta)$$

we arrive at the relations (4.20) with the stated $P_m(\eta)$ and $Q_m(\eta)$. □

Claim 4.2.4. *Let α_k, for $k \in \{1, 2, 3, n\}$, be as in* (2.71) *and* (2.73)*. For all $\eta \geq 3$, we have*

$$\alpha_2^2 > \alpha_3^2 > \alpha_n^2; \tag{4.21}$$

for $\eta = 2$, we have

$$\alpha_2^2 = \alpha_3^2 > \alpha_n^2 = \alpha_1^2. \tag{4.22}$$

Proof. Define the function

$$h(x) = \frac{1}{2(x-(\eta-2))^2 + 2(\eta-1)}.$$

This function has a unique maximum at $x = \eta - 2$ and is even around the line $x = \eta - 2$. Further, we have $h(\lambda_k) = \alpha_k^2$ for $k \in \{1, 2, 3, n\}$. For $\eta \geq 3$ the result follows from the inequalities

$$|\lambda_2 - (\eta-2)| < 1 \leq \eta - 2 < |\lambda_3 - (\eta-2)| < \eta - 1 < |\lambda_n - (\eta-2)|,$$

which, in turn, are obtained from Lemma 2.5.14. For $\eta = 2$, we have $\lambda_1 = \frac{1}{2} + \frac{\sqrt{5}}{2} = -\lambda_n$ and $\lambda_2 = -\frac{1}{2} + \frac{\sqrt{5}}{2} = -\lambda_3$, which yields (4.22). □

Claim 4.2.5. *$f_1(\beta)$ is strictly increasing in β for $\eta \geq 3$.*

Proof. Consider the derivative of $f_1(\beta)$,

$$f_1'(\beta) = \sum_{k \in \{2,3,n\}} \lambda_k \alpha_k^2 e^{\beta \lambda_k} + \frac{e^{-\beta}}{\eta - 1}.$$

We shall use Lemma 2.4.1 to show that the function $f_1'(\beta)$ has no zeros in $(0, \infty)$. First, we have $\lambda_2 \alpha_2^2 > 0$. Second, we consider $\lambda_2 \alpha_2^2 + \lambda_3 \alpha_3^2$. The bounds in Lemma 2.5.14 imply that $\lambda_2 > \eta - 2 \geq 1$ and $-1 < \lambda_3 < 0$ and hence $\lambda_2 + \lambda_3 \geq 0$. Further, Claim 4.2.4 yields $\alpha_2^2 > \alpha_3^2$. Hence, we obtain

$$\lambda_2 \alpha_2^2 + \lambda_3 \alpha_3^2 \geq (\lambda_2 + \lambda_3)\alpha_3^2 \geq 0.$$

This, in turn, also implies

$$\lambda_2 \alpha_2^2 + \lambda_3 \alpha_3^2 + \frac{1}{\eta - 1} > 0.$$

Finally, we use $\frac{1}{\eta - 1} = \sum_{k \in \{1,2,3,n\}} \alpha_k^2$ (see Claim 4.2.3), $\lambda_2 + \lambda_n = \eta - 3$, and $\alpha_2^2 > \alpha_n^2$

(see Claim 4.2.4) to obtain

$$\begin{aligned}\sum_{k\in\{2,3,n\}} \lambda_k\alpha_k^2 + \frac{1}{\eta-1} &= \lambda_2\alpha_2^2 + \lambda_3\alpha_3^2 + \lambda_n\alpha_n^2 + \sum_{k\in\{1,2,3,n\}} \alpha_k^2,\\ &= \lambda_2\alpha_2^2 + \lambda_3\alpha_3^2 + \big((\eta-3)-\lambda_2\big)\alpha_n^2 + \sum_{k\in\{1,2,3,n\}} \alpha_k^2\\ &= (\alpha_2^2-\alpha_n^2)\lambda_2 + (\eta-2)\alpha_n^2 + (1+\lambda_3)\alpha_3^2 + \alpha_2^2 + \alpha_1^2 > 0.\end{aligned}$$

Hence, $f_1'(\beta)$ has constant sign by Lemma 2.4.1. Since, for large β, $f_1'(\beta)$ is dominated by the positive $e^{\beta\lambda_2}$ term, we can deduce that $f_1'(\beta) > 0$ for $\beta \in (0,\infty)$, and therefore f_1 is strictly increasing. □

Claim 4.2.6. *$f_3(\beta)$ is strictly increasing in β.*

Proof. Consider the derivative of $f_3(\beta)$,

$$f_3'(\beta) = \sum_{k\in\{2,3,n\}} (\lambda_k - \eta + 2)\lambda_k\alpha_k^2 e^{\beta\lambda_k}.$$

We shall use, again, Lemma 2.4.1 to show that the function f_3' has no zero in $(0,\infty)$. Using the bounds for the eigenvalues in Lemma 2.5.14 we have that $(\lambda_2-\eta+2)\lambda_2\alpha_2^2 > 0$, $(\lambda_3-\eta+2)\lambda_3\alpha_3^2 > 0$, $(\lambda_n-\eta+2)\lambda_n\alpha_n^2 > 0$, and therefore

$$\begin{aligned}&(\lambda_2-\eta+2)\lambda_2\alpha_2^2 + (\lambda_3-\eta+2)\lambda_3\alpha_3^2 > 0,\\ &(\lambda_2-\eta+2)\lambda_2\alpha_2^2 + (\lambda_3-\eta+2)\lambda_3\alpha_3^2 + (\lambda_n-\eta+2)\lambda_n\alpha_n^2 > 0.\end{aligned}$$

Now, Lemma 2.4.1 implies that f_3' has no zero in $(0,\infty)$. Since for large β, $f_3'(\beta)$ is dominated by the positive $e^{\beta\lambda_2}$ term, this implies that $f_3'(\beta) > 0$ for all $\beta \in (0,\infty)$, and hence $f_3(\beta)$ is strictly increasing. □

Claim 4.2.7. *$f_1(\beta) > f_3(\beta)$ for all $\beta \in [0,\infty)$.*

Proof. We rewrite the function $f_1(\beta) - f_3(\beta)$ to be in the form

$$f_1(\beta) - f_3(\beta) = e^{-\beta}\left[\sum_{k\in\{2,3,n\}} (-\lambda_k+\eta-1)\alpha_k^2 e^{\beta(\lambda_k+1)} - \frac{1}{(\eta-1)}\right]. \tag{4.23}$$

Let $H(\beta)$ be the expression within the square brackets, i.e.

$$H(\beta) = \sum_{k\in\{2,3,n\}} (-\lambda_k + \eta - 1)\alpha_k^2 e^{\beta(\lambda_k+1)} - \frac{1}{\eta-1},$$

and consider the derivative of H,

$$H'(\beta) = \sum_{k\in\{2,3,n\}} (-\lambda_k + \eta - 1)(\lambda_k+1)\alpha_k^2 e^{\beta(\lambda_k+1)}.$$

We will show that the function $H'(\beta)$ has no zeros in $(0,\infty)$. The bounds in Lemma 2.5.14 yield $\eta - 2 < \lambda_2 < \eta - 1$ and $-1 < \lambda_3 < 0$ and hence

$$\begin{aligned}
&(-\lambda_2 + \eta - 1)(\lambda_2+1)\alpha_2^2 > 0,\\
&(-\lambda_2 + \eta - 1)(\lambda_2+1)\alpha_2^2 + (-\lambda_3 + \eta - 1)(\lambda_3+1)\alpha_3^2 > 0.
\end{aligned}$$

Further, we obtain from Claim 4.2.3 that

$$\begin{aligned}
&\sum_{k\in\{2,3,n\}} (-\lambda_k + \eta - 1)(\lambda_k+1)\alpha_k^2\\
&= \sum_{k\in\{1,2,3,n\}} (-\lambda_k + \eta - 1)(\lambda_k+1)\alpha_k^2 + (\lambda_1 - \eta + 1)(\lambda_1+1)\alpha_1^2\\
&= \sum_{k\in\{1,2,3,n\}} \left(-\lambda_k^2\alpha_k^2 + (\eta-2)\lambda_k\alpha_k^2 + (\eta-1)\alpha_k^2\right) + (\lambda_1 - \eta + 1)(\lambda_1+1)\alpha_1^2\\
&= -\frac{\eta^2 - 3\eta + 3}{\eta-1} + \frac{(\eta-2)^2}{\eta-1} + \frac{\eta-1}{\eta-1} + (\lambda_1 - \eta + 1)(\lambda_1+1)\alpha_1^2\\
&= (\lambda_1 - \eta + 1)(\lambda_1+1)\alpha_1^2 > 0.
\end{aligned}$$

Therefore, $H'(\beta)$ has constant sign by Lemma 2.4.1. Since, for large β, $H'(\beta)$ is dominated by the positive $e^{\beta\lambda_2}$ term, we obtain that $H'(\beta) > 0$ for $\beta \in (0,\infty)$, and hence

H is strictly increasing on $[0,\infty)$. We use, again, Claim 4.2.3 to obtain

$$\begin{aligned}
H(0) &= \sum_{k\in\{2,3,n\}} (-\lambda_k+\eta-1)\alpha_k^2 - \frac{1}{\eta-1} \\
&= \sum_{k\in\{1,2,3,n\}} (-\lambda_k+\eta-1)\alpha_k^2 + (\lambda_1-\eta+1)\alpha_1^2 - \frac{1}{\eta-1} \\
&= \sum_{k\in\{1,2,3,n\}} \Big(-\lambda_k\alpha_k^2 + (\eta-1)\alpha_k^2\Big) + (\lambda_1-\eta+1)\alpha_1^2 - \frac{1}{\eta-1} \\
&= -\frac{\eta-2}{\eta-1} + \frac{\eta-1}{\eta-1} + (\lambda_1-\eta+1)\alpha_1^2 - \frac{1}{\eta-1} \\
&= (\lambda_1-\eta+1)\alpha_1^2 > 0,
\end{aligned}$$

which, together with the monotonicity of H, implies that $H(\beta) > 0$ for $\beta \in [0,\infty)$. Now (4.23) shows that $f_1(\beta) > f_3(\beta)$ for $\beta \in [0,\infty)$. □

Claim 4.2.8. *$f_3(\beta) > f_4(\beta)$ for all $\beta \in (0,\infty)$.*

Proof. Consider the function

$$f_3(\beta) - f_4(\beta) = 2(\lambda_2-\eta+2)\alpha_2^2 e^{\beta\lambda_2} + 2(\lambda_n-\eta+2)\alpha_n^2 e^{\beta\lambda_n}.$$

Both summands on the right-hand side are strictly increasing functions of β since $\lambda_2 > 0$, $\lambda_2-\eta+2 > 0$, $\lambda_n < 0$ and $\lambda_n-\eta+2 = -\lambda_2-1 < 0$. Hence $f_3(\beta) - f_4(\beta)$ is strictly increasing in β. It follows from Claim 4.2.3 that

$$\alpha_2^2 + \alpha_n^2 = \frac{1}{2}\left[\sum_{k\in\{1,2,3,n\}} \alpha_k^2 - \sum_{k\in\{1,2,3,n\}} (-1)^{k+1}\alpha_k^2\right] = \frac{1}{2(\eta-1)}$$

and

$$\lambda_2\alpha_2^2 + \lambda_n\alpha_n^2 = \frac{1}{2}\left[\sum_{k\in\{1,2,3,n\}} \lambda_k\alpha_k^2 - \sum_{k\in\{1,2,3,n\}} (-1)^{k+1}\lambda_k\alpha_k^2\right] = \frac{\eta-2}{2(\eta-1)}.$$

From this we obtain

$$\begin{aligned} f_3(0) - f_4(0) &= 2(\lambda_2 - \eta + 2)\alpha_2^2 + 2(\lambda_n - \eta + 2)\alpha_n^2 \\ &= 2\big(\lambda_2\alpha_2^2 + \lambda_n\alpha_n^2\big) - 2(\eta - 2)\big(\alpha_2^2 + \alpha_n^2\big) \\ &= \frac{\eta - 2}{\eta - 1} - (\eta - 2)\frac{1}{\eta - 1} = 0. \end{aligned}$$

Together with the monotonicity of $f_3(\beta) - f_4(\beta)$, this implies that $f_3(\beta) - f_4(\beta) > 0$ for $\beta \in (0, \infty)$. □

Claim 4.2.9. *$f_2(\beta)$ is strictly decreasing in β.*

Proof. Consider the derivative of $f_2(\beta)$, $f_2'(\beta) = \sum_{k\in\{2,3,n\}}(-1)^{k+1}\alpha_k^2\lambda_k e^{\beta\lambda_k}$. We will use Lemma 2.4.1 to show that the function $f_2'(\beta)$ has no zeros for $\beta \in (0, \infty)$. Since $\lambda_2 > 0$ and $\lambda_3 < 0$, we have $-\alpha_2^2\lambda_2 < 0$ and $-\alpha_2^2\lambda_2 + \alpha_3^2\lambda_3 \leq 0$. Further, from Claim 4.2.3, we obtain

$$-\alpha_2^2\lambda_2 + \alpha_3^2\lambda_3 - \alpha_n^2\lambda_n = \sum_{k\in\{1,2,3,n\}}(-1)^{k+1}\alpha_k^2\lambda_k - \alpha_1^2\lambda_1 = -\alpha_1^2\lambda_1 < 0.$$

Therefore, $f_2'(\beta)$ has constant sign on $(0, \infty)$ by Lemma 2.4.1. Since for large β, $f_2'(\beta)$ is dominated by the negative $e^{\beta\lambda_2}$ term, $f_2'(\beta) < 0$ for $\beta \in (0, \infty)$ and hence $f_2(\beta)$ is strictly decreasing. □

Claim 4.2.10. *$f_3(\beta) > f_5(\beta)$ for all $\beta \in [0, \infty)$.*

Proof. Let us consider

$$f_3(\beta) - f_5(\beta) = \sum_{k\in\{2,3,n\}}\Big[(\lambda_k - \eta + 2) - (-1)^{k+1}(\lambda_k - \eta + 2)^2\Big]\alpha_k^2 e^{\beta\lambda_k}.$$

We use Lemma 2.4.1 to show that its derivative,

$$\big(f_3(\beta) - f_5(\beta)\big)' = \sum_{k\in\{2,3,n\}}\Big[(\lambda_k - \eta + 2) - (-1)^{k+1}(\lambda_k - \eta + 2)^2\Big]\lambda_k\alpha_k^2 e^{\beta\lambda_k},$$

has no zero in $(0,\infty)$. First, we know from Lemma 2.5.14 that $\lambda_2-\eta+2>0$ and hence

$$\big[(\lambda_2-\eta+2)+(\lambda_2-\eta+2)^2\big]\lambda_2\alpha_2^2>0.$$

Lemma 2.5.14 also implies that $\lambda_3<0$ and $\lambda_3-\eta+2<0$, which yields

$$\big[(\lambda_2-\eta+2)+(\lambda_2-\eta+2)^2\big]\lambda_2\alpha_2^2+\big[(\lambda_3-\eta+2)-(\lambda_3-\eta+2)^2\big]\lambda_3\alpha_3^2>0.$$

Finally, we obtain from Claim 4.2.3 that

$$\begin{aligned}
&\sum_{k\in\{2,3,n\}}\Big[(\lambda_k-\eta+2)-(-1)^{k+1}(\lambda_k-\eta+2)^2\Big]\lambda_k\alpha_k^2\\
&=\sum_{k\in\{1,2,3,n\}}\Big[(\lambda_k-\eta+2)-(-1)^{k+1}(\lambda_k-\eta+2)^2\Big]\lambda_k\alpha_k^2\\
&\quad-\big[(\lambda_1-\eta+2)-(\lambda_1-\eta+2)^2\big]\lambda_1\alpha_1^2\\
&=\sum_{k\in\{1,2,3,n\}}\Big[\lambda_k^2\alpha_k^2-(\eta-2)\lambda_k\alpha_k^2-(-1)^{k+1}\lambda_k^3\alpha_k^2+2(\eta-2)(-1)^{k+1}\lambda_k^2\alpha_k^2\\
&\quad-(\eta-2)^2\lambda_k\alpha_k^2\Big]+\big[(\lambda_1-\eta+2)^2-(\lambda_1-\eta+2)\big]\lambda_1\alpha_1^2\\
&=\frac{\eta^2-3\eta+3}{\eta-1}-(\eta-2)\frac{\eta-2}{\eta-1}-1+\big[(\lambda_1-\eta+2)^2-(\lambda_1-\eta+2)\big]\lambda_1\alpha_1^2\\
&=\big[(\lambda_1-\eta+2)^2-(\lambda_1-\eta+2)\big]\lambda_1\alpha_1^2>0;
\end{aligned}$$

the last inequality follows since $\lambda_1-\eta+2>1$ by Lemma 2.5.14. Hence, Lemma 2.4.1 implies that $(f_3(\beta)-f_5(\beta))'$ does not change sign in $(0,\infty)$. Since $(f_3(\beta)-f_5(\beta))'$ is dominated by the positive $e^{\beta\lambda_2}$ term, $(f_3(\beta)-f_5(\beta))'>0$ for $\beta\in(0,\infty)$, and therefore $f_3(\beta)-f_5(\beta)$ is monotonic increasing. Now we consider the value at 0: with Claim 4.2.3 we obtain

$$\begin{aligned}
f_3(0)-f_5(0)&=\sum_{k\in\{2,3,n\}}\Big[(\lambda_k-\eta+2)-(-1)^{k+1}(\lambda_k-\eta+2)^2\Big]\alpha_k^2\\
&=\sum_{k\in\{1,2,3,n\}}\Big[(\lambda_k-\eta+2)-(-1)^{k+1}(\lambda_k-\eta+2)^2\Big]\alpha_k^2\\
&\quad-\big[(\lambda_1-\eta+2)-(\lambda_1-\eta+2)^2\big]\alpha_1^2
\end{aligned}$$

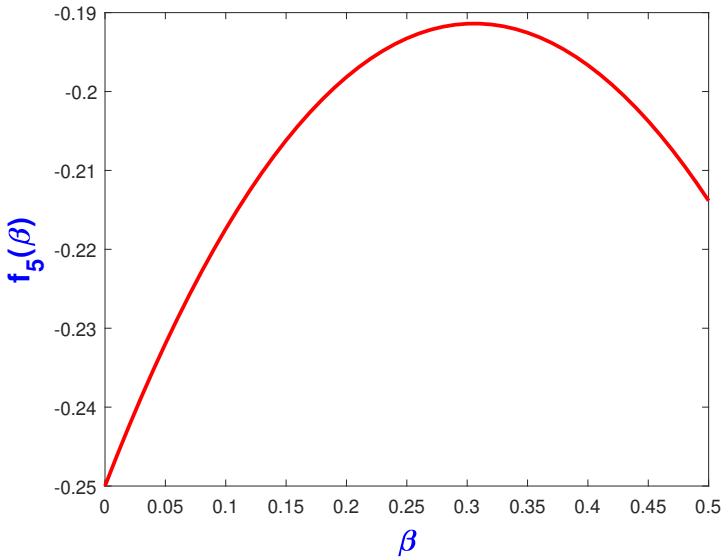

Figure 4.5: Plot of $f_5(\beta)$.

$$
\begin{aligned}
&= \sum_{k\in\{1,2,3,n\}} \Big[\lambda_k\alpha_k^2 - (\eta-2)\alpha_k^2 - (-1)^{k+1}\lambda_k^2\alpha_k^2 + 2(\eta-2)(-1)^{k+1}\lambda_k\alpha_k^2 \\
&\quad - (\eta-2)^2(-1)^{k+1}\alpha_k^2\Big] + \big[(\lambda_1-\eta+2)^2 - (\lambda_1-\eta+2)\big]\alpha_1^2 \\
&= \frac{\eta-2}{\eta-1} - (\eta-2)\frac{1}{\eta-1} + \big[(\lambda_1-\eta+2)^2 - (\lambda_1-\eta+2)\big]\alpha_1^2 \\
&= \big[(\lambda_1-\eta+2)^2 - (\lambda_1-\eta+2)\big]\alpha_1^2 > 0.
\end{aligned}
$$

Together with the monotonicity of $f_3(\beta) - f_5(\beta)$, this shows that $f_3(\beta) - f_5(\beta) > 0$ for all $\beta \in [0,\infty)$. □

Remark 4.2.11. *$f_5(\beta)$ is not necessarily monotonic for $\eta \geq 2$. For example, in Figure 4.5 we plot $f_5(\beta)$ when $\eta = 3$.*

Proposition 4.2.12. *For all $\beta \in (0,\infty)$, $f_1(\beta) > f_j(\beta)$, $j = 2,3,4,5$.*

Proof. We prove the four inequalities separately.

1. The case $j = 2$. It follows from Claims 4.2.5 and 4.2.9 that $f_1 - f_2$ is strictly

increasing on $[0,\infty)$. Moreover, we have

$$\begin{aligned} f_1(0) - f_2(0) &= 2\alpha_2^2 + 2\alpha_n^2 - \frac{1}{(\eta-1)} \\ &= \frac{1}{(\eta-1)} - \frac{1}{(\eta-1)} = 0, \end{aligned}$$

since $\sum_{k\in\{1,2,3,n\}} \alpha_k^2 = \frac{1}{(\eta-1)}$, and $\alpha_2^2 + \alpha_n^2 = \alpha_3^2 + \alpha_1^2$. From this, we obtain that $f_1(\beta) > f_2(\beta)$ for $\beta \in (0,\infty)$.

2. The case $j = 3$. The inequality $f_1(\beta) > f_3(\beta)$, $\beta \in [0,\infty)$, is proved in Claim 4.2.7.

3. The case $j = 4$. It follows from the case $j = 3$ and Claim 4.2.8 that $f_1(\beta) > f_3(\beta) > f_4(\beta)$ for $\beta \in (0,\infty)$.

4. The case $j = 5$. Claims 4.2.7 and 4.2.10 together imply that $f_1(\beta) > f_3(\beta) > f_5(\beta)$ for $\beta \in [0,\infty)$.

□

The take-home message from Proposition 4.2.12 and Claims 4.2.2–4.2.10 is that for all $\beta \in [0,\infty)$ the maximum value of $\Delta G_{pq}(\beta)$ is attained by $f_1(\beta)$, i.e., at entries of $\Delta G(\beta)$ corresponding to two nodes that belong to the same clique V_1 or V_2. Hence, we have proved the following result.

Theorem 4.2.13. *Let K_η–$K_\eta = (V,E)$ be a dumbbell graph and suppose that $\eta \geq 3$. Moreover, assume that the labeling of nodes is given by the matrix of A in* (2.40)*. Then, for all $p \neq q \in V$,*

$$\Delta\tilde{G}_{pq}(\beta) = \begin{cases} 2\sum_{k\in\{2,3,n\}} \alpha_k^2 e^{\beta\lambda_k} - \frac{2e^{-\beta}}{\eta-1}, & \text{if } p,q \in V_1 \text{ or } p,q \in V_2 \\ 2\alpha_3^2 e^{\beta\lambda_3} - \frac{e^{-\beta}}{\eta-1}, & \text{if } p \in V_1, q \in V_2 \\ \sum_{k\in\{2,3,n\}} (\lambda_k - \eta + 3)\alpha_k^2 e^{\beta\lambda_k} - \frac{e^{-\beta}}{\eta-1}, & \text{if } p \in V_1, q = \eta \text{ or } p \in V_2, q = (\eta+1) \\ \sum_{k\in\{2,3,n\}} \left[(-1)^{k+1}(\lambda_k - \eta + 2) + 1\right] \alpha_k^2 e^{\beta\lambda_k} - \frac{e^{-\beta}}{\eta-1}, & \text{if } p \in V_1, q = \eta+1 \text{ or } p \in V_2, q = \eta \\ \sum_{k\in\{2,3,n\}} \left[(-1)^{k+1}(\lambda_k - \eta + 2)^2 + 1\right] \alpha_k^2 e^{\beta\lambda_k} - \frac{e^{-\beta}}{\eta-1}, & \text{if } p = \eta, q = \eta+1. \end{cases}$$

Note that the entries in $\Delta\tilde{G}_{pq}(\beta)$ are

$$2f_1(\beta), \quad f_1(\beta)+f_2(\beta), \quad f_1(\beta)+f_3(\beta), \quad f_1(\beta)+f_4(\beta), \quad f_1(\beta)+f_5(\beta), \tag{4.24}$$

respectively.

4.2.2 Melting in Dumbbell Graphs

To characterize melting, we need to understand in what order the functions in (4.24), corresponding to the different values appearing in the off-diagonal entries of $\Delta\tilde{G}(\beta)$, cross the β-axis and to ensure that such crossing point is unique for each function. We will show that these conditions are verified for all of these function.

Claim 4.2.14. *The function $2f_1(\beta)$ crosses the β-axis exactly once and before all the functions $f_1(\beta)+f_2(\beta)$, $f_1(\beta)+f_3(\beta)$, $f_1(\beta)+f_4(\beta)$ and $f_1(\beta)+f_5(\beta)$.*

Proof. Note that from Claim 4.2.2 we have

$$f_1(0) = \sum_{k\in\{2,3,n\}} \alpha_k^2 - \frac{1}{\eta-1} = -\alpha_1^2 < 0. \tag{4.25}$$

That $2f_1(\beta)$ crosses the β-axis exactly once, follows now from Claim 4.2.5 and the fact that, for large β, the positive $e^{\beta\lambda_2}$ term dominates and therefore $f_1(\beta)\to\infty$ as $\beta\to\infty$. Finally, Proposition 4.2.12 implies that $2f_1(\beta)$ crosses the β-axis first. □

Claim 4.2.15. *The function $f_1(\beta)+f_3(\beta)$ is monotonic increasing and crosses the β-axis once.*

Proof. Monotonicity is obvious as both $f_1(\beta)$ and $f_3(\beta)$ are monotonic increasing by Claims 4.2.5 and 4.2.6, respectively. It follows from (4.25) and Claim 4.2.7 that

$$f_3(0) < f_1(0) < 0.$$

For large β the positive term $e^{\beta\lambda_2}$ dominates and hence $f_1(\beta)+f_3(\beta)$ has crosses the β-axis exactly once. □

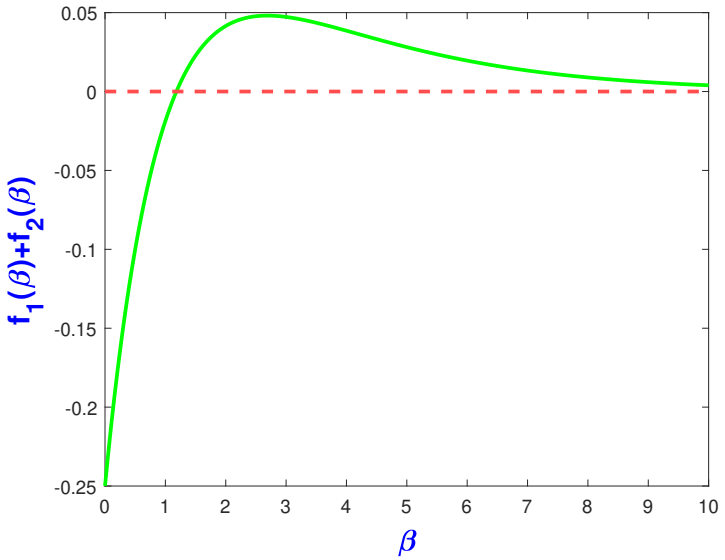

Figure 4.6: Plot for $f_1(\beta) + f_2(\beta)$.

Claim 4.2.16. *$f_1(\beta) + f_2(\beta)$ crosses the β-axis once.*

Proof. By direct computations, the solution of $f_1(\beta) + f_2(\beta) = 2\alpha_3^2 e^{\beta\lambda_3} - \frac{e^{-\beta}}{\eta-1} = 0$ is $\beta = \frac{\log\left[\left(2(\eta-1)\alpha_3^2\right)^{-1}\right]}{\lambda_3+1}$, which is positive since $2(\eta-1)\alpha_3^2 < 1$ by (2.71) and the inequality $\lambda_3 > -1$. □

Note that

$$\lim_{\beta\to\infty} f_1(\beta) + f_2(\beta) = 0.$$

In Figure 4.6, we plot $f_1(\beta) + f_2(\beta)$ when $\eta = 3$.

Claim 4.2.17. *The function $f_1(\beta) + f_4(\beta)$ is monotonic increasing and crosses the β-axis once.*

Proof. To prove that $f_1(\beta) + f_4(\beta)$ is monotonic increasing for all $\beta \in [0, \infty)$, consider the derivative of $f_1(\beta) + f_4(\beta)$:

$$\left(f_1(\beta) + f_4(\beta)\right)' = \sum_{k\in\{2,3,n\}} \left[(-1)^{k+1}(\lambda_k - \eta + 2) + 1\right] \alpha_k^2 \lambda_k e^{\beta\lambda_k} + \frac{e^{-\beta}}{\eta - 1}.$$

We will show, using Lemma 2.4.1, that $(f_1(\beta) + f_4(\beta))'$ has no zeros for $\beta \in [0, \infty)$. We have that

$$\big[-(\lambda_2 - \eta + 2) + 1\big]\lambda_2\alpha_2^2 > 0, \tag{4.26}$$

since from the bounds in Lemma 2.5.14 we have $\lambda_2 - \eta + 2 < 1$. Further, the inequality $(\lambda_3 - \eta + 2) + 1 < 0$ implies

$$\begin{aligned} \big[-(\lambda_2 - \eta + 2) + 1\big]\lambda_2\alpha_2^2 + \big[(\lambda_3 - \eta + 2) + 1\big]\lambda_3\alpha_3^2 > 0, \\ \big[-(\lambda_2 - \eta + 2) + 1\big]\lambda_2\alpha_2^2 + \big[(\lambda_3 - \eta + 2) + 1\big]\lambda_3\alpha_3^2 + \frac{1}{\eta - 1} > 0. \end{aligned} \tag{4.27}$$

Moreover, by Claim 4.2.3, we have

$$\begin{aligned} &\sum_{k\in\{2,3,n\}} \Big[(-1)^{k+1}(\lambda_k - \eta + 2) + 1\Big]\lambda_k\alpha_k^2 \\ &= \sum_{k\in\{2,n\}} \big[-(\lambda_k - \eta + 2) + 1\big]\lambda_k\alpha_k^2 + \big[(\lambda_3 - \eta + 2) + 1\big]\lambda_3\alpha_3^2 \\ &= -\sum_{k\in\{2,n\}} \lambda_k^2\alpha_k^2 + (\eta - 1)\sum_{k\in\{2,n\}} \lambda_k\alpha_k^2 + \big[(\lambda_3 - \eta + 2) + 1\big]\lambda_3\alpha_3^2 \\ &= -\frac{\eta^2 - 3\eta + 3}{2\,(\eta - 1)} + \frac{(\eta - 1)\,(\eta - 2)}{2\,(\eta - 1)} + \big[(\lambda_3 - \eta + 2) + 1\big]\lambda_3\alpha_3^2 \\ &= \frac{-1}{2\,(\eta - 1)} + \big[(\lambda_3 - \eta + 2) + 1\big]\lambda_3\alpha_3^2 \end{aligned}$$

and

$$\begin{aligned} &\sum_{k\in\{2,3,n\}} \Big[(-1)^{k+1}(\lambda_k - \eta + 2) + 1\Big]\lambda_k\alpha_k^2 + \frac{1}{\eta - 1} \\ &= \big[(\lambda_3 - \eta + 2) + 1\big]\lambda_3\alpha_3^2 - \frac{1}{2\,(\eta - 1)} + \frac{1}{\eta - 1} \\ &= \frac{1}{2(\eta - 1)} + \big[(\lambda_3 - \eta + 2) + 1\big]\lambda_3\alpha_3^2 > 0, \end{aligned}$$

where we have used $(\lambda_3 - \eta + 2) + 1 < 0$. Now, Lemma 2.4.1 implies that $(f_1(\beta) + f_4(\beta))'$ does not change sign. Since, for large β, $(f_1(\beta) + f_4(\beta))'$ is dominated by the positive $[-(\lambda_2 - \eta + 2) + 1]\,\alpha_2^2 e^{\beta\lambda_2}$ term, we can deduce that $(f_1(\beta) + f_4(\beta))' > 0$ for $\beta \in (0, \infty)$

and hence $f_1(\beta) + f_4(\beta)$ is strictly increasing. From Claim 4.2.3, we obtain

$$\begin{aligned} f_1(0) + f_4(0) &= \sum_{k\in\{2,3,n\}} \left[\alpha_k^2 + (-1)^{k+1}(\lambda_k - \eta + 2)\alpha_k^2\right] - \frac{1}{\eta - 1} \\ &= \sum_{k\in\{1,2,3,n\}} \left[\alpha_k^2 + (-1)^{k+1}(\lambda_k - \eta + 2)\alpha_k^2\right] - \alpha_1^2 - (\lambda_1 - \eta + 2)\alpha_1^2 - \frac{1}{\eta - 1} \\ &= \frac{1}{\eta - 1} - \alpha_1^2 - (\lambda_1 - \eta + 2)\alpha_1^2 - \frac{1}{\eta - 1} \\ &= -(\lambda_1 - \eta + 3)\alpha_1^2 < 0. \end{aligned}$$

This implies that $f_1(\beta) + f_4(\beta)$ crosses the β axis exactly once. □

Claim 4.2.18. *The function $f_1(\beta) + f_5(\beta)$ has exactly one zero in $(0, \infty)$; this function is negative to the left and positive to the right of this zero.*

Proof. Let us consider the function

$$\begin{aligned} g(\beta) &= \big(f_1(\beta) + f_5(\beta)\big)e^{\beta} \\ &= \sum_{k\in\{2,3,n\}} \Big[1 + (-1)^{k+1}(\lambda_k - \eta + 2)^2\Big]\alpha_k^2 e^{(\lambda_k+1)\beta} - \frac{1}{\eta - 1}. \end{aligned}$$

We show that $g(\beta)$ is monotonic increasing. In what follows, we use Lemma 2.4.1 to show that the derivative,

$$g'(\beta) = \sum_{k\in\{2,3,n\}} \Big[1 + (-1)^{k+1}(\lambda_k - \eta + 2)^2\Big](\lambda_k + 1)\alpha_k^2 e^{(\lambda_k+1)\beta},$$

does not change sign. Since $0 < \lambda_2 - \eta + 2 < 1$ by Lemma 2.5.14, we have

$$\big[1 - (\lambda_2 - \eta + 2)^2\big](\lambda_2 + 1)\alpha_2^2 > 0.$$

Again, by Lemma 2.5.14, we know that $\lambda_3 + 1 > 0$ and hence

$$\big[1 - (\lambda_2 - \eta + 2)^2\big](\lambda_2 + 1)\alpha_2^2 + \big[1 + (\lambda_3 - \eta + 2)^2\big](\lambda_3 + 1)\alpha_3^2 > 0.$$

Finally, we obtain, from Lemma 2.5.14, that $(\lambda_n - \eta + 2)^2 > 1$ and that $\lambda_n + 1 < 0$,

which yields

$$\big[1-(\lambda_2-\eta+2)^2\big](\lambda_2+1)\alpha_2^2+\big[1+(\lambda_3-\eta+2)^2\big](\lambda_3+1)\alpha_3^2 \\ +\big[1-(\lambda_n-\eta+2)^2\big](\lambda_n+1)\alpha_n^2>0.$$

Now, Lemma 2.4.1 implies that $g'(\beta)$ does not change sign. Since, for large β, the positive $e^{(\lambda_2+1)\beta}$ term dominates, we obtain that $g'(\beta)>0$ for all $\beta\in(0,\infty)$, and hence $g(\beta)$ is strictly increasing on $[0,\infty)$. Further, we obtain from Claim 4.2.3 that

$$\begin{aligned}
g(0)&=\sum_{k\in\{2,3,n\}}\Big[1+(-1)^{k+1}(\lambda_k-\eta+2)^2\Big]\alpha_k^2-\frac{1}{\eta-1}\\
&=\sum_{k\in\{1,2,3,n\}}\Big[1+(-1)^{k+1}(\lambda_k-\eta+2)^2\Big]\alpha_k^2-\big[1+(\lambda_1-\eta+2)^2\big]\alpha_1^2-\frac{1}{\eta-1}\\
&=\sum_{k\in\{1,2,3,n\}}\Big[\alpha_k^2+(-1)^{k+1}\lambda_k^2\alpha_k^2-2(\eta-2)(-1)^{k+1}\lambda_k\alpha_k^2+(\eta-2)^2(-1)^{k+1}\alpha_k^2\Big]\\
&\quad-\big[1+(\lambda_1-\eta+2)^2\big]\alpha_1^2-\frac{1}{\eta-1}\\
&=\frac{1}{\eta-1}-\big[1+(\lambda_1-\eta+2)^2\big]\alpha_1^2-\frac{1}{\eta-1}\\
&=-\big[1+(\lambda_1-\eta+2)^2\big]\alpha_1^2<0.
\end{aligned}$$

Since, for large β, $g(\beta)$ is dominated by the positive $e^{(\lambda_2+1)\beta}$ term, the monotonicity of $g(\beta)$ implies that $g(\beta)$ has exactly one zero, it is negative to the left and positive to the right of this zero. Multiplying by the positive factor $e^{-\beta}$ we can deduce that $g_1(\beta)+g_5(\beta)$ has the same properties. □

Proposition 4.2.19. *For every $j=1,2,3,4,5$, the function $f_1(\beta)+f_j(\beta)$ crosses the β axis exactly once.*

Proof. For $j=1,2,3,4,5$ the assertions follow from Claims 4.2.14, 4.2.16, 4.2.15, 4.2.17 and 4.2.18, respectively. □

For $i=1,2,3,4,5$, let us denote by $\beta_i=\beta_i(\eta)$ the unique point where the function $f_1(\beta)+f_i(\beta)$ crosses the β-axis. These points are well defined by Proposition 4.2.19. Next, we discuss the order of these points β_i.

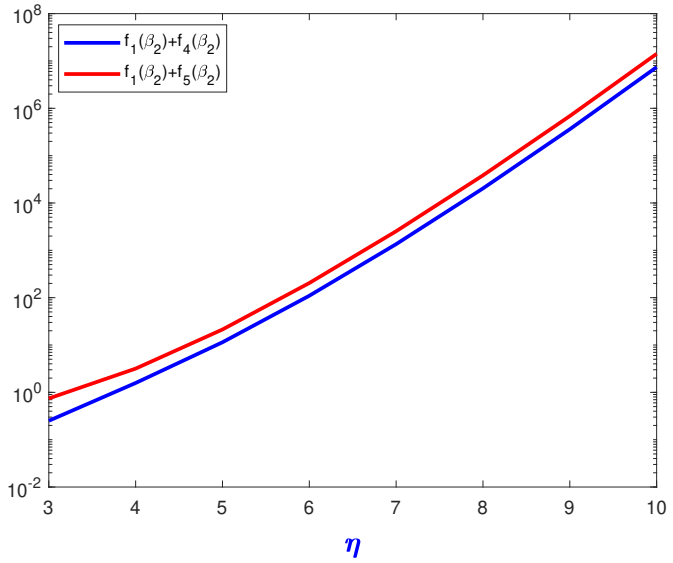

Figure 4.7: The semilogy plot for $f_1(\beta_2) + f_4(\beta_2)$ and $f_1(\beta_2) + f_5(\beta_2)$ versus η.

Proposition 4.2.20. *The following inequalities are true:*

1. $\beta_1 < \beta_i$ *for* $i = 2, 3, 4, 5$;

2. $\beta_3 < \beta_4, \quad \beta_3 < \beta_5$.

Proof. The inequalities in item 1. follow directly from Claim 4.2.14. Further, the relations in item 2. follow from Claims 4.2.8 and 4.2.10, respectively. □

Conjecture 4.2.21. *We conjecture that* $\beta_5 < \beta_4 < \beta_2$.

There is some computational evidence that $\beta_2 > \beta_4$ and $\beta_2 > \beta_5$. Namely, we know from Claim 4.2.16 that $\beta_2 = \frac{\log[(2(\eta-1)\alpha_3^2)^{-1}]}{\lambda_3+1}$. As can be seen from Figure 4.7, the values $f_1(\beta_2) + f_4(\beta_2)$ and $f_1(\beta_2) + f_5(\beta_2)$ are positive for $\eta \in [3, 10]$. This implies that $\beta_4 < \beta_2$ and $\beta_5 < \beta_2$ for those η. We also computed β_4 and β_5 for $\eta \in [3, 10]$, which are displayed in Figure 4.8; this gives computational evidence that $\beta_5 < \beta_4$ for those η.

Claim 4.2.22. $\beta_2(\eta) \to \infty$ *as* $\eta \to \infty$.

Proof. It follows from Lemma 2.5.14 that $\lambda_3 \to 0$ as $\eta \to \infty$. Hence,

$$2(\eta-1)\alpha_3^2 = \frac{\eta-1}{(\lambda_3-\eta+2)^2+\eta-1} \sim \frac{\eta-1}{(\eta-2)^2+\eta-1} \sim \frac{1}{\eta}.$$

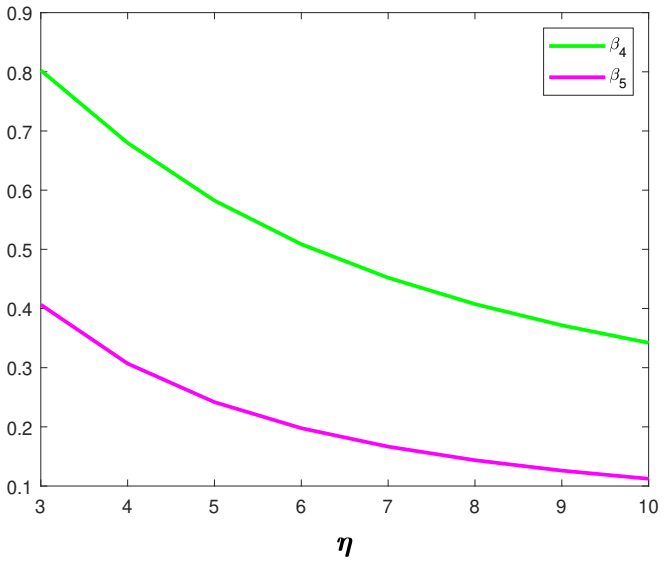

Figure 4.8: Plot of β_4 and β_5 versus η.

Now, Claim 4.2.16 implies

$$\beta_2(\eta) = \frac{\log[(2(\eta-1)\alpha_3^2)^{-1}]}{\lambda_3+1} \sim \log\eta \to \infty$$

as $\eta \to \infty$. □

Claim 4.2.23. *We have that $\beta_i(\eta) \to 0$ as $\eta \to \infty$ for $i = 1, 3, 4, 5$.*

Proof. It is sufficient to prove that $\beta_4(\eta) \to 0$ and $\beta_5(\eta) \to 0$ since we know from Proposition 4.2.20 that $\beta_1(\eta) < \beta_5(\eta)$ and $\beta_3(\eta) < \beta_5(\eta)$.

Let us first determine the asymptotic behaviour of λ_2 as $\eta \to \infty$. With the asymptotic formula $\sqrt{1-x} = 1 - \frac{x}{2} + \mathcal{O}(x^2)$ we obtain

$$\begin{aligned}\lambda_2 &= \frac{\eta-3}{2} + \frac{\sqrt{(\eta+1)^2-4}}{2} = \frac{1}{2}\left[\eta - 3 + (\eta+1)\sqrt{1-\frac{4}{(\eta+1)^2}}\right] \\ &= \frac{1}{2}\left[\eta - 3 + (\eta+1)\left(1 - \frac{2}{(\eta+1)^2} + \mathcal{O}\Big(\frac{1}{(\eta+1)^4}\Big)\right)\right] \\ &= \frac{1}{2}\left[\eta - 3 + \eta + 1 - \frac{2}{\eta+1} + \mathcal{O}\Big(\frac{1}{(\eta+1)^3}\Big)\right] \\ &= \eta - 1 - \frac{1}{\eta+1} + \mathcal{O}\Big(\frac{1}{\eta^3}\Big)\end{aligned}$$

as $\eta \to \infty$. From this we deduce that

$$1 - (\lambda_2 - \eta + 2) = \eta - 1 - \lambda_2 = \frac{1}{\eta+1} + \mathcal{O}\Big(\frac{1}{\eta^3}\Big),$$

$$\begin{aligned}1 - (\lambda_2 - \eta + 2)^2 &= \big[1 + (\lambda_2 - \eta + 2)\big]\big[1 - (\lambda_2 - \eta + 2)\big] \\ &= \left[2 - \frac{1}{\eta+1} + \mathcal{O}\Big(\frac{1}{\eta^3}\Big)\right]\left[\frac{1}{\eta+1} + \mathcal{O}\Big(\frac{1}{\eta^3}\Big)\right] \\ &= \frac{2}{\eta+1} + \mathcal{O}\Big(\frac{1}{\eta^2}\Big) \qquad (4.28)\end{aligned}$$

and

$$\alpha_2^2 = \frac{1}{2[(\lambda_2 - \eta + 2)^2 + \eta - 1]} \sim \frac{1}{2[1 + \eta - 1]} = \frac{1}{2\eta}\,. \qquad (4.29)$$

Now, let us fix $\beta > 0$. We show that

$$f_1(\beta) + f_5(\beta) = \sum_{k\in\{2,3,n\}} \Big[1 + (-1)^{k+1}(\lambda_k - \eta + 2)^2\Big]\alpha_k^2 e^{\beta\lambda_k} - \frac{e^{-\beta}}{\eta - 1} \qquad (4.30)$$

tends to infinity as $\eta \to \infty$. The last term on the right-hand side converges to 0 as $\eta \to \infty$. For $k \in \{3, n\}$, we have that $\eta - 2 \le \eta - 2 - \lambda_k \le \eta$ and hence

$$\begin{aligned}\Big|\big[1 + (-1)^{k+1}(\lambda_k - \eta + 2)^2\big]\alpha_k^2 e^{\beta\lambda_k}\Big| &\le \big[1 + (\eta - 2 - \lambda_k)^2\big]\frac{1}{2[(\eta - 2 - \lambda_k)^2 + \eta - 1]} \\ &\le \frac{1+\eta^2}{2[(\eta-2)^2 + \eta - 1]},\end{aligned}$$

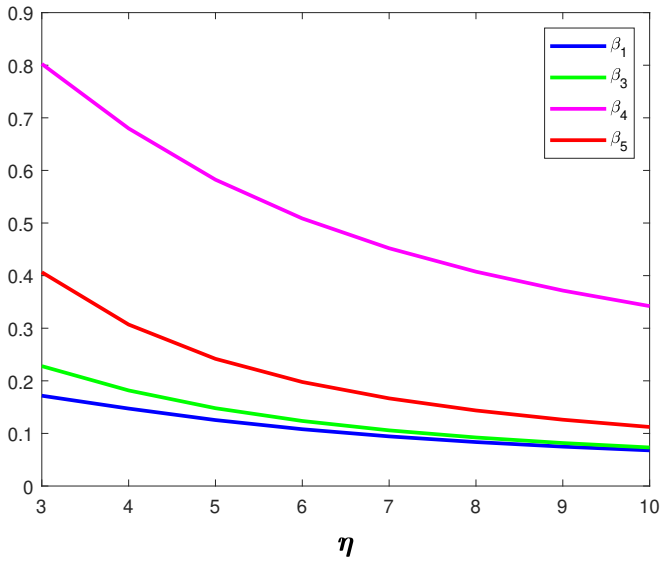

Figure 4.9: Plot of β_1,β_3 β_4 and β_5 versus η.

which is bounded. For the term in (4.30) with $k = 2$ we use (4.28) and (4.29) to obtain

$$\begin{aligned}\left[1-(\lambda_2-\eta+2)^2\right]\alpha_2^2 e^{\beta\lambda_2} &\geq \left[1-(\lambda_2-\eta+2)^2\right]\alpha_2 e^{\beta(\eta-2)} \\ &\sim \frac{2}{\eta+1}\cdot\frac{1}{2\eta^2}e^{\beta(\eta-2)} \to \infty\end{aligned}$$

as $\eta \to \infty$. This implies that $f_1(\beta) + f_5(\beta) \to \infty$ as $\eta \to \infty$ for each fixed $\beta > 0$. In particular, for every fixed $\beta > 0$, we have $f_1(\beta) + f_5(\beta) > 0$ for large enough η and therefore $\beta_5(\eta) < \beta$. This shows that $\beta_5(\eta) \to 0$ as $\eta \to \infty$.

The proof for the fact that $\beta_4(\eta) \to 0$ is very similar and even slightly simpler. □

Conjecture 4.2.24. *The values of β_i in the melting signature for $i = 1, 3, 4, 5$, go to zero as η goes to infinity.*

In Figure 4.9, we see that $\beta_1 < \beta_3 < \beta_5 < \beta_4$ and $\beta_i \to 0$ as $\eta \to \infty$ for $i = 1, 3, 4, 5$.

4.2.3 Melting Signatures of Dumbbell Graphs

We recall that the *melting signature* is the sequence of inverse temperatures β, starting with the lowest, at which the structure of the associated modified communicability

graph changes. In this section we discuss how the structure of the modified communicability graph associated with a given K_η–K_η, for $\eta \geq 3$, changes with $\beta \in [0, \infty)$.

From Propositions 4.2.19 and 4.2.20, and Conjecture 4.2.21 it follows that $f_1(\beta) + f_i(\beta)$, $i = 1, 2, 3, 4, 5$, crosses the β-axis exactly once, and that the functions $f_1(\beta) + f_i(\beta)$, $i = 1, 2, 3, 4, 5$, cross the β-axis in the following order: $2f_1(\beta)$, $f_1(\beta) + f_3(\beta)$, $f_1(\beta) + f_5(\beta)$, $f_1(\beta) + f_4(\beta)$ and, lastly, $f_1(\beta) + f_2(\beta)$. The graphs K_η–K_η have one possible melting signature: $(\beta_1, \beta_3, \beta_5, \beta_4, \beta_2)$. The melting of the associated modified communicability graph proceeds as follows. At $\beta = \beta_1$, the modified communicability graph of K_η–K_η changes from being the null graph N_n to a collection of two complete graphs $K_{\eta-1}$ and two single nodes, and at $\beta = \beta_3$, the modified communicability graph becomes a collection of just two complete graphs K_η. At $\beta = \beta_5$, the modified communicability graph becomes the graph K_η–K_η itself, and at $\beta = \beta_4$, the modified communicability graph becomes a core-satellite graph $\Theta(2, \eta-1, 2)$. Finally, at $\beta = \beta_2$, the modified communicability graph becomes the complete graph $K_{2\eta}$. In Figure 4.10, we show the evolution of the modified communicability graphs of K_5–K_5 as β varies, which exhibits the $(\beta_1, \beta_3, \beta_5, \beta_4, \beta_2)$ melting signature.

4.2.4 Melting in K_2–K_2

The graph K_2–K_2 is the path graph with 4 vertices, and the spectrum of its adjacency matrix can be found from Theorem 2.5.13 by setting $\eta = 2$. The communicability function $G_{pq}(\beta)$ for K_2–K_2 is given by (4.4) in Lemma 4.2.1 with $\eta = 2$. There are four different types of edges; the first case in (4.4) does not appear because V_1 and V_2 are singletons. Hence, we can write the communicability function as follows:

$$G_{pq}(\beta) = \begin{cases} \sum_{k\in\{1,2,3,4\}} (-1)^{k+1} \alpha_k^2 e^{\beta\lambda_k} & \text{if } p, q \in \{1, 4\}, \\ \sum_{k\in\{1,2,3,4\}} \lambda_k \alpha_k^2 e^{\beta\lambda_k} & \text{if } p, q \in \{1, 2\} \text{ or } p, q \in \{3, 4\}, \\ \sum_{k\in\{1,2,3,4\}} (-1)^{k+1} \lambda_k \alpha_k^2 e^{\beta\lambda_k} & \text{if } p, q \in \{1, 3\} \text{ or } p, q \in \{2, 4\}, \\ \sum_{k\in\{1,2,3,4\}} (-1)^{k+1} \lambda_k^2 \alpha_k^2 e^{\beta\lambda_k} & \text{if } p, q \in \{2, 3\}, \end{cases}$$

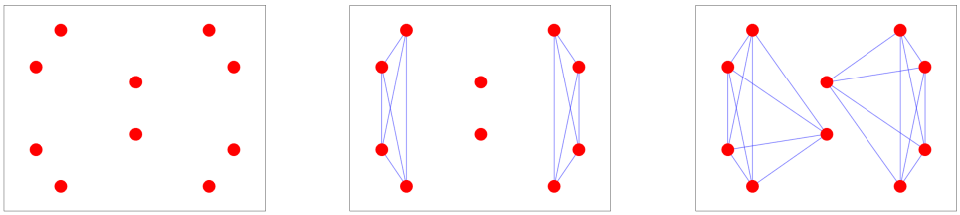

(a) $0 \leq \beta < \beta_1$ (b) $\beta_1 \leq \beta < \beta_3$ (c) $\beta_3 \leq \beta < \beta_5$

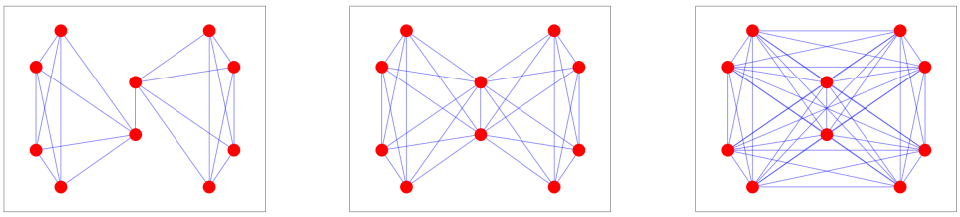

(d) $\beta_5 \leq \beta < \beta_4$ (e) $\beta_4 \leq \beta < \beta_2$ (f) $\beta \geq \beta_2$

Figure 4.10: Illustration of the structure of the modified communicability graph of K_5–K_5 versus β.

where

$$\lambda_1 = \frac{1+\sqrt{5}}{2}, \quad \lambda_2 = \frac{-1+\sqrt{5}}{2}, \quad \lambda_3 = \frac{1-\sqrt{5}}{2}, \quad \lambda_4 = \frac{-1-\sqrt{5}}{2}, \tag{4.31}$$

$$\alpha_k = \left(2\lambda_k^2 + 2\right)^{-\frac{1}{2}} \tag{4.32}$$

for $k \in \{1, 2, 3, 4\}$.

Remark 4.2.25. *It is straightforwardly verified that* $\lambda_1 = -\lambda_4$, $\lambda_2 = -\lambda_3$, $\alpha_1 = \alpha_4$ *and* $\alpha_2 = \alpha_3$.

Now, by removing the $e^{\beta\lambda_1}$ terms from $G_{pq}(\beta)$, we obtain $\Delta G_{pq}(\beta)$:

$$\Delta G_{pq}(\beta) = \begin{cases} \sum_{k\in\{2,3,4\}} \alpha_k^2 e^{\beta\lambda_k} & \text{if } p,q \in \{1,4\}, \\ \sum_{k\in\{2,3,4\}} \lambda_k \alpha_k^2 e^{\beta\lambda_k} & \text{if } p,q \in \{1,2\} \text{ or } p,q \in \{3,4\}, \\ \sum_{k\in\{2,3,4\}} (-1)^{k+1} \lambda_k \alpha_k^2 e^{\beta\lambda_k} & \text{if } p,q \in \{1,3\} \text{ or } p,q \in \{2,4\}, \\ \sum_{k\in\{2,3,4\}} (-1)^{k+1} \lambda_k^2 \alpha_k^2 e^{\beta\lambda_k} & \text{if } p,q \in \{2,3\}, \end{cases}$$

where the four terms of $\Delta G_{pq}(\beta)$ for K_2–K_2 correspond to the functions f_2, f_3, f_4 and

f_5 in (4.15), (4.16), (4.17) and (4.18) when $\eta = 2$, respectively.

Next, to understand the order relations among the different entries in $\Delta G_{pq}(\beta)$, we have the following result.

Proposition 4.2.26. *The following statements are true.*

1. *The equation $f_2(\beta) = f_3(\beta)$ has a unique solution $\beta_0 \approx 0.10029$; this solution also satisfies $f_2(\beta_0) = f_3(\beta_0) < 0$. Moreover, $0 > f_2(\beta) > f_3(\beta)$ for $\beta \in [0, \beta_0)$, and $f_2(\beta) < f_3(\beta)$ for $\beta > \beta_0$.*

2. *$f_3(\beta) > f_4(\beta)$ for all $\beta \in (0, \infty)$.*

3. *$f_3(\beta) > f_5(\beta)$ for all $\beta \in [0, \infty)$.*

Proof. Let us consider the statements in item 1. The function f_2 is strictly decreasing by Claim 4.2.9; f_3 is strictly increasing by Claim 4.2.6. To obtain their values at 0, we use Claim 4.2.3:

$$f_2(0) = \sum_{k\in\{2,3,4\}} (-1)^{k+1}\alpha_k^2 = \sum_{k\in\{1,2,3,4\}} (-1)^{k+1}\alpha_k^2 - \alpha_1^2 = -\alpha_1^2,$$

$$f_3(0) = \sum_{k\in\{2,3,4\}} \lambda_k\alpha_k^2 = \sum_{k\in\{1,2,3,4\}} \lambda_k\alpha_k^2 - \lambda_1\alpha_1^2 = -\lambda_1\alpha_1^2,$$

which yields $f_3(0) < f_2(0) < 0$ since $\lambda_1 > 1$. This implies that there is a unique $\beta_0 > 0$ such that $f_2(\beta_0) = f_3(\beta_0)$. From the monotonicity of f_2 we obtain that $f_2(\beta_0) < 0$. A numerical computation yields $\beta_0 \approx 0.10029$. Clearly, $0 > f_2(\beta) > f_3(\beta)$ for $\beta \in (0, \beta_0)$, and $f_2(\beta) < f_3(\beta)$ for $\beta > \beta_0$.

The assertions in items 2. and 3. were proved in Claims 4.2.8 and 4.2.10, respectively. □

From Proposition 4.2.26 we know that, for all $\beta \geq \beta_0 \approx 0.10029$, the maximum value of $\Delta G_{pq}(\beta)$ for K_2–K_2 is attained at the pair of nodes $p, q \in \{1, 2\}$ or $p, q \in \{3, 4\}$, which correspond to the function $f_3(\beta)$. Hence, for all $\beta \geq \beta_0$, the modified communicability

graph function $\Delta\tilde{G}_{pq}(\beta)$ of K_2–K_2 is given by

$$\Delta\tilde{G}_{pq}(\beta) = \begin{cases} \sum_{k\in\{2,3,4\}} \left(\lambda_k + (-1)^{k+1}\right) \alpha_k^2 e^{\beta\lambda_k} & \text{if } p,q \in \{1,4\}, \\ \sum_{k\in\{2,3,4\}} 2\lambda_k \alpha_k^2 e^{\beta\lambda_k} & \text{if } p,q \in \{1,2\} \text{ or } p,q \in \{3,4\}, \\ 2\lambda_3 \alpha_3^2 e^{\beta\lambda_3} & \text{if } p,q \in \{1,3\} \text{ or } p,q \in \{2,4\}, \\ \sum_{k\in\{2,3,4\}} \left(\lambda_k + (-1)^{k+1}\lambda_k^2\right) \alpha_k^2 e^{\beta\lambda_k} & \text{if } p,q \in \{2,3\}. \end{cases}$$

Proposition 4.2.26 implies that $f_j(\beta) < 0$ for $\beta \in (0, \beta_0]$ and $j = 2,3,4,5$, and that the entries of the modified communicability graph function $\Delta\tilde{G}_{pq}(\beta)$ are of the form $f_2(\beta) + f_j(\beta)$, $j = 2,3,4,5$, which are all negative. We can therefore ignore the interval $(0, \beta_0]$ and concentrate on values β in (β_0, ∞). Let us set $y_j(\beta) = f_3(\beta) + f_j(\beta)$, $j = 2,3,4,5$, which are the entries in $\Delta\tilde{G}_{pq}(\beta)$ for $\beta \in (\beta_0, \infty)$; explicitly, these functions are given by

$$y_1(\beta) = \sum_{k\in\{2,3,4\}} \left(\lambda_k + (-1)^{k+1}\right) \alpha_k^2 e^{\beta\lambda_k}, \tag{4.33}$$

$$y_2(\beta) = \sum_{k\in\{2,3,4\}} 2\lambda_k \alpha_k^2 e^{\beta\lambda_k}, \tag{4.34}$$

$$y_3(\beta) = 2\lambda_3 \alpha_3^2 e^{\beta\lambda_3}, \tag{4.35}$$

$$y_4(\beta) = \sum_{k\in\{2,3,4\}} \left(\lambda_k + (-1)^{k+1}\lambda_k^2\right) \alpha_k^2 e^{\beta\lambda_k}. \tag{4.36}$$

Let us derive some properties of these functions.

Claim 4.2.27. *The function $y_2(\beta)$ is strictly increasing and crosses the β axis exactly once.*

Proof. From Claim 4.2.6 with $\eta = 2$ we obtain that $y_2(\beta) = 2f_3(\beta)$ is strictly increasing on $[0, \infty)$. For large β, $y_2(\beta)$ is dominated by the positive $e^{\beta\lambda_2}$ term. By Proposition 4.2.26, we have $y_2(0) = 2f_3(0) < 0$. Hence $y_2(\beta)$ has exactly one zero. □

Claim 4.2.28. *The function $y_4(\beta)$ is strictly increasing and crosses the β axis exactly once.*

Proof. Consider the derivative $y_4'(\beta) = \sum_{k\in\{2,3,4\}} \left(\lambda_k + (-1)^{k+1}\lambda_k^2\right) \lambda_k \alpha_k^2 e^{\beta\lambda_k}$. Since

$\lambda_4 < -1 < \lambda_3 < 0 < \lambda_2 < 1$, we have

$$\big(\lambda_2 - \lambda_2^2\big)\lambda_2\alpha_2^2 > 0, \qquad \big(\lambda_3 + \lambda_3^2\big)\lambda_3\alpha_3^2 > 0, \qquad \big(\lambda_4 - \lambda_4^2\big)\lambda_4\alpha_4^2 > 0,$$

and hence

$$\big(\lambda_2 - \lambda_2^2\big)\lambda_2\alpha_2^2 + \big(\lambda_3 + \lambda_3^2\big)\lambda_3\alpha_3^2 > 0$$

and

$$\big(\lambda_2 - \lambda_2^2\big)\lambda_2\alpha_2^2 + \big(\lambda_3 + \lambda_3^2\big)\lambda_3\alpha_3^2 + \big(\lambda_4 - \lambda_4^2\big)\lambda_4\alpha_4^2 > 0.$$

Lemma 2.4.1 implies that $y_4'(\beta)$ does not change sign. Since, for large β, $y_4'(\beta)$ is dominated by the positive $e^{\beta\lambda_2}$ term, we have $y_4'(\beta) > 0$ for $\beta \in (0, \infty)$, and therefore $y_4(\beta)$ is strictly increasing. From Proposition 4.2.26, we obtain $y_4(0) = f_3(0) + f_5(0) < 0$, and hence $y_4(\beta)$ has exactly one zero. □

Claim 4.2.29. *We have $y_1(\beta) < 0$ for all $\beta \in [0, \infty)$.*

Proof. Since $0 < \lambda_2 < 1$, $\lambda_3 = -\lambda_2$, $\lambda_4 < 0$ and $\alpha_2^2 = \alpha_3^2$, we have

$$\begin{aligned}(\lambda_2 - 1)\alpha_2^2 < 0, \qquad (\lambda_2 - 1)\alpha_2^2 + (\lambda_3 + 1)\alpha_3^2 = 0,\\ (\lambda_2 - 1)\alpha_2^2 + (\lambda_3 + 1)\alpha_3^2 + (\lambda_4 - 1)\alpha_4^2 < 0.\end{aligned}$$

Hence, the function $y_1(\beta) = \sum_{k\in\{2,3,4\}}\big(\lambda_k + (-1)^{k+1}\big)\alpha_k^2 e^{\beta\lambda_k}$ does not change sign in $(0, \infty)$ by Lemma 2.4.1. For large β, $y_1(\beta)$ is dominated by the negative $e^{\beta\lambda_2}$ term, and therefore $y_1(\beta) < 0$ for $\beta \in (0, \infty)$. Moreover,

$$y_1(0) = (\lambda_2 - 1)\alpha_2^2 + (\lambda_3 + 1)\alpha_3^2 + (\lambda_4 - 1)\alpha_4^2 < 0,$$

which finishes the proof. □

Claim 4.2.30. *We have $y_2(\beta) > y_4(\beta)$ for all $\beta \in [0, \infty)$.*

Proof. Let us consider the derivative

$$\big(y_2(\beta) - y_4(\beta)\big)' = \sum_{k\in\{2,3,4\}}\Big(\lambda_k - (-1)^{k+1}\lambda_k^2\Big)\lambda_k\alpha_k^2 e^{\beta\lambda_k}.$$

Since $\lambda_2 > 0$ and $\lambda_3 > -1$, we have

$$\big(\lambda_2^2 + \lambda_2^3\big)\alpha_2^2 > 0, \qquad \big(\lambda_2^2 + \lambda_2^3\big)\alpha_2^2 + \big(\lambda_3^2 - \lambda_3^3\big)\alpha_3^2 > 0.$$

Moreover, from Claim 4.2.3, we obtain

$$\begin{aligned}\sum_{k\in\{2,3,4\}} \big(\lambda_k^2 - (-1)^{k+1}\lambda_k^3\big)\alpha_k^2 &= \sum_{k\in\{1,2,3,4\}} \big(\lambda_k^2 - (-1)^{k+1}\lambda_k^3\big)\alpha_k^2 - \big(\lambda_1^2 - \lambda_1^3\big)\alpha_1^2 \\ = 1 - 1 - \big(\lambda_1^2 - \lambda_1^3\big)\alpha_1^2 &= \big(\lambda_1^3 - \lambda_1^2\big)\alpha_1^2 > 0.\end{aligned}$$

Hence, by Lemma 2.4.1, $(y_2(\beta) - y_4(\beta))'$ does not change sign in $(0,\infty)$. Since, for large β, $(y_2(\beta) - y_4(\beta))'$ is dominated by the positive $e^{\beta\lambda_2}$ term, we can deduce that $(y_2(\beta) - y_4(\beta))' > 0$ for $\beta \in (0,\infty)$, and therefore $y_2(\beta) - y_4(\beta)$ is monotonic increasing. Finally, we obtain again from Claim 4.2.3 that

$$\begin{aligned}y_2(0) - y_4(0) &= \sum_{k\in\{2,3,4\}} \big(\lambda_k - (-1)^{k+1}\lambda_k^2\big)\alpha_k^2 \\ &= \sum_{k\in\{1,2,3,4\}} \big(\lambda_k - (-1)^{k+1}\lambda_k^2\big)\alpha_k^2 - \big(\lambda_1^1 - \lambda_1^2\big)\alpha_1^2 = \big(\lambda_1^2 - \lambda_1\big)\alpha_1^2 > 0,\end{aligned}$$

which implies that $y_2(\beta) - y_4(\beta) > 0$ for all $\beta \in [0,\infty)$. □

Let us denote by β_2 the unique zero of y_2 and by β_4 the unique zero of y_4; they both exist by Claims 4.2.27 and 4.2.28.

Now, denote by β_2 (resp., β_4) the unique point, if it exists, where the function $y_2(\beta)$ (resp., $y_4(\beta)$) crosses the β-axis. Next, we discuss the order in which the different curves $y_2(\beta)$ and $y_4(\beta)$ cross the β-axis.

Proposition 4.2.31. *The following statements are true:*

1. *$y_1(\beta) < 0$ and $y_3(\beta) < 0$ for all $\beta \in [0,\infty)$.*
2. *Each of y_2 and y_4 has a unique zero in $(0,\infty)$.*
3. *Let us denote the zeros of y_2 and y_4 by β_2 and β_4 respectively; then $\beta_2 < \beta_4$.*

Proof.

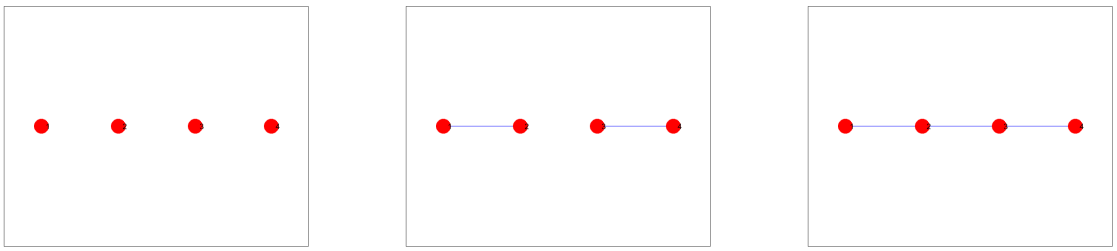

(a) $0 \leq \beta < \beta_2$ (b) $\beta_2 \leq \beta < \beta_4$ (c) $\beta \geq \beta_4$

Figure 4.11: Illustration of the structure of the modified communicability graph of K_2–K_2 versus β.

1. That $y_1(\beta) < 0$ for all $\beta \in [0, \infty)$ is proved in Claim 4.2.29. Since $\lambda_3 < 0$, it is clear that $y_3(\beta) < 0$ for all $\beta \in [0, \infty)$.

2. These statements are proved in Claims 4.2.27 and 4.2.28.

3. From Claim 4.2.30 we know that $y_2(\beta) > y_4(\beta)$ for $\beta \in [0, \infty)$. This, together with the monotonicity of y_2 and y_4 implies that $\beta_2 < \beta_4$.

□

4.2.5 Melting Signatures of K_2–K_2

Let β_2 and β_4 be as in Proposition 4.2.31. It follows from the latter that $\beta_2 < \beta_4$. Hence, the graph K_2–K_2 has one possible melting signature: (β_2, β_4). The melting of the associated modified communicability graph goes as follows. At $\beta = \beta_2$, the modified communicability graph of K_2–K_2 changes from being the null graph N_4 to two complete graphs K_2, and at $\beta = \beta_4$, the modified communicability graph becomes just the graph K_2–K_2 itself, the path graph. In Figure 4.11, we show the evolution of the modified communicability graphs of K_2–K_2 as β varies, which exhibits the (β_2, β_4) melting signature. In Figure 4.12, we plot the modified communicability function of K_2–K_2 as β varies, which exhibits the (β_2, β_4) melting signature.

Thus, in this section, we have proved the following result which fully characterizes the melting signature of dumbbell graphs.

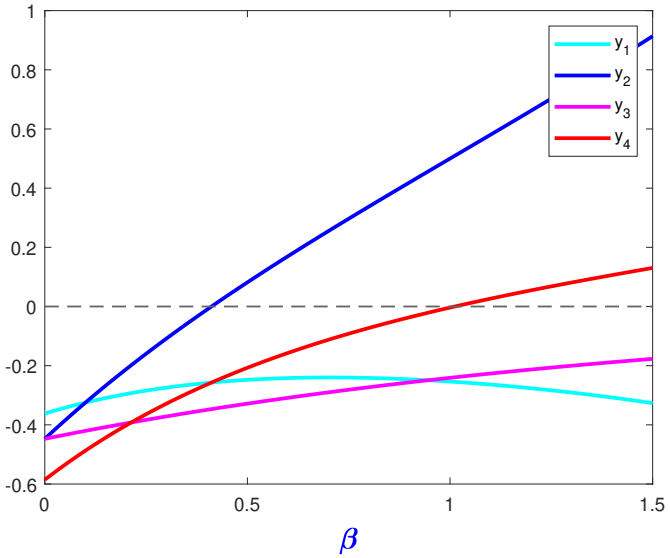

Figure 4.12: Modified communicability graph function $\Delta\tilde{G}_{pq}(\beta)$ of K_2–K_2 versus β.

Theorem 4.2.32. *All graphs K_η–K_η with $\eta \geq 3$ have the $(\beta_1, \beta_3, \beta_5, \beta_4, \beta_2)$ melting signature; only the graph K_2–K_2 has the (β_2, β_4) signature.*

4.2.6 Conclusions

As in the case of windmill graphs, a rather complete picture could be given for melting of dumbbell graphs. Rigorous proofs for most claims were possible because of the small number of different types of edges and the fact that eigenvalues of the adjacency matrix were related by algebraic relations; see Theorem 2.5.13. As in the section about windmill graphs, the main tool we used was Lemma 2.4.1.

However, even in this case there were results, such as the ordering of β_4 and β_5, where we had to rely on numerics to generate conjectures (see Conjecture 4.2.21 and Figure 4.8). The difficulty is that entries in $\Delta\tilde{G}_{pq}(\beta)$ corresponding to different edge types can intersect as β increases, and determining the place of their intersection with respect to the axis is not possible analytically. The final result of our combined analytic and numerical investigation is that the whole class of dumbbell graphs has two types of melting signatures: $(\beta_1, \beta_3, \beta_5, \beta_4, \beta_2)$ in the case of $\eta \geq 3$ and (β_2, β_4) in the case of $\eta = 2$. The reader is referred to Figure 4.10 to see the evolution of the modified

communicability graph as temperature is decreased; in particular, note the core-satellite graph $\Theta(2, \eta - 1, 2)$ in (e).

Also, note that starting at $\beta = 0$ and decreasing the temperature in the case of $\eta \geq 3$ to a sufficiently low value gives us a modified communicability graph that is a complete graph, while for $\eta = 2$, we can only recover the graph K_2–K_2 itself and not K_4.

In the next two chapters we will discuss in more detail this simple fact and will also consider the following observation: in dumbbell graphs, all entries in $\Delta\tilde{G}_{pq}(\beta)$ that correspond to edges that are present in the original graph, are monotone increasing and do not intersect (see, e.g. $f_1(\beta) + f_3(\beta)$ and $f_1(\beta) + f_5(\beta)$ in the case when $\eta \geq 3$, or indeed $y_2(\beta)$ and $y_4(\beta)$ when $\eta = 2$). As in the case of windmill graphs, in this section, the same entry in $\Delta G(\beta)$ provided the maximum for all β in the case when $\eta \geq 3$ (when $\eta = 2$ this was the case for all $\beta \geq \beta_0$). We will discuss an interpretation of this fact in terms of an edge-centrality measure in Chapter 6.

4.3 Melting in Complete Multipartite Graphs

In this section, we investigate melting in complete multipartite graphs $K_{\eta_1,\eta_2,\ldots,\eta_k}$ where $k \geq 2$ and $\eta_i \geq 1$, $i \in \{1, 2, \ldots, k\}$. Recall that $K_{\eta_1,\eta_2,\ldots,\eta_k}$ consists of k sets of vertices, V_i, $i = 1, \ldots, k$, consisting of η_i nodes; if $v \in V_i$ and $w \in V_j$, then there is an edge between v and w if and only if $i \neq j$. We consider these graphs in order to cover the case when the second eigenvalue is non-positive. There are $\frac{k(k+1)}{2}$ different types of edges in the modified communicability graph of $K_{\eta_1,\eta_2,\ldots,\eta_k}$; k different types of edges between the vertices in the same set V_i, and $\frac{k(k-1)}{2}$ different types of edges between the vertices from different sets. We use the explicit formulas for eigenvalues and normalized eigenvectors of the adjacency matrix of complete multipartite graphs to find the communicability function in order to study melting in these graphs. This allows us to find the modified communicability graph function in three cases: for $K_{\eta_1,\eta_2,\ldots,\eta_k}$ when $\eta_1 < \eta_2 < \cdots < \eta_k$, for $K_{\eta,\eta,\ldots,\eta}$, and for $K_{\eta,\eta,l}$ with $\eta < l$. In the two cases of $K_{\eta,\eta,\ldots,\eta}$ and $K_{\eta,\eta,l}$, all the analysis of monotonicity and ordering of the elements of $\Delta G(\beta)$ and $\Delta\tilde{G}_{pq}(\beta)$ can be done analytically since we found the eigenvalues and

their associated eigenvectors for these graphs; see Section 2.5.11. However, in the case of $K_{\eta_1,\eta_2,\ldots,\eta_k}$ when $\eta_1 < \eta_2 < \cdots < \eta_k$, it is very difficult to do the analysis of monotonicity and ordering analytically due to the lack of information about the $k-1$ negative eigenvalues in this situation. However, we can determine explicitly that the modified communicability graphs for these graphs are not connected regardless of the value of β.

4.3.1 Complete Multipartite Graphs $K_{\eta_1,\eta_2,\ldots,\eta_k}$ with Pairwise Distinct Parts Sizes

In this subsection, we consider the case of a complete multipartite graph $K_{\eta_1,\eta_2,\ldots,\eta_k}$ when $\eta_1 < \eta_2 < \cdots < \eta_k$. First we find the communicability function for $K_{\eta_1,\eta_2,\ldots,\eta_k}$. For this we need the eigenvalues and the orthonormal eigenvectors from Section 2.5.11. It follows from Lemma 2.5.6 that A has one positive eigenvalue λ_1, the eigenvalue 0 with multiplicity $n-k$, and $k-1$ negative eigenvalues satisfying

$$-\eta_k < \lambda_n < -\eta_{k-1} < \lambda_{n-1} < -\eta_{k-2} < \cdots < -\eta_2 < \lambda_{n-k+2} < -\eta_1.$$

The non-zero eigenvalues satisfy equation (2.21), and the corresponding eigenvectors have the form

$$\boldsymbol{x}_h = \alpha_h \begin{bmatrix} \frac{1}{\lambda_h+\eta_1}\mathbf{1}_{\eta_1} \\ \frac{1}{\lambda_h+\eta_2}\mathbf{1}_{\eta_2} \\ \vdots \\ \frac{1}{\lambda_h+\eta_k}\mathbf{1}_{\eta_k} \end{bmatrix} \qquad \text{with} \quad \alpha_h = \left(\sum_{i=1}^{k} \frac{\eta_i}{(\lambda_h+\eta_i)^2}\right)^{-\frac{1}{2}}, \qquad h \in \{1, n-k+2, n-k+3, \ldots, n\}. \tag{4.37}$$

The eigenvectors corresponding to the eigenvalue 0 are given by (2.29).

Communicability Function for $K_{\eta_1,\eta_2,\ldots,\eta_k}$

In the next lemma we find the explicit expression for the communicability function $G(\beta) = e^{\beta A}$ for $K_{\eta_1,\eta_2,\ldots,\eta_k}$ when $\eta_1 < \eta_2 < \cdots < \eta_k$. We denote by V_i the subgroups of nodes of the graph, which have size η_i.

Lemma 4.3.1. *Let $K_{\eta_1,\eta_2,\dots,\eta_k} = (V, E)$ be a complete multipartite graph with $n = \sum_{i=1}^{k} \eta_i$ nodes such that $\eta_1 < \eta_2 < \cdots < \eta_k$. Assume the nodes to be partitioned into subgroups $V_1, V_2, \dots, V_k$, and let A be the adjacency matrix defined in* (2.19)*. The communicability function $G_{pq}(\beta)$ of $K_{\eta_1,\eta_2,\dots,\eta_k}$ for all $p, q \in V$ with $p \neq q$ at the inverse temperature β is given by*

$$G_{pq}(\beta) = \begin{cases} \frac{\alpha_1^2}{(\lambda_1+\eta_i)^2} e^{\beta\lambda_1} + \sum_{h=n-k+2}^{n} \frac{\alpha_h^2}{(\lambda_h+\eta_i)^2} e^{\beta\lambda_h} - \frac{1}{\eta_i} & \text{if } p, q \in V_i, \\ \frac{\alpha_1^2}{(\lambda_1+\eta_i)(\lambda_1+\eta_j)} e^{\beta\lambda_1} + \sum_{h=n-k+2}^{n} \frac{\alpha_h^2}{(\lambda_h+\eta_i)(\lambda_h+\eta_j)} e^{\beta\lambda_h} & \text{if } p \in V_i,\ q \in V_j,\ i \neq j, \end{cases}$$

where $\lambda_1 \geq \lambda_2 \geq \cdots \geq \lambda_n$ are the eigenvalues of A and α_h are as in (4.37)*.*

Proof. First, we consider the case when $p, q \in V_i$ for some $i \in \{1, 2, \dots, k\}$. We substitute the eigenvalues and the eigenvectors of A into

$$\begin{aligned} G_{pq}(\beta) &= x_1(p)x_1(q)e^{\beta\lambda_1} + \sum_{h=2}^{n-k+1} x_h(p)x_h(q) + \sum_{h=n-k+2}^{n} x_h(p)x_h(q)e^{\beta\lambda_h} \\ &= \frac{\alpha_1^2}{(\lambda_1+\eta_i)^2} e^{\beta\lambda_1} + \sum_{h=n-k+2}^{n} \frac{\alpha_h^2}{(\lambda_h+\eta_i)^2} e^{\beta\lambda_h} + \sum_{h=2}^{n-k+1} x_h(p)x_h(q). \end{aligned}$$

Since $p, q \in V_i$, in the last sum only terms from the i^{th} block of eigenvectors corresponding to the eigenvalue 0 can be non-zero, i.e., only terms with $h = h_i + j$, $j \in \{1, 2, \dots, \eta_i - 1\}$ where $h_s = 1 + \sum_{s=1}^{i-1}(\eta_s - 1)$; cf. (2.29). The vectors $\boldsymbol{y}_{i,j}$ in (2.29) build an orthonormal system such that $\mathbf{1}_{\eta_i}^T \boldsymbol{y}_{i,j} = 0$. Hence, with $\boldsymbol{y}_{i,\eta_i} = \frac{1}{\sqrt{\eta_i}} \mathbf{1}_{\eta_i}$, the matrix $Y_i = [\boldsymbol{y}_{i,1}, \boldsymbol{y}_{i,2}, \dots, \boldsymbol{y}_{i,\eta_i}]$ is orthogonal. Since $p \neq q$, we have

$$0 = (YY^T)_{pq} = \sum_{j=1}^{\eta_i} y_p^{(i,j)}(p) y_q^{(i,j)} = \sum_{j=1}^{\eta_i - 1} x_{h_i+j}(p) x_{h_i+j}(q) + \frac{1}{\eta_i}, \tag{4.38}$$

which gives the desired result.

Now we consider the case when $p \in V_i$, $q \in V_j$, $i \neq j$. Again, we want to evaluate

$$\begin{aligned} G_{pq}(\beta) &= x_1(p)x_1(q)e^{\beta\lambda_1} + \sum_{h=2}^{n-k+1} x_h(p)x_h(q) + \sum_{h=n-k+2}^{n} x_h(p)x_h(q)e^{\beta\lambda_h} \\ &= \frac{\alpha_1^2}{(\lambda_1+\eta_i)(\lambda_1+\eta_j}e^{\beta\lambda_1)} + \sum_{h=n-k+2}^{n} \frac{\alpha_h^2}{(\lambda_h+\eta_i)(\lambda_h+\eta_j)}e^{\beta\lambda_h} \end{aligned}$$

since the entries for the eigenvectors corresponding to the eigenvalue 0 satisfy the relation $x_h(p)x_h(q) = 0$. □

Modified Communicability Graph Function of $K_{\eta_1,\eta_2,\ldots,\eta_k}$

We will find the modified communicability graph function of $K_{\eta_1,\eta_2,\ldots,\eta_k}$, when $\eta_1 < \eta_2 < \cdots < \eta_k$. First of all, we find the value of $\Delta G_{pq}(\beta)$ for all pairs of distinct nodes in the complete multipartite graphs $K_{\eta_1,\eta_2,\ldots,\eta_k}$ by removing the $e^{\beta\lambda_1}$ terms from $G_{pq}(\beta)$. Thus,

$$\Delta G_{pq}(\beta) = \begin{cases} \displaystyle\sum_{h=n-k+2}^{n} \frac{\alpha_h^2}{(\lambda_h+\eta_i)^2}e^{\beta\lambda_h} - \frac{1}{\eta_i} & \text{if } p,q \in V_i, \\ \displaystyle\sum_{h=n-k+2}^{n} \frac{\alpha_h^2}{(\lambda_h+\eta_i)(\lambda_h+\eta_j)}e^{\beta\lambda_h} & \text{if } p \in V_i,\ q \in V_j,\ i \neq j, \end{cases}$$

where the α_h are as in (4.37). Next, we need to understand the order relations among the different entries in $\Delta G_{pq}(\beta)$. This will allow us to find $\max_{p\neq q} \Delta G_{pq}(\beta)$ for $\beta > 0$ and hence $\Delta\tilde{G}_{pq}(\beta)$. We set

$$f_i(\beta) = \sum_{h=n-k+2}^{n} \frac{\alpha_h^2}{(\lambda_h+\eta_i)^2}e^{\beta\lambda_h} - \frac{1}{\eta_i} \tag{4.39}$$

$$f_{i,j}(\beta) = \sum_{h=n-k+2}^{n} \frac{\alpha_h^2}{(\lambda_h+\eta_i)(\lambda_h+\eta_j)}e^{\beta\lambda_h}. \tag{4.40}$$

The function $f_i(\beta)$ is monotonic decreasing for all $i \in \{1,2,\ldots,k\}$ since $e^{\beta\lambda_h}$ is monotonic decreasing for all $h \in \{n-k+2, n-k+3, \ldots, n\}$, and we have $\lim_{\beta\to\infty} f_i(\beta) = -\frac{1}{\eta_i}$. Let $i \in \{1,2,\ldots,k\}$ and let $p \in V_i$ be arbitrary. With a similar calculation as in (4.38)

we obtain

$$1 = \sum_{j=1}^{\eta_i - 1} \big(x_{h_i+j}(p)\big)^2 + \frac{1}{\eta_i} = \sum_{h=2}^{n-k+1} \big(x_h(p)\big)^2 + \frac{1}{\eta_i},$$

which, together with the orthogonality of the adjacency matrix A, implies

$$\begin{aligned} f_i(0) &= \sum_{h=n-k+2}^{n} \frac{\alpha_h^2}{(\lambda_h + \eta_i)^2} - \frac{1}{\eta_i} = \sum_{h=n-k+2}^{n} \big(x_h(p)\big)^2 - \frac{1}{\eta_i} \\ &= \sum_{h=2}^{n} \big(x_h(p)\big)^2 - 1 = -\big(x_1(p)\big)^2 = -\frac{\alpha_1^2}{(\lambda_1 + \eta_i)^2} < 0. \end{aligned}$$

In a similar way we can deduce that, for $i \neq j$,

$$f_{i,j}(0) = \sum_{h=n-k+2}^{n} \frac{\alpha_h^2}{(\lambda_h + \eta_i)(\lambda_h + \eta_j)} = -\frac{\alpha_1^2}{(\lambda_1 + \eta_i)(\lambda_1 + \eta_j)} < 0.$$

Based on some numerical experiments we make the following conjecture about the maximal values of $f_i(\beta)$ and $f_{i,j}(\beta)$.

Conjecture 4.3.2. *We conjecture that the following statements are true.*

1. *The graphs of the functions $f_{k,k-1}(\beta)$ and $f_k(\beta)$ intersect at a value $\beta_0 > 0$ and $f_{k,k-1}(\beta_0) = f_k(\beta_0) < 0$.*

2. *For $\beta \geq \beta_0$ the maximum of $\Delta G_{pq}(\beta)$ is attained for $p \in V_k$, $q \in V_{k-1}$, i.e., by the value $f_{k,k-1}(\beta)$.*

In Figure 4.13, we illustrate that the graphs of the functions $f_{3,2}(\beta)$ and $f_3(\beta)$ of $K_{2,3,5}$ intersect in the negative area at β_0 and that $f_{3,2}(\beta)$ gives the maximal value for $\beta \geq \beta_0$.

From Conjecture 4.3.2 we have that, for all $\beta \geq \beta_0$, the maximum value of $\Delta G_{pq}(\beta)$ should be attained by $f_{k,k-1}(\beta)$, i.e. at entries of $\Delta G(\beta)$ corresponding to two nodes that belong to the sets of largest size: V_k and V_{k-1}. Hence, we have the following result.

Theorem 4.3.3. *Let $K_{\eta_1,\eta_2,\ldots,\eta_k} = (V, E)$ be a complete multipartite graph with $n = \sum_{i=1}^{k} \eta_i$ nodes such that $\eta_1 < \eta_2 < \cdots < \eta_k$ and assume the nodes to be partitioned by $V_1, V_2, \ldots, V_k$ with adjacency matrix A defined in* (2.19)*. Assuming Conjecture 4.3.2 is*

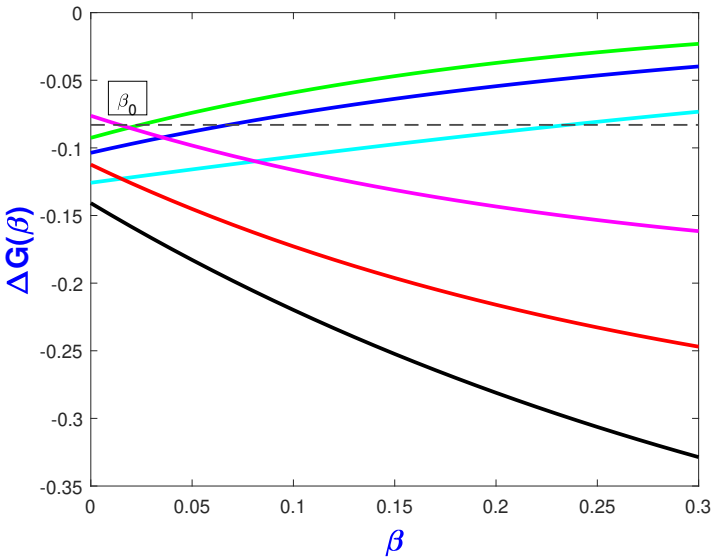

Figure 4.13: The components of the function $\Delta G_{pq}(\beta)$ of $K_{2,3,5}$ as functions of β. The green and the purple curves represent the functions $f_{3,2}(\beta)$ and $f_3(\beta)$ respectively. These curves intersect at $\beta_0 = 0.01889$ such that $f_{3,2}(\beta_0) = f_3(\beta_0) = -0.083$. The functions $f_{3,1}(\beta)$ (dark blue), $f_{2,1}(\beta)$ (light blue), $f_2(\beta)$ (red) and $f_1(\beta)$ (black) are given as well.

true, for all $p \neq q \in V$, $\Delta\tilde{G}_{pq}(\beta)$ *is given by*

$$\begin{cases} \sum_{h=n-k+2}^{n} \left(\frac{\alpha_h^2}{(\lambda_h+\eta_k)(\lambda_h+\eta_{k-1})} + \frac{\alpha_h^2}{(\lambda_h+\eta_i)^2} \right) e^{\beta\lambda_h} - \frac{1}{\eta_i} & \text{if } p,q \in V_i, \\ \sum_{h=n-k+2}^{n} \left(\frac{\alpha_h^2}{(\lambda_h+\eta_k)(\lambda_h+\eta_{k-1})} + \frac{\alpha_h^2}{(\lambda_h+\eta_i)(\lambda_h+\eta_j)} \right) e^{\beta\lambda_h} & \text{if } p \in V_i,\ q \in V_j,\ i \neq j, \end{cases}$$

where α_h *is defined in* (4.37).

To investigate melting, we use another conjecture, which is also based on computational results.

Conjecture 4.3.4. *The function*

$$f_{k,k-1}(\beta) + f_{i,1}(\beta) = \sum_{h=n-k+2}^{n} \left(\frac{\alpha_h^2}{(\lambda_h+\eta_k)(\lambda_h+\eta_{k-1})} + \frac{\alpha_h^2}{(\lambda_h+\eta_i)(\lambda_h+\eta_1)} \right) e^{\beta\lambda_h}$$

is strictly increasing for all $i \in \{2,\ldots,k\}$.

In Figure 4.14, we illustrate that the functions $f_{3,2}(\beta)+f_{3,1}(\beta)$ and $f_{3,2}(\beta)+f_{2,1}(\beta)$

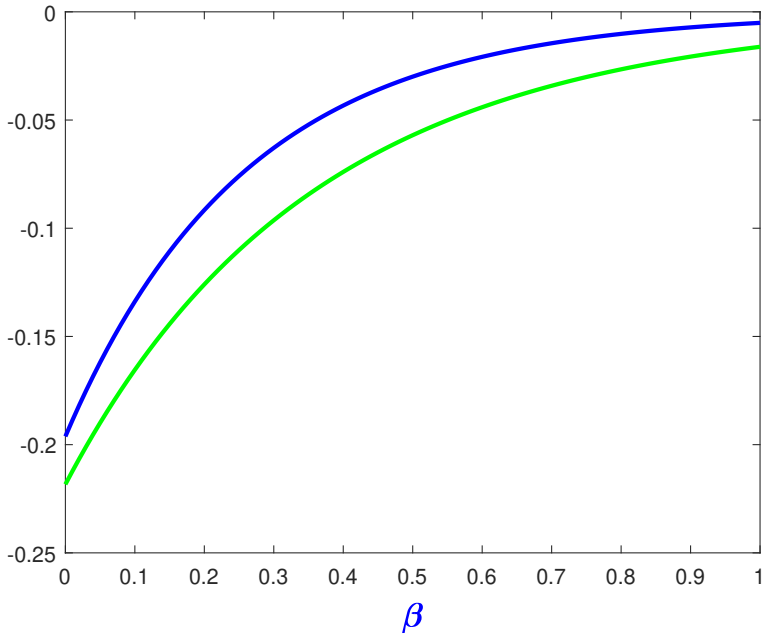

Figure 4.14: The modified communicability graph functions $f_{3,2}(\beta)+f_{3,1}(\beta)$ (blue) and $f_{3,2}(\beta)+f_{2,1}(\beta)$ (green) of $K_{2,3,5}$ as functions of β.

of $K_{2,3,5}$ are strictly increasing functions.

From Conjecture 4.3.4 it follows that $f_{k,k-1}(\beta)+f_{i,1}(\beta) < 0$ for all $\beta > 0$ and $i \in \{2,\dots,k\}$ since the limit of this function if 0 as $\beta \to \infty$. Therefore, we can deduce that the smallest set V_1, which has size η_1, cannot be connected to other sets in the modified communicability graphs of $K_{\eta_1,\eta_2,\dots,\eta_k}$ for any $\beta \geq 0$. Thus, we have the following result.

Theorem 4.3.5. *Let $K_{\eta_1,\eta_2,\dots,\eta_k} = (V,E)$ be a complete multipartite graph with $n = \sum_{i=1}^{k}\eta_i$ nodes such that $\eta_1 < \eta_2 < \cdots < \eta_k$, and assume the nodes to be partitioned by $V_1, V_2, \dots, V_k$ with adjacency matrix A defined in* (2.19)*. Assuming Conjecture 4.3.4 is true, the modified communicability graph of $K_{\eta_1,\eta_2,\dots,\eta_k}$ is not connected regardless of the value of β.*

4.3.2 Complete k-partite Graphs with equal-sized Parts

In this subsection, we consider the case of $K_{\eta_1,\eta_2,\dots,\eta_k}$ when $\eta_1 = \eta_2 = \cdots = \eta_k = \eta$. Recall from Lemma 2.5.10 that the adjacency matrix A has one positive eigenvalue

$\lambda_1 = \eta(k-1)$, one negative eigenvalue $\lambda_n = -\eta$ with multiplicity $k-1$, and 0 as eigenvalue with multiplicity $n-k$. The eigenvectors are also given in that lemma.

Communicability Function of Complete k-partite Graphs with equal-sized Parts

In the next lemma, we find the communicability function for every pair of distinct nodes in $K_{\eta,\eta,\ldots,\eta}$.

Lemma 4.3.6. *Let $K_{\eta,\eta,\ldots,\eta} = (V, E)$ be a complete k-partite graph with $n = \eta k$ nodes and assume the nodes to be partitioned by $V_1, V_2, \ldots, V_k$, with adjacency matrix A defined in (2.19) where $\eta_1 = \eta_2 = \cdots = \eta_k = \eta$. The communicability function $G_{pq}(\beta)$ of $K_{\eta,\eta,\ldots,\eta}$, for all $p \neq q \in V$, at the inverse temperature β, is given by*

$$G_{pq}(\beta) = \begin{cases} \dfrac{1}{n}e^{\beta(k-1)\eta} - \dfrac{1}{n}e^{-\beta\eta} & \text{if } p \in V_i, q \in V_j,\ i \neq j, \\ \dfrac{1}{n}e^{\beta(k-1)\eta} + \dfrac{k-1}{n}e^{-\beta\eta} - \dfrac{1}{\eta} & \text{if } p, q \in V_j. \end{cases}$$

Proof. First, we consider the case when $p \in V_i$, $q \in V_j$, $i \neq j$. Then,

$$\begin{aligned} G_{pq}(\beta) &= x_1(p)x_1(q)e^{\beta(k-1)\eta} + \sum_{h=2}^{n-k+1} x_h(p)x_h(q) + \sum_{h=n-k+2}^{n} x_h(p)x_h(q)e^{-\beta\eta} \\ &= \frac{1}{n}e^{\beta(k-1)\eta} + \sum_{h=n-k+2}^{n} x_h(p)x_h(q)e^{-\beta\eta}, \end{aligned}$$

since the entries of all eigenvectors corresponding to $\lambda = 0$ satisfy $x_h(p)x_h(q) = 0$ for all $h \in \{2, 3, \ldots, n-k+1\}$. In order to simplify the sum, let $X = [\boldsymbol{x}_1, \boldsymbol{x}_2, \ldots, \boldsymbol{x}_n]$ be the orthogonal matrix of eigenvectors of $A(K_{\eta,\eta,\ldots,\eta})$. It is easy to verify that

$$(XX^T)_{pq} = \frac{1}{n} + \sum_{h=n-k+2}^{n} x_h(p)x_h(q) = 0,$$

and hence

$$\sum_{h=n-k+2}^{n} x_h(p)x_h(q) = -\frac{1}{n},$$

which implies the desired result.

Now, we consider the case when $p, q \in V_j$, $1 \leq j \leq k$. Again, we want to evaluate

$$G_{pq}(\beta) = x_1(p)x_1(q)e^{\beta(k-1)\eta} + \sum_{h=2}^{n-k+1} x_h(p)x_h(q) + \sum_{h=n-k+2}^{n} x_h(p)x_h(q)e^{-\beta\eta}.$$

In exactly the same way as in the proof of Lemma 4.3.1, we can show that

$$\sum_{h=2}^{n-k+1} x_h(p)x_h(q) = \sum_{l=2}^{\eta} y_h(p)y_h(q) = -\frac{1}{\eta}.$$

Now, if we let again $X = [\boldsymbol{x}_1, \mathbf{x}_2, \ldots, \boldsymbol{x}_n]$ be the orthogonal matrix of eigenvectors of $A(K_{\eta,\eta,\ldots,\eta})$, then

$$(XX^T)_{pq} = \frac{1}{n} - \frac{1}{\eta} + \sum_{h=n-k+2}^{n} x_h(p)x_h(q) = 0.$$

Thus,

$$\sum_{h=n-k+2}^{n} x_h(p)x_h(q) = \frac{-1}{n} + \frac{1}{\eta} = \frac{k-1}{n},$$

since $n = \eta k$, and we get the desired result. □

Modified Communicability Graph Function of Complete k-partite Graph

To find the modified communicability graph function of $K_{\eta,\eta,\cdots,\eta}$, we first find the value of $\Delta G_{pq}(\beta)$ for all pairs of distinct nodes in the complete multipartite graph $K_{\eta,\eta,\ldots,\eta}$ by removing the $e^{\beta\lambda_1}$ terms from $G_{pq}(\beta)$. Thus,

$$\Delta G_{pq}(\beta) = \begin{cases} -\dfrac{1}{n}e^{-\beta\eta} & \text{if } p \in V_i, q \in V_j,\ i \neq j, \\ \dfrac{k-1}{n}e^{-\beta\eta} - \dfrac{1}{\eta} & \text{if } p, q \in V_j. \end{cases}$$

Next, we need to understand the order relations among the different entries in $\Delta G_{pq}(\beta)$. This will allow us to describe $\max_{p\neq q} \Delta G_{pq}(\beta)$ for $\beta > 0$ and, hence, define $\Delta\tilde{G}(\beta)$.

We set

$$f_1(\beta) = -\frac{1}{n}e^{-\beta\eta},$$
$$f_2(\beta) = \frac{k-1}{n}e^{-\beta\eta} - \frac{1}{\eta}.$$

Clearly, $f_2(\beta)$ is monotonic decreasing, and $f_1(\beta)$ is monotonic increasing. Now, since $f_1(0) = f_2(0) = -\frac{1}{n}$, we have $f_1(\beta) \geq f_2(\beta)$ for all $\beta \in [0, \infty)$, and therefore the maximal term in $\Delta G_{pq}(\beta)$ is the term that corresponds to pairs $p \in V_i$, $q \in V_j$, $i \neq j$. Hence, we have proved the following result.

Theorem 4.3.7. *Let $K_{\eta,\eta,\ldots,\eta} = (V, E)$ be a complete k-partite graph with $n = \eta k$ nodes and assume the nodes to be partitioned by $V_1, V_2, \ldots, V_k$, with adjacency matrix A defined in* (2.19)*. Then, for all $p \neq q \in V$,*

$$\Delta G_{pq}(\beta) = \begin{cases} -\frac{2}{n}e^{-\beta\eta} & \text{if } p \in V_i, q \in V_j,\ i \neq j, \\ \frac{k-2}{n}e^{-\beta\eta} - \frac{1}{\eta} & \text{if } p, q \in V_j. \end{cases}$$

Now, assume that $k \geq 2$. Then $f_1(\beta) + f_2(\beta)$ is monotonic decreasing in β and does not cross the β axis since $f_1(0) + f_2(0) = -\frac{2}{\eta} < 0$. The function $2f_1(\beta)$ is monotonic increasing but does not cross the β axis since $\lim_{\eta\to\infty} 2f_1(\beta) = 0$. Thus, for all $p \neq q \in V$, $\Delta\tilde{G}_{pq}(\beta) < 0$ for all β. Thus, we have proved the following result.

Theorem 4.3.8. *Let $K_{\eta,\eta,\ldots,\eta} = (V, E)$ be a complete k-partite graph with $n = \eta k$ nodes where $k \geq 2$ and assume that the nodes are partitioned by $V_1, V_2, \ldots, V_k$, with adjacency matrix A defined in* (2.19)*. Then, the modified communicability graph of $K_{\eta,\eta,\ldots,\eta}$ is N_n regardless of the value of β.*

4.3.3 A Class of Complete 3-partite Graphs

In this subsection, we consider the case of complete 3-partite graphs when $\eta_1 = \eta_2 = \eta$ and $\eta_3 = l$, i.e., we have three subsets: V_1,V_2 of size η, and V_3 of size l with $l > \eta$. The

adjacency matrix of a complete 3-partite graph $K_{\eta,\eta,l}$ is an $n \times n$ matrix of the form

$$A = \begin{pmatrix} O_{\eta\times\eta} & 1_{\eta\times\eta} & 1_{\eta\times l} \\ 1_{\eta\times\eta} & O_{\eta\times\eta} & 1_{\eta\times l} \\ 1_{l\times\eta} & 1_{l\times\eta} & O_{l\times l} \end{pmatrix}. \tag{4.41}$$

Recall from Lemma 2.5.11 that A has one positive eigenvalue λ_1 given in (2.33), the simple eigenvalue $-\eta$, another simple negative eigenvalue $\lambda_n \in (-l, -\eta)$ given in (2.34), and the eigenvalue 0 with multiplicity $n-3$.

Communicability Function of Complete 3-partite Graphs

We find the explicit expression for the communicability function $G(\beta) = e^{\beta A}$ for any distinct pair of nodes of $K_{\eta,\eta,l}$ in order to find the modified communicability graph functions for this graph. We have the following result.

Lemma 4.3.9. *Let $K_{\eta,\eta,l} = (V, E)$ be a complete 3-partite graph with $n = 2\eta + l$ nodes and assume the nodes to be partitioned by V_1, V_2 and V_3. The communicability function $G_{pq}(\beta)$ of $K_{\eta,\eta,l}$, for all $p \neq q \in V$, at the inverse temperature β, is given by*

$$G_{pq}(\beta) = \begin{cases} \frac{\lambda_1^2}{2\eta\lambda_1^2+4\eta^2 l}e^{\beta\lambda_1} + \frac{\lambda_n^2}{2\eta\lambda_n^2+4\eta^2 l}e^{\beta\lambda_n} + \frac{1}{2\eta}e^{-\beta\eta} - \frac{1}{\eta} & \text{if } p,q \in V_1 \text{ or } p,q \in V_2, \\ \frac{4\eta^2}{2\eta\lambda_1^2+4\eta^2 l}e^{\beta\lambda_1} + \frac{4\eta^2}{2\eta\lambda_n^2+4\eta^2 l}e^{\beta\lambda_n} - \frac{1}{l} & \text{if } p,q \in V_3, \\ \frac{\lambda_1^2}{2\eta\lambda_1^2+4\eta^2 l}e^{\beta\lambda_1} + \frac{\lambda_n^2}{2\eta\lambda_n^2+4\eta^2 l}e^{\beta\lambda_n} - \frac{1}{2\eta}e^{-\beta\eta} & \text{if } p \in V_1,\ q \in V_2, \\ \frac{2\eta\lambda_1}{2\eta\lambda_1^2+4\eta^2 l}e^{\beta\lambda_1} + \frac{2\eta\lambda_n}{2\eta\lambda_n^2+4\eta^2 l}e^{\beta\lambda_n} & \text{if } p \in V_1 \cup V_2,\ q \in V_3, \end{cases}$$

where λ_1 and λ_n are given in (2.33) and (2.34), respectively.

Proof. Throughout the proof, we shall make use of the results presented in Lemma 2.5.11.

First, we consider the case when $p, q \in V_1$ or $p, q \in V_2$ with $p \neq q$. Then

$$\begin{aligned} G_{pq}(\beta) &= x_1(p)x_1(q)e^{\beta\lambda_1} + \sum_{h=2}^{n-2} x_h(p)x_h(q) + x_{n-1}(p)x_{n-1}(q)e^{-\beta\eta} + x_n(p)x_n(q)e^{\beta\lambda_n} \\ &= \frac{\lambda_1^2}{2\eta\lambda_1^2 + 4\eta^2 l}e^{\beta\lambda_1} + \sum_{h=2}^{n-2} x_h(p)x_h(q) + \frac{\lambda_n^2}{2\eta\lambda_n^2 + 4\eta^2 l}e^{\beta\lambda_n} + \frac{1}{2\eta}e^{-\beta\eta}. \end{aligned}$$

For the term corresponding to the eigenvalue 0 we can use calculations that are similar to the one in the proof of Lemma 4.3.1 to show that $\sum_{h=2}^{n-2} x_h(p)x_h(q) = -\frac{1}{\eta}$.

Next, we consider the case when $p, q \in V_3$, $p \neq q$. Using again the form of the eigenvectors in Lemma 2.5.11, we obtain

$$\begin{aligned} G_{pq}(\beta) &= x_1(p)x_1(q)e^{\beta\lambda_1} + \sum_{h=2}^{n-2} x_h(p)x_h(q) + x_{n-1}(p)x_{n-1}(q)e^{-\beta\eta} + x_n(p)x_n(q)e^{\beta\lambda_n} \\ &= \frac{4\eta^2}{2\eta\lambda_1^2 + 4\eta^2 l}e^{\beta\lambda_1} + \sum_{h=2}^{n-2} x_h(p)x_h(q) + \frac{4\eta^2}{2\eta\lambda_n^2 + 4\eta^2 l}e^{\beta\lambda_n} \\ &= \frac{4\eta^2}{2\eta\lambda_1^2 + 4\eta^2 l}e^{\beta\lambda_1} - \frac{1}{l} + \frac{4\eta^2}{2\eta\lambda_n^2 + 4\eta^2 l}e^{\beta\lambda_n}, \end{aligned}$$

where we used again a similar calculation as in the proof of Lemma 4.3.1 and the fact that the term corresponding to the eigenvalue $\lambda_{n-1} = -\eta$ satisfies $x_{n-1}(p)x_{n-1}(q) = 0$.

The third case is when $p \in V_1$ and $q \in V_2$, where we have

$$\begin{aligned} G_{pq}(\beta) &= x_1(p)x_1(q)e^{\beta\lambda_1} + \sum_{h=2}^{n-2} x_h(p)x_h(q) + x_{n-1}(p)x_{n-1}(q)e^{-\beta\eta} + x_n(p)x_n(q)e^{\beta\lambda_n} \\ &= \frac{\lambda_1^2}{2\eta\lambda_1^2 + 4\eta^2 l}e^{\beta\lambda_1} + \frac{\lambda_n^2}{2\eta\lambda_n^2 + 4\eta^2 l}e^{\beta\lambda_n} - \frac{1}{2\eta}e^{-\beta\eta} \end{aligned}$$

since the entries for all the eigenvectors that correspond to the eigenvalue $\lambda = 0$ satisfy $x_h(p)x_h(q) = 0$ for all $h \in \{2, 3, \ldots, n-2\}$.

Finally, we consider the case when $p \in V_1$ or $q \in V_2$, and $q \in V_3$. With similar

considerations as above we obtain

$$\begin{aligned} G_{pq}(\beta) &= x_1(p)x_1(q)e^{\beta\lambda_1} + \sum_{h=2}^{n-2} x_h(p)x_h(q) + x_{n-1}(p)x_{n-1}(q)e^{-\beta\eta} + x_n(p)x_n(q)e^{\beta\lambda_n} \\ &= \frac{2\eta\lambda_1}{2\eta\lambda_1^2 + 4\eta^2 l}e^{\beta\lambda_1} + \frac{2\eta\lambda_n}{2\eta\lambda_n^2 + 4\eta^2 l}e^{\beta\lambda_n}. \end{aligned}$$

This finishes the proof. □

Modified Communicability Graph Function of Complete 3-partite Graphs

First of all, we find the value of $\Delta G_{pq}(\beta)$ for all pairs of distinct nodes in the complete 3-partite graphs:

$$\Delta G_{pq}(\beta) = \begin{cases} \frac{\lambda_n^2}{2\eta\lambda_n^2+4\eta^2 l}e^{\beta\lambda_n} + \frac{1}{2\eta}e^{-\beta\eta} - \frac{1}{\eta} & \text{if } p,q \in V_1 \text{ or } p,q \in V_2, \\ \frac{4\eta^2}{2\eta\lambda_n^2+4\eta^2 l}e^{\beta\lambda_n} - \frac{1}{l} & \text{if } p,q \in V_3, \\ \frac{\lambda_n^2}{2\eta\lambda_n^2+4\eta^2 l}e^{\beta\lambda_n} - \frac{1}{2\eta}e^{-\beta\eta} & \text{if } p \in V_1,\ q \in V_2, \\ \frac{2\eta\lambda_n}{2\eta\lambda_n^2+4\eta^2 l}e^{\beta\lambda_n} & \text{if } p \in V_1 \cup V_2,\ q \in V_3. \end{cases}$$

Next, we need to understand the order relations among the different entries in $\Delta G_{pq}(\beta)$. This will allow us to describe $\max_{p\neq q} \Delta G_{pq}(\beta)$ for $\beta > 0$ and hence, to define $\Delta\tilde{G}_{pq}(\beta)$. We set

$$\begin{aligned} f_1(\beta) &= \frac{\lambda_n^2}{2\eta\lambda_n^2 + 4\eta^2 l}e^{\beta\lambda_n} + \frac{1}{2\eta}e^{-\beta\eta} - \frac{1}{\eta}, \\ f_2(\beta) &= \frac{4\eta^2}{2\eta\lambda_n^2 + 4\eta^2 l}e^{\beta\lambda_n} - \frac{1}{l}, \\ f_3(\beta) &= \frac{\lambda_n^2}{2\eta\lambda_n^2 + 4\eta^2 l}e^{\beta\lambda_n} - \frac{1}{2\eta}e^{-\beta\eta}, \\ f_4(\beta) &= \frac{2\eta\lambda_n}{2\eta\lambda_n^2 + 4\eta^2 l}e^{\beta\lambda_n}. \end{aligned}$$

Claim 4.3.10. *We have $f_4(\beta) > f_3(\beta)$ for all $\beta \in [0, \infty)$.*

Proof. First we observe that $\lambda_n + \eta < 0$ and $\lambda_n + l > 0$. Hence, for all $\beta \in [0, \infty)$, we

have

$$\begin{aligned} f_4(\beta) - f_3(\beta) &= \frac{2\eta\lambda_n - \lambda_n^2}{2\eta(\lambda_n^2 + 2\eta l)} e^{\beta\lambda_n} + \frac{1}{2\eta} e^{-\beta\eta} \\ &= e^{-\beta\eta}\left[\frac{2\eta\lambda_n - \lambda_n^2}{2\eta(\lambda_n^2 + 2\eta l)} e^{\beta(\lambda_n+\eta)} + \frac{1}{2\eta}\right] \\ &\geq e^{-\beta\eta}\left[\frac{2\eta\lambda_n - \lambda_n^2}{2\eta(\lambda_n^2 + 2\eta l)} + \frac{1}{2\eta}\right] \\ &= e^{-\beta\eta}\frac{2\eta\lambda_n - \lambda_n^2 + \lambda_n^2 + 2\eta l}{2\eta(\lambda_n^2 + 2\eta l)} = e^{-\beta\eta}\frac{\lambda_n + l}{\lambda_n^2 + 2\eta l} > 0, \end{aligned}$$

which proves the claim. □

Claim 4.3.11. *We have $f_3(\beta) \geq f_1(\beta)$ for all $\beta \in [0, \infty)$.*

Proof. For $\beta \in [0, \infty)$, we have

$$f_3(\beta) - f_1(\beta) = -\frac{1}{\eta} e^{-\beta\eta} + \frac{1}{\eta} = \frac{1}{\eta}\big(1 - e^{-\beta\eta}\big) \geq 0.$$

□

Claim 4.3.12. *The function $f_2(\beta)$ is strictly decreasing; the function $f_4(\beta)$ is strictly increasing. There is a unique point $\beta_0 > 0$ where the graphs of f_2 and f_4 intersect, i.e., a unique number such that $f_2(\beta_0) = f_4(\beta_0)$. Further, $f_4(0) < f_2(0) < 0$.*

Proof. The function $f_2(\beta)$ is strictly decreasing and $f_4(\beta)$ is strictly increasing since the coefficients of $e^{\beta\lambda_n}$ are positive and negative respectively. For the values at 0 we have

$$f_2(0) = \frac{2\eta}{\lambda_n^2 + 2\eta l} - \frac{1}{l} = -\frac{\lambda_n^2}{(\lambda_n^2 + 2\eta l)l} < 0$$

and

$$f_2(0) - f_4(0) = -\frac{\lambda_n^2}{(\lambda_n^2 + 2\eta l)l} - \frac{\lambda_n}{\lambda_n^2 + 2\eta l} = -\frac{\lambda_n(\lambda_n + l)}{(\lambda_n^2 + 2\eta l)l} > 0$$

since $\lambda_n + l > 0$. Moreover, we have $\lim_{\beta\to\infty} f_2(\beta) = -\frac{1}{l}$ and $\lim_{\beta\to\infty} f_4(\beta) = 0$, which implies that the graphs of f_2 and f_4 intersect at a unique positive point $\beta_0 > 0$. □

Proposition 4.3.13. *We have the following relations among the functions $f_i(\beta)$.*

1. *$f_4(\beta) \geq f_3(\beta) \geq f_1(\beta)$ for all $\beta \in [0, \infty)$.*

2. *For $\beta_0 > 0$ as in Claim 4.3.12 we have $f_2(\beta) > f_4(\beta)$ for $\beta \in [0, \beta_0)$, and $f_2(\beta) < f_4(\beta)$ for $\beta \in [\beta_0, \infty)$.*

3. *$f_i(\beta) < 0$ for all $\beta \in [0, \infty)$ and $i = 1, 2, 3, 4$.*

Proof. The first two items follow directly from Claims 4.3.10 4.3.11 and 4.3.12.

Now let us consider the statements in item 3. Since $f_4(\beta)$ is strictly increasing and $\lim_{\beta\to\infty} f_4(\beta) = 0$, it follows that $f_4(\beta) < 0$ for all $\beta \in [0, \infty)$. The fact that $f_2(0) < 0$ (proved in Claim 4.3.12) and the monotonicity of $f_2(\beta)$ imply that $f_2(\beta) < 0$ for all $\beta \in [0, \infty)$. Finally, we use item 1. to obtain $f_1(\beta) \leq f_3(\beta) \leq f_4(\beta) < 0$ for all $\beta \in [0, \infty)$. □

From Proposition 4.3.13, we see that, for $\beta \in [0, \beta_0)$, the maximum value of $\Delta G_{pq}(\beta)$ is attained by $f_2(\beta)$, and for $\beta \in [\beta_0, \infty)$, the maximum value of $\Delta G_{pq}(\beta)$ is attained by $f_4(\beta)$; for $\beta \in [0, \beta_0)$ this corresponds to pairs of nodes $p, q \in V_3$, and for $\beta \in [\beta_0, \infty)$ this corresponds to pairs of nodes $p \in V_1 \cup V_2$ and $q \in V_3$. Hence we have proved the following result.

Theorem 4.3.14. *Let $K_{\eta,\eta,l} = (V, E)$ be a complete 3-partite graph with $n = 2\eta + l$ nodes. Assume that the nodes are partitioned by V_1, V_2, V_3 with $\eta < l$, and let the adjacency matrix A be as in (4.41). The modified communicability graph function $\Delta\tilde{G}_{pq}(\beta)$ of $K_{\eta,\eta,l}$ is, for all $p, q \in V$, $p \neq q$, given by*

$$\Delta\tilde{G}_{pq}(\beta) = \begin{cases} \frac{\lambda_n^2+4\eta^2}{2\eta\lambda_n^2+4\eta^2 l} e^{\beta\lambda_n} + \frac{1}{2\eta} e^{-\beta\eta} - \frac{1}{\eta} - \frac{1}{l} & \text{if } p, q \in V_1 \text{ or } p, q \in V_2, \\ \frac{8\eta^2}{2\eta\lambda_n^2+4\eta^2 l} e^{\beta\lambda_n} - \frac{2}{l} & \text{if } p, q \in V_3, \\ \frac{\lambda_n^2+4\eta^2}{2\eta\lambda_n^2+4\eta^2 l} e^{\beta\lambda_n} - \frac{1}{2\eta} e^{-\beta\eta} - \frac{1}{l} & \text{if } p \in V_1,\ q \in V_2, \\ \frac{2\eta\lambda_n+4\eta^2}{2\eta\lambda_n^2+4\eta^2 l} e^{\beta\lambda_n} - \frac{1}{l} & \text{if } p \in V_1 \cup V_2,\ q \in V_3 \end{cases}$$

when $\beta \in [0, \beta_0)$*, and*

$$\Delta\tilde{G}_{pq}(\beta) = \begin{cases} \frac{\lambda_n^2+2\eta\lambda_n}{2\eta\lambda_n^2+4\eta^2 l}e^{\beta\lambda_n} + \frac{1}{2\eta}e^{-\beta\eta} - \frac{1}{\eta} & \text{if } p,q \in V_1 \text{ or } p,q \in V_2, \\ \frac{4\eta^2+2\eta\lambda_n}{2\eta\lambda_n^2+4\eta^2 l}e^{\beta\lambda_n} - \frac{1}{l} & \text{if } p,q \in V_3, \\ \frac{\lambda_n^2+2\eta\lambda_n}{2\eta\lambda_n^2+4\eta^2 l}e^{\beta\lambda_n} - \frac{1}{2\eta}e^{-\beta\eta} & \text{if } p \in V_1,\ q \in V_2, \\ \frac{4\eta\lambda_n}{2\eta\lambda_n^2+4\eta^2 l}e^{\beta\lambda_n} & \text{if } p \in V_1 \cup V_2,\ q \in V_3 \end{cases}$$

when $\beta \in [\beta_0, \infty)$*.*

From Proposition 4.3.13, $f_i(\beta) < 0$ for all $\beta \in [0, \infty)$ and all $i \in \{1, 2, 3, 4\}$. Hence, all entries of the modified communicability graph function $\Delta\tilde{G}_{pq}(\beta)$ are negative, i.e., none of the entries crosses the β axis. Thus, we proved the following result.

Theorem 4.3.15. *Let* $K_{\eta,\eta,l} = (V, E)$ *be a complete* 3*-partite graph with* $n = 2\eta + l$ *nodes. Assume that the nodes are partitioned by* V_1, V_2, V_3 *with* $\eta < l$*, and let the adjacency matrix* A *be as in* (4.41)*. Then, the modified communicability graph of* $K_{\eta,\eta,l}$ *is* N_n *regardless of the value of* β*.*

4.3.4 Conclusions

Finding the explicit formulas for eigenvalues and normalized eigenvectors of the adjacency matrix allowed us to find the communicability function and the modified communicability graph function for complete multipartite graphs $K_{\eta,\eta,\ldots,\eta}$ and $K_{\eta,\eta,l}$. In the two cases of $K_{\eta,\eta,\ldots,\eta}$ and $K_{\eta,\eta,l}$, all the analysis of monotonicity and ordering of the elements of $\Delta G(\beta)$ and $\Delta\tilde{G}_{pq}(\beta)$ can be done analytically. However, in the case of $K_{\eta_1,\eta_2,\ldots,\eta_k}$ when $\eta_1 < \eta_2 < \cdots < \eta_k$, it was very difficult to do the analysis of monotonicity and ordering analytically. We found the maximum of $\Delta G(\beta)$ and the connectivity of the function $\Delta\tilde{G}_{pq}(\beta)$ for $K_{\eta_1,\eta_2,\ldots,\eta_k}$ when $\eta_1 < \eta_2 < \cdots < \eta_k$ based on experiments; see Conjunctures 4.3.2 and 4.3.4. To sum up, we determined explicitly that, in the cases considered in this section, the modified communicability graph for complete multipartite graphs is not connected regardless the value of β.

Chapter 5

Melting Phase transition

5.1 Melting in Cycle Graphs

In Chapter 4, we studied melting in three families of graphs. Two families, namely, windmill graphs and dumbbell graphs, have the property that the second largest eigenvalue λ_2 is positive and the number of different types of edges in the associated modified communicability graph is very low. In this section, we study the melting of cycle graphs C_n, $n \geq 5$, in which case the second largest eigenvalue is positive and the number of different types of edges in the associated modified communicability graph is increasing as n increases; it is $\frac{n-1}{2}$ if n is odd and $\frac{n}{2}$ if n is even. Based on the considerations below, we conjecture that all functions corresponding to different types of edges in the associated modified communicability graph function of C_n, $n \notin \{6, 8\}$ change sign (cross the β-axis) as β increases, except one function, which is concave and either does not cross the β-axis at all or crosses it twice, which is inconsistent with our proposed melting theory for graphs. However, if we exclude this concave function, we can determine computationally that there is one possible melting signature when n is even and one possible melting signature when n is odd for the modified communicability graph of C_n. We also determine the melting signatures for C_6 and C_8; for both graphs, there are two functions that do not cross the β-axis: one is concave and one is monotonic increasing and converging to 0.

Let $n \in \mathbb{N}$ with $n \geq 5$ and consider the cycle graph $C_n = (V, E)$ with n vertices.

Recall from (2.8) that the spectrum of the adjacency matrix A consists of the eigenvalues

$$\lambda_k = 2\cos\left(\frac{2\pi(k-1)}{n}\right), \qquad \begin{cases} k = 0, 1, \ldots, \frac{n+1}{2} & \text{if } n \text{ is odd,} \\ k = 0, 1, \ldots, \frac{n+2}{2} & \text{if } n \text{ is even.} \end{cases}$$

(We have shifted the index by one so that the largest eigenvalue is λ_1.) The eigenvalue $\lambda_1 = 2$, and in the case of even n also $\lambda_{\frac{n+2}{2}} = -2$, are simple with eigenvector $\boldsymbol{x}_1$ and $\boldsymbol{x}_{\frac{n+2}{2}}$ respectively; all other eigenvalues have multiplicity two with eigenvectors $\boldsymbol{x}_k$ and $\boldsymbol{x}_{n-k}$ where

$$\boldsymbol{x}_k = \frac{1}{\sqrt{n}} \begin{bmatrix} 1 \\ \omega_n^{k-1} \\ \omega_n^{2(k-1)} \\ \vdots \\ \omega_n^{(n-1)(k-1)} \end{bmatrix}, \qquad k = 1, 2, \ldots, n, \qquad \text{with} \quad \omega_n = e^{\frac{2\pi i}{n}}.$$

Let us find the communicability function $G_{p,q}$ when n is odd. Since the eigenvectors we chose have nonreal entries, we have

$$\begin{aligned} G_{pq}(\beta) &= x_1(p)\overline{x_1(q)}e^{\beta\lambda_1} + \sum_{k=2}^{\frac{n+1}{2}} \Big[x_k(p)\overline{x_k(q)} + x_{n-k}(p)\overline{x_{n-k}(q)} \Big] e^{\lambda_k \beta} \\ &= \frac{1}{n}e^{2\beta} + \sum_{k=2}^{\frac{n+1}{2}} \frac{1}{n} \Big[\omega_n^{(p-1)(k-1)} \omega_n^{-(q-1)(k-1)} + \omega_n^{(p-1)(n-k-1)} \omega_n^{-(q-1)(n-k-1)} \Big] e^{\lambda_k \beta} \\ &= \frac{1}{n}e^{2\beta} + \sum_{k=2}^{\frac{n+1}{2}} \frac{1}{n} \Big[\omega_n^{(p-q)(k-1)} + \omega_n^{-(p-q)(k-1)} \Big] e^{\lambda_k \beta} \\ &= \frac{1}{n}e^{2\beta} + \sum_{k=2}^{\frac{n+1}{2}} \frac{2}{n} \Big[e^{\frac{2\pi i(p-q)(k-1)}{n}} + e^{-\frac{2\pi i(p-q)(k-1)}{n}} \Big] e^{\lambda_k \beta} \\ &= \frac{1}{n}e^{2\beta} + \sum_{k=2}^{\frac{n+1}{2}} \frac{2}{n} \cos\left(\frac{2\pi|p-q|(k-1)}{n}\right) e^{\lambda_k \beta}, \end{aligned}$$

where we have used that $\omega_n^n = 1$. In a similar way, we can consider the case when n is

even, where we also have a term corresponding to the eigenvalue $\lambda_{\frac{n+2}{2}} = -2$ and hence obtain

$$G_{pq}(\beta) = \frac{1}{n}e^{2\beta} + \sum_{k=2}^{\frac{n}{2}} \frac{2}{n}\cos\left(\frac{2\pi|p-q|(k-1)}{n}\right)e^{\lambda_k\beta} + \frac{1}{n}(-1)^{|p-q|}e^{-2\beta}.$$

By subtracting the term corresponding to $\lambda_1 = 2$ we obtain

$$\Delta G_{pq}(\beta) = \begin{cases} \frac{2}{n}\sum_{k=2}^{\frac{n+1}{2}} \cos\left(\frac{2\pi|p-q|(k-1)}{n}\right)e^{\lambda_k\beta} & \text{if } n \text{ is odd,} \\ \frac{2}{n}\sum_{k=2}^{\frac{n}{2}} \cos\left(\frac{2\pi|p-q|(k-1)}{n}\right)e^{\lambda_k\beta} + \frac{1}{n}(-1)^{|p-q|}e^{-2\beta} & \text{if } n \text{ is even.} \end{cases} \tag{5.1}$$

Let us introduce the functions $f_d(\beta) = \Delta G_{1,1+d}(\beta)$, which correspond to pairs of nodes that are distance d apart:

$$f_d(\beta) = \begin{cases} \frac{2}{n}\sum_{k=2}^{\frac{n+1}{2}} \cos\left(\frac{2\pi d(k-1)}{n}\right)e^{\lambda_k\beta} & \text{if } n \text{ is odd,} \\ \frac{2}{n}\sum_{k=2}^{\frac{n}{2}} \cos\left(\frac{2\pi d(k-1)}{n}\right)e^{\lambda_k\beta} + \frac{1}{n}(-1)^{d}e^{-2\beta} & \text{if } n \text{ is even,} \end{cases} \tag{5.2}$$

$d = 1, \ldots, \frac{n}{2}$ if n is even, and $d = 1, \ldots, \frac{n-1}{2}$ if n is odd. In the following subsections we consider different values of n.

5.1.1 Melting in C_5

The graph $C_5 = (V, E)$ is a simple graph with 5 vertices, and the spectrum of its adjacency matrix consists of $\lambda_1 = 2$, $\lambda_2 = 2\cos\left(\frac{2\pi}{5}\right) = \frac{\sqrt{5}-1}{2} \approx 0.618$ and $\lambda_3 = 2\cos\left(\frac{4\pi}{5}\right) = -\frac{\sqrt{5}+1}{2} \approx -1.618$ where λ_2 and λ_3 have multiplicity two. The functions $f_d(\beta)$ from (5.2) become

$$f_d(\beta) = \frac{2}{5}\cos\left(\frac{2\pi d}{5}\right)e^{\lambda_2\beta} + \frac{2}{5}\cos\left(\frac{4\pi d}{5}\right)e^{\lambda_3\beta}, \qquad d = 1, 2,$$

which yields

$$f_1(\beta) = ae^{\lambda_2\beta} + be^{\lambda_3\beta},$$
$$f_2(\beta) = be^{\lambda_2\beta} + ae^{\lambda_3\beta},$$

where $a = \frac{2}{5}\cos\left(\frac{2\pi}{5}\right) = \frac{2}{5}\cos\left(\frac{8\pi}{5}\right) \approx 0.1236$ and $b = \frac{2}{5}\cos\left(\frac{4\pi}{5}\right) \approx -0.3236$. The derivatives of $f_1(\beta)$ and $f_2(\beta)$ satisfy

$$f_1'(\beta) = a\lambda_2 e^{\lambda_2\beta} + b\lambda_3 e^{\lambda_3\beta} > 0,$$
$$f_1'(\beta) = b\lambda_2 e^{\lambda_2\beta} + a\lambda_3 e^{\lambda_3\beta} < 0,$$

and hence $f_1(\beta)$ is strictly increasing, and $f_2(\beta)$ is strictly decreasing. Moreover, we have

$$f_1(0) = f_2(0) = a + b = \frac{\sqrt{5}-1}{10} - \frac{\sqrt{5}+1}{10} = \frac{1}{5},$$

which implies that $f_1(\beta) \geq f_2(\beta)$ for all $\beta \in [0, \infty)$. This shows that the maximum value of $\Delta G_{pq}(\beta)$ is attained by $f_1(\beta)$, which corresponds to pairs of nodes (p, q) that are connected in the graph C_5. Hence the modified communicability graph function $\Delta\tilde{G}_{pq}(\beta)$ of C_5, for all $\beta \geq 0$, is given by

$$\Delta\tilde{G}_{pq}(\beta) = \begin{cases} 2ae^{\lambda_2\beta} + 2be^{\lambda_3\beta} & \text{if } (p,q) \in E, \\ (a+b)e^{\lambda_2\beta} + (a+b)e^{\lambda_3\beta} & \text{if } (p,q) \notin E. \end{cases}$$

In Figure 5.1, we show the modified communicability graph function $\Delta\tilde{G}_{pq}(\beta)$ of C_5 versus β. Since $a + b = -\frac{1}{5} < 0$, we have $f_1(\beta) + f_2(\beta) < 0$ for all $\beta \in [0, \infty)$, whereas $2f_1(\beta)$ is strictly increasing and crosses the β-axis exactly once. Thus, the graph C_5 has one possible melting signature, (β_1). The melting of the associated modified communicability graph goes as follows. At $\beta = \beta_1$, the modified communicability graph of C_5 changes from being the null graph N_5 to C_5.

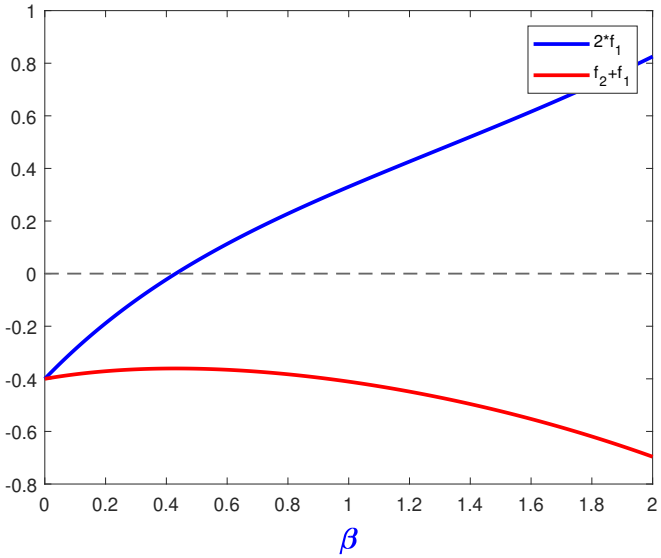

Figure 5.1: Modified communicability graph function $\Delta\tilde{G}_{pq}(\beta)$ of C_5 versus β.

5.1.2 Melting in C_6

The graph $C_6 = (V, E)$ is a simple graph with 6 vertices, and the spectrum of its adjacency matrix consists of $\lambda_1 = 2$, $\lambda_2 = 1$, $\lambda_3 = -1$ and $\lambda_4 = -2$ where λ_2 and λ_3 have multiplicity two. It follows from (5.1) that

$$\Delta G_{pq}(\beta) = \frac{1}{3}\cos\Big(\frac{\pi|p-q|}{3}\Big)e^{\beta} + \frac{1}{3}\cos\big(\frac{2\pi|p-q|}{3}\Big)e^{-\beta} + \frac{1}{6}(-1)^{|p-q|}e^{-2\beta}$$

$$= \begin{cases} \frac{1}{6}\big(e^{\beta} - e^{-\beta} - e^{-2\beta}\big) & \text{if } (p,q) \in E, \\ \frac{1}{6}\big(-e^{\beta} - e^{-\beta} + e^{-2\beta}\big) & \text{if } |p-q| = 2 \text{ or } |p-q| = 4, \\ \frac{1}{6}\big(-2e^{\beta} + 2e^{-\beta} - e^{-2\beta}\big) & \text{if } |p-q| = 3. \end{cases}$$

As in (5.2) let us define $f_d(\beta)$ as follows:

$$f_1(\beta) = \frac{1}{6}\big(e^{\beta} - e^{-\beta} - e^{-2\beta}\big),$$

$$f_2(\beta) = \frac{1}{6}\big(-e^{\beta} - e^{-\beta} + e^{-2\beta}\big),$$

$$f_3(\beta) = \frac{1}{6}\big(-2e^{\beta} + 2e^{-\beta} - e^{-2\beta}\big).$$

Claim 5.1.1. *The function $f_2(\beta)$ is monotonic decreasing in β.*

Proof. Consider the derivative of $f_2(\beta)$,

$$f_2'(\beta) = -\frac{1}{6}e^{\beta} + \frac{1}{6}e^{-\beta} - \frac{1}{3}e^{-2\beta}.$$

It follows from Lemma 2.4.1 that $f_2'(\beta) < 0$ since $-\frac{1}{6} < 0$, $-\frac{1}{6}+\frac{1}{6} = 0$ and $-\frac{1}{6}+\frac{1}{6}-\frac{1}{3} < 0$. This implies that $f_2(\beta)$ is monotonic decreasing. □

Claim 5.1.2. *The function $f_3(\beta)$ is monotonic decreasing in β.*

Proof. Consider the derivative of $f_3(\beta)$,

$$f_3'(\beta) = -\frac{1}{3}e^{\beta} - \frac{1}{3}e^{-\beta} + \frac{1}{3}e^{-2\beta}.$$

We can, again, use Lemma 2.4.1 to show that $f_3'(\beta) < 0$ since $-\frac{1}{3} < 0$, $-\frac{1}{3} - \frac{1}{3} < 0$ and $-\frac{1}{3} - \frac{1}{3} + \frac{1}{3} < 0$. Hence, $f_3(\beta)$ is monotonic decreasing. □

We also know that $f_1(\beta)$ is strictly increasing since $f_1'(\beta) = \frac{1}{6}e^{\beta} + \frac{1}{6}e^{-\beta} + \frac{1}{3}e^{-2\beta}$ is clearly positive. Further, $f_1(0) = f_2(0) = f_3(0) = -\frac{1}{6}$. This, together with Claims 5.1.1 and 5.1.2, implies that maximum value of $\Delta G_{pq}(\beta)$ is attained by $f_1(\beta)$, which corresponds to pairs (p, q) that are connected in the graph C_6. Hence the modified communicability graph function $\Delta\tilde{G}_{pq}(\beta)$ of C_6 is, for all $\beta \geq 0$, given by

$$\Delta\tilde{G}_{pq}(\beta) = \begin{cases} \frac{1}{3}\left(e^{\beta} - e^{-\beta} - e^{-2\beta}\right) & \text{if } (p,q) \in E, \\ -\frac{1}{3}e^{-\beta} & \text{if } |p-q| = 2 \text{ or } |p-q| = 4, \\ \frac{1}{6}\left(-e^{\beta} + e^{-\beta} - 2e^{-2\beta}\right) & \text{if } |p-q| = 3. \end{cases}$$

The function $2f_1(\beta)$ is monotonic increasing in β and crosses the β-axis exactly once. On the other hand, the function $f_1(\beta)+f_2(\beta)$ is monotonic increasing but does not cross the β-axis. The function $f_1(\beta)+f_3(\beta)$ is concave and does not cross β-axis. The latter can again be seen by applying Lemma 2.4.1 since $-\frac{1}{6} < 0$, $-\frac{1}{6}+\frac{1}{6} = 0$ and $-\frac{1}{6}+\frac{1}{6}-\frac{1}{3} < 0$ and hence $f_1(\beta) + f_3(\beta) < 0$. In Figure 5.2, we show the modified communicability graph function $\Delta\tilde{G}_{pq}(\beta)$ of C_6 versus β. Thus, the graph C_6 has one possible melting

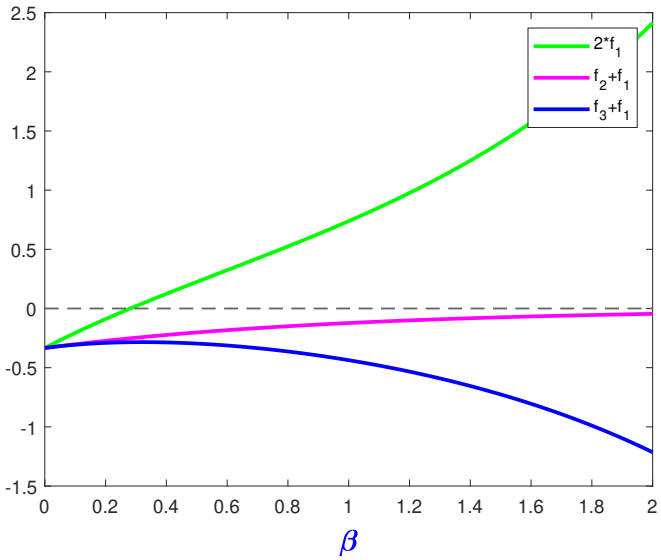

Figure 5.2: Modified communicability graph function $\Delta\tilde{G}_{pq}(\beta)$ of C_6 versus β.

signature, (β_1). The melting of the associated modified communicability graph goes as follows. At $\beta = \beta_1$ the modified communicability graph of C_6 changes from being the null graph N_6 to C_6.

5.1.3 Melting in C_n

Let us now consider the general case C_n, $n \geq 5$. We have studied the melting in C_n for $n = 7, 8, \ldots, 13$. In the following conjecture we summarize what we believe happens in the general case. The cases $n = 5$ and $n = 6$ have actually been discussed rigorously above.

Conjecture 5.1.3. *We conjecture that, for the cycle graph $C_n = (V, E)$, $n \geq 5$, the following statements are true.*

1. *For all β, the maximum of $\Delta G_{pq}(\beta)$ for C_n is the function $f_1(\beta)$, which corresponds to the pairs (p, q) that are connected in the graph C_n (i.e. $(p, q) \in E$). Hence, the entries of the modified communicability graph function $\Delta\tilde{G}_{pq}(\beta)$ are $f_1(\beta) + f_d(\beta)$, $d = 1, \ldots, \frac{n}{2}$ if n is even, and $d = 1, \ldots, \frac{n-1}{2}$ if n is odd.*

2. *For C_5, the function $2f_1(\beta)$ is strictly increasing and crosses the β-axis exactly*

once. The function $f_1(\beta) + f_2(\beta)$ is concave and does not cross the β-axis.

3. *For C_6, the function $2f_1(\beta)$ is strictly increasing and crosses the β-axis exactly once. The function $f_1(\beta) + f_2(\beta)$ is strictly increasing and converges to 0 and hence does not cross the β-axis. The function $f_1(\beta) + f_3(\beta)$ is concave and does not cross the β-axis.*

4. *For C_7, the functions $2f_1(\beta)$ and $f_1(\beta) + f_2(\beta)$ are strictly increasing and cross the β-axis exactly once. The function $f_1(\beta) + f_3(\beta)$ is concave and does not cross the β-axis.*

5. *For C_8, the functions $2f_1(\beta)$ and $f_1(\beta) + f_2(\beta)$ are strictly increasing and cross the β-axis exactly once. The function $f_1(\beta) + f_3(\beta)$ is strictly increasing and converges to 0 and hence does not cross the β-axis. The function $f_1(\beta) + f_4(\beta)$ is concave and does not cross the β-axis.*

6. *For C_n with $n \geq 9$, the functions $f_1(\beta) + f_d(\beta)$, $d = 1, \ldots, \frac{n}{2} - 1$ when n is even, and $d = 1, \ldots, \frac{n-1}{2} - 1$ when n is odd, are strictly increasing and cross the β-axis exactly once. The function $f_1(\beta) + f_{\frac{n}{2}}(\beta)$ when n is even, or $f_1(\beta) + f_{\frac{n-1}{2}}(\beta)$ when n is odd, is concave and crosses the β-axis twice.*

The graphs C_5 and C_6 have melting signature (β_1) as discussed above. Moreover, the graphs C_7 and C_8 have melting signature (β_1, β_2); in both cases the modified communicability graph changes at $\beta = \beta_1$ from being the null graph N_n to C_n (which is a regular graph with average degree 2), and at $\beta = \beta_2$ it becomes a regular graph with average degree 4 (vertices are connected in the modified communicability graph if the distance of the vertices is 1 or 2 in C_n).

For $n \geq 9$, we encounter the problem that the function $f_1(\beta) + f_{\frac{n}{2}}(\beta)$ (when n is even) or $f_1(\beta) + f_{\frac{n-1}{2}}(\beta)$ (when n is odd) crosses the β-axis twice. However, if we exclude this concave function with two crossings, then we can still obtain a sensible melting signature, namely $(\beta_1, \beta_2, \ldots, \beta_{\frac{n-2}{2}})$ if n is even and $(\beta_1, \beta_2, \ldots, \beta_{\frac{n-3}{2}})$ if n is odd. The modified communicability graph changes at $\beta = \beta_1$ from being the null graph

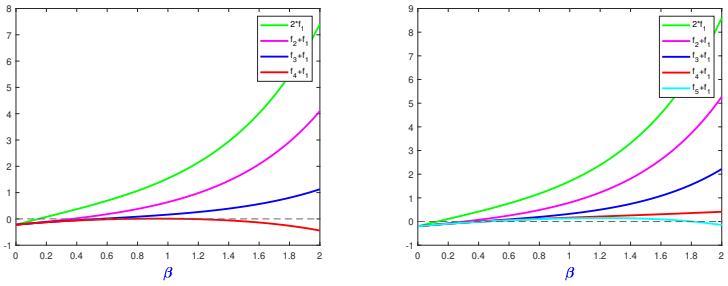

(a) (b)

Figure 5.3: Modified communicability graph function $\Delta\tilde{G}_{pq}(\beta)$ of C_9 and C_{10} versus β in (a) and (b), respectively.

N_n to C_n; at $\beta = \beta_2$ it becomes a regular graph with average degree 4; at $\beta = \beta_3$ it becomes a regular graph with average degree 6, etc.

In Figure 5.3, we plot the modified communicability functions for C_9 and C_{10} as β varies, which exhibits the $(\beta_1, \beta_2, \beta_3)$ and $(\beta_1, \beta_2, \beta_3, \beta_4)$ melting signatures, respectively. The term $f_1(\beta) + f_4(\beta)$ (red curve) in the modified communicability graph function for C_9 is a concave function and crosses the β-axis twice. Similarly, in the modified communicability graph function for C_{10}, the function $f_1(\beta) + f_5(\beta)$ (cyan curve) is concave and crosses the β-axis twice. In both examples, we ignore this function to obtain sensible melting signatures. In Figure 5.4, we show the evolution of the modified communicability graphs of C_{10} as β varies, which exhibits the $(\beta_1, \beta_2, \beta_3, \beta_4)$ melting signature.

5.2 Freezing order of the edges

We recall that the modified communicability graph is the null graph when the communicability between the nodes is very low (i.e. $\Delta\tilde{G}_{pq}(\beta) < 0$ for all $p, q \in V$). However, the communicability between the nodes increases as β increases from zero. The nodes p and q are connected (freeze) by an edge in the modified communicability graph if $\Delta\tilde{G}_{pq}(\beta) \geq 0$. We call this process *freezing* of an edge. The modified communicability graph is fully connected when the communicability between the nodes is very high (i.e. $\Delta\tilde{G}_{pq}(\beta) \geq 0$ for all $p, q \in V$).

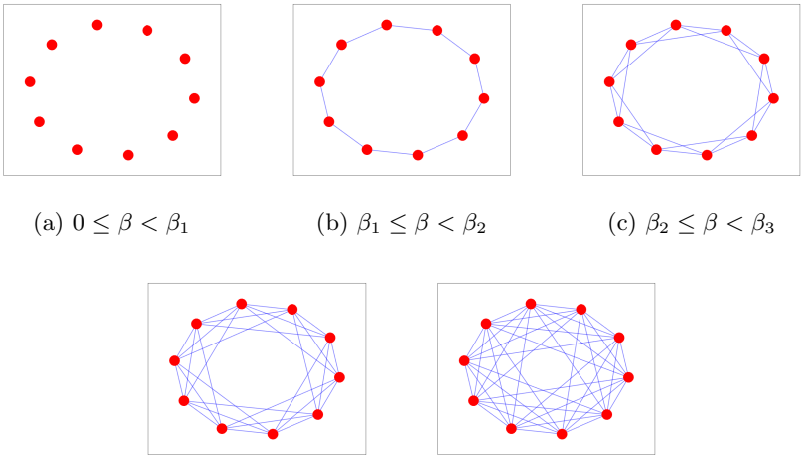

(a) $0 \leq \beta < \beta_1$ (b) $\beta_1 \leq \beta < \beta_2$ (c) $\beta_2 \leq \beta < \beta_3$

(d) $\beta_3 \leq \beta < \beta_4$ (e) $\beta \geq \beta_4$

Figure 5.4: Illustration of the structure of the modified communicability graph of C_{10} versus increase β.

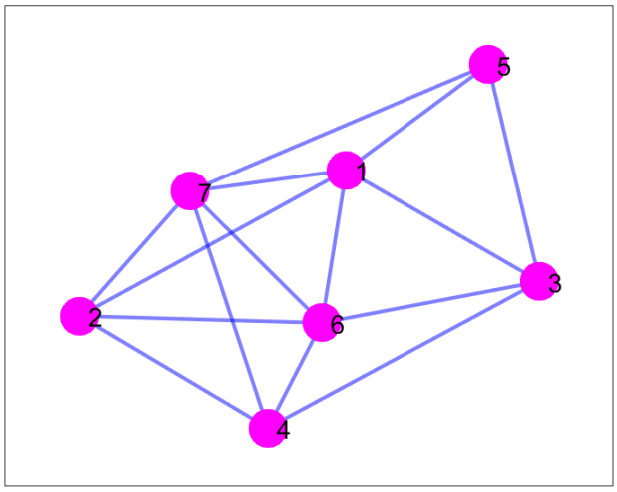

Figure 5.5: Small graph Γ with degree sequence 3, 4, 4, 4, 5, 5, 5.

In this section, we consider a small graph Γ with 7 nodes and degree sequence 3, 4, 4, 4, 5, 5, 5 presented in Figure 5.5. We investigate the order of freezing of the edges as β increases from zero. The second largest eigenvalue of the adjacency matrix A of the graph Γ is $\lambda_2 \approx 0.9246$, and the number of different types of edges in the associated modified communicability graph is $\frac{n(n-1)}{2} = 21$; in other words, each edge freezes at a different value of β. We find, computationally, that freezing in the modified communicability graph of Γ starts with the existing edges in Γ and then freezing continues to other possible edges as β increases, one by one, until the modified communicability graph changes to be the complete graph K_7. In Table 5.1, we label the edges according to their freezing order such that the first edge $(3, 5)$ freezes at $\beta \approx 0.17$ and when β increases to be 0.2, the second edge $(1, 5)$ freezes and so on until all the possible edges freeze. The values of β by which the corresponding edges freeze are in the fourth column. In the last column, we include the communicability for the corresponding edges (i.e. the communicability function at $\beta = 1$). In the third column, d_1, we include the sum of end nodes degrees of the edge, such as

$$d_1(v_i, v_j) = d(v_i) + d(v_j),$$

where $d(v_i)$ is the degree of the node v_i. We find that freezing of the edges in the modified communicability graph of Γ can be ordered according to d_1 starting from the edge of the lowest d_1. Moreover, the freezing order for the edges of the graph Γ explains that the maximum value of the modified communicability graph function is a function that corresponds to edges that are connected in the original graph, and that is what we observed in all windmill graphs, dumbbell graphs, complete multipartite graphs and cycle graphs. In Figure 5.6, we plot the freezing values of $\beta = \beta(e)$ of the edges in x-axis versus the communicability of the corresponding edges in y-axis. However, it was really difficult to find a relationship that could relate that freezing values $\beta(e)$ of edges in the modified communicability graph of Γ and the communicability of the corresponding edges. This could be related to some other structural characterization of nodes that connect these edges. In the next chapter, we will investigate this further.

Freezing order	Edge	d_1	$\beta(e)$	Comm.
1	(3,5)	7	0.17	7.7046
2	(1,5)	8	0.2	9.4583
3	(7,5)	8	0.224	9.1912
4	(3.4)	8	0.248	9.6801
5	(2,4)	8	0.255	10.9212
6	(3,1)	9	0.285	11.4798
7	(6,4)	9	0.2976	12.7005
8	(7,2)	9	0.306	12.8015
9	(6,3)	9	0.315	11.7866
10	(6,2)	9	0.325	13.169
11	(7,4)	9	0.334	12.1266
12	(2,1)	9	0.38	12.4079
13	(1,7)	9	0.41	14.1928
14	(6,7)	9	0.465	14.6984
15	(6,1)	9	0.468	14.5145
16	(3,7)	9	1.3	11.0304
17	(6,5)	9	1.4	8.9513
18	(1,4)	9	1.55	11.5193
19	(3,2)	10	2.2	9.5579
20	(5,4)	10	10.3	7.1664
21	(2,5)	10	10.5	7.4788

Table 5.1: Labelling for the edges according to their freezing order. The values of β by which the corresponding edges freeze are in the fourth column. In the last column we include the communicability for the corresponding edges. In the third column d_1 we include the sum of end node degrees of the corresponding edge.

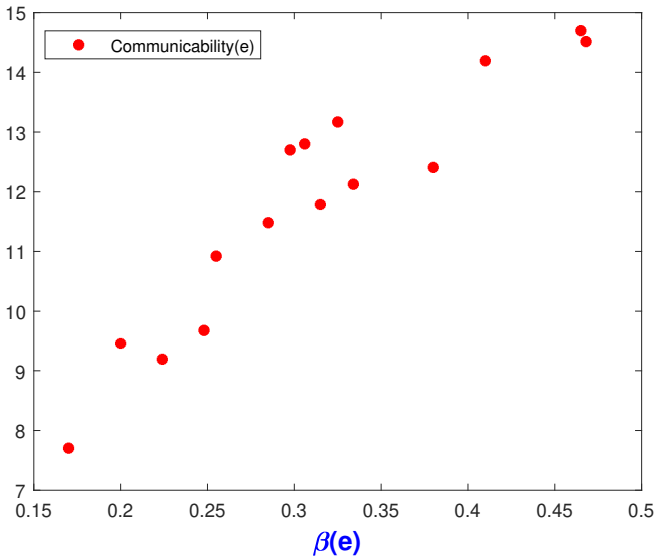

Figure 5.6: Plot for the freezing values of β of the edges in x-axis versus the communicability of the corresponding edges in y-axis.

5.3 Melting Phase Transition

We recall that the critical value β_c (melting temperature or the melting phase transition) of a graph Γ is the value of β which makes the modified communicability graph of Γ transfer from being connected to being a disconnected graph. The modified communicability graph of a graph Γ starts melting when deleting one or more edges. The modified communicability graph is a complete graph when the communicability between the nodes is very high (i.e. $\Delta\tilde{G}_{pq}(\beta) \geq 0$ for all $p, q \in V$). The communicability between the nodes decreases as β decreases, where the modified communicability graph is the null graph when $\Delta\tilde{G}_{pq}(\beta) < 0$, for all $p, q \in V$.

However, in the modified communicability graph there could be edges connecting pairs of nodes which are not connected in the original graph Γ. Also, in reality there is no disconnection in the edges but just change in the communicability of the edges. That is, in reality there is no disconnection of edges in the network at β_c, but a significant change in the behavior of the communicability for the different edges of the network. For this reason, we examine what exactly is this change that is taking place in the communicability function, where the communicability is accounting for all walks that

permit the flow of information from one node to another.

In this section, we state our results about the existence of the melting phase transition in simple graphs. In Chapter 4, we found in Theorem 4.3.5 (which is based on Conjecture 4.3.4) that for complete multipartite graphs where the second largest eigenvalue of their adjacency matrix $\lambda_2 \leq 0$, the modified communicability graph is not connected regardless of the value of β. Thus, we can deduce that there is no melting phase transition (value of β) in the modified communicability graphs of complete multipartite graphs by which the modified communicability graph changes from connected to disconnected.

Moreover, in Chapter 4 we considered two graph families that have $\lambda_2 > 0$: windmill and dumbbell graphs; the cycle graphs considered in Section 5.1 also have this property. We found that the modified communicability graph functions for windmill graphs, dumbbell graphs and cycle graphs change sign as β increases and the modified communicability graphs turn to be connected as β increases in Theorem 4.1.12, Theorem 4.2.32 and Conjecture 5.1.3, respectively. Thus, we have the following two conjectures about the existence of the melting phase transition in the modified communicability graphs and the maximum of $\Delta G_{pq}(\beta)$ for simple graphs with $\lambda_2 > 0$.

Conjecture 5.3.1. *Let $\Delta\tilde{G}_{pq}(\beta)$ be the modified communicability graph function for a simple connected graph $\Gamma = (V, E)$ with adjacency matrix A, and $\lambda_1 > \lambda_2 \geq \cdots \geq \lambda_n$ be the eigenvalues of A such that $\lambda_2 > 0$ and $\lambda_2 \gg \lambda_3$. Then, there exists $\beta_c \in (0, \infty)$, a melting phase transition for Γ, such that*

1. *$\Delta\tilde{G}_{pq}(\beta)$ is disconnected for all $\beta < \beta_c$,*
2. *$\Delta\tilde{G}_{pq}(\beta)$ is connected for all $\beta \geq \beta_c$.*

Conjecture 5.3.2. *The maximum of $\Delta G_{pq}(\beta)$ for a simple connected graph $\Gamma = (V, E)$ is a function that corresponds to pairs (p, q) which are connected in Γ (i.e. $(p,q) \in E$) for all β.*

It is important to mention that in reality the melting point for a substance is not affected by increasing the size. However, our proposed melting phase transition is

affected by increasing the size (number of nodes). For instance, in Conjuncture 4.1.13 for windmill graphs, the melting signatures go to zero as the number of the nodes goes to infinity. Moreover, in Claim 4.2.22 and Conjuncture 4.2.24 for dumbbell graphs, the melting signatures go to zero or infinity as the number of the nodes goes to infinity.

5.4 Granular Materials in Network Theory

A granular material is a collection of discrete and microscopic particles, where two particles interact when they are in contact. Examples of such materials are sands and grains. These materials are non-equilibrium materials due to their lack of rearrangement when they have thermal fluctuations applied to them [89].

Early work in the study of the theory surrounding granular materials was done by Maxwell [77]. Traditionally, granular materials have been commonly modelled using either particulate-based or continuum-based frameworks. It is challenging to model the structural organization of granular materials due to their component behaviour.

In 1998, tools from network theory [85, 10] and mathematics were used successfully to study the properties of such kind of materials. Smart and Ottino [99] were the first to suggest the formal use of graph theory to study the physical behaviour of granular materials.

In graph theory, a contact network is the simplest way to represent granular materials [4, 89]. In this network, each particle is represented by a node and two particles are connected by an edge if they are in contact with each other. However, determining the physical contact may not be possible; so we need to approximate the contact of particles. For instance, we can approximate the contact based on particle positions and the particle size. Granular materials have been successfully modelled using different approaches in network theory in order to study the structure and physical behaviour of these systems when applied to external perturbations [4, 89]. However, it is Newton's laws of motion that are most commonly used to model the contact of particles [89, 94]. In this work, we model the granular material systems as simple networks and we assume that the particles are identical.

5.5 Melting of Granular Solids

In this section, we study the influence of order and randomness on the melting phase transition in granular materials, an aspect at the basis of many physical problems. In particular, here we are interested in comparison between the physical properties and our melting phase transition of granular materials with ordered structures and random structures. The classical example of an ordered system is a crystal, and the amorphous solids are good examples of random-like materials.

5.5.1 Crystalline and Amorphous Solids

Crystalline solids or crystals are defined as solids which have highly regular and ordered microscopic structures of atoms or molecules. Crystalline atoms are organized and packed to be very close to each other and form a crystalline lattice. Crystals have sharp melting points which occur at high temperatures. There are many examples of this kind of solids including sugar, diamond, zinc oxide, and sodium chloride [108, 116]. Crystals can be represented using regular lattices in which atoms correspond to nodes and the interactions between them correspond to the edges [90].

Amorphous solids are solids that have a particular lack of arrangement among their atoms or molecules and so an unspecified geometrical structure. In this kind of solid, the distances between the atoms vary and are irregular. Amorphous solids are gradually and softly melted generally at higher temperature than many other solids. Common examples of amorphous solids are glass, plastics, and solid polymers [2, 116]. In order to model a random-like granular material, we consider here a type of random graph known as *Gabriel graph* (see Chapter 2 for more details). The reason why we consider random neighbourhood graphs, like Gabriel graphs, instead of other types of random graphs is as follows. To keep the analogy with solid granular materials we should maintain certain geometric disposition of the nodes. This geometric arrangement of nodes is possible in so-called random geometric graphs (RGG) as well as in random neighbourhood graphs (RNG). The RGG are nonplanar graphs, which means that a node A can interact with another node B, even in the case of a third node C being exactly in the middle between

A and B. This, of course, is not a realistic scenario for the interaction between granular particles and not appropriate for representing a granular material. However, Gabriel graphs are planar graphs and avoid the interaction between such nodes. Consequently, they are appropriate for modelling amorphous granular materials.

The differences between ordered and random arrangements of particles in crystalline and amorphous granular materials mean that they differ significantly in the way that they change from solid to liquid. This dichotomy between the manner in which crystalline and amorphous solids transition is one of the fundamental differences between them. While a crystalline solid has a sharp transition from solid to liquid, the amorphous solid does not. Instead, it displays a very smooth transition for a long range of temperatures [116]. The second characteristic feature is that for the same material in amorphous and crystalline forms, the amorphous one melts at a higher temperature than the crystalline one [116]. For instance, crystalline quartz melts at 1,550 and amorphous quartz melts in the range of 1,500–2,000. We are interested in investigating this physical phenomenon here as an analogy for our crystalline and amorphous granular material graphs.

5.5.2 Melting of Crystalline versus Amorphous Solids Networks

In this subsection, we investigate and compare the physical properties of crystalline and amorphous solids networks with resilience to increase temperature, the number of connected components and evolution of the melting process.

Resilience to an Increase in Temperature

In order to investigate the physical phenomenon that the amorphous solids are more resilient to an increase in temperature than other types of solids, we plot, in Figure 5.7, the change in the number of connected components in the modified communicability graph against the change of β for a 10×10 square grid and a Gabriel graph with $n = 100$ nodes and $m = 180$ edges. The main difference between these two kinds of graphs resides in the order/randomness of the nodes in a unit square. The main observation from this experiment is that the crystalline granular material (green curve)

displays a sharp increase in the number of connected components with a decrease in β (increase in the temperature). On the other hand, the amorphous solids graph (blue curve) displays a very smooth increase in the number of connected components with a decrease in β. Thus, the amorphous solids graphs are more resilient to an increase in temperature than crystalline graphs.

Melting Temperature

The second important observation from Figure 5.7 is that the structure of the crystalline graph is destroyed more quickly than that of the amorphous one. For instance,a crystalline graph melts approximately 50% and 100% of its nodes at $\beta = 0.0017$ and $\beta = 0.0005$, respectively (see Figure 5.7). On the other hand, an amorphous solid graph melts approximately 50% and 100% of the nodes at $\beta = 0.0001$ and $\beta = 0.001$, respectively (see Figure 5.7), which are less than that observed for the crystal graph. Thus, an amorphous solids graph needs a higher temperature to complete melting 50% and 100% of its nodes than a crystal graph. If we consider the temperature at which all the nodes in these graphs melt, as a melting temperature for these two materials, then that reflects the physical phenomenon for melting of the solids. That is, the melting temperature of amorphous solids is higher than that of crystal.

Evolution of Melting Process

Another feature of the current approach is that it allows us to visualize the evolution of the topological melting process in granular materials in order to gain insights into the mechanism. In Figure 5.8 (a), (b) and (c) we illustrate some snapshots of the change in the Lindemann graph structure with the change of β for the square lattice. We represent in red the nodes for which all of their edges have been removed, and which are disconnected from the giant connected component, that is, those particles which are in the liquid state. In blue, we represent those nodes which form the giant connected component of the graph, i.e. the nodes still in the solid phase.

When the temperature is very high at $\beta = 0.00005$ (see Figure 5.8 (c)) the Lindemann graph structure is almost melted (i.e. most of the nodes are isolated), so the

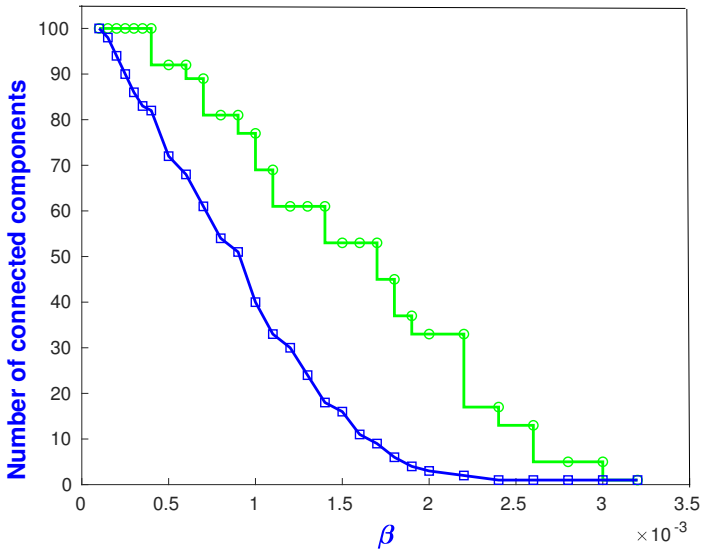

Figure 5.7: Change in the number of connected components in the modified communicability graph for the 10×10 square lattice (green curve) and Gabriel graph (blue curve) with $n = 100$ nodes and $m = 182$ edges as β increases.

material is almost in the liquid state. As the temperature drops, β increases, certain patterns start to emerge. In particular, for $\beta = 0.000075$ (Figure 5.8 (b)), an annulus external part of the lattice is solidified into a single connected component and only the central part of the granular material remains melted. As the temperature drops below $\beta = 0.000085$ (Figure 5.8 (a)), the melted region (red nodes) shrinks to the very centre of the lattice. The observed pattern of melting the square lattice is similar to the one observed experimentally for crystalline granular (colloidal) material.

In Figure 5.8 (d), we illustrate the results of Wang et al. [100] for the melting of colloidal crystals, which show such patterns of central melting. In the case of amorphous granular materials, there is no repeating pattern in them, and it is impossible to find a general structural pattern of the evolution of the melting process. A few snapshots of the process are given in Figure 5.9. The temperature needed to melt these graphs is significantly higher (smaller β) than the ones needed to melt square lattices of the same size, which coincides with our previous observations as well as with the experimental results for crystalline and amorphous solids.

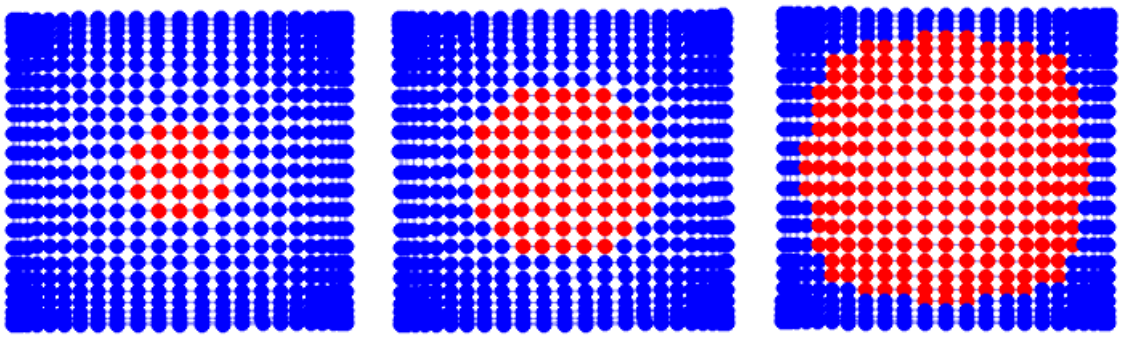

(a) (b) (c)

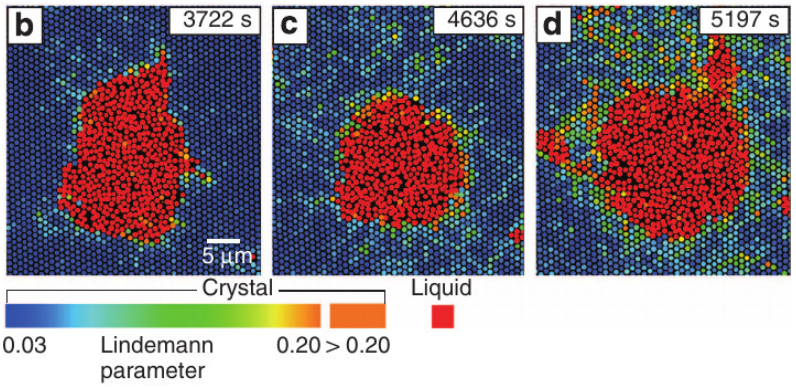

(d)

Figure 5.8: Illustration of melting of Lindemann graph of a 25×25 square lattice at $\beta = 0.000085$ (a), $\beta = 0.000075$ (b) and $\beta = 0.00005$ (c). Results for melting of colloidal crystals obtained by Wang et al. [100]. In plots (a)–(c), the nodes not in the giant connected component are in red.

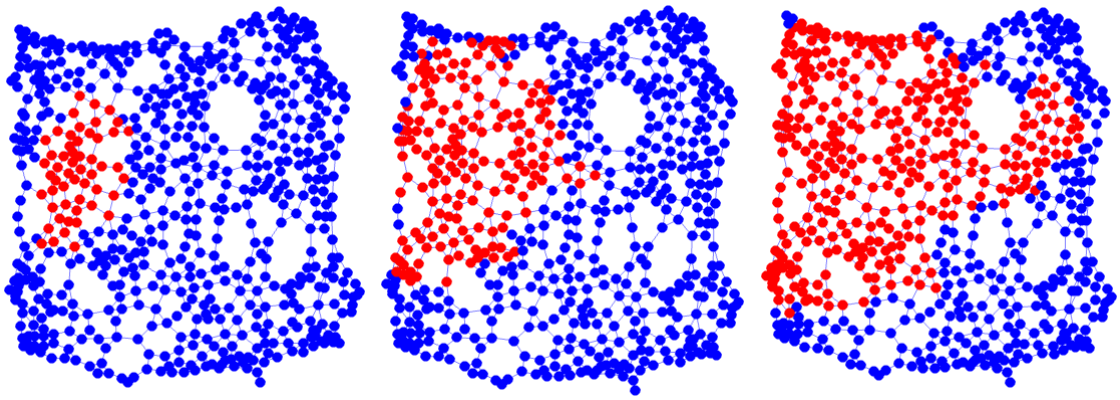

Figure 5.9: Nodes in each of the connected components of the Lindemann graph corresponding to the Gabriel graph with $n = 625$ nodes studied here for $\beta = 10^{-9}$, 10^{-10} and 10^{-11} from left to right. The nodes not in the giant connected component are in red.

5.6 Summary

In this chapter, we have studied computationally melting in C_n, $n \geq 5$, where the second largest eigenvalue is positive and the number of different types of edges in the associated modified communicability graph is not low and increases as n increases. We found that all corresponding functions of equivalence classes of edges in the associated modified communicability graph function of C_n, $n \geq 9$, cross the β-axis exactly once as β increases except for one function, which crosses the β-axis twice and is concave. Thus, we excluded this concave function and found computationally that there is one possible melting signature when n is even and one possible melting signature when n is odd for the modified communicability graphs of C_n. Also, we determined the melting signatures for C_5, C_6, C_7 and C_8. In these latter cases, there are one or two functions that do not cross the β-axis.

The main observation from this chapter is that the maximum of $\Delta G_{pq}(\beta)$ is a function that corresponds to connected edges in the original graph for all β and that freezing of the edges starts from the existing edges in the original graph. Also, we found that freezing of the edges in the modified communicability graph can be ordered according to the sum of end node degrees of the edges (d_1) starting from the edge of the lowest d_1. Moreover, from the work in graph families that we considered in Chapter 4

and the work for C_n, we stated our conjecture about the existence of the melting phase transition in simple graphs when $\lambda_2 > 0$ and $\lambda_2 \gg \lambda_3$.

Furthermore, we included some basics about melting solids physically, namely, about granular materials in network theory, and melting of crystalline versus amorphous solids networks. In this way, regular-like graphs such as square lattices are easier to melt than more irregular structures, such as spatial random graphs. These differences resemble the known dissimilarities between crystalline and amorphous granular materials in their melting process.

Chapter 6

Topological Melting Analysis of Complex Networks

The use of graphs and networks to represent many physical, biological, social and engineering systems has triggered their relevance as an object of study in applied mathematics and physics. In this context, many physical metaphors are typically used to study processes taking place in complex systems represented by networks. This includes, for instance, the use of theoretical tools developed in polymer physics, spin glass studies, Ising model simulations, discrete scaling and the theory of liquids to study complex systems [28, 29, 86]. In this chapter, we point out that the study of melting processes of graphs can bring some insights in analysing and studying the robustness of complex systems.

We provide an interpretation of the melting process of communicability paths in complex networks, when the parameter β is changed systematically towards zero. We also study the existence and characteristics of this phenomenon in real-world networks. We discover in this chapter that the main driver for node melting (node getting disconnected) is the eigenvector centrality of the corresponding node. That is, nodes with higher values of the Perron–Frobenius eigenvector melt (get disconnected) at lower temperatures than those with smaller values of it. Thus, being "more central" according to the eigenvector centrality also indicates to be "more at risk" of triggering a "melt down" of the network communicability, which is an abrupt variation in the rate of

change of this function with the parameter β.

6.1 Interpretation of Melting Graphs Based on Communicability

We proposed (in Chapter 5) that for simple connected graphs with $\lambda_2 > 0$ and $\lambda_2 \gg \lambda_3$, there is a melting point β_c. However, in reality there is no disconnection in the edges but just change in the communicability of the edges. In this section, we study that change in the communicability of the edges. In other words, we study the effects of β on the communicability of the edges. In this section, we provide an interpretation of the phenomenon of graph melting based on the communicability. We should start by remarking that the idea of graph melting should be interpreted as a physical metaphor for a completely mathematical phenomenon taking place in network communicability when the parameter β is approaching zero. That is, in reality there is no disconnection of edges in the network at β_c, but also a significant change in the behaviour of the communicability for the different edges of the network. We explore what exactly this change is that is taking place in the communicability function.

The first thing we need to consider here is that, for $p, q \in V$, $p \neq q$,

$$G_{pq}(\Gamma, 0) = (e^{0A})_{pq} = (I)_{pq} = 0, \tag{6.1}$$

where I is the $n \times n$ identity matrix. Thus, because $G_{pq}(\Gamma, \beta) > 0$, for $p \neq q$ and $\beta > 0$, we have a natural decreasing trend in the communicability when $\beta \to 0$. That is, when β decreases, the communicability for any pair of distinct nodes also decreases up to the point where it reaches the value of zero when $\beta = 0$. Therefore, the difference between one graph and another is in the rate at which the communicability decays as a function of β. In Figure 6.1, we illustrate the decay of $G_{pq}(\Gamma, \beta)$ as a function of β for three graphs with $n = 8$, in which we have selected an edge from each of the graphs for calculating the communicability. As can be seen from Figure 6.1, the decay of the communicability with β follows two trends, for larger values of β it follows an exponential decay and then a power law. The power law behaviour starts, for these

three graphs, at approximately close to $\beta = 1$. If we select the straight line in the log-log plot between $\beta = 1$ and $\beta_c > 0$, we can obtain the slope of this line by

$$s = \frac{\log(G_{pq}(\mathit{\Gamma}, 1)) - \log(G_{pq}(\mathit{\Gamma}, \beta_c))}{-\log(\beta_c)}.$$

From this we can obtain $\log \beta_c$,

$$\log \beta_c = \frac{\log(G_{pq}(\mathit{\Gamma}, \beta_c)) - \log(G_{pq}(\mathit{\Gamma}, 1))}{s},$$

and hence also the value of β_c,

$$\beta_c = \left(\frac{G_{pq}(\Gamma, \beta_c)}{G_{pq}(\Gamma, 1)}\right)^{1/s}. \tag{6.2}$$

However, an obvious problem is that we do not know the value of β_c, and so we cannot determine the value of $G_{pq}(\mathit{\Gamma}, \beta_c)$ for a given graph. We found computationally that, for the three graphs considered in Figure 6.1, $G_{pq}(\mathit{\Gamma}, \beta_c)$ follows a power law as a function of $G_{pq}(\mathit{\Gamma}, 1)$,

$$G_{pq}(\mathit{\Gamma}, \beta_c) \approx 0.006761\big(G_{pq}(\mathit{\Gamma}, 1)\big)^{2.117}.$$

Thus, with (6.2) we obtain an estimate for β_c,

$$\beta_c \approx \Big(0.006761\big(G_{pq}(\Gamma, 1)\big)^{1.117}\Big)^{1/s}.$$

An important remark here is that an increase in s causes a decrease in β_c. That is, a large value of s indicates a fast decay of the communicability with β. When this happens, the graph has a relatively small value of β_c. On the other hand, if s is small, or close to zero, then the graph has a relatively high value of β_c. In order to interpret these results physically we again borrow a metaphor from the physics of melting. In this case, we use the differences in melting between crystalline and amorphous materials. In graphs resembling more a crystalline material, and thus having a more regular structural patterns, the melting process occurs like in the case (c) in Figure 6.1 with a more abrupt transition of the communicability with β and at higher values of β_c. On the other hand,

	$\ln(\delta)$	$\bar{l}$	$\ln(Ef)$
$\ln(\beta_c)$	$r = 0.795$	$r = -0.716$	$r = 0.722$

Table 6.1: Pearson correlation coefficient r of semi-log correlations between $\ln(\beta_c)$ and the parameters $\ln(\delta)$, $\bar{l}$ and $\ln(Ef)$ of 47 complex networks arising from different scenarios (see Appendix A, Table A.1).

those graphs resembling more an amorphous solid, in other words those having more irregular structural patterns, will have melting more similar to that of case (a) in Figure 6.1 with a slow change of the communicability with β and a smaller value of β_c.

6.2 Global Analysis of Melting in Complex Networks

In this section, we consider a collection of 47 complex networks arising from different scenarios (see Appendix A, Table A.1). In order to analyse the melting properties based on our communicability phase transition β_c, we will correlate global properties of these networks with their melting phase transition β_c. The global parameters investigated in this section are: edge density δ, average degree $\bar{k}$, maximum degree K_{max}, average Watts–Strogatz clustering coefficient $\bar{C}$, average path length $\bar{l}$, shortest path efficiency Ef, second largest eigenvalue of the adjacency matrix λ_2, spectral gap $\lambda_2 - \lambda_3$, number of nodes n, average communicability distance $\bar{\xi}$, average resistance distance $\bar{\Omega}$, and average communicability angle $\bar{\theta}$ (see Chapter 2). We review more details about these parameters. Further, see Appendix B for MATLAB codes for the computation of these parameters.

We start by explicitly computing, for each network, the value of $\beta = \beta_c$ at which the Lindemann graph transfers from connected to disconnected. Then, we will relate the values of β_c to some simple global descriptors of the network, in order to shed light on the structural dependence of this transition. We investigate any correlation between these measures and the values of β_c for the 47 complex networks (see Appendix A, Table A.2 and Table A.3). The most significant correlations are noted in Table 6.1. Furthermore, in Figure 6.2 we illustrate these correlations in a log-log plot; more explicitly, we plot β_c against (a) δ (b) Ef and (c) $\bar{l}$. The correlations observed for $\ln(\beta_c)$ in Table

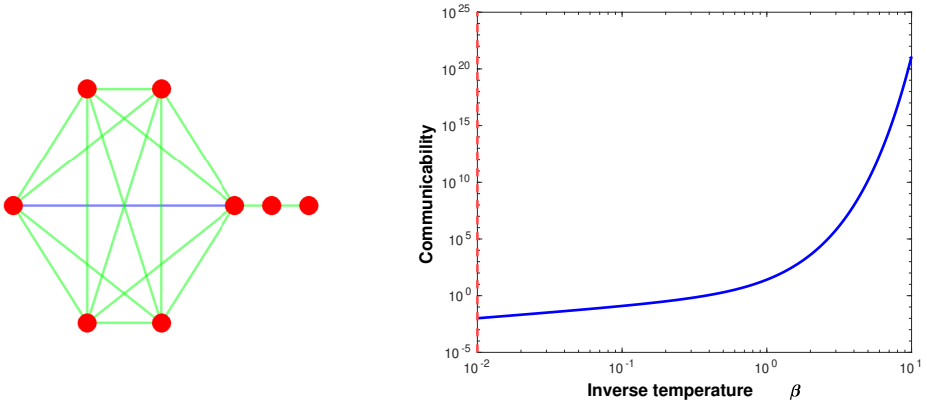

(a)

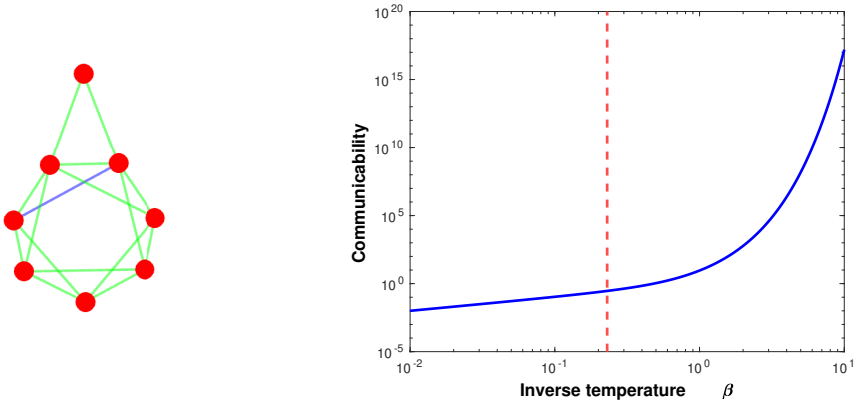

(b)

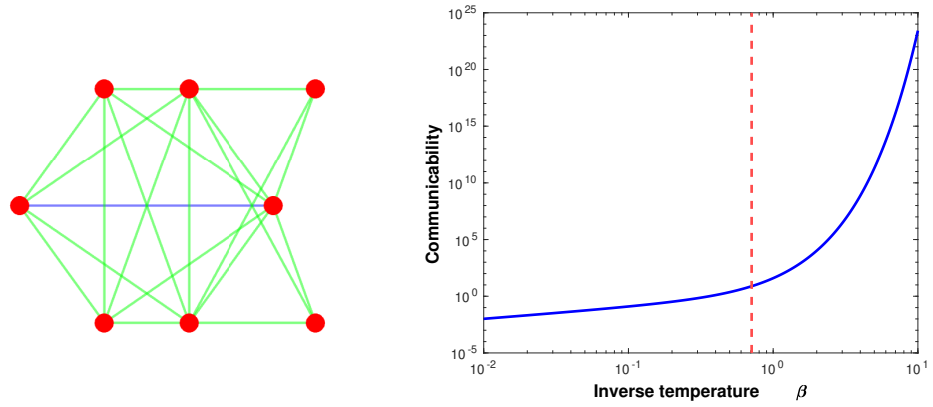

(c)

Figure 6.1: Illustration of the variation of $G_{pq}(\Gamma, \beta)$ with β for a single edge (highlighted by blue colour) in three different graphs with $n = 8$ nodes. The values of β_c for the corresponding graphs are: 0.01 (a), 0.23 (b) and 0.71 (c), and these values are represented by the intersection of the vertical red dashed line with x axis. The plots are in log - log scale.

6.1 with some of the previous structural parameters may encode something about the real structural characteristic of networks that influence their melting properties, such as the positive correlation between δ and β_c. Our intuition tells us that, under all other structural conditions being the same, high density networks should melt at higher temperatures, (lower β_c), than less dense ones. This is exactly what has been observed in molecular crystals of nonpolar molecules, such as linear alkanes [9]. Then, the fact that smaller and denser real-world networks in our data set are the ones having the largest β_c, implies that Lindemann graphs are easier to disconnect. This may indicate that the homogeneity in degree of these networks, rather than their sizes or densities, is the real driver of their melting.

In order to capture these degree irregularities, we use the heterogeneity [49] to combine some structural parameters in order to find a new index that may reflect the reality of graph melting. We start by recalling the definition of the average degree of a network $\bar{k}$ in matrix form

$$\bar{k} = \frac{2m}{n} = \frac{\mathbf{1}^T A \mathbf{1}}{\mathbf{1}^T \mathbf{1}}.$$

The right-hand side of the previous equation is useful to think about the spectral radius of the adjacency matrix as a sort of average degree, where

$$\lambda_1 = \frac{\boldsymbol{\psi}_1^T A \boldsymbol{\psi}_1}{\boldsymbol{\psi}_1^T \boldsymbol{\psi}_1}.$$

Notice that $\bar{k} \leq \lambda_1$ [28]; thus the term $\frac{\lambda_1}{\bar{k}}$ is the ratio between the global environment of a node to its local one. That is, the ratio $\frac{\lambda_1}{\bar{k}}$ indicates how a node "sees" on average its global environment in relation to its nearest neighbours. In a regular graph we have $\lambda_1 = \bar{k}$, and hence $\frac{\lambda_1}{\bar{k}}$=1. Therefore, we define the following index of global to local degree heterogeneity,

$$\varrho(G) = \frac{\lambda_1}{\bar{k}}, \tag{6.3}$$

where $(n-1)\varrho(G) = \frac{\lambda_1}{\delta}$, which may explain the previously observed correlation between $\ln(\beta_c)$ and $\ln(\delta)$. We use $\varrho(G)$ as an indicator of the global to local heterogeneity of the 47 real-world networks studied in this chapter. In Figure 6.2(d) we show the plot of $\varrho(G)$ versus β_c which has Pearson correlation coefficient $r = -0.776$.

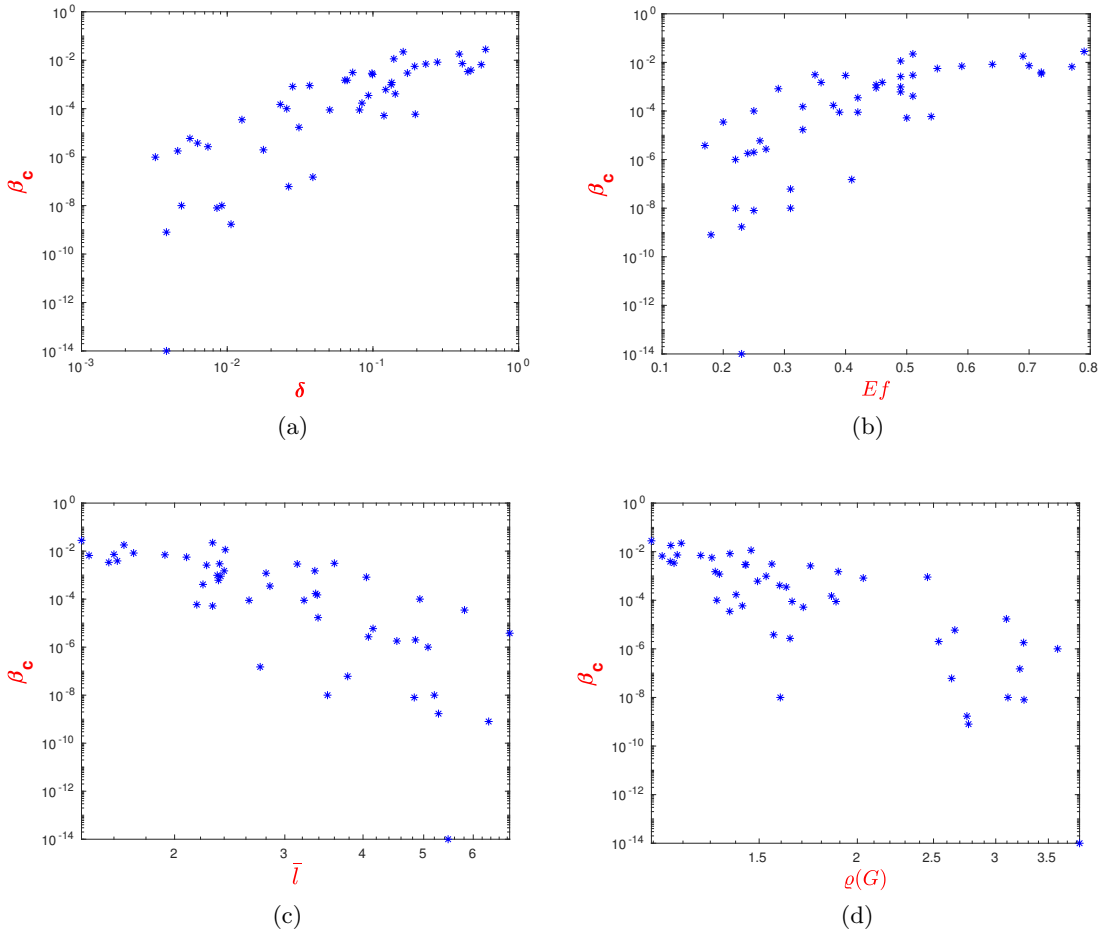

Figure 6.2: Changes in β_c for 47 real-world networks as a function of edge density δ, (a), shortest path efficiency Ef, (b), average path length $\bar{l}$, (c) and global to local degree heterogeneity $\varrho(G)$, (d).

The most important insight of this section is the following. The disconnection of the Lindemann graph of a given graph (its melting), is correlated with the differences between global and local degree heterogeneities of the network. Regular graphs are easier to melt than non-regular ones, and the more irregular in terms of global to local degree heterogeneities, the more robust the graph with the smallest value of β_c is, in other words, it is more difficult to melt.

6.3 Local Analysis of Melting in Complex Networks

We investigate computationally the effects of a decrease in β on the topological structure of the Lindemann graph. Our analysis is divided into two subsections.

6.3.1 How Do the Nodes of a Network Melt?

We begin by investigating how nodes in a network melt (get disconnected). We consider some of the real-world networks which were studied in the last section. We find the value of β for each node by which it is disconnected from the giant connected component of the modified communicability graph. Also, we create a melting barcode plot in which we plot the number of melted nodes in the y-axis versus the values of β in the x-axis. In Figure 6.3, we illustrate the melting barcodes of four real-world networks: Neurons (a), Little Rock (b), Corporate elite (c), and Roget (d). To understand the melting process of these networks in their plots, we need to read it from right to left as the melting process starts at higher values of β. There are significant differences in the four barcodes presented in Figure 6.3 which point to differences existing in their melting processes. First, we observe that the shapes of the melting barcodes are different. Whilst in Neurons (Figure 6.3(a)) and Roget (Figure 6.3(d)) the decay resembles an exponential curve, in Little Rock (Figure 6.3(b)) it is almost linear and the Corporate elite network (Figure 6.3(c)) displays a more skewed shape.

We investigate the rate of change of the melting process in the networks analysed by considering the shape of the histogram of the number of nodes melted at a given temperature. In general, we observe that the decay of the number of nodes of these networks at a given temperature, are exponentially related to inverse temperature

$$\eta = a \exp(\zeta \beta), \tag{6.4}$$

where η is the number of nodes melted at a given value β and a, ζ are constants.

However, in the smallest networks it was not possible to find regularities or any particular law of the decay of the number of melted nodes η as a function of β. These were the cases of the networks of Benguela ($n = 29$), Coachella ($n = 30$), Social3

Network	a	ζ	$\lvert r\rvert$
Prison	88.25	-2299	0.92
Neurons	345.3	$-6.836.10^4$	0.80
Small World	395	$-1.025.10^4$	0.72
Ythan1	182.5	-3596	0.87
Electronic1	121.2	$-4.885.10^4$	0.90
PIN H. pylori	694.2	$-2.678.10^6$	0.73
Macaque	89.24	-176	0.97
Stony	236	-3090	0.98
PIN B. subtilis	82.23	-9685	0.71
Roget	974.8	$-2.703.10^6$	0.85
Software_Abi	932.3	-7.063	0.54
Corporate elite	1398	$-2.492.10^8$	0.87

Table 6.2: Values of the fitting parameters for equation (6.4) displaying the relation between the number of nodes melted at a given value of β as a function of β for several real-word networks. The values $|r|$ are the absolute values of Pearson correlation coefficient for these relations

($n = 32$), and St.Marks ($n = 48$) as well as for the network of Little Rock, which is not so small ($n = 181$) but it also has a very disperse histogram. For the rest of the networks analysed we display the parameters of fitting equation (6.4) as an exponential function with the values of β, and the absolute values of Pearson correlation coefficient $|r|$ for these relations in Table 6.2.

The fitting parameters given in Table 6.2, indicate the differences in the rates of melting of the networks analysed. These rates of melting represent a new measure for the robustness of networks to the effects of the external stress (the inverse temperature β) to which the network is submitted.

In comparing these networks in their β_c (see Appendix A, Table A.3), it is clear that the social network of Prison and the food web Ythan1 networks are significantly less robust to the external stress than the protein–protein interaction network PIN H.pylori. Furthermore, the Macaque network, which represents the visual cortex of macaque, melts very quickly and at a much lower temperature when compared to the other networks analysed. This indicates that once the external stress has triggered the melting process, the nodes of this network get disconnected very quickly from the giant connected component of the modified communicability graph.

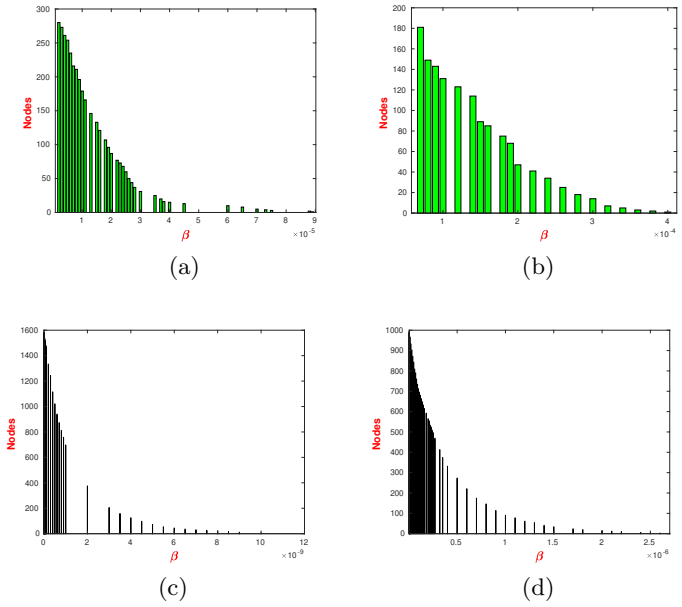

Figure 6.3: Number of melted nodes vesus some values of β, where $\beta \leq \beta_c$ for the networks Neurons (a), Little Rock (b), Corporate elite (c), and Roget (d).

6.3.2 Which Structural Parameter Drives the Melting Process of the Nodes?

We investigate in this subsection the main factors that affect the melting process of the nodes. In particular, we consider the role of node centrality in the melting of the corresponding node. We analyse the relationship between the value of β at which a node becomes disconnected from the giant component of the modified communicability graph with some node centralities such as closeness centrality CC, betweenness centrality BC, eigenvector centrality EC and subgraph centrality SC (see Chapter 2 for more details and see Appendix B for MATLAB codes for these parameters). In general, we observed that the value of β at which a node melts from the giant connected component of the network presents the highest correlation with the corresponding entry of the eigenvector centrality EC. The larger size networks (see Table 6.3) studied have a Pearson correlation coefficient higher than 0.9, between the values of β at which the nodes melt and their corresponding EC entries, with one exception of the network of the Macaque visual cortex. In Table 6.3, we list the values of the Pearson correlation

coefficient and the variation in CV of the values of β at which the nodes melt from the giant connected component, estimated from a linear regression with EC. The coefficient of variation CV measures the dispersion to the values of β, at which the nodes of each graph melt with their corresponding EC entries. The coefficients of variation CV for the listed graphs are in general very small, the small values of CV indicate that there is no dispersion in these correlations. Consequently, the small values of CV indicate a more reliable (consistent) measurement, since all the values of CV are less than 5. According to the values of the Pearson correlation coefficient r in Table 6.3, we found that the correlation between the values of β, at which the nodes melt, with its corresponding EC entries are very strong for all the networks.

Furthermore, in Figure 6.4, we plot the relation between values β at which the nodes melt versus their corresponding EC entries, for some of the networks as, Small World (a), Electronic1 (b), PIN B. subtilis (c) and Prison (d).

In general, we observed that when β_c is arbitrarily small, the correlation between the melting values of β of the nodes and EC is better than when β_c is relatively large. The reason for that difference is the following.

Let us recall the modified communicability graph function $\Delta\tilde{G}_{pq}(\beta)$, that is

$$\begin{aligned}\Delta\tilde{G}_{pq}(\beta) &= \sum_{j=2}^{n} \psi_j(p)\psi_j(q)e^{\beta\lambda_j} + M(\Gamma,\beta),\\ &= \sum_{j=2}^{n} \psi_j(p)\psi_j(q)e^{\beta\lambda_j} + \max_{s\neq t\in V} \sum_{j=2}^{n} \psi_j(s)\psi_j(t)e^{\beta\lambda_j}.\end{aligned}$$

As $\beta_c \to 0$, we have $e^{\beta_c\lambda_j} \to 1$, $j \in \{1, 2, \ldots, n\}$, and thus

$$\Delta\tilde{G}_{pq}(\beta_c) = \sum_{j=2}^{n} \psi_j(p)\psi_j(q) + \max_{s\neq t\in V} \sum_{j=2}^{n} \psi_j(s)\psi_j(t), \tag{6.5}$$

$$= -\psi_1(p)\psi_1(q) - \min_{s\neq t\in V} \psi_1(s)\psi_1(t), \tag{6.6}$$

since $\sum_{j=1}^{n} \psi_j(p)\,\psi_j(q) = 0$ for all $p \neq q \in V$. Equation (6.6) explains the dependency of $\Delta\tilde{G}_{pq}(\beta_c)$ on the eigenvector centrality EC entries, especially when β_c for a given graph is arbitrarily small. Then also $\Delta\tilde{G}_{pq}(\grave{\beta})$ depends on the corresponding entries

of EC, where $\grave{\beta}$ is the melting value of β of a node $p \in V$ and $\grave{\beta} \leq \beta_c$. This then represents the dependency of the value of $\grave{\beta}$ by which the node p disconnects from the giant connected component of the modified communicability graph on the corresponding eigenvector centrality entry of the node. That clearly explains the observed high positive correlation between the values of β at which a node p melts and $\psi_1(p)$ for the networks which have β_c very close to zero. Also, this explains why those networks for which β_c is not sufficiently small display bad correlation between the values of β at which a node melts and $\psi_1(p)$.

This result has important consequences for the robustness of networks. Those networks displaying a high robustness to external stresses, for which we expect β_c is very close to zero, start their melting process from the nodes that are most central according to EC. That is, if we consider a network like the USA air transportation network, which has β_c to the order of 10^{-7}, we will observe that the first airports to be disconnected from the giant connected component are the most important ones in terms of their EC. Here we give the list of the first airports separated from the giant connected component in the modified communicability graph: Chicago O'Hare, Dallas/Forth Worth Int., The William B. Hartsfield (Atlanta), Detroit Metropolitan, Pittsburgh Intel., Lambert-St. Louis, Charlotte/Douglas Int. (see Figure 6.5).

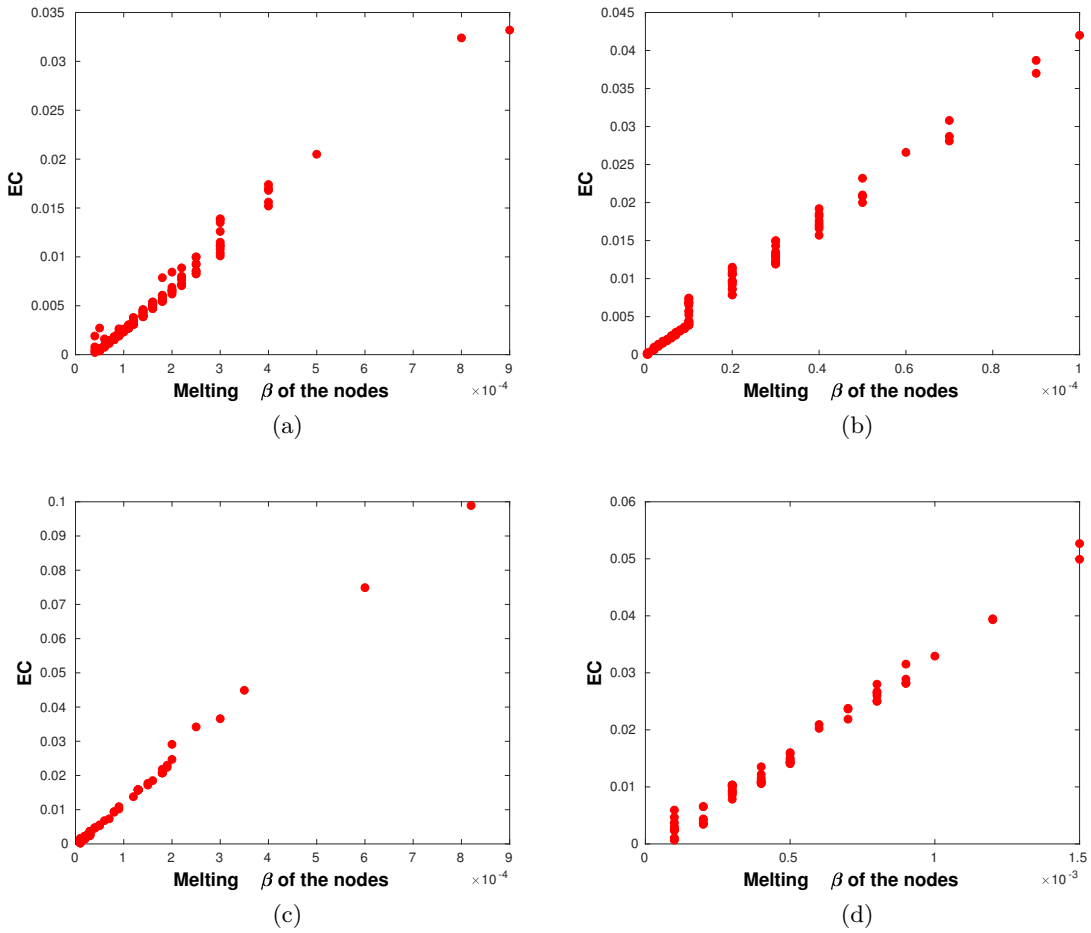

Figure 6.4: The values of β at which the nodes melt versus their corresponding EC entries, for the networks of Small World (a), Electronic1 (b), PIN B. subtilis (c) and Prison (d).

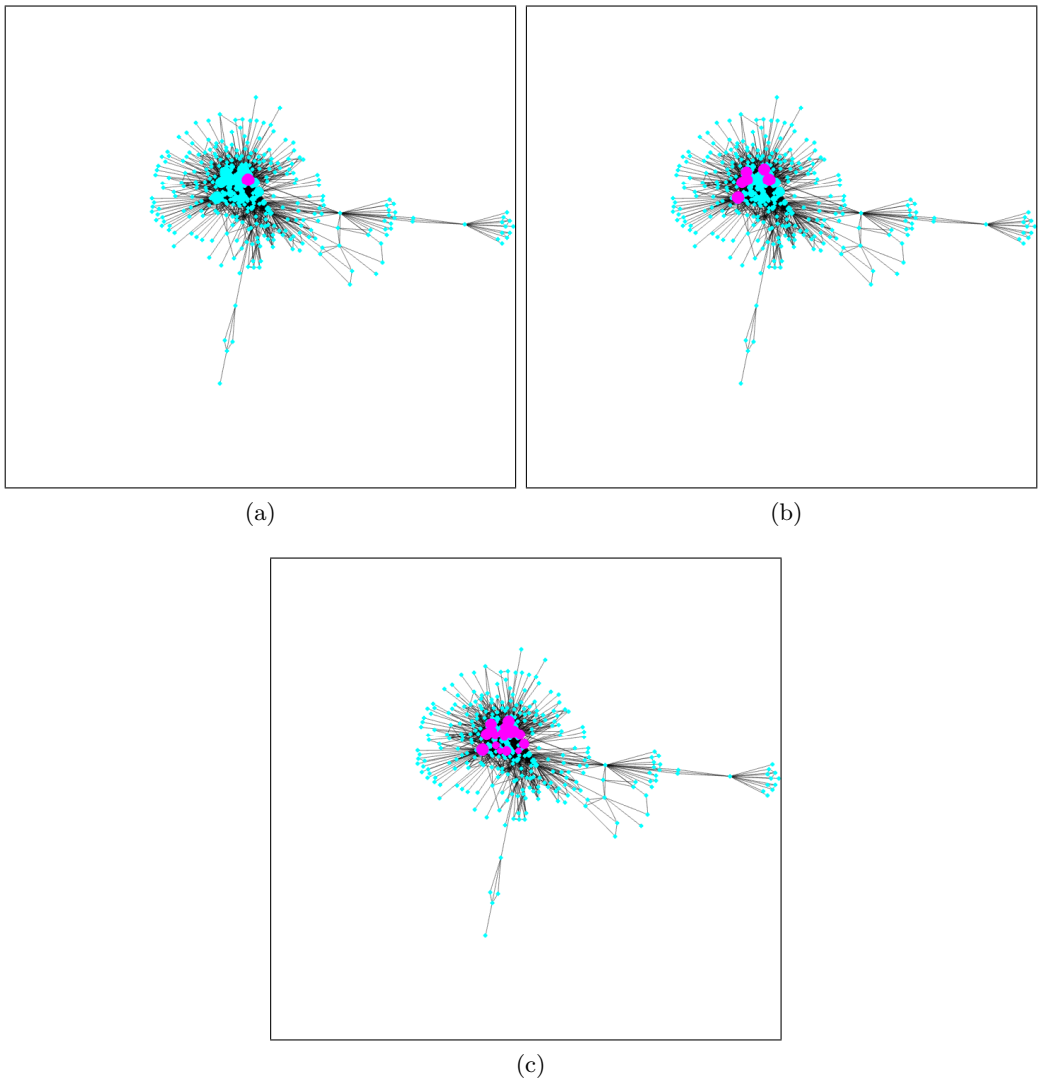

(a) (b)

(c)

Figure 6.5: Snapshots of the melting process of the USAir97 network at three different values of β, $\beta = 1.5.10^{-7}$ (a), $\beta = 1.25.10^{-7}$ (b) and $\beta = 1.0.10^{-7}$ (c). The red coloured nodes represent the melted nodes at the corresponding values of β, and the blue coloured nodes represent the giant connected component of the network. The melting starts at Chicago O'Hare and propagates through the central eastern area of the US.

Network	r	CV
Benguela	0.96	0.403
Coachela	0.93	0.402
Social3	0.95	0.595
Macaque	0.81	0.365
St. Marks	0.97	0.48
Prison	0.993	0.70
PIN B. subtilis	0.998	1.232
Stony	0.945	0.428
Electronic1	0.992	1.082
Ythan1	0.989	0.761
Small World	0.99	0.722
Little Rock	0.987	0.475
Neurons	0.998	0.841
Roget	0.997	1.164
PIN H. pylori	0.997	1.383
Software Abi	0.9958	2.163
Corporate elite	0.9901	1.295

Table 6.3: Illustration of the values of Pearson correlation coefficient r and the coefficient of variation CV to the values of β at which the nodes melt with its corresponding EC entries.

6.4 Summary

The analysis of a series of real-world networks has given us the possibility of exploring the global and local structural characteristics of networks which drive their melting process. At the global topological level, we have shown that the value β_c at which the melting of a network occurs depends mainly on the differences between the local and global degree heterogeneities existing in the graph. At the local level we have observed that the melting is triggered by the nodes having the higher eigenvector centrality in the network, particularly in those cases of networks where the melting phase transition (β_c) is very close to zero. This means that "being too central is too dangerous" as it may trigger a catastrophic melt down of the network.

Chapter 7

Conclusions

In this work, we considered the communicability function as a new approach in order to find a melting phase transition for networked systems. This phase transition allows us to study network robustness. The communicability function that we consider in our work is based on the Lindemann criterion for melting solids, which allows us to define the melting process of a networked system in graph-theoretical terms. The Lindemann criterion for melting solids states that melting in substances is initiated when the vibrations between nodes exceed a critical threshold. In graph theory, the vibrations between nodes can be related to the communicability function of pairs of nodes. We proposed a new communicability graph function which considers the maximum vibration of all pairs of distinct nodes in the graph as the critical threshold for melting.

In this work we found a topological melting phase transition in simple connected graphs with $\lambda_2 > 0$ and $\lambda_2 \gg \lambda_3$, which resembles the melting process of a given system. We found that there is a critical threshold in the connectivity of the modified communicability graphs of simple connected graphs with $\lambda_2 > 0$ and $\lambda_2 \gg \lambda_3$.

Mathematically, our work is based on the spectral properties of the adjacency matrix of the graph and the change in its exponential matrix function, $\exp(\beta A)$, where $\beta \in [0, \infty)$. The melting phenomenon considered in this work is driven by the parameter β (inverse temperature) which acts as a thermal bath for the whole network.

We study and investigate melting in certain graphs with positive second largest eigenvalue, namely, melting in windmill graphs, dumbbell graphs and cycle graphs.

Also, we investigated melting in complete multipartite graphs where the second largest eigenvalue is non-positive. We found a melting phase transition in simple connected graphs with $\lambda_2 > 0$ and $\lambda_2 \gg \lambda_3$, which resembles the melting process of a given system. We found that there is no melting phase transition in complete multipartite graphs. Through that we found the spectral decomposition for dumbbell graphs and complete multipartite graphs, which until now have not been done. The spectral decomposition of the adjacency matrices are, in general, very useful in studying different areas of research in graph theory. Also, we found mathematical expressions for the communicability functions of windmill and dumbbell graphs.

Moreover, we examined the melting phase transition in two different kinds of graphs, namely, random and regular graphs. We have modelled amorphous and crystalline solids within a graph-theoretical framework theory. There are many differences between these two kinds of solids. The main difference is related to their structures and particular arrangements of their atoms and molecules. Crystalline solids can be modelled in graph theory by a square lattice (grid graph), whereas amorphous solids are represented by Gabriel graphs.

We observed that the differences in the melting phase transitions of regular and irregular graphs resemble the differences in melting of crystalline and amorphous solids. The melting phase transition satisfies the main two physical phenomena of melting these two kinds of solids. That is, the melting temperature of an amorphous solid is higher than that of a crystalline solid. Additionally, amorphous solids are more resilient than crystalline solids when faced with an increase in temperature. Crystalline solids also display a sharp increase in melting percentage with an increase in the temperature, while amorphous solids softly melt in contrast.

We found correlations between the melting phase transition and certain global and local properties of the network by investigating a number of real-world networks. Our analysis addresses the following two main questions: How do nodes of a network melt? And which structural parameter drives this melting process of the nodes?

At the global topological level, we have found that the critical phase transition of a graph, β_c, correlates well with the difference between the local and global degree

heterogeneity in the graph. We have observed, at a local topological level, that melting of graphs with β_c close to zero is initiated by the nodes having a higher eigenvector centrality in the network.

7.1 Future Work

The analysis of network melting based on the communicability function opens up many new areas for further analysis. There are many mathematical and computational questions, that remain open, about the study of network robustness based on the communicability between the nodes when they are subjected to external stresses. These questions and research directions include, but are not limited to the following:

1. Does there exist a unique value $\beta_c \in (0, \infty)$ for the modified communicability graphs of a simple connected graph $\Gamma = (V, E)$ with adjacency matrix A, and $\lambda_1 > \lambda_2 \geq \lambda_3 \geq \cdots \geq \lambda_n$ the eigenvalues of A such that $\lambda_2 > 0$ and $\lambda_2 \simeq \lambda_3$?

2. Conduct a more exhaustive analysis of the topological (global and local) drivers that could drive network melting.

3. Can real world networks be systematically classified according to their melting processes?

4. Archimedean lattices are 2-dimensional regular planar graphs, which tile the plane uniformly with one type or more of polygons. These lattices are described and classified into 11 (Archimedean) lattices [58]. Three of these lattices have identical polygons (one type of face), which are square (4^4), triangular (3^6), the hexagonal (6^3) lattices, while the other eight have more than one polygon, see Figure 7.1. The notation for each lattice refers to the polygons around a node in the clockwise direction. For example, the notation $(3^3, 4^2)$ indicates that around each node, there are 3 triangles and 2 squares. We distinguish the lattices by the type of polygons. For instance, the lattices $(3^3, 4^2)$ and $(3^2, 4, 3, 4)$ have the same polygons but are different types (see Figure 7.1).

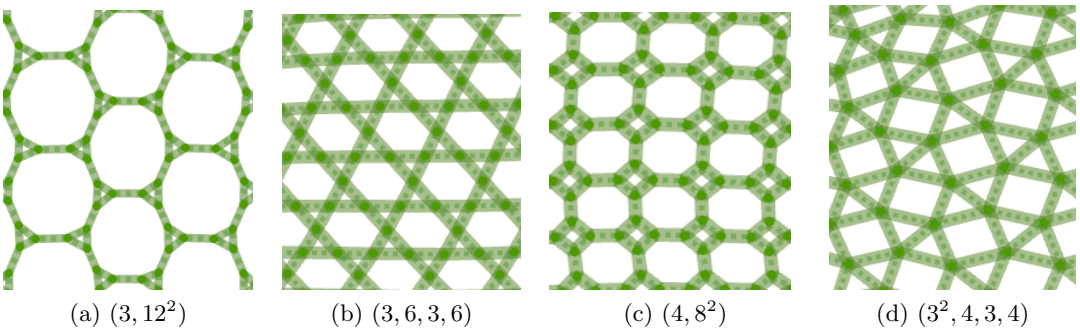

(a) $(3, 12^2)$ (b) $(3, 6, 3, 6)$ (c) $(4, 8^2)$ (d) $(3^2, 4, 3, 4)$

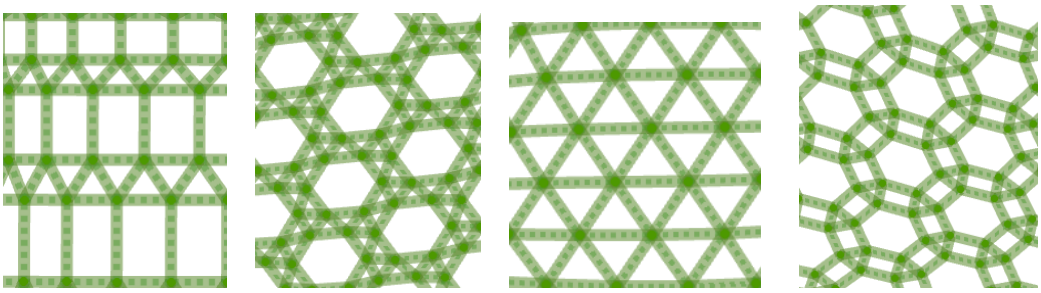

(e) $(3^3, 4^2)$ (f) $(3^4, 6)$ (g) (3^6) (h) $(3, 4, 6, 4)$

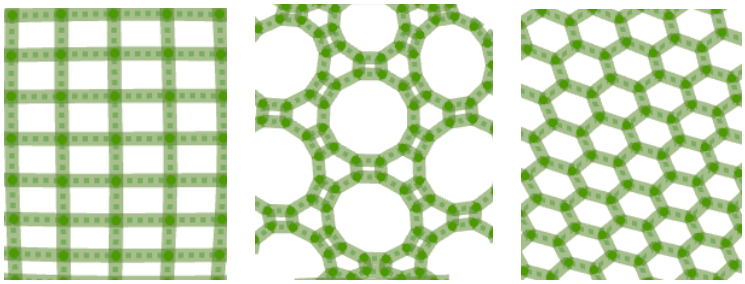

(i) (4^4) (j) $(4, 6, 12)$ (k) (6^3)

Figure 7.1: The 11 Archimedean lattices.

By studying the melting phase transition on the 11 Archimedean lattices, one could explore and determine the relationship between β_c and the specific kind of lattice or even the dimension of the lattice. I have already started working on this problem, by creating MATLAB codes for the 11 Archimedean lattices (see Appendix B).

5. Studying the melting phase transition on the β-skeleton graphs when $\beta = 2$ (relative neighbourhood graphs) in 2 and in 3 dimensions.

6. Investigating the effects of adding some edges randomly or systematically to a network on the communicability function.

Appendix A

Datasets and Tables

Real-World Networks Datasets

The real-world networks used in this work belong to different domains: ecological (includes food webs and ecosystems), social (networks of friendships, communication networks, corporate relationships), technological (internet, transport, software development networks), informational (vocabulary networks, citations) and biological (protein-protein interaction networks, transcription regulation networks, brain networks). The dataset comprises networks of different sizes, ranging from $n = 29$ to $n = 1586$ nodes, which are listed in Table A.1.

Table A.1: Networks Datasets

	Dataset	Domain	Description and reference
1	Benguela	ecological	Marine ecosystem of Benguela off the southwest coast of South Africa [114].
2	Coachella	ecological	Wide range of highly aggregated taxa from the Coachella Valley desert in southern California [111].

Table A.1: Networks Datasets

	Dataset	Domain	Description and reference
3	Sicail3	social	Social network among college students participating in a course about leadership. The students choose which three members they want to have on a committee [117].
4	Macaque	biological	The brain networks of macaque visual cortex and cat cortex, after the modifications introduced by Sporn and Kötter [102].
5	PIN A. fulgidus	biological	Protein-protein interaction network in A. fulgidus [83].
6	Hitech	ecological	Friendship ties among the employees in a small high-tech computer firm which sells, installs, and maintains computer systems [18].
7	Chesapeake	social	The pelagic portion of an eastern U.S. estuary, with an emphasis on larger fishes [60].
8	Zackary	social	Social network of friendship between members of the Zackary karate club. [115].
9	Skipwith	ecological	Invertebrates in an English pond [114].
10	Sawmill	social	Social communication network within a sawmill, where employees were asked to indicate the frequency with which they discussed work matters with each of their colleagues [79].
11	St. Martin	ecological	Birds and predators and arthropod prey of Anolis lizards on the island of St. Martin, which is located in the northern Lesser Antilles [76].

Table A.1: Networks Datasets

	Dataset	Domain	Description and reference
12	Trans Urchin	biological	Developmental transcription network for sea urchin endomesoderm development [80].
13	St. Marks	ecological	Mostly macroinvertebrates, fishes, and birds associated with an estuarine seagrass community, Halodule wrightii, at St. Marks Refuge in Florida [44].
14	Reef Small	ecological	Caribbean coral reef ecosystem from the Puerto Rico-Virgin Island shelf complex [88].
15	PIN KSHV	biological	Protein-protein interaction networks in *Kaposi sarcoma herpes virus*[106].
16	Dolphins	social	Social network of a bottlenose dolphins (Tursiops truncates) population near New Zealand [69].
17	Prison	social	Social network of inmates in prison who chose "Which fellows on the tier are you closest friends with?" [72].
18	Bridge Brook	ecological	Pelagic species from the largest of a set of 50 New York Adirondack lake food webs [92].
19	World Trade	economic	World trade network of miscellaneous manufacture of metals (MMM) in 1994 [8].
20	Shelf	ecological	Marine ecosystem on the northeast US shelf [68].
21	PIN B. subtilis	biological	Protein-protein interaction network in B. subtilis [87].
22	Ythan2	ecological	Reduced version of Ythan1 with no parasites [46].

Table A.1: Networks Datasets

	Dataset	Domain	Description and reference
23	Canton	ecological	Primarily invertebrates and algae in a tributary, surrounded by pasture, of the Taieri River in the South Island of New Zealand [105].
24	Stony	ecological	Primarily invertebrates and algae in a tributary, surrounded by pasture, of the Taieri River in the South Island of New Zealand in native tussock habitat [5].
25	Electronic1	technological	Electronic sequential logic circuits parsed from the ISCAS89 benchmark set, where nodes represent logic gates and flip-flops [81].
26	Ythan1	ecological	Mostly birds, fishes, invertebrates, and metazoan parasites in a Scottish Estuary [52].
27	Software Digital	technological	Software network development for Digital [84].
28	Scotch Broom	ecological	Trophic interactions between the herbivores, parasitoids, predators and pathogens associated with broom, Cytisus scoparius, collected in Silwood Park, Berkshire, England, UK [78].
29	El Verde	ecological	Insects, spiders, birds, reptiles and amphibians in a rainforest in Puerto Rico [95].
30	Little Rock	ecological	Pelagic and benthic species, particularly fishes, zooplankton, macroinvertebrates, and algae of the Little Rock Lake, Wisconsin, U.S. [48].
31	PIN Malaria	biological	Rock Lake, Wisconsin, USA. Protein-protein interaction network in P. falciparum (malaria parasite) [61].
32	PIN E. coil	biological	Protein-protein interaction network in E. coli [12].

Table A.1: Networks Datasets

	Dataset	Domain	Description and reference
33	Small World	informational	Citation network of papers that cite S. Milgram's 1967 Psychology Today paper or use Small World in title [7].
34	Electronic2	technological	Electronic sequential logic circuits parsed from the ISCAS89 benchmark set, where nodes represent logic gates and flip-flops [81].
35	Neurons	biological	Neuronal synaptic network of the nematode *C. elegans*. Included all data except muscle cells and using all synaptic connections [113].
36	Trans E. coli	biological	B. subtilis. Protein-protein interaction network in E. coli [80].
37	USAir97	technological	Airport transportation network between airports in the US in 1997 [7].
38	Electronic3	technological	Electronic sequential logic circuits parsed from the ISCAS89 benchmark set, where nodes represent logic gates and flip-flops [81].
39	Drugs	social	Social network of injecting drug-users (IDUs) who have shared a needle in the last six months [8].
40	Trans Yeast	biological	Zealand. Transcriptional regulation between genes in Saccaromyces cerevisiae [80].
41	PIN H. pyroli	biological	Protein-protein interaction network in H. pyroli [65].
42	Software_VTK	technological	MySQL. Software network development for VTK [84].
43	Software_XMMS	technological	VTK. Software network development for XMMS [84].

Table A.1: Networks Datasets

	Dataset	Domain	Description and reference
44	Roget	informational	Vocabulary network of words related by their definitions in Roget's Thesaurus of English. Two words are connected if one is used in the definition of the other [96].
45	Software Abi	technological	Software network development for Abi [84].
46	Software MySQL	technological	Software network development for MySQL [84].
47	Corporate elite	social	American corporate elite formed by the directors of the 625 largest corporations that reported the compositions of their boards, selected from the Fortune 1,000 in 1999 [21].

Tables of Simulation Results

Values of several topological parameters of networks, namely, edge density δ, average degree $\bar{K}$, maximum degree K_{max}, average Watts-Strogatz clustering coefficient $\bar{C}$, average path length $\bar{l}$, shortest path efficiency Ef, and the spectral radius of the adjacency matrix λ_1 for 47 complex real-world networks are used in this work. These parameters are listed in Table A.2. In Table A.3, we illustrate the values of several other global structural parameters for the 47 networks, namely, the second largest eigenvalue of the adjacency matrix λ_2, spectral gap of the adjacency matrix Δ, average communicability distance $\bar{\xi}$, average resistance distance $\bar{\Omega}$, average communicability angle $\bar{\theta}$ and melting phase transition β_c.

Table A.2: Topological parameters of networks

Network	Nodes	edges	δ	$\overline{k}$	k_{max}	$\bar{C}$	$\bar{l}$	Ef	λ_2
Benguela	29	191	0.47	13.17	24	0.57	1.62	0.72	4.0807
Coachella	30	241	0.554	16.7	25	0.71	1.46	0.77	5.0895
Sicail3	32	80	0.161	5	13	0.33	2.30	0.51	3.8096
Macaque	32	194	0.391	12.13	22	0.65	1.66	0.69	7.3329
PIN A. fulgidus	32	36	0.072	2.25	9	0.06	3.60	0.35	2.7694
Hitech	33	91	0.172	5.52	16	0.45	2.36	0.51	4.0791
Chesapeake	33	71	0.134	4.30	10	0.20	2.80	0.45	4.5301
Zackary	34	78	0.139	4.59	17	0.57	2.41	0.49	4.9771
Skipwith	35	353	0.593	20.17	32	0.63	1.42	0.79	3.4282
Sawmill	36	62	0.098	3.44	13	0.31	3.14	0.4	3.2714
St. Martin	44	218	0.23	9.91	27	0.33	1.93	0.59	6.972
Trans Urchin	45	80	0.08	3.56	14	0.21	3.22	0.39	2.9482
St. Marks	48	218	0.193	9.08	19	0.28	2.09	0.55	4.9313
Reef Small	50	503	0.41	20.12	39	0.61	1.6	0.70	8.5789
PIN KSHV	50	114	0.093	4.56	16	0.13	2.84	0.42	3.6109
Dolphins	62	159	0.084	5.13	12	0.26	3.36	0.38	5.9363
Prison	67	142	0.064	4.24	11	0.31	3.35	0.36	4.616
Bridge Brook	75	542	0.195	14.45	41	0.20	2.17	0.54	12.9665
World Trade	80	875	0.276	21.88	77	0.75	1.72	0.64	10.6077
Shelf	81	1451	0.447	35.83	69	0.59	1.57	0.72	11.7232
PIN B. subtilis	84	98	0.028	2.33	17	0.04	4.05	0.29	3.7738
Ythan2	92	416	0.099	9.04	50	0.22	2.25	0.49	6.1364
Canton	108	707	0.122	13.09	47	0.05	2.35	0.49	7.035
Stony	112	830	0.133	14.82	45	0.07	2.34	0.49	6.2789
Electronic1	122	189	0.025	3.10	10	0.06	4.93	0.25	3.6308
Ythan1	134	593	0.066	8.85	65	0.23	2.40	0.46	7.4653
Software Digital	150	198	0.017	2.64	25	0.05	4.85	0.25	4.8417

Table A.2: Topological parameters of networks

Network	Nodes	edges	δ	$\overline{k}$	k_{max}	$\bar{C}$	$\bar{l}$	Ef	λ_2
Scotch Broom	154	366	0.031	4.75	36	0.14	3.39	0.33	6.2284
El Verde	156	1439	0.119	18.45	83	0.21	2.30	0.5	9.4123
Little Rock	181	2318	0.142	25.61	105	0.35	2.22	0.51	26.1729
PIN Malaria	229	604	0.023	5.28	35	0.17	3.38	0.33	7.9178
PIN E. coil	230	695	0.026	6.04	36	0.22	3.78	0.31	8.5681
Small World	233	994	0.036	8.53	147	0.56	2.37	0.45	14.7231
Electronic2	252	399	0.012	3.17	14	0.06	5.81	0.2	3.9621
Neurons	280	1973	0.05	14.09	77	0.28	2.63	0.42	14.0663
Trans E. coli	328	456	0.008	2.78	72	0.11	4.83	0.25	6.2972
USAir97	332	2126	0.038	12.81	139	0.63	2.74	0.41	17.3085
Electronic3	512	819	0.006	3.20	22	0.05	6.86	0.17	4.1209
Drugs	616	2012	0.010	6.53	58	0.55	5.28	0.23	14.2338
Trans Yeast	662	1062	0.004	3.21	71	0.05	5.20	0.22	8.4518
PIN H. pyroli	710	1396	0.005	3.93	55	0.02	4.15	0.26	8.2499
Software_VTK	771	1357	0.004	3.52	83	0.06	4.53	0.24	8.7069
Software_XMMS	971	1802	0.003	3.71	36	0.05	6.35	0.18	8.9324
Roget	994	3640	0.007	7.32	28	0.15	4.08	0.27	9.8092
Software Abi	1035	1719	0.003	3.32	89	0.06	5.08	0.22	7.6764
Software MySQL	1480	4190	0.003	5.66	220	0.16	5.47	0.23	14.4141
Corporate elite	1586	11540	0.009	14.55	65	0.50	3.51	0.31	19.2296

Table A.3: Topological parameters and β_c of networks

Network	ϱ	β_c	$\lambda_1 - \lambda_2$	$\lambda_2 - \lambda_3$	$\bar{\xi}$	$\bar{\theta}$	$\bar{\Omega}$
Benguela	1.156	$4.0.10^{-3}$	11.1477	1.6585	160.9	1.22	104.3
Coachella	1.129	$6.7.10^{-3}$	13.0578	1.404	622.1	0.25	71.6
Sicail3	1.194	$22.3.10^{-3}$	2.1617	0.4974	3.61	52.1	288.8
Macaque	1.158	$18.1.10^{-3}$	6.7087	3.2987	91.5	3.6	119.1
PIN A. fulgidus	1.557	$3.2.10^{-3}$	0.7359	0.5219	2.1	79.3	1233.2
Hitech	1.440	$29.7.10^{-4}$	3.8629	1.1479	7.2	39.2	416.5
Chesapeake	1.335	$1.3.10^{-3}$	1.2151	1.5505	3.7	60.6	575.4
Zackary	1.465	$11.5.10^{-3}$	1.7486	2.0606	4.6	45.4	470.2
Skipwith	1.094	$2.9.10^{-2}$	18.6481	0.4785	3327.9	0.015	66.1
Sawmill	1.443	$3.0.10^{-3}$	1.7004	0.1365	2.9	71.4	879.07
St. Martin	1.264	$7.1.10^{-3}$	5.5589	3.6695	41.7	6.1	354.4
Trans Urchin	1.879	$9.0.10^{-5}$	3.7353	0.1617	4.2	61.8	2002.8
St. Marks	1.306	$5.7.10^{-3}$	6.9337	0.1482	33.2	8.2	396.1
Reef Small	1.180	$7.4.10^{-3}$	15.1769	3.3023	8975.4	0.04	175.2
PIN KSHV	1.624	$3.6.10^{-3}$	3.7953	0.2489	5.17	51.5	1380.2
Dolphins	1.402	$1.8.10^{-4}$	1.2573	1.106	5.9	65.3	1864.3
Prison	1.319	$1.6.10^{-3}$	0.9748	0.4963	3.8	76.5	2352.7
Bridge Brook	1.428	$6.0.10^{-5}$	7.9428	8.957	2041.5	2	829.4
World Trade	1.3774	$8.4.10^{-3}$	19.5234	1.2534	185830	0.006	439.01
Shelf	1.169	$3.5.10^{-3}$	30.1925	5.0688	61317000	0.00003	234.6
PIN B. subtilis	2.035	$8.3.10^{-4}$	0.9766	0.2854	2.5	81.7	8801
Ythan2	1.743	$2.7.10^{-3}$	9.6343	0.2525	180.7	2.03	2202.1
Canton	1.493	$6.2.10^{-4}$	12.5243	0.9162	1103.8	0.46	2781.7
Stony	1.531	$9.9.10^{-4}$	16.4232	0.8835	5372	0.09	2784.1
Electronic1	1.325	$1.1.10^{-4}$	0.4755	0.1264	2.6	86.1	1308.2
Ythan1	1.891	$1.6.10^{-3}$	9.2716	0.7321	251.8	2.1	5066.1
Software Digital	2.538	$3.0.10^{-6}$	1.8603	1.3521	3.2	81.6	33732

Table A.3: Topological parameters and β_c of networks

Network	ϱ	β_c	$\lambda_1 - \lambda_2$	$\lambda_2 - \lambda_3$	$\bar{\xi}$	$\bar{\theta}$	$\bar{\Omega}$
Scotch Broom	3.095	$1.8.10^{-5}$	8.4851	0.9613	95.2	30.3	18878
El Verde	1.707	$5.3.10^{-5}$	22.0819	0.9165	393310	0.006	4554.7
Little Rock	1.593	$4.2.10^{-4}$	14.6429	11.2706	37086000	0.05	4022.7
PIN Malaria	1.854	$1.6.10^{-4}$	1.8626	1.9766	8.6	55.03	21314
PIN E. coil	2.636	$6.2.10^{-8}$	7.363	1.6578	147.9	39.7	43692
Small World	2.456	$9.1.10^{-4}$	6.2385	6.1129	1459.4	5.05	17115
Electronic2	1.376	$3.6.10^{-5}$	0.3979	0.0809	2.7	87.9	58313
Neurons	1.652	$9.0.10^{-5}$	9.2266	3.124	4575.4	1.5	10342
Trans E. coli	3.259	$9.0.10^{-9}$	2.7664	1.1304	5.1	77.4	136090
USAir97	3.219	$1.6.10^{-7}$	23.9249	7.3098	37249000	0.002	45538
Electronic3	1.565	$3.9.10^{-6}$	0.8891	0.0468	2.82	88.8	251490
Drugs	2.757	$1.8.10^{-9}$	3.7761	0.6647	245.2	64	348790
Trans Yeast	3.109	$2.0.10^{-8}$	1.5243	0.6435	7.1	83.3	450470
PIN H. pyroli	2.661	$6.0.10^{-6}$	2.2159	1.4565	7.1	67.5	370530
Software_VTK	3.255	$2.0.10^{-6}$	2.7514	0.6763	9.7	70.1	563410
Software_XMMS	2.770	$9.0.10^{-10}$	1.3513	1.7303	6.4	84.3	1011600
Roget	1.642	$3.0.10^{-6}$	2.2181	0.7447	14.8	65.7	316670
Software Abi	3.596	$2.0.10^{-6}$	4.269	0.3969	9.2	72.8	1233700
Software MySQL	3.835	$2.0.10^{-14}$	7.3001	1.9879	895.5	45.6	1700500
Corporate elite	1.596	$2.0.10^{-8}$	3.9	1.004	2099.8	15.5	337470

Statistical Tools for Correlation

To investigate the relationship between network robustness and network's structural properties, we use two correlation coefficients. There are many measures of correlations in the literature, however, in this thesis we consider the Pearson correlation coefficient and the coefficient of variation [39, 103].

Definition A.0.1. The Pearson correlation coefficient r between two variables $X = (x_1, x_2, \ldots, x_n)$ and $Y = (y_1, y_2, \ldots, y_n)$ is defined by

$$r = \frac{n\sum_{i=1}^{n} x_i y_i - \sum_{i=1}^{n} x_i \sum_{i=1}^{n} y_i}{\sqrt{n\sum_{i=1}^{n} x_i^2 - (\sum_{i=1}^{n} x_i)^2}\sqrt{n\sum_{i=1}^{n} y_i^2 - (\sum_{i=1}^{n} y_i)^2}}. \tag{A.1}$$

The Pearson correlation coefficient is bounded by $0 \leq |r| \leq 1$. A positive value of r indicates that Y increases as X increases, and a negative value implies that X and Y are inversely related where Y decreases as X increases. If $|r| = 0$, then there is no relationship between the variables X and Y. If $|r| = 1$ then X and Y are completely correlated.

Definition A.0.2. The coefficient of variation CV of the variables $X_1, X_2, \ldots, X_n$ is the standard deviation divided by the mean of these variables,

$$CV = \frac{\sqrt{\frac{\sum_{i=1}^{n}(X_i - \frac{\sum_{i=1}^{n} X_i}{n})^2}{n}}}{\frac{\sum_{i=1}^{n} X_i}{n}}. \tag{A.2}$$

Appendix B

MATLAB© Scripts

B.1 Script for Global to Local Degree Heterogeneity Index and some basic Parameters for the Adjacency Matrix of Simple Connected Networks.

```
% A is adjacency matrix of the network
A=max(A,A');
A=A-diag(diag(A));
[V,D]=eig(A);
b=sort(diag(D))
n=length(A)              % number of nodes
m=sum(sum(A))/2          % number of links
k=(2*m)/n                % average-degree(A)
t=sum(A);
k_max=max(t)             % max-degree(A)
h=2*m/(n*(n-1))          % edge density
lambda1=b(n)             % lambda_1 of A
lambda2=b(n-1)           % lambda_2 of A
c1=b(n)-b(n-1)           % Spectral gap
% global to local degree heterogeneity
q=n*lambda1/k;
```

B.2 Script for calculating the Kirchhoff Index Kf

```
L=diag(sum(A))-A ;     % L Laplacian Matrix,  % A is adjacency matrix
  of the network
[V,D]= eig(L);
b=sort(diag(D));
un = b(end);
u2 = b(2) ;
n=length(A);
D=zeros(n,n);
for i=1:n;
   for j=1:n;
       D(i,j)==0;
       for k=2:n;
D(i,j)=D(i,j)+((1/b(k))*((V(i,k)-V(j,k))^2));
       end
   end
end
D;
Kf=0;
for i=1:n-1;
  for   j=i+1:n;
        Kf=Kf+D(i,j);
   end
end
Kf       % kirchhoff index
```

B.3 Script for calculating the Clustering Coefficient and some other Parameters.

```
deg = sum(A);    % A is adjacency matrix of the network
B=(1/2)*diag(A^3);
n=length(A) ;
cc=zeros(n,1);
for i=1:n
if deg(i)>1
cc(i)=(1/n)*(2*B(i)/(deg(i)*(deg(i)-1)));
end
end
cl=sum(cc)          % clustering coefficient cl
G=expm(A) ;         % Communicability matrix
sc=diag(G) ;        %Vector of self-communicabilities
u=ones(n,1);
CD=(sc*u'+u*sc'-2*G);
%Squared Communicability distance matrix
X=CD.^0.5 ;    %Communicability distance matrix
An=acosd(G./((sc*u').*(u*sc')).^0.5);
Average_Angle=sum(sum(An))/(n*(n-1))    % Average communicability
  angle
Average_dist=sum(sum(X))/(n*(n-1))      % Average communicability
  distance
```

B.4 Script for calculating Diameter and Shorteast Path Length Efficiency.

```
A=sparse(A);  % A is adjacency matrix of the network
D=graphallshortestpaths(A,'Directed',false);
Di=max(D(:)); % Diameter Di
% average path length l
n=length(A);
l = sum(sum(D))/(n^2-n)
% shorteast path length efficiency l1
r=zeros(n);
r=(1./D);
for i=1:n
r(i,i)=0;
end
l1 =( 1/(n^2-n))*(sum(sum(r)))
```

B.5 Script for calculating the Pearson Correlation Coefficient.

```
r;  b;    % r, b are vectors
n=length(r); br=zeros(n,1);
for k=1:n
br(k)=b(k)*r(k);          % finding br
end
rr=zeros(n,1);
for k=1:n
rr(k)=r(k)*r(k);          % finding r^2
end
bb=zeros(n,1);
for k=1:n
bb(k)=b(k)*b(k);          % finding b^2
end
p=(n*sum(br)-sum(b)*sum(r))/(sqrt((n*sum(rr)-sum(r)^2))*
sqrt((n*sum(bb)-sum(b)^2)))  % pearson correlation coefficient p
```

B.6 Script for calculating the Beta Critical and Number of Connected Components.

```
A=A-diag(diag(A)); % A is adjacency matrix
for beta= 0.000025 ;
[a,b] = sort(diag(D));
lambda1 = D(b(end),b(end)) ;
gamma1 = V(:,b(end));
gamma1=abs(gamma1) ;
C1=(gamma1*exp(beta*lambda1)*gamma1');
H=diag(exp(beta*diag(D)));
G=V*H*V';
DG=G-C1 ;
DG=DG-diag(diag(DG)); HH=DG+max(max(DG));
n=length(A);
sgnDG=zeros(n,n);
for i=1:n;
for j=1:n;
if HH(i,j)>=0
sgnDG(i,j)=1;
else sgnDG(i,j)=0;
end;end;end;
AC=sgnDG-diag(diag(sgnDG));
L=diag(sum(AC))-AC;
[V,D]= eig(L);
[a1,b2] = sort(diag(D));
nc=numel(find(a1<10^(-5))) % number connected components
h=beta
end
```

B.7 Script for calculating the Coefficient of Variation and some other Parameters.

```
% finding melted nodes
% AC is the communicability graph adjacency matrix
% A is adjacency matrix of the network
n=length(AC);
beta_melt=zeros(n,1);
for r=1:n;
 if AC(r,:)==0
   beta_melt(r,1)=beta ;
 end;
end;
beta_melt;
% highlighting melted nodes
h =plot(graph(A),'Layout','force','EdgeColor','b',
'NodeColor','b', 'MarkerSize',7,'NodeLabel',{},
'LineWidth',0.75)
highlight(h,[melted nodes],'NodeColor','r')
axis off
% Eigenvector Centrality EC
G=graph(A); EC=centrality(G,'eigenvector')
% Supgraph Centrality SE
B=expm(A); SE=diag(B);
% Coefficient of variation cv
% r is vector
n=length(r); m=sum(r)/n; Se=0;
for i=1:n
Se=Se+(r(i)-m)^2;
end
d=sqrt(Se/n); cv=(d/m);
```

B.8 Script for Communicability Function of Dumbbell Graphs

```
n=5; % n is number of nodes in each clique
z1=ones(n,n); z1=z1-eye(n);
A=blkdiag(z1,z1); A(n,n+1) =1;
A=max(A,A'); A=A-diag(diag(A))
[V,D]= eig(A); b=sort(diag(D))
format long
G=expm(A);
y1=1/(sqrt((2*(1+((n-1)/(b(2*n)-n+2)^2)))));
x1=(1/(b(2*n)-n+2))*y1;
y2=1/(sqrt((2*(1+((n-1)/(b(2*n-1)-n+2)^2)))));
x2=(1/(b(2*n-1)-n+2))*y2;
y3=1/(sqrt((2*(1+((n-1)/(b(2*n-2)-n+2)^2)))));
x3=(1/(b(2*n-2)-n+2))*y3;
y2n=1/(sqrt((2*(1+((n-1)/(b(1)-n+2)^2)))));
x2n=(1/(b(1)-n+2))*y2n;
G3=((x1)^2)*exp(b(2*n))+((x2)^2)*exp(b(2*n-1))+((x3)^2)*exp(b(2*n-2))
  +((x2n)^2)*exp(b(1))-exp(-1)*((x1)^2+(x2)^2+(x3)^2+(x2n)^2)
G4=(y1*x1)*exp(b(2*n))+(y2*x2)*exp(b(2*n-1))+(y3*x3)*exp(b(2*n-2))+(
  y2n*x2n)*exp(b(1))
G5=(y1*x1)*exp(b(2*n))-(y2*x2)*exp(b(2*n-1))+(y3*x3)*exp(b(2*n-2))-(
  y2n*x2n)*exp(b(1))
G6=((x1)^2)*exp(b(2*n))-((x2)^2)*exp(b(2*n-1))+((x3)^2)*exp(b(2*n-2))
  -((x2n)^2)*exp(b(1))+exp(-1)*(-(x1)^2+(x2)^2-(x3)^2+(x2n)^2)
G7=((y1)^2)*exp(b(2*n))-((y2)^2)*exp(b(2*n-1))+((y3)^2)*exp(b(2*n-2))
  -((y2n)^2)*exp(b(1))
figure (1)
h=plot(graph(A),'Layout','force','EdgeColor','b','NodeColor','r','
  MarkerSize',12,'LineWidth',1,'NodeLabel',{})
axis off
```

B.9 Script for Communicability Function of Windmill Graphs

```
% n is number of nodes in each clique.
% d is number of cliques.
n=2; d=3;
z2=ones(n,n); c=eye(d);
B=kron(c,z2); A=blkdiag(0,B) ;
A(1,2:d*n+1)=1; A=max(A,A');
A=A-diag(diag(A)); [V,D]= eig(A);
b=sort(diag(D))
format long
G=expm(A)
p = [1 (1-n) -d*n];
r = roots(p)
x1=1/sqrt(d*n+(r(1)-n+1)^2);
y1=(r(1)-n+1)*x1;
x2=1/sqrt(d*n+(r(2)-n+1)^2);
y2=(r(2)-n+1)*x2;
x3=1/sqrt(d*n);
r(3)=n-1;
G3=(x1*y1)*exp(r(1))+(x2*y2)*exp(r(2))
G4=((x1)^2)*exp(r(1))- ((x1)^2+(x2)^2-(1/n))*exp(r(3))+((x2)^2)*exp(r
  (2))-exp(-1)*(1/n)
G5=((x1)^2)*exp(r(1))+((x2)^2)*exp(r(2))-((x1)^2+(x2)^2)*exp(r(3))
figure (1)
h =plot(graph(A),'Layout','force','EdgeColor','b','NodeColor','r','
  MarkerSize',12,'LineWidth',1,'NodeLabel',{})
axis off
```

B.10 Script for Archimedean Lattice $(3, 12^2)$.

```
n=12; % n is natural number
A=[0 1 1
    1 0  1
    1 1 0];
n=n^2; c=eye(n);
d=kron(c,A); d=max(d,d'); m=sqrt(n);
for j=0:m-1;
   for i=3:3:3*m-3
                d(i+3*m*j,i+3*m*j+1)=1;
                d(i+3*m*j+1,i+3*m*j)=1;
       end
end
for j=0:2:m-2;
    for i=2:6:3*m-1
              d(i+3*m*j,i+3*m*(j+1))=1;
              d(i+3*m*(j+1),i+3*m*j)=1;
       end
end
for j=1:2:m-2;
    for i=5:6:3*m-1
        d(i+3*m*j,i+3*m*(j+1))=1;
        d(i+3*m*(j+1),i+3*m*j)=1;
     end
end
d=max(d,d');
hold on
h = plot(graph(d),'EdgeColor','k', 'NodeColor','[0.3, 0.6,0]', '
  MarkerSize',6,'EdgeColor', '[0.3, 0.5,0.1]','LineWidth', 5 )
h = plot(graph(d),'EdgeColor','k', 'NodeColor','[0.3, 0.6,0]', '
  MarkerSize',6,'EdgeColor', '[0.3, 0.6,0.2]','LineStyle',':','
  LineWidth',3 )
hold off
axis off
```

B.11 Script for Archimedean Lattice $(3, 6, 3, 6)$.

```
n=23; % n is natural number
A=[0 1 1
    1 0  1
    1 1 0];
n=n^2; c=eye(n);
d=kron(c,A); d=max(d,d'); n=sqrt(n)
for j=0:n-1;
    for i=3:3:3*n-3;
        d(i+3*j*n,i+3*j*n+1)=1;
        d(i+3*j*n+1,i+3*j*n)=1;
    end;
end;
for j=0:2:n-2;
    for i=5:3:3*n-1;
        d(i+3*j*n,i+3*(j+1)*n-2)=1;
        d(i+3*j*n,i+3*(j+1)*n-1)=1;
     end;
end;
for j=0:2:n-2;
            d(2+3*j*n,2+3*(j+1)*n-1)=1;
            d(2+3*(j+1)*n-1,2+3*j*n)=1;
end;
for j=1:2:n-2;
    for i=2:3:3*n-4;
        d(i+3*j*n,i+3*(j+1)*n+1)=1;
        d(i+3*j*n,i+3*(j+1)*n+2)=1;
        d(i+3*(j+1)*n+1,i+3*j*n)=1;
        d(i+3*(j+1)*n+2,i+3*j*n)=1;
    end;
end;
for j=1:2:n-2;
    for i=3*n-1;
        d(i+3*j*n,i+3*(j+1)*n+1)=1;
        d(i+3*(j+1)*n+1,i+3*j*n)=1;
     end;
```

```
end;
d=max(d,d');
hold on
h = plot(graph(d),'EdgeColor','k', 'NodeColor','[0.3, 0,0.6]', '
  MarkerSize',6,'EdgeColor', '[0.3, 0.1,0.5]','LineWidth', 5 )
h = plot(graph(d),'EdgeColor','k', 'NodeColor','[0.3, 0,0.6]', '
  MarkerSize',6,'EdgeColor', '[0.3, 0.2,0.6]','LineStyle',':','
  LineWidth',3 )
hold off
axis off
```

B.12 Script for Archimedean Lattice $(4, 8^2)$.

```
n=5; % n is natural number
A=[0 1 1 0
    1 0 0 1
    1 0 0 1
    0 1 1 0];
n=n^2; c=eye(n);
f=kron(c,A); f=max(f,f'); c=zeros(n*4);
for i=4:4:n*4-1;
    c(i,i+1)=1;
end
m=sqrt(n);
for i=m*4:m*4:n*4-1;
  c(i,i+1)=0;
end
c=max(c,c');
c2=zeros(n*4);
for i=2:4:4*n-4*m;
    c2(i,i+4*m+1)=1;
end
c2=max(c2,c2');
r=c+f+c2; r=max(r,r');
hold on
h = plot(graph(r),'EdgeColor','k', 'NodeColor','[0.3, 0,0.6]', '
```

```
  MarkerSize',6,'NodeLabel',{},'EdgeColor', '[0.3, 0.1,0.5]','
  LineWidth', 5 )
h = plot(graph(r),'EdgeColor','k', 'NodeColor','[0.3, 0,0.6]', '
  MarkerSize',6,'NodeLabel',{},'EdgeColor', '[0.3, 0.2,0.6]','
  LineStyle',':','LineWidth',3 )
hold off
axis off
```

B.13 Script for Archimedean Lattice $(3^2, 4, 3, 4)$.

```
n= 40; % n is even number
el =zeros(n-1,3);
el = [[1:n-1]' [2:n]' ones(n-1,1)];
nodes=sort(unique([el(:,1) el(:,2)])); % get all nodes, sorted
n=numel(nodes) % number of unique nodes
A=zeros(n);    % initialize adjacency matrix
for i=1:size(el,1); % across all edges
A(find(nodes==el(i,1)),find(nodes==el(i,2)))=el(i,3);
end
A=max(A,A'); A=A-diag(diag(A)); c=eye(n);
d=kron(c,A)+kron(A,c);
for j=0:n-2;
    for i=1:n;
        d(i+j*n,i+(j+1)*n)=0;
        d(i+(j+1)*n,i+j*n)=0;
     end;
end;
for j=0:8:n-2;
    for i=1:3:n-1;
        d(i+j*n,i+(j+1)*n)=1;
        d(i+j*n,i+(j+1)*n+1)=1;
     end
end
for j=0:8:n-2;
    for i=1:3:n;
         d(i+j*n,i+(j+1)*n)=1;
```

```
      end
end
for j=0:8:n-2;
     for i=2:3:n-1;
         d(i+j*n,i+(j+1)*n+1)=1;
         d(i+j*n+1,i+(j+1)*n+1)=1;
     end
end
for j=4:8:n-2;
     for i=1:3:n-1;
         d(i+j*n,i+(j+1)*n)=1;
         d(i+j*n+1,i+(j+1)*n)=1;
      end
end
for j=4:8:n-2;
    for i=1:3:n;
        d(i+j*n,i+(j+1)*n)=1;
    end
end
for j=4:8:n-2;
     for i=3:3:n;
        d(i+j*n,i+(j+1)*n-1)=1;
        d(i+j*n,i+(j+1)*n)=1;
    end
end
for j=3:4:n-1;
    d(n*j,n*j+1)=1;
end
for j=2:4:n-2;
     for i=1:3:2*n-3
         d(i+j*n,i+j*n+2)=1;
        d(i+j*n+1,i+j*n+3)=1;
     end
end
for j=2:4:n-2;
    for i=1:3:2*n-2
        d(i+j*n,i+j*n+2)=1;
```

```
64        end
65  end
66  for j=2:4:n-2;
67      for i=5:6:2*n-3
68          d(i+j*n,i+j*n+1)=0;
69          d(i+j*n+1,i+j*n)=0;
70        end
71  end
72  for j=2:4:n-2;
73     for i=4:6:2*n-3
74          d(i+j*n,i+j*n+3)=1;
75       end
76  end
77  for j=1:8:n-3;
78      for i=1:3:n-1;
79          d(i+j*n,2*i+(j+1)*n)=1;
80          d(i+j*n+1,2*i+(j+1)*n)=1;
81      end
82  end
83  for j=1:8:n-3;
84      for i=1:3:n;
85         d(i+j*n,2*i+(j+1)*n)=1;
86        end
87  end
88  for j=1:8:n-3;
89      for i=2:3:n-2;
90          d(i+j*n,2*i+1+(j+1)*n)=1;
91          d(i+j*n+1,2*i+1+(j+1)*n)=1;
92          d(i+j*n+2,2*i+1+(j+1)*n)=1;
93      end
94  end
95  for j=4:8:n-2;
96      for i=1:3:n-1;
97          d(i+j*n,2*i+1+(j-2)*n)=1;
98          d(i+j*n+1,2*i+1+(j-2)*n)=1;
99      end
100 end
```

```
for j=4:8:n-2;
    for i=2:3:n-2;
        d(i+j*n,2*i+2+(j-2)*n)=1;
        d(i+j*n+1,2*i+2+(j-2)*n)=1;
        d(i+j*n+2,2*i+2+(j-2)*n)=1;
      end
end
for j=5:8:n-3;
    for i=1:3:n-2;
        d(i+j*n+1,2*i+(j+1)*n)=1;
        d(i+j*n+2,2*i+(j+1)*n)=1;
    end
end
for j=5:8:n-3;
    for i=1:3:n-1;
         d(i+j*n+1,2*i+(j+1)*n)=1;
       end
end
for j=5:8:n-2;
    for i=2:3:n-3;
        d(i+j*n+1,2*i+1+(j+1)*n)=1;
        d(i+j*n+2,2*i+1+(j+1)*n)=1;
        d(i+j*n+3,2*i+1+(j+1)*n)=1;
     end
end
for j=5:8:n-2;
  for i=2:3:n-1;
     d(i+j*n+1,2*i+1+(j+1)*n)=1;
   end
end
for j=5:8:n-2;
     for i=2:3:n-2;
        d(i+j*n+2,2*i+1+(j+1)*n)=1;
     end
end
for j=8:8:n-2;
    for i=1:3:n-2;
```

```
138         d(i+j*n+1,2*i+1+(j-2)*n)=1;
139         d(i+j*n+2,2*i+1+(j-2)*n)=1;
140     end
141 end
142 for j=8:8:n-2;
143     for i=1:3:n-1;
144         d(i+j*n+1,2*i+1+(j-2)*n)=1;
145        end
146 end
147 for j=8:8:n-2;
148    for i=2:3:n-3;
149         d(i+j*n+1,2*i+2+(j-2)*n)=1;
150         d(i+j*n+2,2*i+2+(j-2)*n)=1;
151         d(i+j*n+3,2*i+2+(j-2)*n)=1;
152     end
153 end
154 for j=8:8:n-2;
155    for i=2:3:n-1;
156        d(i+j*n+1,2*i+2+(j-2)*n)=1;
157    end
158 end
159 for j=8:8:n-2;
160     for i=2:3:n-2;
161       d(i+j*n+2,2*i+2+(j-2)*n)=1;
162    end
163 end
164 d=max(d,d');
165 hold on
166 h = plot(graph(d),'EdgeColor','k', 'NodeColor','[0.3, 0.6,0]', '
    MarkerSize',5,'NodeLabel',{},'EdgeColor', '[0.3, 0.5,0.1]','
    LineWidth', 5 )
167 h = plot(graph(d),'EdgeColor','k', 'NodeColor','[0.3, 0.6,0]', '
    MarkerSize',5,'NodeLabel',{},'EdgeColor', '[0.3, 0.6,0.2]','
    LineStyle',':','LineWidth',3 )
168 hold off
169 axis off
```

B.14 Script for Archimedean Lattice $(3^3, 4^2)$.

```
n=40; % n is natural number
el =zeros(n-1,3);
el = [[1:n-1]' [2:n]' ones(n-1,1)];
nodes=sort(unique([el(:,1) el(:,2)])); % get all nodes, sorted
n=numel(nodes) % number of unique nodes
A=zeros(n);   % initialize adjacency matrix
for i=1:size(el,1); % across all edges
A(find(nodes==el(i,1)),find(nodes==el(i,2)))=el(i,3);
end
A=max(A,A');  A=A-diag(diag(A));
c=eye(n);
d=kron(c,A)+kron(A,c);
for j=0:4:n-2;
    for i=2:n;
    d(i+j*n,(j+1)*n+i-1)=1;
   end
end
for j=2:4:n-2;
   for i=1:n-1;
        d(i+j*n,(j+1)*n+i+1)=1;
    end
end
d=max(d,d');
hold on
h = plot(graph(d),'EdgeColor','k', 'NodeColor','[0.3, 0.6,0]', '
  MarkerSize',6,'NodeLabel',{},'EdgeColor', '[0.3, 0.5,0.1]','
  LineWidth', 5 )
h = plot(graph(d),'EdgeColor','k', 'NodeColor','[0.3, 0.6,0]', '
  MarkerSize',6,'EdgeColor', '[0.3, 0.6,0.2]','LineStyle',':','
  LineWidth',3 )
hold off
axis off
```

B.15 Script for Archimedean Lattice $(3^4, 6)$.

```
n=40;      % n=10, 16, 22 ,..
el =zeros(n-1,3);
el = [[1:n-1]' [2:n]' ones(n-1,1)];
nodes=sort(unique([el(:,1) el(:,2)])); % get all nodes, sorted
n=numel(nodes) % number of unique nodes
A=zeros(n);   % initialize adjacency matrix
for i=1:size(el,1); % across all edges
A(find(nodes==el(i,1)),find(nodes==el(i,2)))=el(i,3);
end
A=max(A,A'); A=A-diag(diag(A));
c=eye(n);
d=kron(c,A)+kron(A,c);
for j=0:3:n-1;
    for i=2:6:n-1;
        d(i+j*n,i+j*n+1)=0;
        d(i+j*n+1,i+j*n)=0;
      end;
end;
for j=1:3:n-1;
    for i=6:6:n-1;
        d(i+j*n,i+j*n+1)=0;
        d(i+j*n+1,i+j*n)=0;
      end;
end;
for j=2:3:n-1;
    for i=4:6:n-1;
        d(i+j*n,i+j*n+1)=0;
        d(i+j*n+1,i+j*n)=0;
    end;
end;
for j=0:3:n-2;
    for i=2:6:n-1;
d(i+j*n,i+(j+1)*n-1)=1;
d(i+(j+1)*n-1,i+j*n)=1;
    end;
```

```
end;
for j=0:3:n-2;
    for i=3:6:n-3;
d(i+j*n,i+(j+1)*n+1)=1;
d(i+j*n+1,i+(j+1)*n+2)=1;
d(i+j*n+2,i+(j+1)*n+3)=1;
d(i+(j+1)*n+1,i+j*n)=1;
d(i+(j+1)*n+2,i+j*n+1)=1;
d(i+(j+1)*n+3,i+j*n+2)=1;
    end;
end;
for j=1:3:n-2;
   for i=6:6:n-3;
d(i+j*n,i+(j+1)*n-1)=1;
d(i+j*n+1,i+(j+1)*n+2)=1;
d(i+(j+1)*n+2,i+j*n+1)=1;
d(i+(j+1)*n-1,i+j*n)=1;
d(i+j*n-5,i+(j+1)*n-4)=1;
d(i+j*n-4,i+(j+1)*n-3)=1;
d(i+j*n-3,i+(j+1)*n-2)=1;
d(i+(j+1)*n-4,i+j*n-5)=1;
d(i+(j+1)*n-3,i+j*n-4)=1;
d(i+(j+1)*n-2,i+j*n-3)=1;
     end;
end;
for j=1:3:n-2;
    for i=6:6:n;
d(i+j*n-5,i+(j+1)*n-4)=1;
d(i+j*n-4,i+(j+1)*n-3)=1;
d(i+j*n-3,i+(j+1)*n-2)=1;
d(i+(j+1)*n-4,i+j*n-5)=1;
d(i+(j+1)*n-3,i+j*n-4)=1;
d(i+(j+1)*n-2,i+j*n-3)=1;
     end;
end;
for j=1:3:n-2;
     for i=6:6:n;
```

```
d(i+j*n-5,i+(j+1)*n-4)=1;
d(i+j*n-4,i+(j+1)*n-3)=1;
d(i+j*n-3,i+(j+1)*n-2)=1;
d(i+(j+1)*n-4,i+j*n-5)=1;
d(i+(j+1)*n-3,i+j*n-4)=1;
d(i+(j+1)*n-2,i+j*n-3)=1;
     end;
end;
for j=1:3:n-2
d(n-2+j*n,n+(j+1)*n-1)=1;
d(n-1+j*n,n+1+(j+1)*n-1)=1;
d(n+1+(j+1)*n-1,n-1+j*n)=1;
d(n+(j+1)*n-1,n-2+j*n)=1;
end
for j=0:3:n-2
     i=n-1;
d(i+j*n,i+1+(j+1)*n)=1;
d(i+1+(j+1)*n,i+j*n)=1;
end
for j=2:3:n-2;
   for i=1:6:n-3;
d(i+j*n,i+(j+1)*n+1)=1;
d(i+j*n+3,i+(j+1)*n+2)=1;
d(i+(j+1)*n+1,i+j*n)=1;
d(i+(j+1)*n+2,i+j*n+3)=1;
    end;
end;
for j=2:3:n-2;
   for i=5:6:n-3;
d(i+j*n,i+(j+1)*n+1)=1;
d(i+j*n+1,i+(j+1)*n+2)=1;
d(i+j*n+2,i+(j+1)*n+3)=1;
d(i+(j+1)*n+1,i+j*n)=1;
d(i+(j+1)*n+2,i+j*n+1)=1;
d(i+(j+1)*n+3,i+j*n+2)=1;
    end;
end;
```

```
d=max(d,d');
hold on
h = plot(graph(d),'EdgeColor','k', 'NodeColor','[0.3, 0.6,0]', '
  MarkerSize',6,'NodeLabel',{},'EdgeColor', '[0.3, 0.5,0.1]','
  LineWidth', 5 )
h = plot(graph(d),'EdgeColor','k', 'NodeColor','[0.3, 0.6,0]', '
  MarkerSize',6,'NodeLabel',{},'EdgeColor', '[0.3, 0.6,0.2]','
  LineStyle',':','LineWidth',3 )
hold off
axis off
```

B.16 Script for Archimedean Lattice (3^6).

```
n=40; % n is natural number
el =zeros(n-1,3);
el = [[1:n-1]' [2:n]' ones(n-1,1)];
nodes=sort(unique([el(:,1) el(:,2)])); % get all nodes, sorted
n=numel(nodes) % number of unique nodes
A=zeros(n);   % initialize adjacency matrix
for i=1:size(el,1); % across all edges
A(find(nodes==el(i,1)),find(nodes==el(i,2)))=el(i,3);
end
A=max(A,A'); A=A-diag(diag(A));
c=eye(n);
d=kron(c,A)+kron(A,c);
% j=0:((n-1)/2)-1 if n is odd or j=0:(n/2)-1 if n is even
for j=0:((n)/2)-1;
    for i=2:n;
    d(i+2*j*n,(2*j+1)*n+i-1)=1;
   end
end
% j=0:((n-1)/2)-1 if n is odd or j=0:(n/2)-2 if n is even
for j=0:((n)/2)-2;
    for i=2:n;
    d((2*j+1)*n+i-1,i+2*(j+1)*n)=1;
   end
```

```
end
d=max(d,d');
hold on
h = plot(graph(d),'EdgeColor','k', 'NodeColor','[0.3, 0,0.6]', '
  MarkerSize',6,'NodeLabel',{},'EdgeColor', '[0.3, 0.1,0.5]','
  LineWidth', 5 )
h = plot(graph(d),'EdgeColor','k', 'NodeColor','[0.3, 0,0.6]', '
  MarkerSize',6,'NodeLabel',{},'EdgeColor', '[0.3, 0.2,0.6]','
  LineStyle',':','LineWidth',3 )
hold off
axis off
```

B.17 Script for Archimedean Lattice $(3, 4, 6, 4)$.

```
n=40; % n is natural number
el =zeros(n-1,3);
el = [[1:n-1]' [2:n]' ones(n-1,1)];
nodes=sort(unique([el(:,1) el(:,2)])); % get all nodes, sorted
n=numel(nodes) % number of unique nodes
A=zeros(n);   % initialize adjacency matrix
for i=1:size(el,1); % across all edges
A(find(nodes==el(i,1)),find(nodes==el(i,2)))=el(i,3);
end
A=max(A,A'); A=A-diag(diag(A));
c=eye(n);
d=kron(c,A)+kron(A,c);
for j=0:n-2;
    for i=1:n;
        d(i+j*n,i+(j+1)*n)=0;
        d(i+(j+1)*n,i+j*n)=0;
     end;
end;
for j=0:4:n-2;
    for i=1:3:n-1;
        d(i+j*n,i+(j+1)*n)=1;
        d(i+j*n,i+(j+1)*n+1)=1;
```

```
23          d(i+(j+1)*n,i+j*n)=1;
24          d(i+(j+1)*n+1,i+j*n)=1;
25       end
26  end
27  for j=0:4:n-2;
28      for i=2:3:n-1;
29          d(i+j*n,i+(j+1)*n+1)=1;
30          d(i+j*n+1,i+(j+1)*n+1)=1;
31          d(i+(j+1)*n+1,i+j*n)=1;
32          d(i+(j+1)*n+1,i+j*n+1)=1;
33      end
34  end
35  for j=2:4:n-2;
36     for i=1:3:n-1;
37           d(i+j*n,i+(j+1)*n)=1;
38           d(i+j*n+1,i+(j+1)*n)=1;
39           d(i+(j+1)*n,i+j*n)=1;
40           d(i+(j+1)*n,i+j*n+1)=1;
41       end
42  end
43  for j=2:4:n-2;
44     for i=3:3:n;
45         d(i+j*n,i+(j+1)*n-1)=1;
46         d(i+j*n,i+(j+1)*n)=1;
47         d(i+(j+1)*n-1,i+j*n)=1;
48         d(i+(j+1)*n,i+j*n)=1;
49       end
50  end
51  for j=1:4:n-2;
52      for i=1:3:n-1;
53        d(i+j*n,i+(j+1)*n)=1;
54        d(i+j*n+1,i+(j+1)*n+1)=1;
55        d(i+(j+1)*n,i+j*n)=1;
56        d(i+(j+1)*n+1,i+j*n+1)=1;
57      end;
58  end;
59  for j=3:4:n-2;
```

```
60    for i=2:3:n-1;
61       d(i+j*n,i+(j+1)*n)=1;
62      d(i+j*n+1,i+(j+1)*n+1)=1;
63      d(i+(j+1)*n,i+j*n)=1;
64      d(i+(j+1)*n+1,i+j*n+1)=1;
65    end;
66 end;
67 d=max(d,d');
68 hold on
69 h = plot(graph(d),'EdgeColor','k', 'NodeColor','[0.3, 0,0.6]', '
   MarkerSize',6,'NodeLabel',{},'EdgeColor', '[0.3, 0.1,0.5]','
   LineWidth', 5 )
70 h = plot(graph(d),'EdgeColor','k', 'NodeColor','[0.3, 0,0.6]', '
   MarkerSize',6,'NodeLabel',{},'EdgeColor', '[0.3, 0.2,0.6]','
   LineStyle',':','LineWidth',3 )
71 hold off
72 axis off
```

B.18 Script for Archimedean Lattice (4^4).

```
1  n=4;  % n is natural number
2  el =zeros(n-1,3);
3  el = [[1:n-1]' [2:n]' ones(n-1,1)];
4  nodes=sort(unique([el(:,1) el(:,2)])); % get all nodes, sorted
5  n=numel(nodes) % number of unique nodes
6  A=zeros(n);   % initialize adjacency matrix
7  for i=1:size(el,1); % across all edges
8  A(find(nodes==el(i,1)),find(nodes==el(i,2)))=el(i,3);
9  end
10 A=max(A,A'); A=A-diag(diag(A));
11 c=eye(n);
12 d=kron(c,A)+kron(A,c);
13 d=max(d,d');
14 hold on
15 h = plot(graph(d),'EdgeColor','k', 'NodeColor','[0.3, 0,0.6]', '
   MarkerSize',6,'NodeLabel',{},'EdgeColor', '[0.3, 0.1,0.5]','
```

```
  LineWidth', 5 )
h = plot(graph(d),'EdgeColor','k', 'NodeColor','[0.3, 0,0.6]', '
  MarkerSize',6,'NodeLabel',{},'EdgeColor', '[0.3, 0.2,0.6]','
  LineStyle',':','LineWidth',3 )
hold off
axis off
```

B.19 Script for Archimedean Lattice $(4, 6, 12)$.

```
n=40;     % n is even number
el =zeros(n-1,3);
el = [[1:n-1]' [2:n]' ones(n-1,1)];
nodes=sort(unique([el(:,1) el(:,2)])); % get all nodes, sorted
n=numel(nodes) % number of unique nodes
A=zeros(n);   % initialize adjacency matrix
for i=1:size(el,1); % across all edges
A(find(nodes==el(i,1)),find(nodes==el(i,2)))=el(i,3);
end
A=max(A,A');
A=A-diag(diag(A));
c=eye(n);
d=kron(c,A)+kron(A,c);
[V,D]= eig(d);
b=sort(diag(D));
for j=0:n-2;
    for i=1:n;
        d(i+j*n,i+(j+1)*n)=0;
        d(i+(j+1)*n,i+j*n)=0;
      end;
end;
for j=n:2*n:n*n-n;
         d(j,j+1)=1;
        d(j+1,j)=1;
end;
for j=0:4:n/2-2;
   for i=1:6:2*n;
```

```
28          d(i+j*2*n,i+(j+1)*2*n)=1;
29          d(i+j*2*n+1,i+(j+1)*2*n+1)=1;
30          d(i+(j+1)*2*n,i+j*2*n )=1;
31          d(i+(j+1)*2*n+1,i+j*2*n+1)=1;
32      end;
33  end;
34  for j=0:4:n/2-2;
35    for i=3:6:2*n-3;
36           d(i+j*2*n,i+(j+1)*2*n+2)=1;
37          d(i+j*2*n+1,i+(j+1)*2*n+3)=1;
38          d(i+(j+1)*2*n+2,i+j*2*n)=1;
39          d(i+(j+1)*2*n+3,i+j*2*n+1)=1;
40      end;
41  end;
42  for j=2:4:n/2-2;
43      for i=1:6:2*n;
44         d(i+j*2*n,i+(j+1)*2*n)=1;
45          d(i+j*2*n+1,i+(j+1)*2*n+1)=1;
46          d(i+(j+1)*2*n,i+j*2*n )=1;
47          d(i+(j+1)*2*n+1,i+j*2*n+1)=1;
48      end;
49  end;
50  for j=2:4:n/2-2;
51     for i=5:6:2*n-3;
52           d(i+j*2*n,i+(j+1)*2*n-2)=1;
53          d(i+j*2*n+1,i+(j+1)*2*n-1)=1;
54          d(i+(j+1)*2*n-2,i+j*2*n)=1;
55          d(i+(j+1)*2*n-1,i+j*2*n+1)=1;
56       end;
57  end;
58  for j=1:4:n/2-2;
59      for i=3:6:2*n-1;
60         d(i+j*2*n,i+(j+1)*2*n)=1;
61          d(i+j*2*n+1,i+(j+1)*2*n+1)=1;
62          d(i+(j+1)*2*n,i+j*2*n )=1;
63          d(i+(j+1)*2*n+1,i+j*2*n+1)=1;
64     end;
```

```
end;
for j=3:4:n/2-2;
    for i=5:6:2*n-1;
       d(i+j*2*n,i+(j+1)*2*n)=1;
       d(i+j*2*n+1,i+(j+1)*2*n+1)=1;
       d(i+(j+1)*2*n,i+j*2*n )=1;
       d(i+(j+1)*2*n+1,i+j*2*n+1)=1;
    end;
end;
d=max(d,d');
hold on
h = plot(graph(d),'EdgeColor','k', 'NodeColor','[0.3, 0,0.6]', '
  MarkerSize',6,'NodeLabel',{},'EdgeColor', '[0.3, 0.1,0.5]','
  LineWidth', 5 )
h = plot(graph(d),'EdgeColor','k', 'NodeColor','[0.3, 0,0.6]', '
  MarkerSize',6,'NodeLabel',{},'EdgeColor', '[0.3, 0.2,0.6]','
  LineStyle',':','LineWidth',3 )
hold off
axis off
```

B.20 Script for Archimedean Lattice (6^3).

```
n=20;  % n is natural number
el =zeros(n-1,3);
el = [[1:n-1]' [2:n]' ones(n-1,1)];
nodes=sort(unique([el(:,1) el(:,2)])); % get all nodes, sorted
n=numel(nodes) % number of unique nodes
A=zeros(n);   % initialize adjacency matrix
for i=1:size(el,1); % across all edges
A(find(nodes==el(i,1)),find(nodes==el(i,2)))=el(i,3);
end
A=max(A,A'); A=A-diag(diag(A));
c=eye(n);
d=kron(c,A)+kron(A,c);
for j=0:2:n-2;
    for i=2:2:n;
```

```
15          d(i+j*n,i+(j+1)*n)=0;
16          d(i+(j+1)*n,i+j*n)=0;
17      end
18  end
19  for j=1:2:n-2;
20      for i=1:2:n;
21          d(i+j*n,i+(j+1)*n)=0;
22          d(i+(j+1)*n,i+j*n)=0;
23      end
24  end
25  d=max(d,d');
26  hold on
27  h = plot(graph(d),'EdgeColor','k', 'NodeColor','[0.3, 0,0.6]', '
      MarkerSize',6,'NodeLabel',{},'EdgeColor', '[0.3, 0.1,0.5]','
      LineWidth', 5 )
28  h = plot(graph(d),'EdgeColor','k', 'NodeColor','[0.3, 0,0.6]', '
      MarkerSize',6,'NodeLabel',{},'EdgeColor', '[0.3, 0.2,0.6]','
      LineStyle',':','LineWidth',3 )
29  hold off
30  axis off
```

Bibliography

[1] N. Alalwan, A. Arenas, and E. Estrada. Topological melting in networks of granular materials. *Journal of Mathematical Chemistry*, 57(3):875–894, 2019.

[2] S. Alexander. Amorphous solids: their structure, lattice dynamics and elasticity. *Physics Reports*, 296(2-4):65–236, 1998.

[3] V. Alexiades. *Mathematical modeling of melting and freezing processes*. Routledge, 2017.

[4] A. Amon, P. Born, K. E. Daniels, J. A. Dijksman, K. Huang, D. Parker, M. Schröter, R. Stannarius, and A. Wierschem. Preface: Focus on imaging methods in granular physics, 2017.

[5] D. Baird and R. E. Ulanowicz. The seasonal dynamics of the Chesapeake Bay ecosystem. *Ecological Monographs*, 59(4):329–364, 1989.

[6] R. Bandyopadhyay, D. Liang, J. L. Harden, and R. L. Leheny. Slow dynamics, aging, and glassy rheology in soft and living matter. *Solid State Communications*, 139(11-12):589–598, 2006.

[7] V. Batagelj and A. Mrvar. Pajek datasets, 2001.

[8] V. Batagelj and A. Mrvar. *Analysis of large networks*. 2006.

[9] R. Boese, H.-C. Weiss, and D. Bläser. The melting point alternation in the short-chain n-alkanes: single-crystal x-ray analyses of propane at 30 k and of n-butane to n-nonane at 90 k. *Angewandte Chemie International Edition*, 38(7):988–992, 1999.

[10] B. Bollobás. Random graphs. In *Modern graph theory*, pages 215–252. Springer, 1998.

[11] M. Born. Thermodynamics of crystals and melting. *The Journal of Chemical Physics*, 7(8):591–603, 1939.

[12] G. Butland, J. M. Peregrín-Alvarez, J. Li, W. Yang, X. Yang, V. Canadien, A. Starostine, D. Richards, B. Beattie, N. Krogan, M. Davey, J. Parkinson, J. Greenblatt, and A. Emili. Interaction network containing conserved and essential protein complexes in Escherichia coli. *Nature*, 433(7025):531–537, 2005.

[13] R. W. Cahn. Melting and the surface. *Nature*, 323(6090):668–669, 1986.

[14] I. M. Campbell, R. A. James, E. S. Chen, and C. A. Shaw. Netcomm: a network analysis tool based on communicability. *Bioinformatics*, page 536, 2014.

[15] I. M. Campbell, M. Rao, S. D. Arredondo, S. R. Lalani, Z. Xia, S.-H. L. Kang, W. Bi, A. M. Breman, J. L. Smith, C. A. Bacino, A. L. Beaudet, A. Patel, S. W. Cheung, J. R. Lupski, P. Stankiewicz, M. B. Ramocki, and C. A. Shaw. Fusion of large-scale genomic knowledge and frequency data computationally prioritizes variants in epilepsy. *PLoS Genet*, 9(9):e1003797, 2013.

[16] G. Canright and K. Engø-Monsen. Roles in networks. *Science of Computer Programming*, 53(2):195–214, 2004.

[17] H. Chan and L. Akoglu. Optimizing network robustness by edge rewiring: a general framework. *Data Mining and Knowledge Discovery*, 30(5):1395–1425, 2016.

[18] R. R. Christian and J. J. Luczkovich. Organizing and understanding a winter's seagrass foodweb network through effective trophic levels. *Ecological Modelling*, 117(1):99–124, 1999.

[19] J. J. Crofts, D. J. Higham, R. Bosnell, S. Jbabdi, P. M. Matthews, T. Behrens, and H. Johansen-Berg. Network analysis detects changes in the contralesional hemisphere following stroke. *Neuroimage*, 54(1):161–169, 2011.

[20] G. D'Agostino and A. Scala. *Networks of networks: the last frontier of complexity*, volume 340. Springer, 2014.

[21] G. F. Davis, M. Yoo, and W. E. Baker. The small world of the American corporate elite, 1982-2001. *Strategic Organization*, 1(3):301–326, 2003.

[22] N. M. M. De Abreu. Old and new results on algebraic connectivity of graphs. *Linear Algebra and its Applications*, 423(1):53–73, 2007.

[23] F. Esser and F. Harary. On the Spectrum of a Complete Multipartite Graph. *European Journal of Combinatorics*, 1(3):211–218, 1980.

[24] E. Estrada. Characterization of 3D molecular structure. *Chemical Physics Letters*, 319(5-6):713–718, 2000.

[25] E. Estrada. Community detection based on network communicability. *Chaos: An Interdisciplinary Journal of Nonlinear Science*, 21(1):016103, 2011.

[26] E. Estrada. The communicability distance in graphs. *Linear Algebra and its Applications*, 436(11):4317–4328, 2012.

[27] E. Estrada. Complex networks in the euclidean space of communicability distances. *Physical Review E*, 85(6):066122, 2012.

[28] E. Estrada. *The structure of complex networks: theory and applications*. Oxford University Press, 2012.

[29] E. Estrada. Graph and network theory. *Mathematical Tools for Physicists, Wiley*, 2013.

[30] E. Estrada. When local and global clustering of networks diverge. *Linear Algebra and its Applications*, 488:249–263, 2016.

[31] E. Estrada and M. Benzi. Core–satellite graphs: Clustering, assortativity and spectral properties. *Linear Algebra and its Applications*, 517:30–52, 2017.

[32] E. Estrada and N. Hatano. Statistical-mechanical approach to subgraph centrality in complex networks. *Chemical Physics Letters*, 439(1):247–251, 2007.

[33] E. Estrada and N. Hatano. Communicability in complex networks. *Physical Review E*, 77(3):036111, 2008.

[34] E. Estrada and N. Hatano. Communicability graph and community structures in complex networks. *Applied Mathematics and Computation*, 214(2):500–511, 2009.

[35] E. Estrada and N. Hatano. Communicability angle and the spatial efficiency of networks. *SIAM Review*, 58(4):692–715, 2016.

[36] E. Estrada, N. Hatano, and M. Benzi. The physics of communicability in complex networks. *Physics Reports*, 514(3):89–119, 2012.

[37] E. Estrada and D. J. Higham. Network properties revealed through matrix functions. *SIAM Review*, 52(4):696–714, 2010.

[38] E. Estrada and J. A. Rodríguez-Velázquez. Spectral measures of bipartivity in complex networks. *Physical Review E*, 72(4):046105, 2005.

[39] M. Ezekiel. Methods of correlation analysis. 1941.

[40] M. Fiedler. Algebraic connectivity of graphs. *Czechoslovak Mathematical Journal*, 23(2):298–305, 1973.

[41] L. C. Freeman. A set of measures of centrality based on betweenness. *Sociometry*, pages 35–41, 1977.

[42] L. C. Freeman. Centrality in social networks conceptual clarification. *Social networks*, 1(3):215–239, 1978.

[43] E. N. Gilbert. Random plane networks. *Journal of the Society for Industrial and Applied Mathematics*, 9(4):533–543, 1961.

[44] L. Goldwasser and J. Roughgarden. Construction and analysis of a large Caribbean food web. *Ecology*, 74(4):1216–1233, 1993.

[45] M. Grandjean. A social network analysis of Twitter: Mapping the digital humanities community. *Cogent Arts & Humanities*, 3(1):1171458, 2016.

[46] S. Hanna. Spectral comparison of large urban graphs. Royal Institute of Technology (KTH), 2009.

[47] F. Harary. *Graph Theory*. Addison-Wesley, Reading, MA, 1969.

[48] K. Havens. Scale and structure in natural food webs. *Science (Washington)*, 257(5073):1107–1109, 1992.

[49] J. P. Higgins, S. G. Thompson, J. J. Deeks, and D. G. Altman. Measuring inconsistency in meta-analyses. *BMJ: British Medical Journal*, 327(7414):557, 2003.

[50] M. Hiraiwa, M. A. Ghanem, S. P. Wallen, A. Khanolkar, A. A. Maznev, and N. Boechler. Complex contact-based dynamics of microsphere monolayers revealed by resonant attenuation of surface acoustic waves. *Physical Review Letters*, 116(19):198001, 2016.

[51] R. A. Horn and C. R. Johnson. *Matrix Analysis*. Cambridge University Press, 1990.

[52] M. Huxham, S. Beaney, and D. Raffaelli. Do parasites reduce the chances of triangulation in a real food web? *Oikos*, pages 284–300, 1996.

[53] Y. Ida. Theory of melting based on lattice instability. *Phys. Rev.*, 187:951–958, Nov 1969.

[54] Y. Iturria-Medina. Anatomical brain networks on the prediction of abnormal brain states. *Brain connectivity*, 3(1):1–21, 2013.

[55] G. J. O. Jameson. Counting zeros of generalised polynomials: Descartes' rule of signs and laguerre's extensions. *The Mathematical Gazette*, 90(518):223–234, 2006.

[56] J. W. Jaromczyk and G. T. Toussaint. Relative neighborhood graphs and their relatives. *Proceedings of the IEEE*, 80(9):1502–1517, 1992.

[57] Z. Jin, P. Gumbsch, K. Lu, and E. Ma. Melting mechanisms at the limit of superheating. *Physical Review Letters*, 87(5):055703, 2001.

[58] J. Kepler. *Harmonices mundi (Linz, 1619), liv.* IV.

[59] D. J. Klein and M. Randić. Resistance distance. *Journal of Mathematical Chemistry*, 12(1):81–95, 1993.

[60] D. Krackhardt. The ties that torture: Simmelian tie analysis in organizations. *Research in the Sociology of Organizations*, 16(1):183–210, 1999.

[61] D. J. LaCount, M. Vignali, R. Chettier, A. Phansalkar, R. Bell, J. R. Hesselberth, L. W. Schoenfeld, I. Ota, S. Sahasrabudhe, and C. Kurschner. A protein interaction network of the malaria parasite Plasmodium falciparum. *Nature*, 438(7064):103–107, 2005.

[62] V. Latora and M. Marchiori. Efficient behavior of small-world networks. *Physical Review Letters*, 87(19):198701, 2001.

[63] P. D. Lax. *Functional Analysis.* Wiley-Interscience, 2002.

[64] Y. Li, V. Jewells, M. Kim, Y. Chen, A. Moon, D. Armao, L. Troiani, S. Markovic-Plese, W. Lin, and D. Shen. Diffusion tensor imaging based network analysis detects alterations of neuroconnectivity in patients with clinically early relapsing-remitting multiple sclerosis. *Human Brain Mapping*, 34(12):3376–3391, 2013.

[65] C.-Y. Lin, C.-L. Chen, C.-S. Cho, L.-M. Wang, C.-M. Chang, P.-Y. Chen, C.-Z. Lo, and C. A. Hsiung. hp-dpi: Helicobacter pylori database of protein interactomesembracing experimental and inferred interactions. *Bioinformatics*, 21(7):1288–1290, 2005.

[66] F. A. Lindemann. The calculation of molecular eigen-frequencies. *Phys. Z.*, 11:609–612, 10 1910.

[67] F. A. Lindemann. The calculation of molecular eigen-frequencies. *Phys. Z.,(West Germany)*, 11(14):609–612, 1910.

[68] J. Link. Does food web theory work for marine ecosystems? *Marine Ecology Progress Series*, 230:1–9, 2002.

[69] D. Lusseau, K. Schneider, O. J. Boisseau, P. Haase, E. Slooten, and S. M. Dawson. The bottlenose dolphin community of Doubtful Sound features a large proportion of long-lasting associations. *Behavioral Ecology and Sociobiology*, 54(4):396–405, 2003.

[70] X. Ma and L. Gao. Predicting protein complexes in protein interaction networks using a core-attachment algorithm based on graph communicability. *Information Sciences*, 189:233–254, 2012.

[71] B. D. MacArthur, A. Sevilla, M. Lenz, F.-J. Müller, B. M. Schuldt, A. A. Schuppert, S. J. Ridden, P. S. Stumpf, M. Fidalgo, and A. Maayan. Nanog-dependent feedback loops regulate murine embryonic stem cell heterogeneity. *Nature Cell Biology*, 14(11):1139–1147, 2012.

[72] D. MacRae. Direct factor analysis of sociometric data. *Sociometry*, 23(4):360–371, 1960.

[73] M. Mancini, M. A. De Reus, L. Serra, M. Bozzali, M. P. Van Den Heuvel, M. Cercignani, and S. Conforto. Network attack simulations in Alzheimer's disease: The link between network tolerance and neurodegeneration. In *Biomedical Imaging (ISBI), 2016 IEEE 13th International Symposium on*, pages 237–240. IEEE, 2016.

[74] L. Mander, S. C. Dekker, M. Li, W. Mio, S. W. Punyasena, and T. M. Lenton. A morphometric analysis of vegetation patterns in dryland ecosystems. *Open Science*, 4(2):160443, 2017.

[75] L. Mander, M. Li, W. Mio, C. C. Fowlkes, and S. W. Punyasena. Classification of grass pollen through the quantitative analysis of surface ornamentation and texture. *Proceedings of the Royal Society of London B: Biological Sciences*, 280(1770):20131905, 2013.

[76] N. D. Martinez. Artifacts or attributes? Effects of resolution on the Little Rock Lake food web. *Ecological Monographs*, 61(4):367–392, 1991.

[77] J. C. Maxwell. L. On the calculation of the equilibrium and stiffness of frames. *The London, Edinburgh, and Dublin Philosophical Magazine and Journal of Science*, 27(182):294–299, 1864.

[78] J. Memmott, N. Martinez, and J. Cohen. Predators, parasitoids and pathogens: species richness, trophic generality and body sizes in a natural food web. *Journal of Animal Ecology*, 69(1):1–15, 2000.

[79] J. H. Michael and J. G. Massey. Modeling the communication network in a sawmill. *Forest Products Journal*, 47(9):25, 1997.

[80] R. Milo, S. Itzkovitz, N. Kashtan, R. Levitt, S. Shen-Orr, I. Ayzenshtat, M. Sheffer, and U. Alon. Superfamilies of evolved and designed networks. *Science*, 303(5663):1538–1542, 2004.

[81] R. Milo, S. Shen-Orr, S. Itzkovitz, N. Kashtan, D. Chklovskii, and U. Alon. Network motifs: simple building blocks of complex networks. *Science*, 298(5594):824–827, 2002.

[82] M. Z. Miskin and H. M. Jaeger. Adapting granular materials through artificial evolution. *Nature Materials*, 12(4):326, 2013.

[83] M. Motz, I. Kober, C. Girardot, E. Loeser, U. Bauer, M. Albers, G. Moeckel, E. Minch, H. Voss, and C. Kilger. Elucidation of an archaeal replication protein network to generate enhanced PCR enzymes. *Journal of Biological Chemistry*, 277(18):16179–16188, 2002.

[84] C. R. Myers. Software systems as complex networks: Structure, function, and evolvability of software collaboration graphs. *Physical Review E*, 68(4):046116, 2003.

[85] M. Newman. *Networks: An Introduction*. Oxford University Press, Inc., USA, 2010.

[86] M. E. J. Newman. The structure and function of complex networks. *SIAM Review*, 45(2):167–256, 2003.

[87] P. Noirot and M.-F. Noirot-Gros. Protein interaction networks in bacteria. *Current Opinion in Microbiology*, 7(5):505–512, 2004.

[88] S. Opitz. *Trophic interactions in Caribbean coral reefs*, volume 1085. WorldFish, 1996.

[89] L. Papadopoulos, M. A. Porter, K. E. Daniels, and D. S. Bassett. Network analysis of particles and grains. *Journal of Complex Networks*, 6(4):485–565, 2018.

[90] S. R. Phillpot, S. Yip, and D. Wolf. How do crystals melt? *Computers in Physics*, 3(6):20–31, 1989.

[91] D. Plavšić, S. Nikolić, N. Trinajstić, and Z. Mihalić. On the Harary index for the characterization of chemical graphs. *Journal of Mathematical Chemistry*, 12(1):235–250, 1993.

[92] G. A. Polis. Complex trophic interactions in deserts: an empirical critique of food-web theory. *The American Naturalist*, 138(1):123–155, 1991.

[93] M. A. Porter, P. G. Kevrekidis, and C. Daraio. Granular crystals: Nonlinear dynamics meets materials engineering. *Physics Today*, 68(LA-UR-15-21727), 2015.

[94] T. Pöschel and T. Schwager. *Computational granular dynamics: models and algorithms*. Springer Science & Business Media, 2005.

[95] D. P. Reagan and R. B. Waide. *The food web of a tropical rain forest*. University of Chicago Press, 1996.

[96] P. M. Roget. Roget's Thesaurus of English Words and Phrases, Project Gutenberg, 2002.

[97] B. Rudra, Y. Jiang, Y. Li, and J. Shim. A class of diatomic 2-D soft granular crystals undergoing pattern transformations. *Soft Matter*, 13(35):5824–5831, 2017.

[98] S. Sibi, A. Thamizharasi, S. Priya, and O. Nayak. Using graph theory concepts to determine boiling point formulae for choloalkanes. *International Journal of Engineering Trends and Technology (IJETT)*, 5(3), 2013.

[99] A. Smart, P. Umbanhowar, and J. Ottino. Effects of self-organization on transport in granular matter: A network-based approach. *EPL (Europhysics Letters)*, 79(2):24002, 2007.

[100] J. H. Smith. Some properties of the spectrum of a graph. In *Combinatorial Structures and their Applications (Proc. Calgary Internat. Conf., Calgary, Alta., 1969)*, pages 403–406. Gordon and Breach, New York, 1970.

[101] J. H. Smith. Some properties of the spectrum of a graph. *Combinatorial Structures and their Applications*, pages 403–406, 1970.

[102] O. Sporns and R. Kötter. Motifs in brain networks. *PLoS Biol*, 2(11):e369, 2004.

[103] R. Taylor. Solution of the linearized equations of multicomponent mass transfer. *Industrial & Engineering Chemistry Fundamentals*, 21(4):407–413, 1982.

[104] G. T. Toussaint. The relative neighbourhood graph of a finite planar set. *Pattern Recognition*, 12(4):261–268, 1980.

[105] C. Townsend. Disturbance, resource supply, and food-web architecture in streams. *Ecology Letters*, 1:200–209, 1998.

[106] P. Uetz, Y.-A. Dong, C. Zeretzke, C. Atzler, A. Baiker, B. Berger, S. V. Rajagopala, M. Roupelieva, D. Rose, and E. Fossum. Herpesviral protein networks and their interaction with the human proteome. *Science*, 311(5758):239–242, 2006.

[107] F. Vecchio, F. Miraglia, F. Piludu, G. Granata, R. Romanello, M. Caulo, V. Onofrj, P. Bramanti, C. Colosimo, and P. M. Rossini. "Small world" architecture in brain connectivity and hippocampal volume in alzheimer's disease: a study via graph theory from eeg data. *Brain Imaging and Behavior*, 11(2):473–485, Apr 2017.

[108] S. R. Vippagunta, H. G. Brittain, and D. J. Grant. Crystalline solids. *Advanced Drug Delivery Reviews*, 48(1):3–26, 2001.

[109] L. Von Collatz and U. Sinogowitz. Spektren endlicher Grafen. In *Abhandlungen aus dem Mathematischen Seminar der Universität Hamburg*, volume 21, pages 63–77. Springer, 1957.

[110] D. M. Walker and A. Tordesillas. Topological evolution in dense granular materials: a complex networks perspective. *International Journal of Solids and Structures*, 47(5):624–639, 2010.

[111] P. H. Warren. Spatial and temporal variation in the structure of a freshwater food web. *Oikos*, pages 299–311, 1989.

[112] D. J. Watts and S. H. Strogatz. Collective dynamics of small-world networks. *Nature*, 393(6684):440, 1998.

[113] J. G. White, E. Southgate, J. N. Thomson, and S. Brenner. The structure of the nervous system of the nematode Caenorhabditis elegans. *Philos Trans R Soc Lond B Biol Sci*, 314(1165):1–340, 1986.

[114] P. Yodzis. Diffuse effects in food webs. *Ecology*, 81(1):261–266, 2000.

[115] W. W. Zachary. An information flow model for conflict and fission in small groups. *Journal of Anthropological Research*, 33(4):452–473, 1977.

[116] R. Zallen. *The physics of amorphous solids*. John Wiley and Sons, 2008.

[117] L. D. Zeleny. Adaptation of research findings in social leadership to college classroom procedures. *Sociometry*, 13(4):314–328, 1950.